Newcastle University

Phosphine-Borane-Stabilised Carbanion Complexes of Main Group Elements

Casey Dixon

A thesis submitted to Newcastle University in candidature for the Degree of Doctor of Philosophy

School of Chemistry

June 2016

Abstract

An array of phosphorus-stabilised-carbanion complexes of group 1, 2 and 14 elements and their behaviour in the solid state is reviewed, along with a brief overview of the chemistry of phosphine-boranes, stannyl-stannylenes, heteroleptic stannylenes and oxidative addition. The synthesis and characterisation of a range of novel phosphine-borane precursors is described: $[Me_2P(BH_3)CH_2SiMe_2CH_2]_2$ (**1**), $[Ph_2P(BH_3)CH_2Si(Me_2)CH_2]_2$ (**2**), 1,2-$C_6H_4\{CH_2P^iPr_2(BH_3)\}_2$ (**3**), 1,2-$C_6H_4\{CH_2PPh_2(BH_3)\}_2$ (**4**), 1,2-$C_6H_4\{CH_2PCy_2(BH_3)\}_2$ (**5**), $C_6H_5CH_2P^iPr_2(BH_3)$ (**6**), $C_6H_5CH_2PPh_2(BH_3)$ (**7**), $C_6H_5CH_2PCy_2(BH_3)$ (**8**), $C_6H_5\{CH_2SiMe_3PCy_2(BH_3)$ (**9**), $\{CH_2CH_2PCy_2(BH_3)\}_2$ (**10**).

Treatment of **1** and **2** with two equivalents of ^{n}BuLi and tetramethylethylenediamine (tmeda) in THF yields the corresponding complexes $[Li(tmeda)]_2[Me_2P(BH_3)CHSi(Me_2)CH_2]_2$ (**1a**) and $[Li(THF)_2]_2[Ph_2P(BH_3)CHSi(Me_2)CH_2]_2$ (**2a**), respectively, as monomeric units where the metal centre is bound to the carbanion along with agostic-type B-H···Li interactions. Similarly, the reaction between **2** and two equivalents of BnK ($PhCH_2K$) in the presence of the pentamethyldiethylenetriamine (pmdeta), followed by recrystallisation from hot toluene yields the potassium complex $[K(pmdeta)]_2[CH_2SiMe_2CHP(BH_3)Ph_2]_2$ (**2b**), which has an unusual cyclic structure.

The *o*-phenylene-bridged bis(phosphine-boranes) **3-5** undergo α-metalation with two equivalents of ^{n}BuLi and tmeda to yield the corresponding phosphine-borane-stabilised carbanions $[1,2\text{-}C_6H_4\{CHP(BH_3)R_2\}_2][Li(tmeda)]_2\cdot n$L (R = ^{i}Pr, n = 0 (**3a**); R = Ph, nL = THF (**4a**); R = Cy, nL = 2$PhCH_3$ (**5a**)) after recrystallisation. Compounds **3a**-**5a** adopt similar structures where each Li is positioned on the opposite sides of an essentially planar $C_6H_4(CP)_2$ fragment and has interactions with the carbanion and BH_3 unit. Treatment of **3-5** with two equivalents of $PhCH_2K$ and pmdeta yields the corresponding phosphine-borane-stabilised carbanions $[K(pmdeta)]_2[1,2\text{-}C_6H_4\{CHPR_2(BH_3)\}_2]$ (R = ^{i}Pr (**3b**), Ph (**4b**) and (**5b**)). Compound **5b** crystallises as a discrete monomer, in which each potassium is bound to the carbanion, the pmdeta co-ligand, an η^1 contact to the BH_3 unit and has additional short contacts with an *ipso* carbon atom in the *o*-phenylene linker.

The benzyl-substituted phosphine-boranes **6**, **7** and **8** undergo α-metalation with one equivalent of ^{n}BuLi and tmeda to yield the corresponding phosphine-borane-stabilised carbanions $[C_6H_5CHP(BH_3)R_2][Li(tmeda)]$ (R = ^{i}Pr (**6a**), Ph (**7a**) and Cy (**8a**)). Compound **8a**

crystallises as a discrete molecular species with coordination between the Li and the carbanion centre, BH_3 hydrogens in an η^2-fashion, the hydrogen atom associated with the carbanion centre and with the coordination sphere completed by two contacts to the two nitrogen atoms in one molecule of tmeda. Treatment of compound **8** with an excess of BnK in THF results in the phosphine-borane-stabilised carbanion complex $K[C_6H_5CHPCy_2(BH_3)]$ (**8b**); which crystallises as a sheet polymer,

The synthesis of group 2 complexes of **6** and **8** was investigated using three different methods in which included the use of ^{n}BuLi followed by the group 2 halide, BnK followed by the group 2 halide and the use of previously prepared Bn_2M (M = Ca, Sr, Ba).

Treatment of *in situ*-generated **5a** with one equivalent of Cp_2Sn in toluene yields pale yellow crystals of the unusual agostically-stabilised stannyl-stannylene $[[1,2\text{-}C_6H_4\{CHP(BH_3)Cy_2\}_2]Sn]_2\cdot 1½PhMe$ (**11**). Compound **11** crystallises as a discrete molecular species containing two different Sn centres with formal oxidation states of I and III, joined by a formal Sn-Sn σ-bond.

Treatment of one equivalent of $SnCl_2$ with two equivalents of *in situ*-generated $[Li(tmeda)][C_6H_5CHPR_2(BH_3)]$ (R = ^{i}Pr (**6a**) and Cy (**8a**)) in diethyl ether yields $Sn[C_6H_5CHPR_2(BH_3)]_2$ (R = ^{i}Pr (***rac*-6c**) and Cy (***rac*-8c**)). Both ***rac*-6c** and ***rac*-8c** have interactions between the Sn centre and one H atom from each of two separate BH_3 units in an η^1-fashion.

Treatment of one equivalent of $SnCl_2$ with one equivalent of *in situ*-generated $Li[C_6H_5CHPR_2(BH_3)]$ (R = ^{i}Pr (**6a**), Cy (**8a**)) in diethyl ether yields $SnCl[C_6H_5CHPR_2(BH_3)]$ (R = ^{i}Pr (**6d**), Cy (**8d**)). Treatment of a diethyl ether solution of **6c** with one equivalent of methyl iodide or benzyl bromide yields the corresponding oxidative addition products $[C_6H_5CHP^iPr_2(BH_3)]_2Sn(Me)I$ (**12)** and $[C_6H_5CHP^iPr_2(BH_3)]_2Sn(Bn)Br$ (**13)**, respectively. Compound **12** crystallises as a discrete monomer where the tin has contacts with two phosphine-borane fragments via the carbanion centre, a bond to the methyl carbon atom and a contact with an iodide in a distorted tetrahedral geometry; this compound has no agostic-type interactions between the borane hydrogens and the tin. The solution state structure of **12** was determined using multi-element and multi-nuclear NMR spectroscopy.

Acknowledgements

I would first like to thank my supervisor Dr Keith Izod for his continued support and guidance over the past four years in both the production of this thesis and in the laboratory. Many thanks also to Professor Bill Clegg, Dr Ross Harrington, Dr Michael Probert and Dr Paul Waddell for their vital help with X-ray crystallography, and to Professor William McFarlane and Dr Corinne Wills for their guidance with NMR spectroscopy.

I would also like to thank Emma McMeekin and Peter Evans for their advice in the laboratory.

Finally, I would like to say a huge thank you to my family, past and present, for their continued support during my education, in particular, to my partner Barney McManners, to whom I dedicate this thesis.

Publications from this work

Chapter 3

- K. Izod, C. M. Dixon, E. McMeekin, L. Rodgers, R. W. Harrington and U. Baisch, *Organometallics*, 2014, **33**, 378-386.

Chapter 5

- K. Izod, C. M. Dixon, R. W. Harrington and M. R. Probert, *Chemical Communications*, 2015, **51**, 679-681.

List of Abbreviations

Å	angstrom	μ_n	n-bridging
^{n}Bu	*n*-butyl	Hz	hertz
^{t}Bu	*t*-butyl	tmeda	*N*, *N*, *N′*, *N′*-tetramethylethylenediamine
VT	variable temperature	Cy	cyclohexyl
C_n	*n*-fold rotation	pmdeta	*N*, *N*, *N′*, *N″*, *N″*-pentamethyldiethylenetriamine
d	doublet	ppm	parts per million
dd	doublet of doublets	s	singlet
d	deuterated	t	triplet
m	multiplet	q	quartet

Table of important compounds

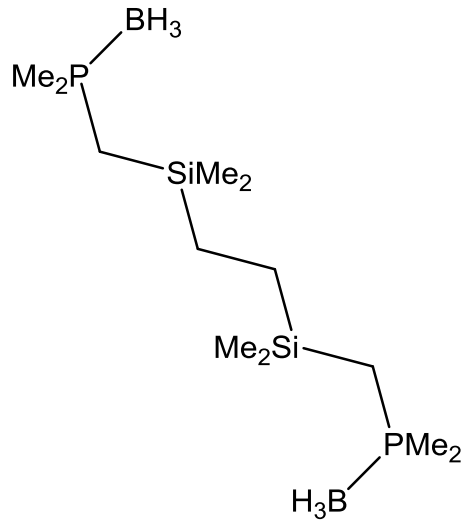 **37**	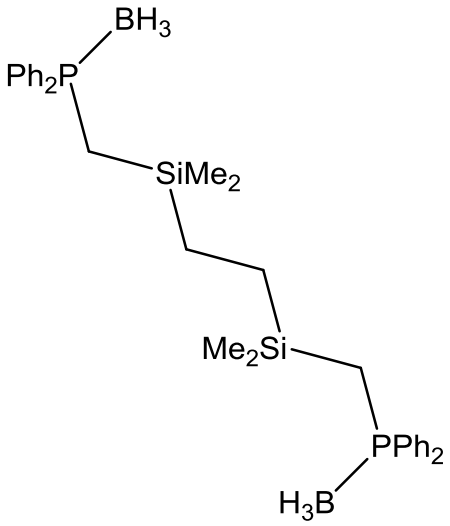 **40**
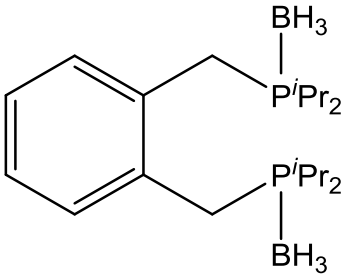 **44**	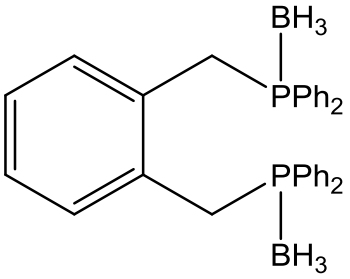 **45**
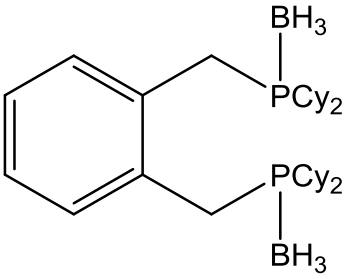 **46**	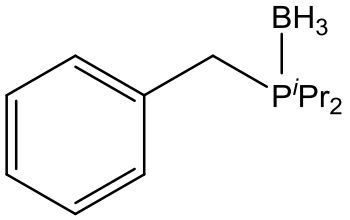 **47**
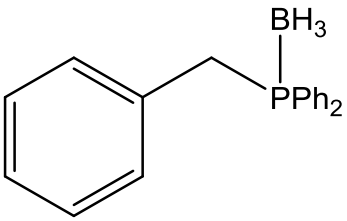 **48**	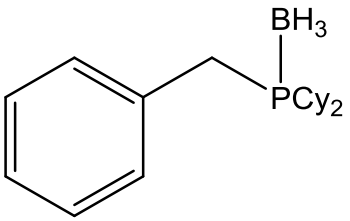 **49**

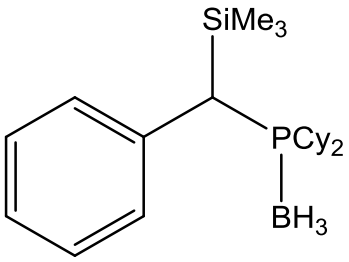

50

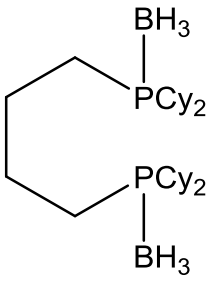

51

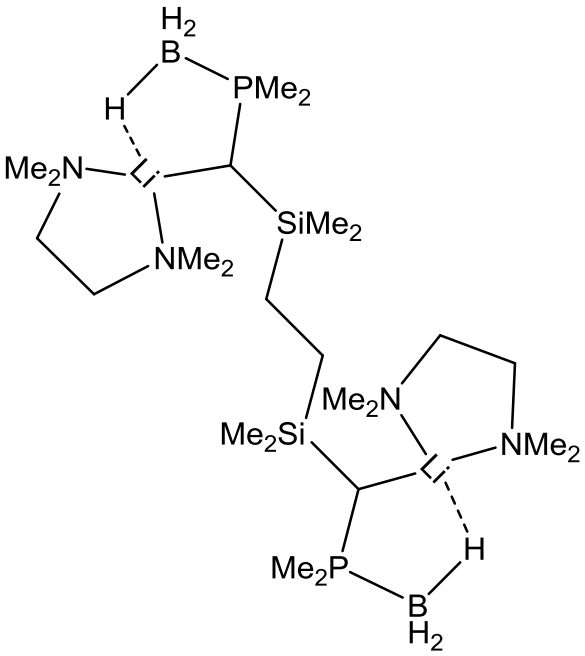

37a

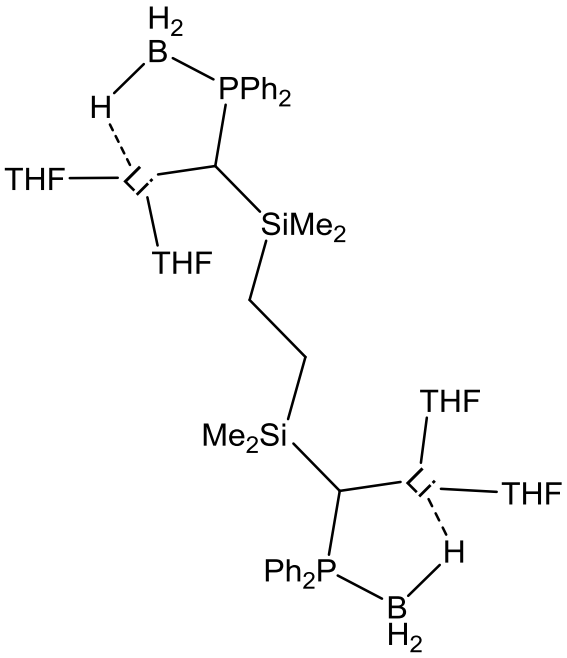

40a

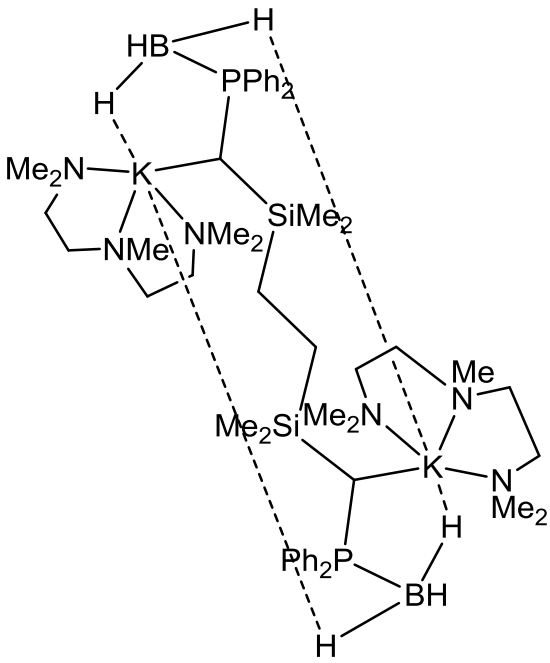

40b

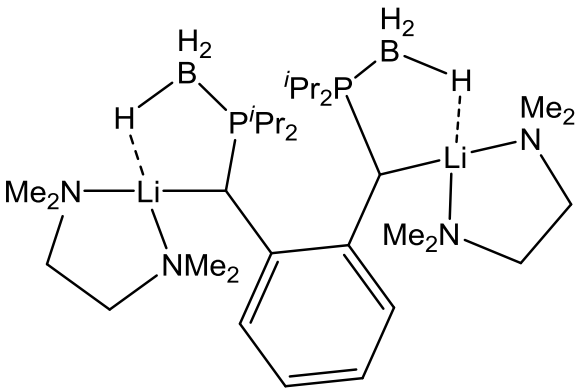

44a

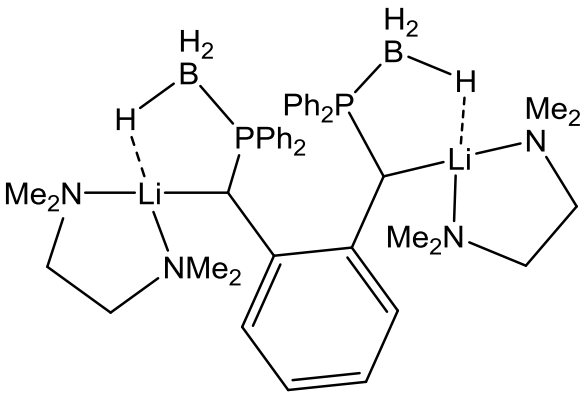

45a

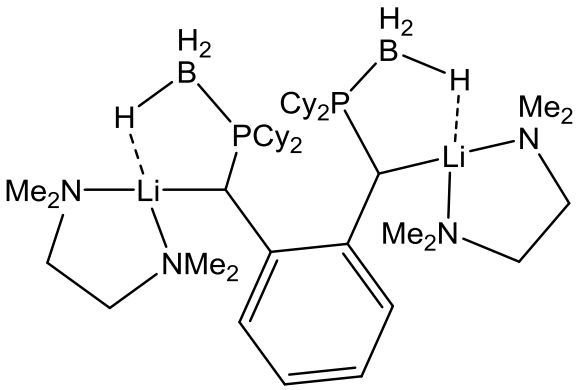

46a

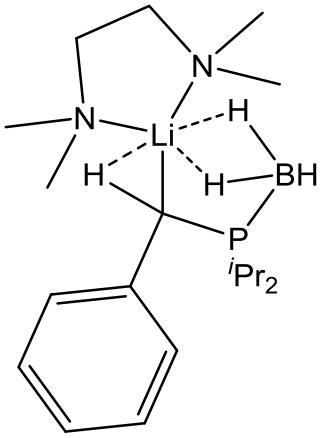

47a

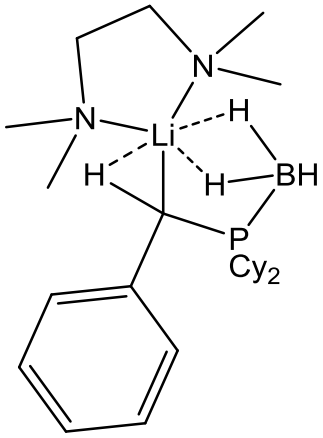

49a

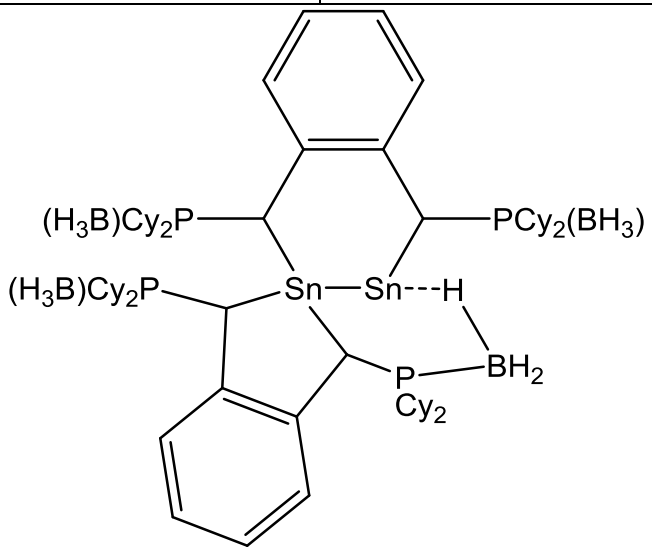

58

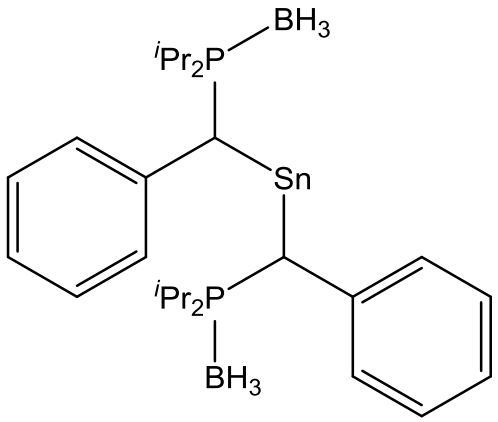 BH3 iPr2P Sn iPr2P BH3	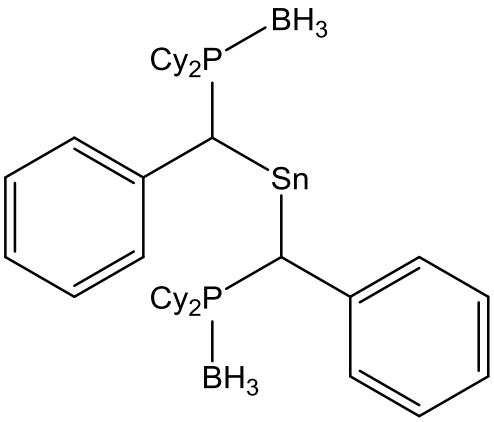 BH3 Cy2P Sn Cy2P BH3
64	**65**
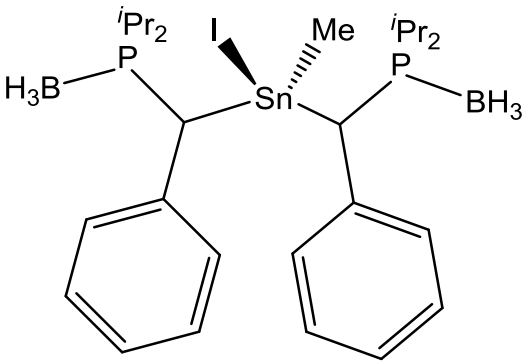 iPr2 P H3B I Me Sn iPr2 P BH3	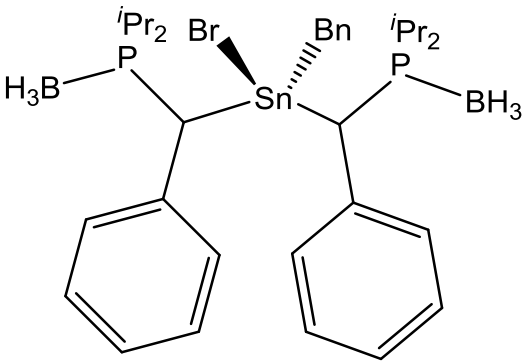 iPr2 P H3B Br Bn Sn iPr2 P BH3
86	**87**

Table of Contents

Chapter 1. Introduction

1.1 Group 1 metal organometallics

Organometallic reagents are very important in synthetic chemistry due to their ability to act as both a base and nucleophile; their use in many reactions is common. The first organolithium was reported by Wilhelm Schlenk[1, 2] in 1914 and its discovery led to the synthesis of an array of group 1 metal organometallics.[3-5]

It is surprising, however, that even with the widespread use of alkali metal organometallics, the understanding of their reactivity is still relatively limited. In order to better understand the reactivity of these species, the determination of their structures in solution and the solid-state is vital, along with their tendency towards aggregation. Advances in X-ray crystallography have been fundamental to this and now a great deal of structural data is available for this class of compound. In addition to X-ray crystallography, analytical methods such as NMR, UV-Vis and IR spectroscopies have improved the ease with which these compounds may be characterised. However, there is still a lot more work to be done in order to fully understand the reactivity of alkali organometallics; especially with regards to heavier alkali metals such as sodium and potassium. Sodium and potassium organometallics pose a slightly different problem to those of lithium due to their increased sensitivity towards moisture and oxygen; alkali metal organometallics must be handled under an inert atmosphere (usually N_2) using Schlenk techniques to prevent hydrolysis and/or oxidation via a hydroperoxide salt (Scheme 1.1).

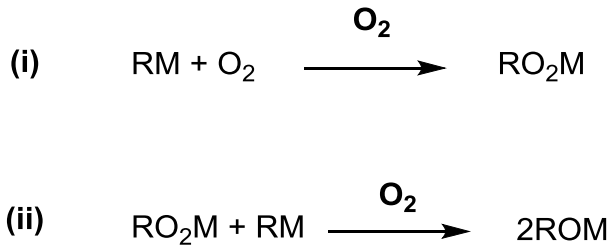

Scheme 1.1: Decomposition of alkali metal organometallic compounds with oxygen.

Not only are alkali metal organometallics reactive towards oxygen, but they are also known to deprotonate ethereal solvents, such as diethyl ether and THF; this decomposition has been studied in detail by Maercher and co-workers who used deuterium-labelled ethers

and witnessed α-, β-, and α,β-eliminations, as well as Wittig rearrangements, resulting in many products (Scheme 1.2).[6]

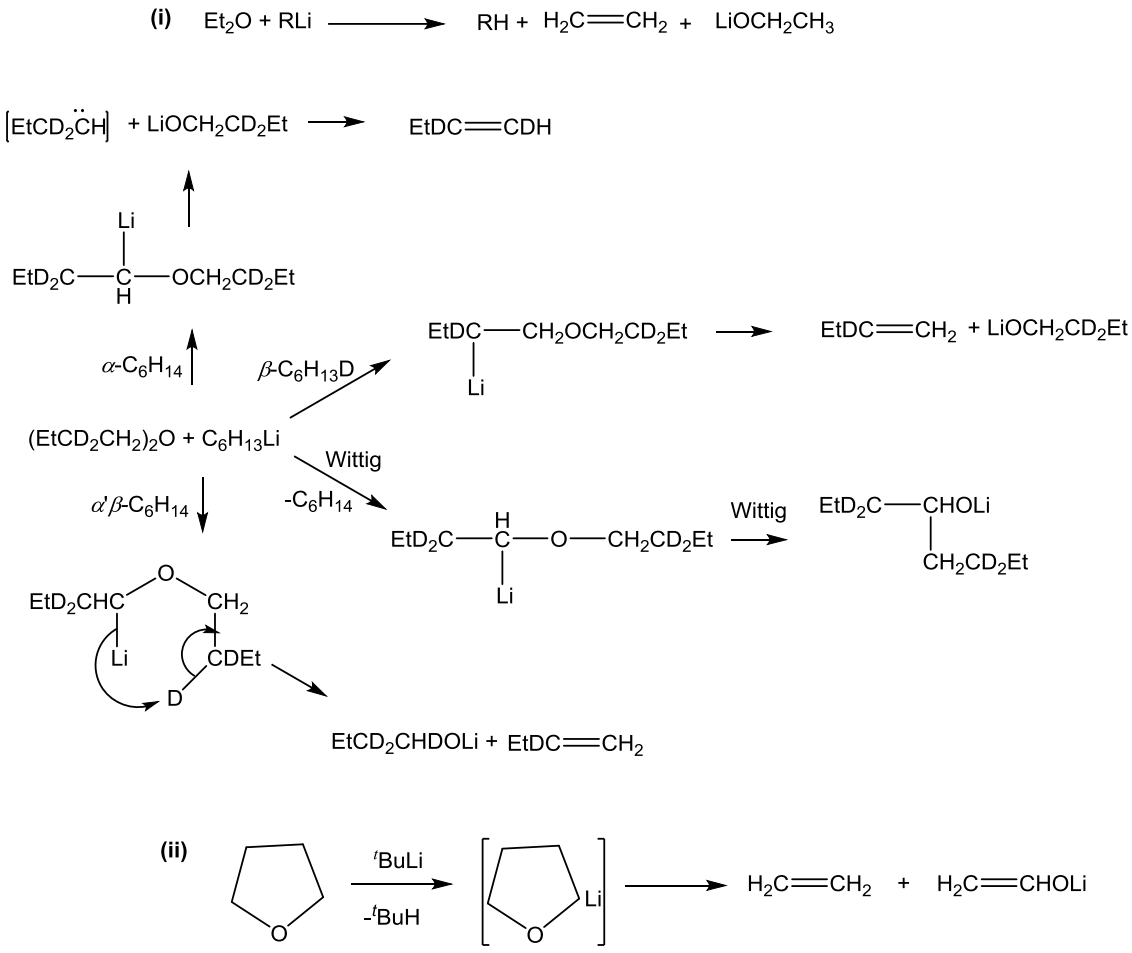

Scheme 1.2: (i) Reaction of diethyl ether with deuterated alkali metal organometallics, (ii) Reaction of THF with ^{t}BuLi.

The factors in alkali metal organometallic compounds which determine structure and reactivity are: i) charge to size ratio, which decreases as the group is descended, ii) ionicity, which generally increases as you go down the group and iii) atomic radii, which increase as you go down the group. The size of the cation is important as it tends to dictate the coordination number of the metal centre; as the cation radius increases, so does the coordination number, leading to a greater tendency towards aggregation.

Overall, now that spectroscopic methods have improved over the last 3 decades, so has our understanding of the reactivity and structure of alkali organometallics. The size of the

cation and aggregation properties are very important as aggregation is a common problem in alkali metal organometallics; this can affect the reactivity of the reagent and so it is quite common to use amines to decrease aggregation and thereby increase the reactivity. As knowledge of alkali metal organometallics increases, so will their uses and the ability to be selective in the use of these types of compounds during synthetic approaches.

1.2 Phosphorus-stabilised carbanions

Phosphorus-stabilised carbanions have been recognised as useful reagents for a variety of important organic reactions, such as variants of the Wittig olefination reaction (Horner or Horner-Wadsworth-Emmons reactions).[7-10] It has been found that phosphorus-stabilised carbanions (phosphinomethanides) have increased reactivity compared to neutral ylide species in the Wittig reaction. These phosphorus-stabilised carbanions can be used as ligands, and complexes of metallic elements from groups 1, 2, 13, 14 and 15 are known.[10] The reason why phosphorus (or other third row elements) can stabilise a carbanion is due to a combination of electrostatic interactions (due to the greater electropositivity of the heteroatom); greater polarisability of the 2nd row elements, negative hyperconjugation, which stabilises the carbanion by donation of the carbanion lone pair into a low lying σ^* orbital on the heteroatom (Figure 1.1 (I)), and dπ-pπ interactions (Figure 1.1 (II)). However, dπ-pπ interactions are now thought not to be very stabilising, since the 3d-orbitals are too high in energy for good overlap with the lone pair (l.p.) orbital on the carbanion centre. Also, studies have shown that any stabilisation in the gas phase is lost on complexation with lithium or sodium ions due to these metals localising the charge on the carbanion centre, although this effect is diminished in complexes with the less charge-localising heavier alkali metal cations.[10]

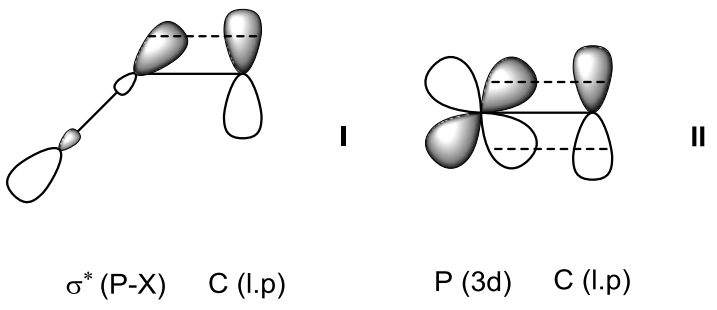

Figure 1.1: Negative hyperconjugation (I) and dπ-pπ interactions (II) between phosphorus and an adjacent carbanion.

Phosphorus(III)-stabilised carbanions can act as monodentate (**i** and **ii**), bidentate (**iii**) and bridging (**iv**) ligands due to the presence of lone pairs on both the P(III) centre and the carbanion, the similar electronegativities of P and C, and the fact that both atoms are valence isoelectronic (Figure 1.2). These factors enable the two atoms to compete as donor ligands, hence the ability to act as a bidentate and bridging ligand.[10]

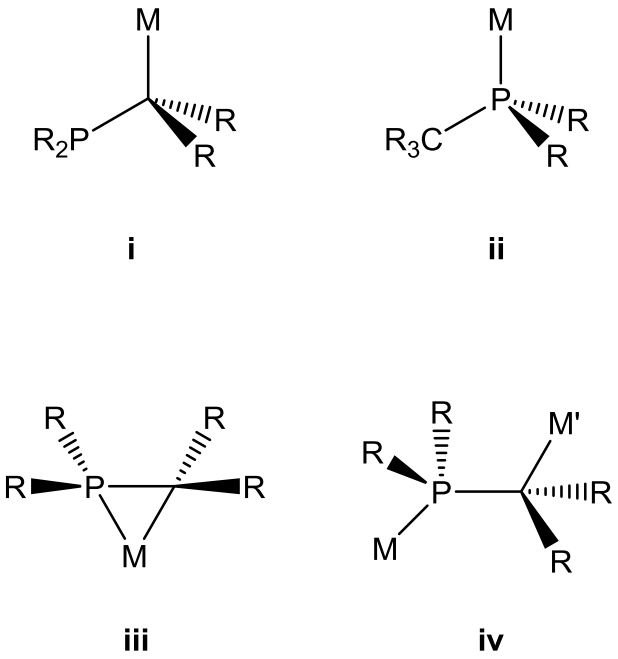

Figure 1.2: Binding modes of phosphinomethanide ligands.

1.2.1 Phosphinomethanide complexes of the alkali metals

The structure adopted by a phosphinomethanide complex depends on the nature of the metal, the nature of the substituents on the carbanion and phosphorus centres and the presence of co-ligands or coordinating solvents. If a charge-delocalising or sterically demanding substituent (e.g. $SiMe_3$) is bound to the carbanion, then the nucleophilicity of the centre decreases and so coordination through the phosphorus atom is favoured. There are a number of structures that have been published from the Izod group, such as the α-lithiated phosphinomethanide $Li[C(SiMe_3)_2\{P(C_6H_4CH_2NMe_2\text{-}2)_2\}]$ (**1**) (Figure 1.3) in which the Li ion is bound to the P and two N atoms of the ligand, but has no short Li-C contacts.[11]

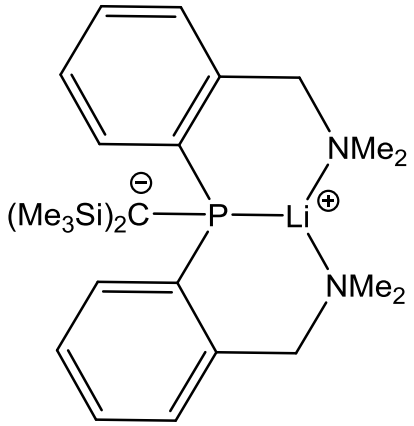

Figure 1.3: α-lithiated phosphinomethanide Li[C(SiMe$_3$)$_2${P(C$_6$H$_4$CH$_2$NMe$_2$-2)$_2$}] (**1**).

The first example of a phosphinomethanide with a co-ligand-free lithium ion [Li{C(SiMe$_3$)$_2$PMe$_2$}]$_2$ (**2**) (Figure 1.4) was reported by Karsch and co-workers in 1990 [this compound exhibits binding modes similar to **iv** (Figure 1.2)].[12] The two lithium cations exhibit a six-membered chair conformation where the lithium cations in the ring are bridged by the phosphinomethanide ligands; the coordination sphere of each lithium ion is completed by additional weak intermolecular and intramolecular Si-Me···Li interactions.[12]

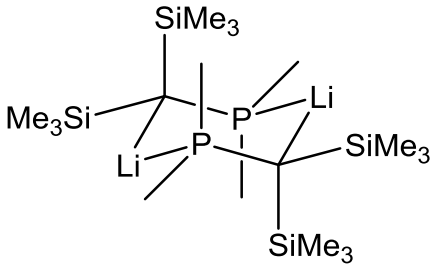

Figure 1.4: Compound **2** in a chair conformation.

1.3 Phosphine-boranes

1.3.1 Introduction

For many years phosphine-boranes have been used extensively for the synthesis of phosphines due to the P-B serving as a protecting group against oxidation. For example, phosphine-borane adducts are important intermediates used to synthesise polyphosphines, such as the chiral diphosphine DIPAMP (Scheme 1.3).[13, 14] More recently, phosphine-boranes have also become of interest as ligands for transition metal complexes.[15] The key features of

phosphine-borane adducts include: (i) the P-B bond shows particular stability, and so the phosphorus atom is protected from oxidation; this enables the easy handling of air-sensitive trivalent phosphines, which would otherwise need to be handled under air- and moisture-free conditions; (ii) the formation of an adduct between a phosphine and a borane is often reversible; and (iii) CH protons α to the phosphorus atom are activated towards deprotonation (using a strong base such as ^{n}BuLi), giving highly stabilised carbanions.[16] Surprisingly, relatively little is known about the structures of these carbanions in solution or the solid state.

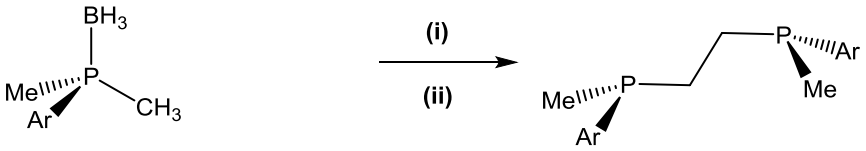

Scheme 1.3: Synthesis of DIPAMP using a phosphine-borane-stabilised carbanion. Reaction conditions: i) ^{s}BuLi{(-)-sparteine}, ii) $Cu(OPiv)_2$ and Et_2NH.

The first example of a phosphine-borane, phosphine trichloroborane ($H_3P{\cdot}BCl_3$) was reported by Besson in 1890.[17] However, detailed investigations were not carried out until the mid-20th century when the next phosphine-borane was published by Gamble and Gilmont in 1940.[18] Based on Stock's[19] work it was first thought that diborane diphosphine ($B_2H_6{\cdot}2PH_3$) had been synthesized, however, on further investigations the simplest example of a phosphine-borane adduct ($PH_3{\cdot}BH_3$) was identified. This phosphine-borane was monomeric and a white solid which did not show any decomposition.[20]

1.3.2 Preparation of phosphine-boranes

An array of secondary and tertiary alkyl-functionalised phosphine-boranes ($R_2PH{\cdot}BH_3$ and $R_3P{\cdot}BH_3$) have been synthesised and published ($Me_3P{\cdot}BH_3$, $Me_2PH{\cdot}BH_3$, $MePH_2{\cdot}BH_3$, $Me_2PH{\cdot}BHMe_2$ and $Me_2PH{\cdot}BMe_3$).[21] It was found that secondary and tertiary phosphine-borane adducts are significantly more stable than primary phosphine-borane adducts due to the phosphorus centre being much higher in basicity for the secondary and tertiary compounds due to increased electron donation from the alkyl substituents. This donation leads to a much stronger phosphorus-boron bond and so will prevent dissociation, which is a common feature in monoalkyl-substituted phosphine-boranes.[15]

In early synthetic experiments it was common to use diborane (B_2H_6) and the required phosphine to yield the corresponding phosphine-borane. However, due to the toxicity and pyrophoric nature of diborane, this synthesis is very rarely used today. The modern approach in research labs is to carry out adduct formation via direct addition of primary, secondary or tertiary phosphines to BH_3·THF or BH_3·SMe_2 (Scheme 1.4) where the strongly donating phosphine rapidly displaces the weaker Lewis base; these reactions are usually clean and quantitative.[18]

Scheme 1.4: Preparation of a phosphine-borane using a borane adduct.

In situations where large quantities of reagents are needed a number of procedures have been used to synthesise phosphine-boranes. The first example is reduction of a phosphine oxide with a mixture of $LiAlH_4$, $NaBH_4$ and $CeCl_3$ (Scheme 1.5, Reaction 1).[22] The cerium trichloride is essential for this reaction to occur as the reduction will not proceed if the cerium complex is not present. The cerium forms a coordination complex with the oxygen on the phosphine oxide to improve the electrophilic nature of the P-centre which will then aid the $LiAlH_4$ to deoxygenate at the phosphorus. A second, widely used method is the use of borohydride reagents with mono/dichlorophosphines to produce the corresponding phosphine-borane adduct (Scheme 1.5, Reaction 2).[23, 24] The main advantage to this is the elimination of handling reactive primary and secondary phosphines. A third and more recent approach is the reaction of $NaBH_4$ and a proton source with a secondary or tertiary phosphine (Scheme 1.5, Reaction 3).[25] The $NaBH_4$ and proton source generate BH_3 *in situ* which then reacts with the phosphine, producing the phosphine-borane.

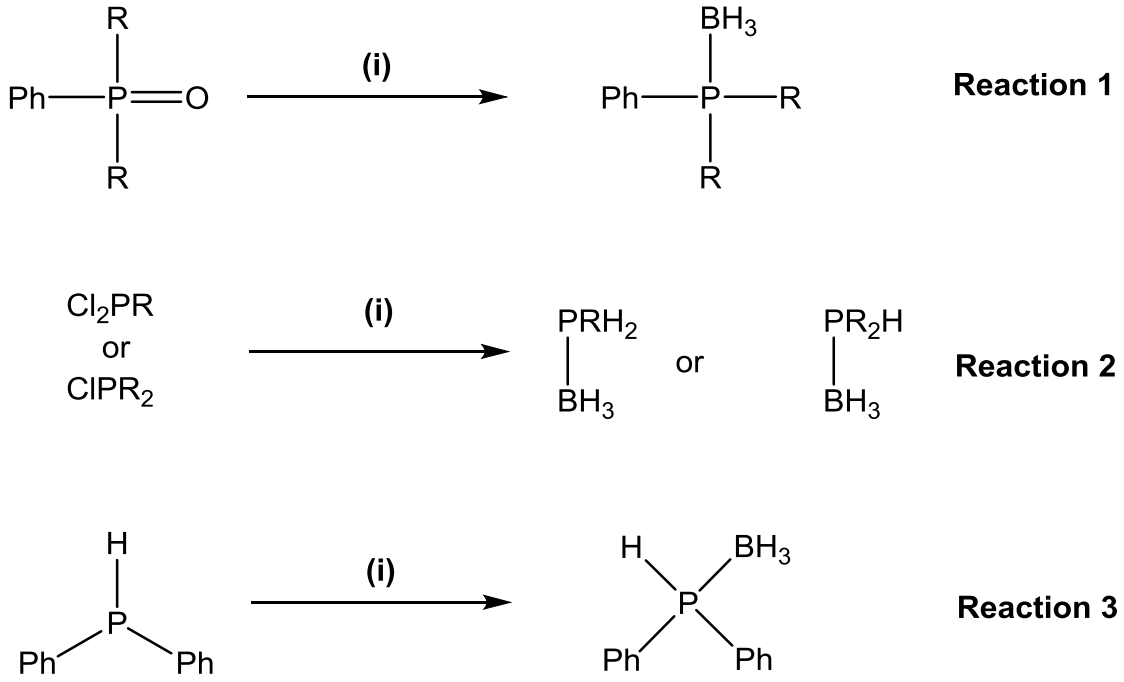

Scheme 1.5: Alternative reactions for the synthesis of phosphine-borane adducts. Reaction conditions. Reaction 1, i) $LiAlH_4$, $NaBH_4$, $CeCl_3$, 25 °C, THF. Reaction 2, i) sodium borohydride. Reaction 3, i) $NaBH_4$, THF and HOAc, THF.

The three alternative methods for synthesising phosphine-borane adducts (Scheme 1.5) are advantageous on a much larger scale due to the instability of the adduct (BH_3·THF) or the large production of noxious gases (BH_3·SMe_2). Sodium borohydride is much more readily available due to its low cost and convenient long term storage.

A fourth alternative method for the synthesis of phosphine-borane adducts is via a phosphine-amine exchange reaction where the amine-borane adduct can be treated with a large excess of the phosphine to yield the phosphine-borane adduct. Due to this reaction being an equilibration process, there are a number of factors which will affect the position of the equilibrium, such as the relative donor ability of the amine and phosphine, which depends on its substituents in relation to its sterics and electronic effects.[15] It should be noted that this synthesis would not be ideal for expensive phosphines, such as $HPCy_2$, as a large excess of phosphine is needed to favour the production of the corresponding phosphine-borane adduct.

Many different functionalised tertiary phosphine-borane adducts have been synthesised from secondary phosphine-boranes by the Imamoto group (Chart 1.1).[13]

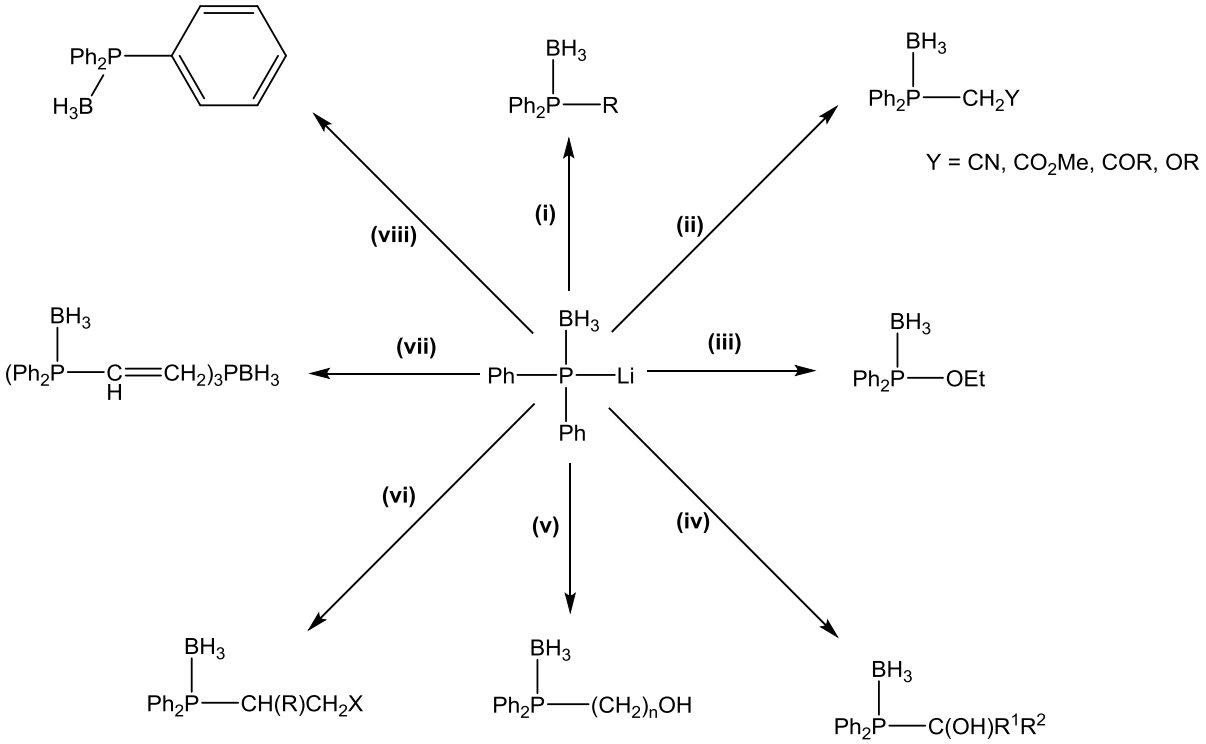

Chart 1.1: Various reactions of the lithium derivative of diphenylphosphine-borane with a number of different electrophiles to form tertiary phosphine-boranes. Reaction conditions: i) RX. ii) XCH_2Y. iii) $Br(CH_2)_2Br$, EtOH. iv) R^1COR^2. v) $O(CH_2)_n$, n = 2, 3. vi) RHCCHX. vii) $(CH_2CH)_3PBH_3$. viii) PhI, $Pd(Ph_3P)_4$.

Imamoto and co-workers investigated the reactions of secondary phosphine-boranes where the corresponding phosphine-borane-stabilised-carbanion can be easily made with an organometallic reagent (BuLi). These anions will then react with an array of electrophiles yielding functionalised phosphine-boranes (Chart 1.1). Due to the stability of the P-B bond and the versatility in which these types of compounds can be synthesised and used, these species are starting to show an increasing demand within asymmetric catalysis.[13]

1.3.3 Decomplexation of boranes

As mentioned above, a useful feature of phosphine-boranes is that their formation is often reversible. The use of an excess of an amine such as diethylamine will often drive the reaction so that the BH_3 will bind to the nitrogen in preference to phosphorus (Scheme 1.6). This was first reported by Imamato, who used a large excess of diethylamine to cleave the P-B bond in a variety of phosphine-borane compounds.[22, 26] The limiting factor in the use of secondary amines in this way is that their use is not always suitable for phosphine-boranes that contain other functional groups, such as carbonyl groups. This problem was first

overcome by using DABCO (1, 4-diazabicyclo[2.2.2]octane) or tmeda [tmeda = *N*,*N*,*N*′,*N*′-tetramethylethylenediamine].[27] Decomplexation can then be achieved under mild conditions, while retaining other functional groups within the newly made phosphine.

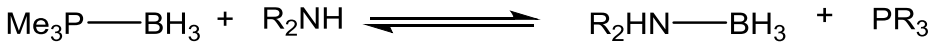

Scheme 1.6: Decomplexation of a phosphine-borane.

Other methods of decomplexation include the use of acids, such as $HBF_4 \cdot OMe_2$, methane- and trifluoromethanesulfonic acid, or zeolites along with alcoholysis.[28] Although the exact mechanism of decomplexation using acids is not understood, the production of hydrogen gas is observed and it is believed that the BH_3 unit may undergo nucleophilic substitution (Scheme 1.7).[26, 29, 30]

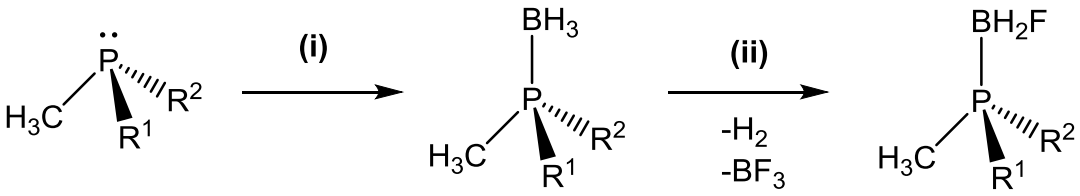

Scheme 1.7: Nucleophilic substitution of a generic phosphine-borane. Reaction conditions: i) $BH_3 \cdot SMe_2$. ii) $HBF_4 \cdot OMe_2$.

1.4 Phosphine-borane-stabilised carbanions

Deprotonation of a phosphine-borane adduct α- to a P-BH_3 group yields the corresponding phosphine-borane-stabilised carbanion. However, until as recently as 2006, only four species of this kind had been isolated and structurally characterised.[31-34] All of these compounds adopted a different structure in the solid state (Figure 1.5).

$[Me_2P(BH_3)CHPMe_2(BH_3)][Li(tmeda)_2]$ (**3**) crystallises as a separated ion pair with no contact between the carbanion centre and the lithium ion.[31] The dicarbanion complex $[(Me_3Si)\{n\text{-}Pr_2P(BH_3)\}CCH_2]Li(pmdeta)]_2$ (**4**) was synthesised via a Schlenk dimerisation of the alkene $\{Pr^n{}_2P(BH_3)\}(Me_3Si)C{=}CH_2$; this compound is stabilised by both phosphine-borane and silyl groups [pmdeta = *N*,*N*,*N*′,*N*″,*N*″-pentamethyldiethylenetriamine]. Compound **4** crystallises as a contact ion multiple in which the lithium cations are bound at either end of the dicarbanionic ligand by two H atoms of the BH_3 moiety rather than the carbanion centres.

The P-C and Si-C distances [1.711(2) and 1.808(2) Å, respectively] are shorter than usual bond lengths for P-C single bonds, which is consistent with a significant degree of negative hyperconjugation.[32]

The α-metalated phenylphosphine-borane (**5**) crystallises as a monomeric species with a direct C-Li bond but no Li-BH_3 interactions,[33] whereas the sterically hindered α-metalated phosphine-borane $(THF)_3Li\{(Me_3Si)_2CPMe_2(BH_3)\}_2Li$ (**6**) crystallises as a contact ion multiple ate complex where one Li ion is bound by two carbanion centres of two phosphine-borane-stabilised carbanions and has a short contact to one of the H atoms of a BH_3 moiety from one ligand, whereas the second lithium cation is bound in an η^3-fashion by the H atoms of a BH_3 group. Therefore, the solid state structure exhibits both C-Li and BH_3-Li contacts (Figure 1.6).

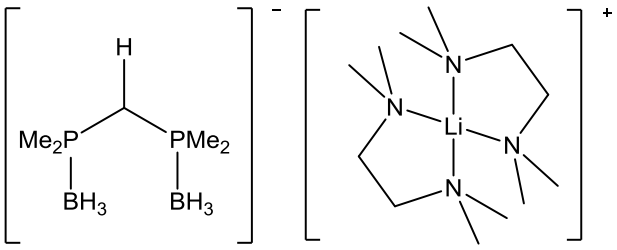

3

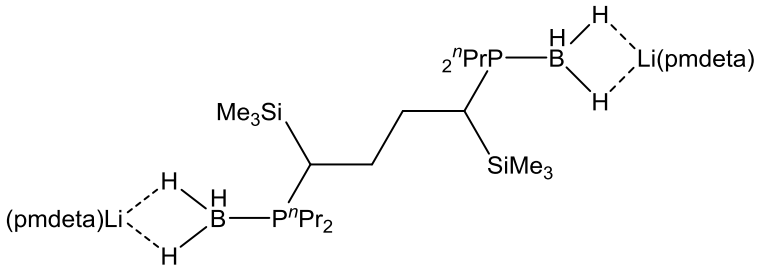

4

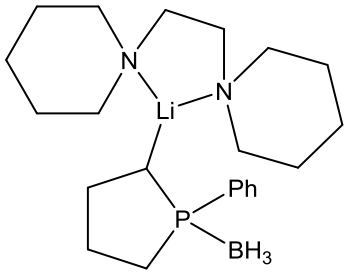

5

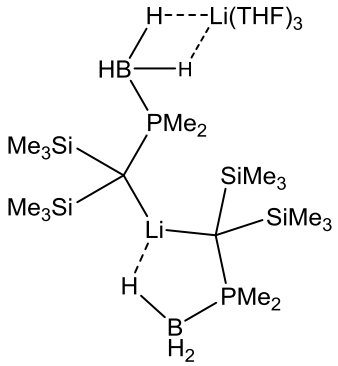

6

Figure 1.5: Different structural motifs observed for phosphine-borane-stabilised carbanions in the solid state.

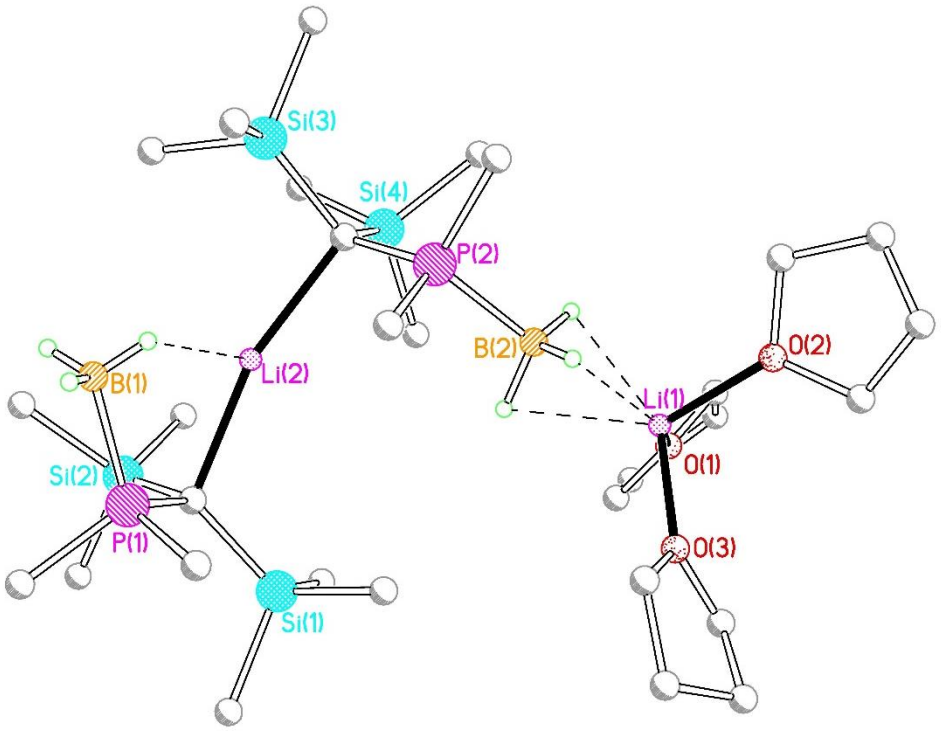

Figure 1.6: Crystal structure of **6** with all H atoms (except for those bound to boron) omitted for clarity.

During an extended study of the synthesis and structures of α-metalated phosphine-boranes, Izod and co-workers found that the structures of these compounds are influenced by a number of different factors, including: (i) the degree of charge delocalisation at the carbanion centre, (ii) the nature of the substituents at the phosphorus, and (iii) the presence of co-ligands such as tmeda and pmdeta.[34]

Even though the first example of a dialkyllithate complex was reported 50 years ago, very few have been isolated and structurally characterised by X-ray crystallography. The few complexes of this type are limited to tris(trimethylsilyl)methyl derivatives $[Li(L)_n][\{Me_3Si)_3C\}_2Li]$ [$Li(L)_n$ = $Li(THF)_4$ (**7**)[35], $Li(tmeda)_2$ (**8**)[36], (pmdeta)LiClLi(pmdeta)][37], cyclic systems such as $[Li(tmeda)_2][\{(Me_3Si)_2C(SiMe_2CH_2)\}_2Li]$ (**9**)[38] and $[Li(tmeda)_2][(tmeda)Li(CH_2Ph)_2]$ (**10**).[39]

In the carbanion complex **6** the negative charge may be delocalised across both the silyl and phosphine-borane groups and so the binding modes adopted may be influenced by the steric and electronic properties of the bulky silyl groups. It is also important to note that Me_2PBH_3 and Me_3Si groups are isoelectronic to each other which is why the dialkyllithate section of compound **6** is very similar to the dialkyllithate anions in compounds **7-10**. The lengthening of the Li(2)-C bonds in **6** [2.249(8) and 2.252(8) Å] compared to the

corresponding bonds in compounds **7**-**10** [2.16(1), 2.20(1), 2.213(5), and 2.156(4) Å] is due to the increased coordination at **7** with a H atom of the BH_3 moiety.[34] Variable-temperature NMR spectroscopy of compound **6** reveals dynamic behaviour (Figure 1.7).

In order to investigate the level of stabilisation that could be achieved by the effect of the phosphine-borane group only, a new phosphine-borane $Me_3P(BH_3)$ was examined.[40] Treatment of $Me_3P(BH_3)$ with either one equivalent of ^{n}BuLi or MeNa gave the corresponding complexes $\{Me_2P(BH_3)CH_2\}M$ [M = Li (**11**), Na (**12**)] (Scheme 1.8).[40] The sodium derivative crystallises to form a polymeric chain where a sodium cation is bound through a carbanion centre and through one hydrogen on one borane group to give a pseudo-four-membered chelate ring (Figure 1.8 and 1.9).[40]

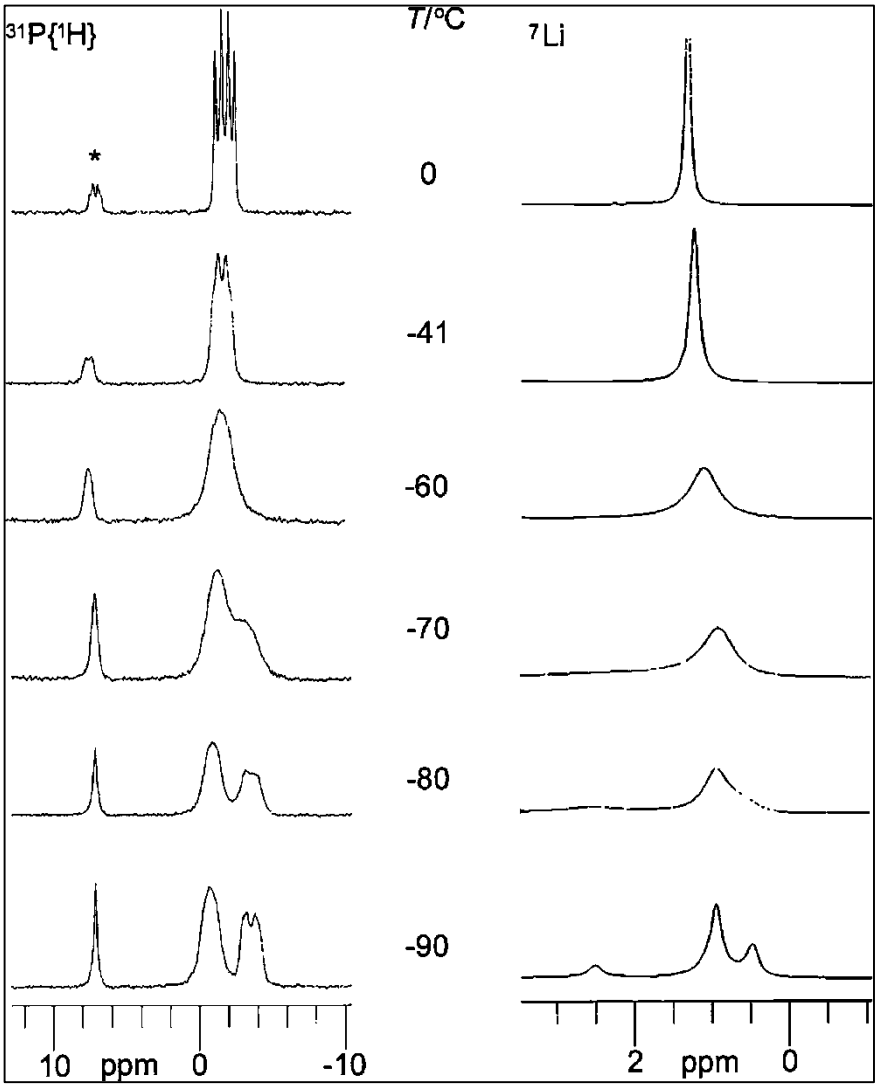

Figure 1.7: Variable-temperature $^{31}P\{^1H\}$ and ^7Li NMR spectra of **6** in d_8-toluene [* Free phosphine-borane $(Me_3Si)_2CHPMe_2(BH_3)$].

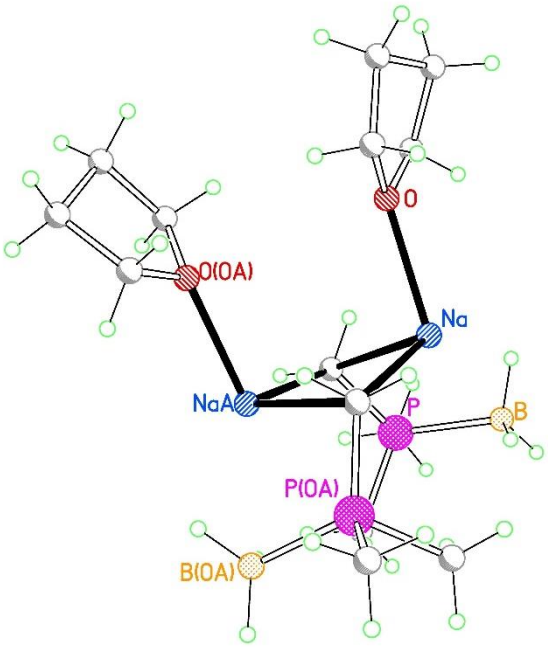

Figure 1.8. Repeat unit of polymeric **12**.

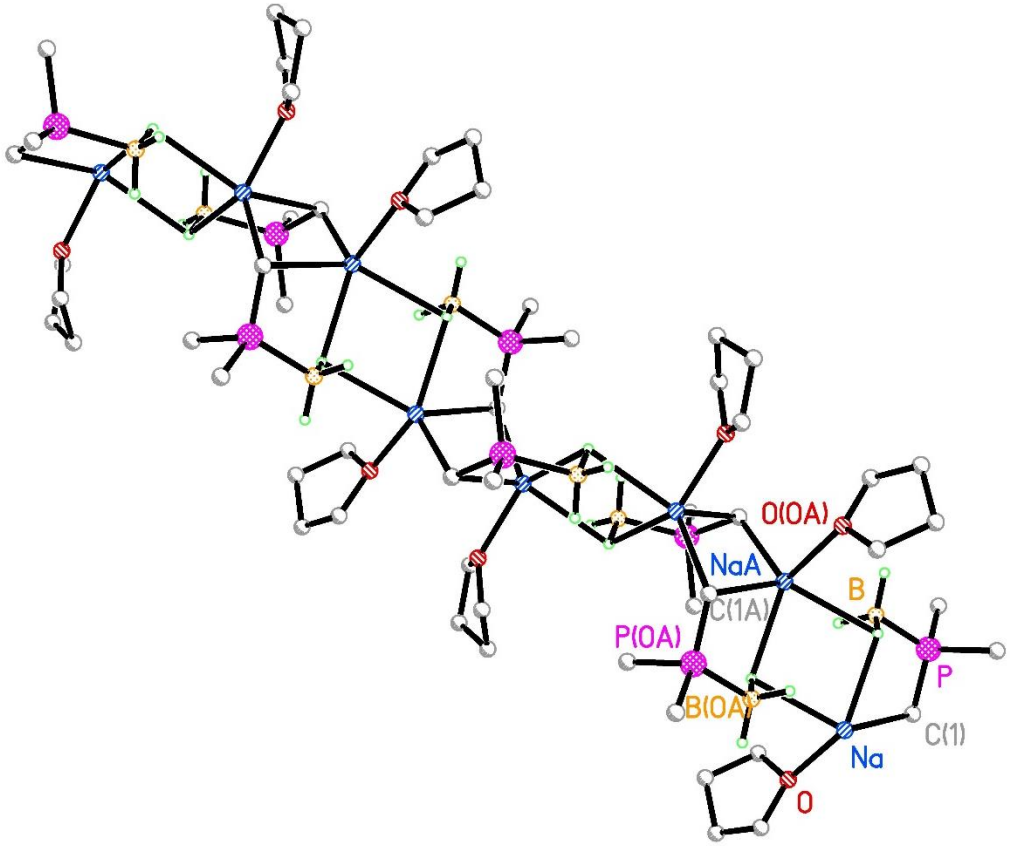

Figure 1.9: Polymer chain of **12** with H atoms (except those bound to B) omitted for clarity.

However, the lithium complex **11** undergoes a rapid reaction with silicone grease to give a cluster complex $\{Me_2P(BH_3)CHSiMe_2OLi\}_4Li_4(Et_2O)_{2.75}(THF)_{1.25}$ (**13**), which contains a siloxy-functionalised alkyl ligand (Scheme 1.8 and Figure 1.10). [40]

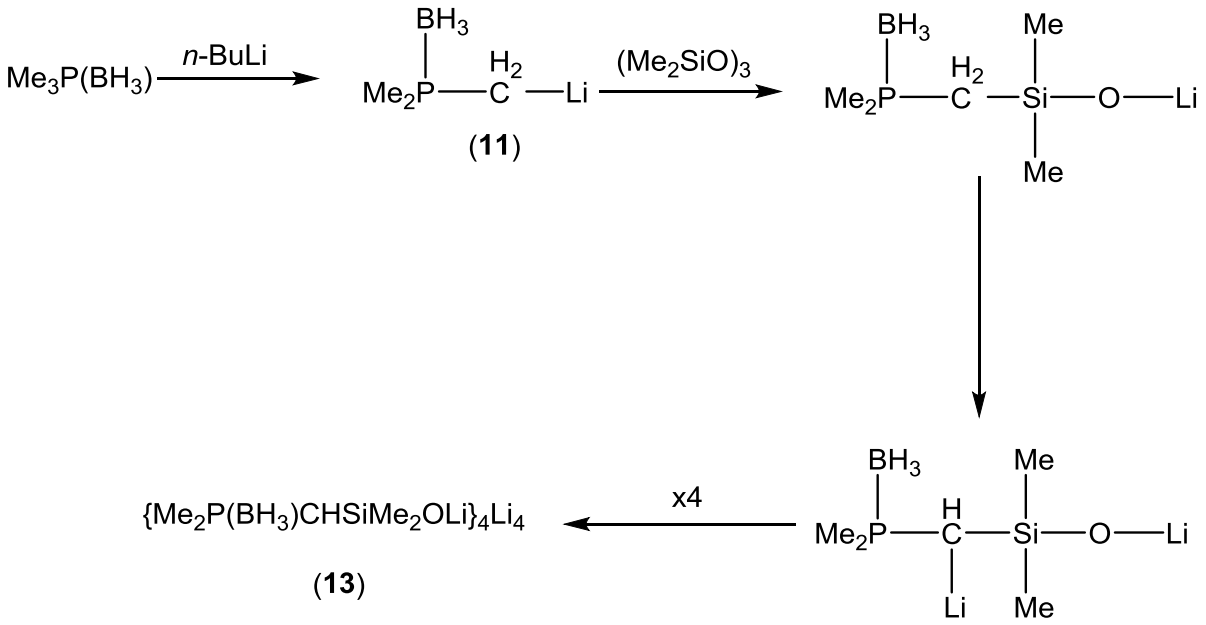

Scheme 1.8: Synthesis of the cluster complex $\{Me_2P(BH_3)CHSiMe_2OLi\}_4Li_4(Et_2O)_{2.75}(THF)_{1.25}$ (**13**).

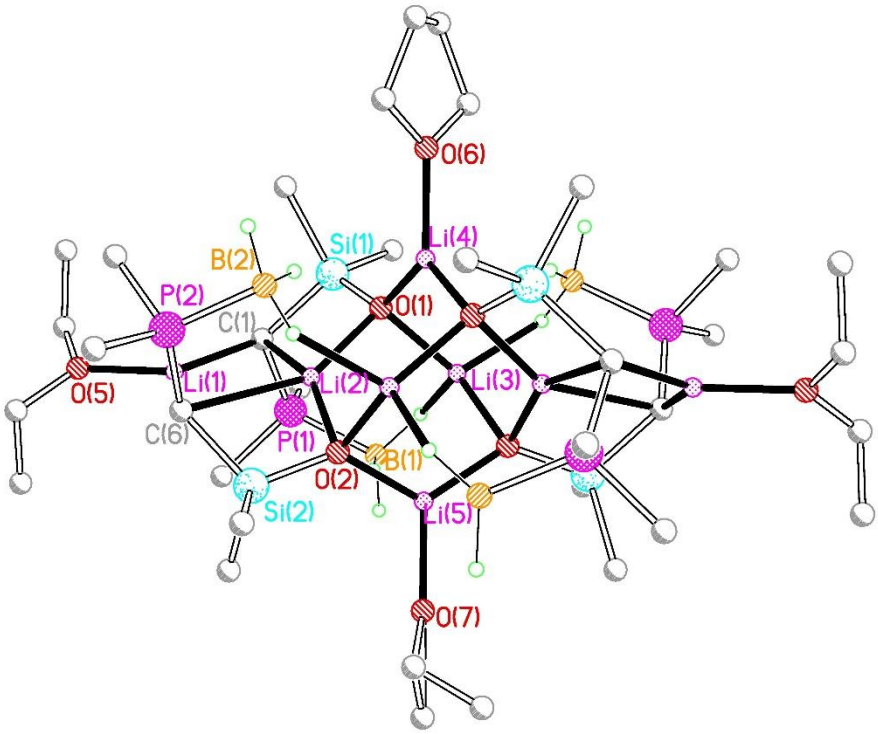

Figure 1.10. Crystal structure of **13** with all H atoms (except those bound to boron) and disorder components omitted for clarity.

The greater reactivity of the lithium salt of trimethylphosphine-borane towards the siloxanes in silicone grease compared to $[(Me_3Si)_2\{Me_2P(BH_3)\}C]^-$ may be due to an increase in negative charge on the carbanion centre from a decrease in negative hyperconjugation, which leads to an increase in nucleophilicity at the carbanion centre. Attempts to isolate the lithiated complex $\{Me_2P(BH)CH_2\}Li$ were unsuccessful.[40]

1.4.1 Heavier alkali metal complexes

In 2006, the Izod group set out to study how the size and polarisability of the metal cation can affect the solid and solution state structure of complexes of the heavier alkali metals with the sterically hindered phosphine-borane-stabilised carbanion $[(Me_3Si)_2\{Me_2P(BH_3)\}C]^-$.[16]

Reactions between $(Me_2Si)_2\{Me_2P(BH_3)\}CH$ and one equivalent of either MeNa or MeK in cold diethyl ether gave the compounds $[(Me_3Si)_2\{Me_2P(BH_3)\}C]M$ [M = Na (**14**), K (**15**)].[16] It was concluded that the solid state structures of these species varied significantly with increasing ionic radius of the metal. The sodium complex **14** crystallises as a one-

dimensional polymer, where each sodium ion is coordinated by the carbanion centre of one ligand and by an η^2-BH_3 group of an adjacent ligand, giving a pseudo-four-coordinate sodium ion with a distorted tetrahedral geometry (Figure 1.11). The potassium complex **15**, however, crystallises with a complex two-dimensional sheet structure, in which there are two distinct ligand environments. For both structures it was evident that M-BH_3 contacts appeared to be the essential feature along with contacts from the metal cation to the carbanion centre.[16]

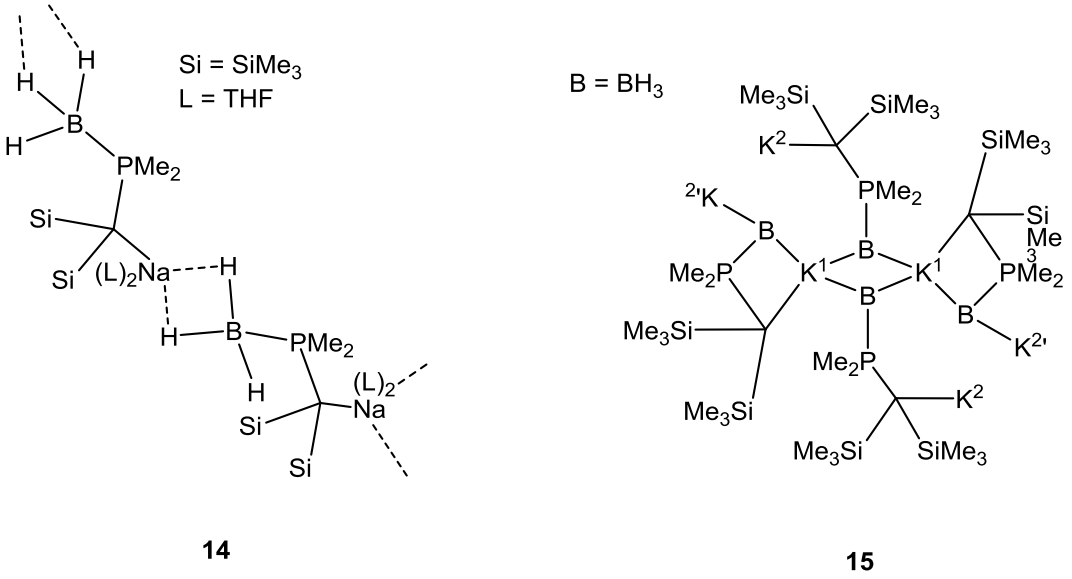

Figure 1.11: Structures of compounds **14** and **15**.

It is well known that co-ligands such as tmeda and pmdeta can affect the aggregation state and ligand binding modes of organo-alkali metal complexes. In 2007 Izod and co-workers investigated the effect of changing the co-ligand on the structure of the previously published potassium salt [[$(Me_3Si)_2${$Me_2P(BH_3)$}C]K] (**16**) and showed that the solid state structures of the potassium complexes **16**, [$(Me_3Si)_2${$Me_2P(BH_3)$}C]K$(THF)_{0.5}$] (**17**), [[$(Me_3Si)_2${$Me_2P(BH_3)$}C]K(tmeda)]$_2$ (**18**), [[$(Me_3Si)_2${$Me_2P(BH_3)$}C]K(pmdeta)]$_2$ (**19**) and [$(Me_3Si)_2${$Me_2P(BH_3)$}C][K(12-crown-4)]$_2$ (**20**) were defined by the respective co-ligand.[41] In each case, except **20**, B-H···K contacts seemed to be the important feature in the structures.

Izod and co-workers have also investigated the influence of aromatic ring substituents on the structures of phosphine-borane-stabilised carbanion complexes (Scheme 1.9).[42]

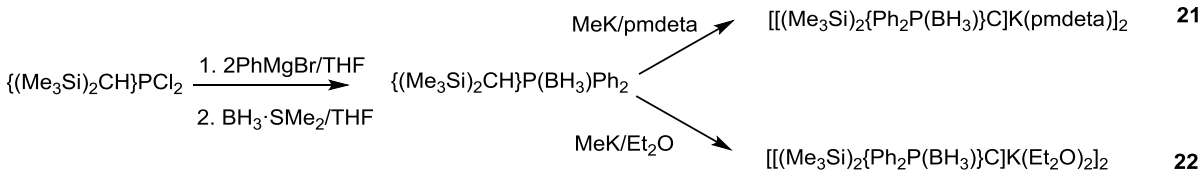

Scheme 1.9: Synthesis of compounds **21** and **22** with methylpotassium.

This study concluded that the phenyl substituents affected the coordination mode of the carbanion.[42] Compound **22** exhibited a preference for coordination through the BH_3 hydrogens with no metal-carbanion centre contact. In the presence of the weaker, monodentate diethyl ether ligands in **22** there was significant competition for coordination of the potassium cation by the aryl rings of the respective phosphine-borane-stabilised carbanion.[42]

1.4.2 Alkaline earth metal complexes

Since the early 20th century, when the first organomagnesium compound was published by Barbier and Grignard, these compounds have been widely exploited in synthetic organic and organometallic chemistry.[43] However, until recently there were still very few organo-heavier alkaline earth metal complexes and these were largely limited to complexes of cyclopentadienyl and substituted cyclopentadienyl ligands.[43, 44] This was thought to be due to difficulties with their synthesis and manipulation due to their large ionic radii and the highly polar nature of the M-C σ-bonds.[45-47] These properties tend to make compounds of this kind highly reactive, even towards the solvents they are prepared in. The first heavier alkaline earth metal analogue of a Grignard reagent was reported in 1905 by Beckmann,[48] but the first structurally characterised organocalcium, $\{(Me_3Si)_2CH\}_2Ca$(1,4-dioxane) was not reported until 1991 by Cloke and co-workers.[49] Significant progress has recently been made in this area, yielding an array of heavier alkaline earth metal organometallics including benzyl, acetylide, aryl, heteroatom-stabilised alkyl compounds, heterometallic species and organocalcium halides.[43]

Izod and co-workers have reported some new organo-heavier alkaline earth metal compounds using the ligand $[(Me_3Si)_2\{Me_2(BH_3)P\}C]^-$.[43] It was found that heavier alkaline earth metal complexes of the phosphine-borane-stabilised carbanion were easily accessible, however, their stabilities, especially towards THF were dependent on the nature of the cation. Treatment of AeI_2 [Ae = Mg, Ca, Sr, Ba] with two equivalents of $[(Me_3Si)_2\{Me_2(BH_3)P\}C]K$

in toluene or THF yielded the complexes $[(Me_3Si)_2\{Me_2(BH_3)P\}C]_2Ae(THF)_n$ [Ae = Mg (**23**), n = 0; Ca (**24**), n = 4; Sr (**25**), n = 5; Ba (**26**), n = 5] (Scheme 1.10).[43]

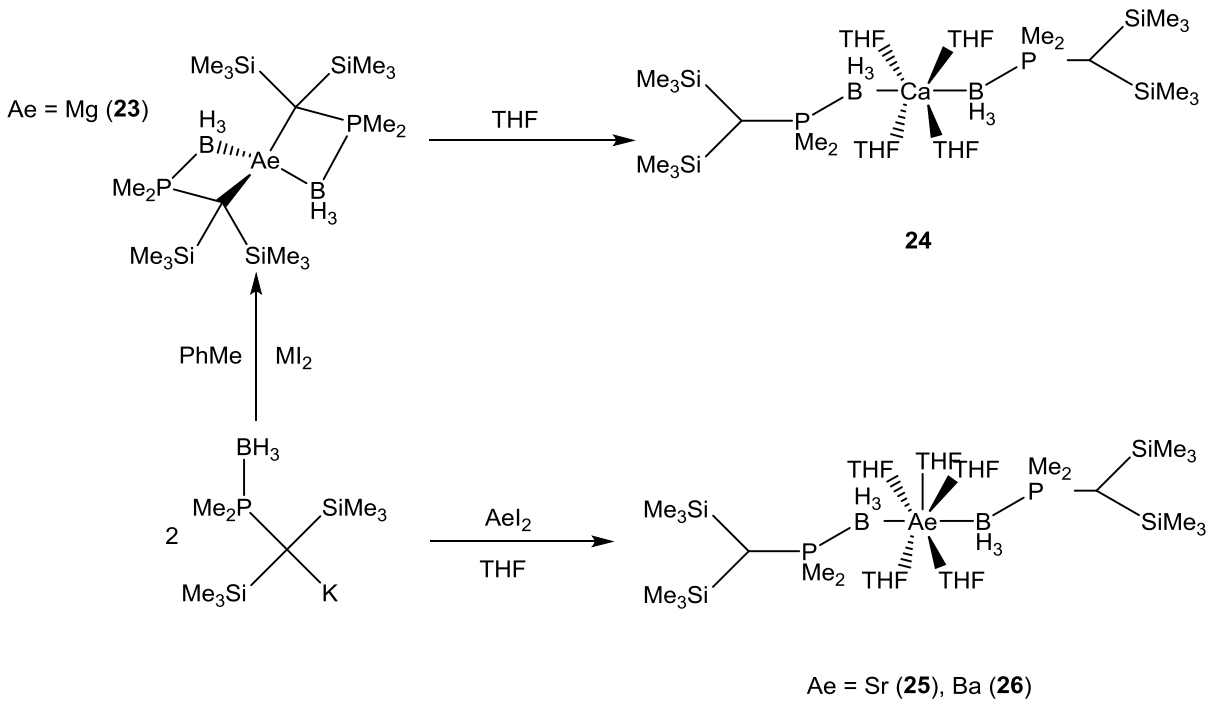

Scheme 1.10: Synthesis of group 2 complexes of a phosphine-borane-stabilised carbanion.

Compound **23** crystallises solvent-free, with chelating ligands, whereas **24**, **25** and **26** crystallise as THF solvates, where the phosphine-borane-stabilised carbanions bind to the metal centres via their borane H atoms only, such that there is no contact between the metal and the carbanion centres in these compounds.[43] Compounds **22** and **23** are stable indefinitely in THF, however, **23** and **24** react slowly with THF at room temperature to give the free phosphine-borane as the sole phosphorus-containing product.[43]

Westerhausen and co-workers, and Harder and co-workers have independently published the same example of a heavier alkaline earth metal complex of phosphine-borane-stabilised carbanion $[(THF)Ca\{CH(PPh_2BH_3)_2\}_2]$ (**27**).[50, 51] In compound **27** one anion exclusively binds through the hydrogen atoms of the BH_3 unit whereas the other ligand binds via the carbanion centre (Figure 1.12).[50, 51]

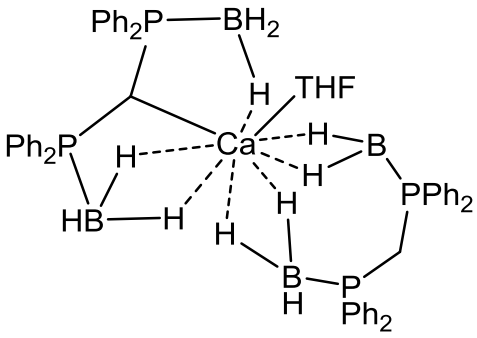

Figure 1.12: Structure of **27**.

In summary, it has been shown that phosphine-borane-stabilised carbanions adopt a wide variety of coordination modes in their complexes (Figure 1.13), including (i) a chelating mode (I), (ii) a number of bridging modes (II-V), and (iii) a terminal BH_3-donor mode (VI). The coordination mode adopted depends on the nature of the metal, the presence of co-ligands and on the steric and electronic properties of the substituents at the P and C centres.[41]

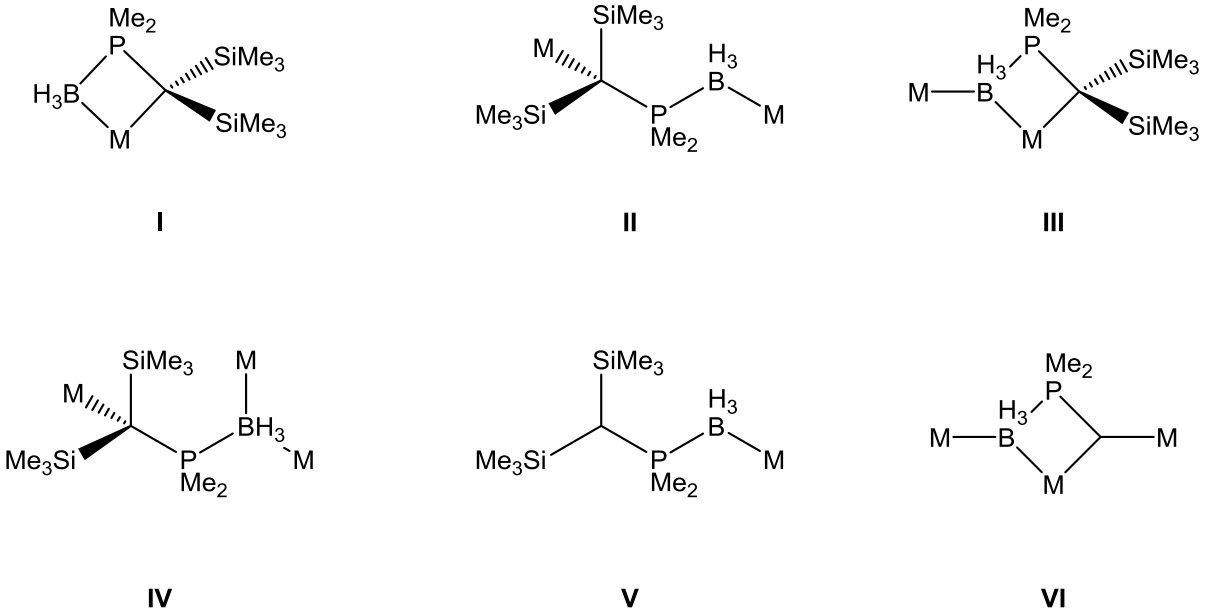

Figure 1.13: Range of ligand binding modes for phosphine-borane-stabilised carbanions.

1.5 Heavier group 14 carbene analogues [tetrylenes, R_2E (E = Ge, Sn, Pb)]

Carbene chemistry has seen a huge rise in popularity since Arduengo and co-workers reported the first stable *N*-heterocyclic carbene (NHC).[52] Over the last 3 decades there has been significant progress with regards to the synthesis of heavier group 14 carbene analogues (tetrylenes) R_2E (E = Ge, Sn or Pb).[53] The vast majority of these tetrylenes are stabilised by heteroatoms which are adjacent to the tetrel centre, for example the diaminotetrylenes, $(R_2N)_2E$, which are analogues of the Arduengo-type diaminocarbenes. Within these compounds the electron deficient tetrel centre is thermodynamically stabilised by efficient overlap between the heteroatom lone pairs and the vacant tetrylene p_π orbital (Figure 1.14).[32]

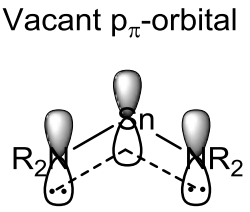

Figure 1.14: Molecular orbital diagram illustrating electron donation from the heteroatom into the vacant p-orbital of the Sn centre.

In comparison to diaminotetrylenes, there are far fewer examples of diorganotetrylenes i.e. diaryl- or dialkyl-tetrylenes.[54] This is due to the fact that thermodynamic stabilisation is absent in these compounds and therefore these compounds solely relied on kinetic stabilisation by sterically bulky groups.[55, 56] In the absence of sufficient steric bulk these species typically dimerise to the corresponding ditetrene analogues $R_2E{=}ER_2$ or else oligomerise to cyclic species (e.g. $[(Cy_2Sn)_6]$).

Lappert and co-workers reported the first dialkylstannylene $\{(Me_3Si)_2CH\}_2Sn$ (**28**) in the 1970s (Figure 1.15). Compound **28** exists as a monomeric structure in the gas phase, but dimerises to the corresponding distannene **28a** in the solid state; compounds **28** and **28a** are in a dynamic equilibrium in solution.[57]

With the ongoing investigation into the chemistry of phosphine-borane-stabilised carbanions Izod and co-workers have recently reported several examples of cyclic and acyclic dialkyltetrylenes which are stabilised by the presence of sterically demanding groups and by agostic-type B-H···E interactions (Figure 1.16).[54, 58] This stabilising effect means that monomeric dialkylstannylene and plumbylene compounds may be isolated even with relatively small alkyl substituents.[54, 58]

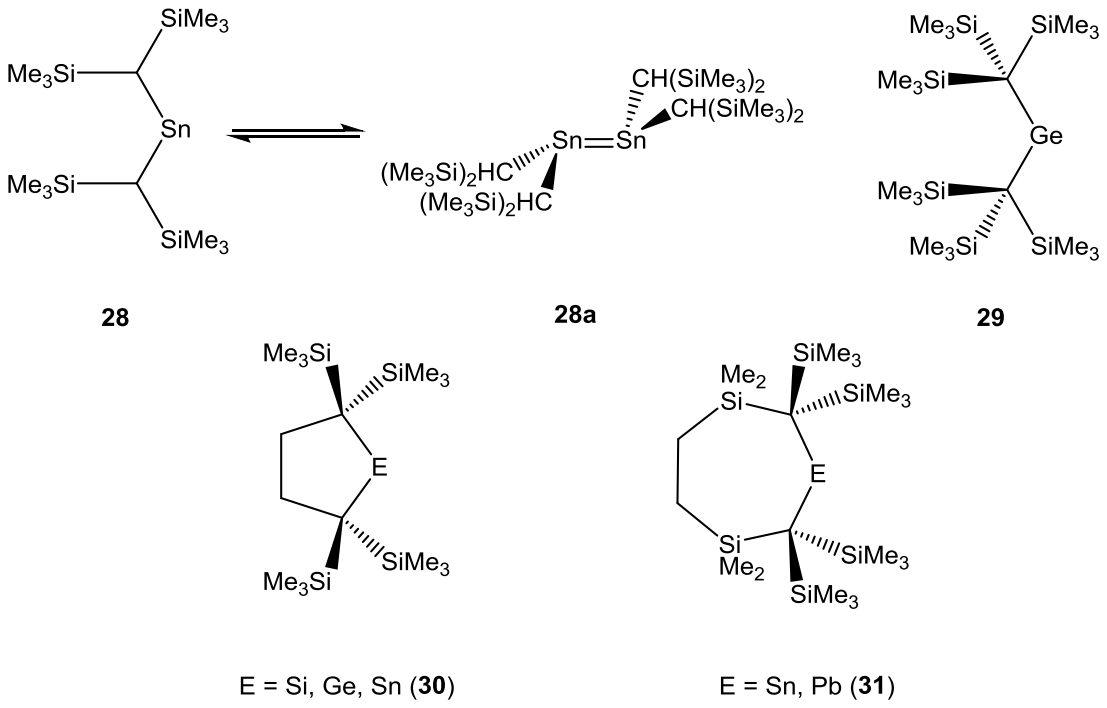

Figure 1.15: An array of cyclic and acyclic heavier group 14 tetrylenes.

The first and second examples of dialkylstannylenes shown to exist as a monomer in the solid state that did not contain heteroatoms were reported by Kira and co-workers in 1991 (**30**), and Eaborn, Smith and co-workers in 2000 (**31**), respectively (Figure 1.15).[59, 60]

The first example of a B-H···Sn agostic-type interaction involving low oxidation-state main group metal centres was reported by Izod and co-workers (**32**)[53] (Figure 1.16), which is similar to Kira's dialkylstannylene (**30**), however, **30** and **32** exhibit different structures and electronic behaviour.

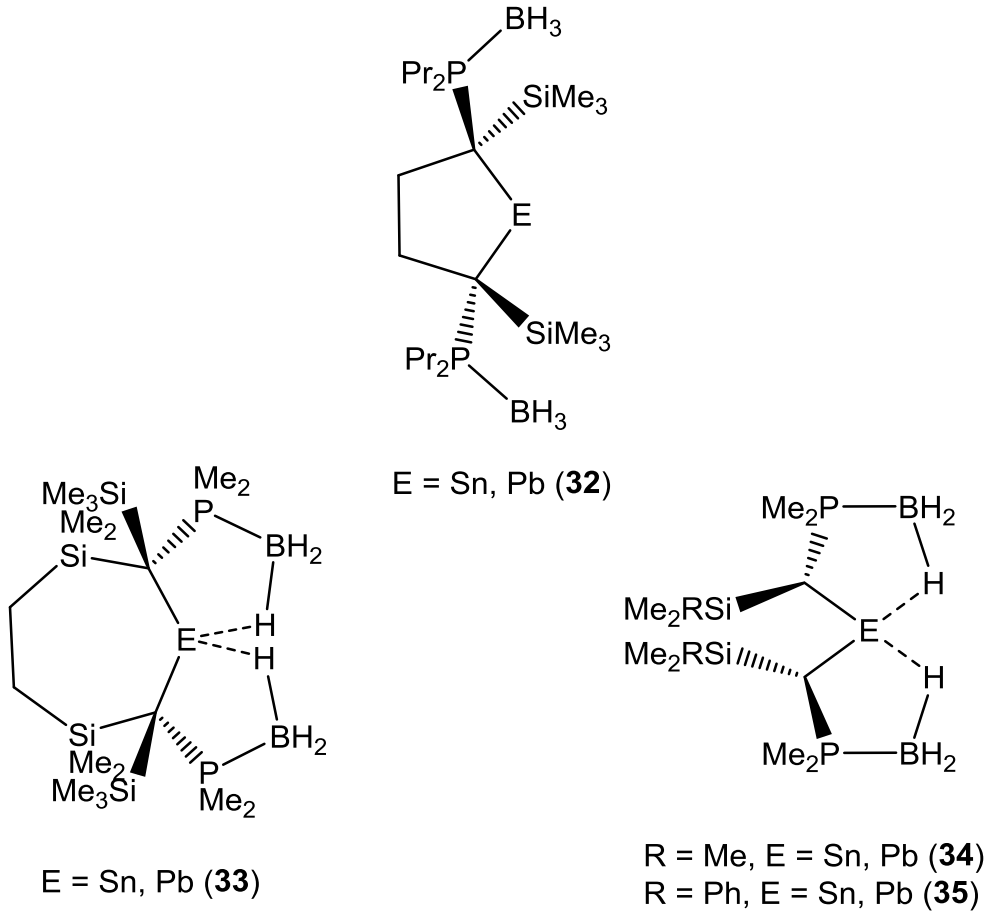

Figure 1.16: An array of cyclic and acyclic heavier group 14 phosphine-borane-stabilised tetrylenes.

Kira and co-workers noted difficulties in the isolation of **30** cleanly and in good yields, whereas compound **32** was isolated in very good yields and with high purity. Izod and co-workers attributed this characteristic to compound **32** exhibiting a higher charge delocalisation away from the carbanion centres, which may be due to the $R_2P(BH_3)$ group.[53] This would then decrease the nucleophilic character of the carbanion centres, reducing the tendency towards reduction of Sn(II) to elemental tin. Compound **32** was isolated as a 1:1 mixture of the *rac* and *meso* diastereomers (Figure 1.17).[53]

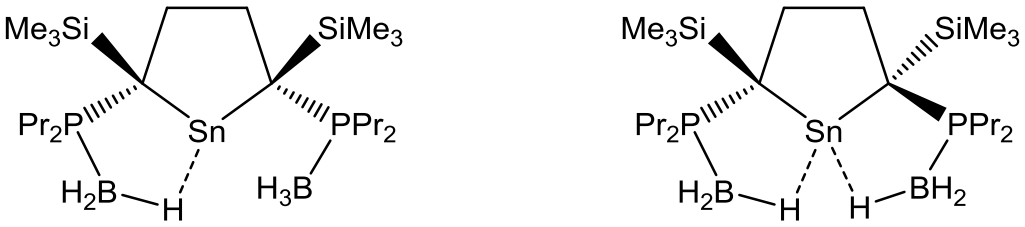

meso-**32** *rac*-**32**

Figure 1.17: Compound **32** existing as *rac* and *meso* diastereomers with B-H···Sn agostic-type interactions.

Spectroscopic studies of compound **32** clearly show that the solid state structure is persistent in solution, where the $^{119}Sn\{^{1}H\}$ NMR chemical shifts are more than 1500 ppm lower than the chemical shifts for compound **30**, indicating the B-H···Sn interactions have a remarkable influence on the electronic structure.[53] Multi-element NMR spectroscopy indicated that *meso*-**32** exhibited dynamic behaviour which was clearly seen in the variable-temperature $^{31}P\{^{1}H\}$ and $^{11}B\{^{1}H\}$ NMR spectra and which was attributed to the competitive binding of the two BH_3 units to the Sn(II) centre (Figure 1.18) as well as restricted rotation about the highly sterically hindered P-C bond of the phosphine-borane ligands (Figure 1.19).[53]

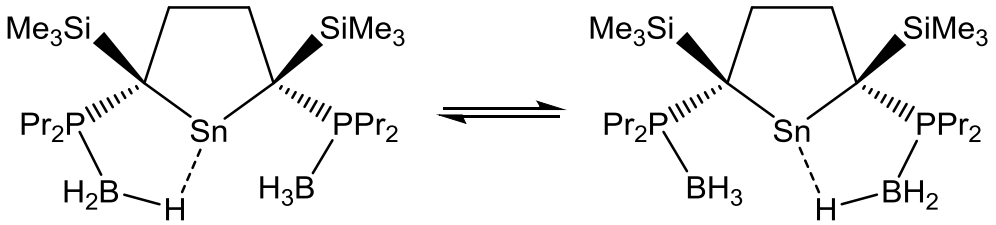

meso-**32**

Figure 1.18: Competition of the binding of two BH_3 units to the Sn(II) centre.

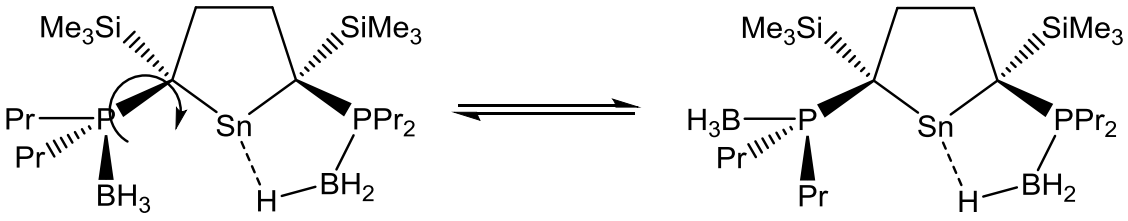

meso-**32**

Figure 1.19: Restricted rotation around the highly hindered P-C bond.

The first acyclic phosphine-borane-substituted dialkylstannylenes (**34** and **35**) were reported by Izod and co-workers in 2009 (Figure 1.16).[54] Compounds **34** and **35** were isolated as the *rac* diastereomers and $^{31}P\{^{1}H\}$ NMR spectra showed no evidence for the formation of the *meso* diastereomer, which is different compared to compound **32** where both the *rac* and *meso* diastereomers are formed.[53, 54] Izod and co-workers proposed that the formation of only the *rac* isomer was due to the formation of two B-H agostic-type interactions being much more favourable than in the *meso* diastereomer, where only one such type of interaction is seen.[54] There was also no evidence to suggest that compounds **34** and **35** dimerise in solution and DFT studies show that dimerisation is significantly disfavoured.[54]

This chapter has provided a brief overview of the chemistry involved in phosphine-boranes, phosphine-borane-stabilised carbanions of group 1, 2 and heavier group 14, and organometallics, with a particular emphasis on the different structural motifs. It is clear that information regarding α-metalated phosphine-boranes is scarce, compared to their Si-substituted analogues. The work presented in this thesis is the synthesis of an array of α-metalated phosphine-boranes and phosphine-borane-substituted heavier group 14 carbene analogues (Sn) with either a flexible backbone or a rigid linker, with particular interest in both the solid and solution-state structures of these complexes. These investigations are vital in order to focus on the extent of the stabilisation effects of the agostic interactions between the heavier group 14 cation and the hydrogen atoms on the BH_3 unit. Also whether the incorporation of a rigid linker yields differences in the solid and solution-state structures compared to their flexible linker analogues.

1.6 References

1. W. Schlenk, A. J, A. Michael and A. Thal, *Ber. Dtsch. Chem. Ges.*, 1914, **47**, 473.
2. W. Schlenk and J. Holtz, *Ber. Dtsch. Chem. Ges.*, 1917, **50**, 262.
3. J. L. Wardell, *Comprehensive Organometallic Chemistry I*, Vol. 1, Eds: E. Abel, F. G. A. Stone, G. Wilkinson, Chapt. 2, Elsevier, 1982, pp 48-50.
4. E. Weiss, *Angew. Chem. Int. Ed. Engl.*, 1993, **32**, 1501
5. M. A. Beswick and D. S. Wright, *Comprehensive Organometalic Chemistry II*, Vol. 1, Eds: E. Abel, F. G. A. Stone, G. Wilkinson, Chapt. 1, Pegamon, Oxford, 1995, pp 1-34.
6. A. Maercker and W. Demuth, *Liebigs Ann. Chem.*, 1977, 1909.
7. L. Horner, H. Hoffman, H. G. Wippel and G. Klahre, *Chem. Ber.*, 1958, **91**, 61.
8. L. Horner, H. Hoffman, H. G. Wippel and G. Klahre, *Chem. Ber.*, 1959, **92**, 2499.
9. W. S. Wadsworth and W. D. Emmons, *J. Am. Chem. Soc.*, 1961, **83**, 1733.
10. K. Izod, *Coord. Chem. Rev.*, 2002, **227**, 153-173.
11. W. Clegg, S. Doherty, K. Izod and P. O'Shaughnessy, *Chem. Commun.*, 1988, 1129.
12. H. H. Karsch, K. Zellner, P. Mikulcik, J. Lachmann and G. Muller, *Organometallics*, 1990, **9**, 190-194.
13. T. Imamoto, *Pure Appl. Chem.*, 1993, **65**, 655-660.
14. A. R. Muci, K. R. Campos and D. A. Evans, *J. Am. Chem. Soc.*, 1995, **117**, 9075-9076.
15. A. Staubitz, A. P. M. Robertson, M. E. Sloan and I. Manners, *Chem. Rev.*, 2010, **110**, 4023-4078.
16. K. Izod, C. Wills, W. Clegg and R. W. Harrington, *Organometallics*, 2006, **25**, 5326-5332.
17. A. Besson, *Comptes Rendus Academie des Sciences*, 1890, **110**, 516.
18. E. Gamble and P. Gilmont, *J. Am. Chem. Soc*, 1940, **62**, 717.
19. A. Stock, *Ber.*, 1923, **56B**.
20. R. W. Rudolph, R. W. Parry and C. F. Farran, *Inorg. Chem.*, 1966, **5**, 723-726.
21. A. B. Burg and R. I. Wagner, *J. Am. Chem. Soc.*, 1953, **75**, 3872-3877.
22. T. Imamoto, T. Kusumoto, N. Suzuki and K. Sato, *J. Am. Chem. Soc.*, 1985, **107**, 5301-5303.
23. J. M. Brunel, B. Faure and M. Maffei, *Coord. Chem. Rev.*, 1998, **178**, 665-698.
24. A. B. Burg and P. J. Slota, *J. Am. Chem. Soc.*, 1960, **82**, 2145-2148.
25. J. McNulty and Y. H. Zhou, *Tetrahedron Lett.*, 2004, **45**, 407-409.

26. T. Imamoto, T. Oshiki, T. Onozawa, T. Kusumoto and K. Sato, *J. Am. Chem. Soc.*, 1990, **112**, 5244-5252.
27. H. Brisset, Y. Gourdel, P. Pellon and M. L. Corre, *Tetrahedron Lett.*, 1997, 4523.
28. L. McKinstry, J. J. Overberg, C. Soubra-Ghaoui, D. S. Walsh, K. A. Robins, T. T. Toto and J. L. Toto, *J. Org. Chem.*, 2000, **65**, 2261-2263.
29. T. Imamoto and T. Oshiki, *Tetrahedron Lett.*, 1989, **30**, 383-384.
30. L. Mckinstry and T. Livinghouse, *Tetrahedron*, 1995, **51**, 7655-7666.
31. H. Schmidbaur, E. Weiss and B. Zimmergasser, *Angew. Chem. Int. Ed. Engl.*, 1979, **18**, 782-784.
32. K. Izod, W. McFarlane, B. V. Tyson, W. Clegg and R. W. Harrington, *Chem. Commun.*, 2004, 570-571.
33. X. M. Sun, K. Manabe, W. W. L. Lam, N. Shiraishi, J. Kobayashi, M. Shiro, H. Utsumi and S. Kobayashi, *Chem. Euro. J.*, 2004, **11**, 361-368.
34. K. Izod, C. Wills, W. Clegg and R. W. Harrington, *Organometallics*, 2006, **25**, 38-40.
35. C. Eaborn, P. B. Hitchcock, J. D. Smith and A. C. Sullivan, *J. Chem. Soc. Chem. Commun.*, 1983, 827-828.
36. A. G. Avent, C. Eaborn, P. B. Hitchcock, G. A. Lawless, P. D. Lickiss, M. Mallien, J. D. Smith, A. D. Webb and B. Wrackmeyer, *J. Chem. Soc. Dalton Trans.*, 1993, 3259-3264.
37. N. H. Buttrus, C. Eaborn, P. B. Hitchcock, J. D. Smith, J. G. Stamper and A. C. Sullivan, *J. Chem. Soc. Chem. Commun.*, 1986, 969-970.
38. C. Eaborn, Z. R. Lu, P. B. Hitchcock and J. D. Smith, *Organometallics*, 1996, **15**, 1651-1655.
39. U. J. Bildmann and G. Muller, *Organometallics*, 2001, **20**, 1689-1691.
40. K. Izod, C. Wills, W. Clegg and R. W. Harrington, *Organometallics*, 2007, **26**, 2861-2866.
41. K. Izod, C. Wills, W. Clegg and R. W. Harrington, *Dalton Trans.*, 2007, 3669-3675.
42. K. Izod, C. Wills, W. Clegg and R. W. Harrington, *J. Organomet. Chem.*, 2007, **692**, 5060-5064.
43. K. Izod, C. Wills, W. Clegg and R. W. Harrington, *Inorg. Chem.*, 2007, **46**, 4320-4325.
44. T. P. Hanusa, *Chem. Rev.*, 1993, **93**, 1023-1036.
45. J. S. Alexander and K. Ruhlandt-Senge, *Eur. J. Inorg. Chem.*, 2002, 2761-2774.
46. T. P. Hanusa, *Coord. Chem. Rev.*, 2000, **210**, 329-367.
47. M. Westerhausen, *Angew. Chem. Int. Ed.*, 2001, **40**, 2975-2977.

48. E. Beckmann, *Chem. Ber.*, 1905, 904.
49. F. G. N. Cloke, P. B. Hitchcock, M. F. Lappert, G. A. Lawless and B. Royo, *J Chem. Soc. Chem. Commun.*, 1991, 724-726.
50. J. Langer, K. Wimmer, H. Goerls and M. Westerhausen, *Dalton Trans.*, 2009, 2951-2957.
51. L. Orzechowski, G. Jansen, M. Lutz and S. Harder, *Dalton Trans.*, 2009, 2958-2964.
52. F. E. Hahn and M. C. Jahnke, *Angew. Chem. Int. Ed.*, 2008, **47**, 3122-3172.
53. K. Izod, W. McFarlane, B. V. Tyson, I. Carr, W. Clegg and R. W. Harrington, *Organometallics*, 2006, **25**, 1135-1143.
54. K. Izod, C. Wills, W. Clegg and R. W. Harrington, *Organometallics*, 2009, **28**, 5661-5668.
55. P. J. Davidson and M. F. Lappert, *J. Chem. Soc. Chem. Commun.*, 1973, 317-317.
56. D. E. Goldberg, D. H. Harris, M. F. Lappert and K. M. Thomas, *J. Chem. Soc. Chem. Commun.*, 1976, 261-262.
57. D. E. Goldberg, D. H. Harris, M. F. Lappert and K. M. Thomas, *J. Chem. Soc. Chem. Commun.*, 1976, 261-262.
58. C. Wills, K. Izod, W. Clegg and R. W. Harrington, *Dalton Trans.*, 2010, **39**, 2379-2384.
59. M. Kira, R. Yauchibara, R. Hirano, C. Kabuto and H. Sakurai, *J. Am. Chem. Soc.*, 1991, **113**, 7785-7787.
60. C. Eaborn, M. S. Hill, P. B. Hitchcock, D. Patel, J. D. Smith and S. B. Zhang, *Organometallics*, 2000, **19**, 49-53.

Chapter 2. Synthesis of phosphine-borane precursors

2.1 Introduction

Phosphine-borane adducts are important intermediates used to synthesise polyphosphines, such as the chiral diphosphine DIPAMP (Scheme 2.1).[1, 2]

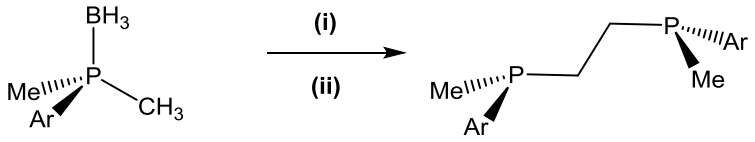

Scheme 2.1: Synthesis of DIPAMP using a phosphine-borane-stabilised carbanion. Reaction conditions: i) ^{s}BuLi{(-)-sparteine}, ii) $Cu(OPiv)_2$ and Et_2NH.

An array of phosphine-borane adducts and phosphine-borane-stabilised carbanions has been synthesised and characterised over the past century (see sections 1.3.2 and 1.4 for more detail). Despite the widespread use of phosphine-borane-stabilised carbanions, little is known about their reactivity and structure. In order to investigate the incorporation of a rigid backbone linker and its effect on the structure of heavier group 14 tetrylenes, an array of mono- and bis(phosphine-boranes) with flexible and rigid linkers has been prepared, these compounds are described below. The compounds can be classified into 4 groups. Group A includes the linear bis(phosphine-boranes) $[Me_2P(BH_3)CH_2SiMe_2CH_2]_2$ (**37**) and $[Ph_2P(BH_3)CH_2SiMe_2CH_2]_2$ (**40**), group B includes the bis(phosphine-boranes) with rigid spacers 1,2-$C_6H_4\{CH_2PR_2(BH_3)\}_2$ [R = ^{i}Pr (**44**), Ph (**45**) and Cy (**46**)], group C includes the mono(phosphine-boranes) $C_6H_5\{CH_2PR_2(BH_3)\}$ [R = ^{i}Pr (**47**), Ph (**48**) and Cy (**49**)] and group D includes the linear phosphine-boranes $C_6H_5\{CH_2SiMe_3PCy_2(BH_3)\}$ (**50**) and $\{CH_2CH_2PCy_2(BH_3)\}_2$ (**51**).

2.2 Synthesis and characterisation of Group A precursors [linear bis(phosphine-boranes)]

2.2.1 $Me_3P(BH_3)$ (36)

There are several methods that have been published which describe the synthesis of this precursor, all of which include the reaction of Me_3P with one of the following: i) $NaBH_4$ activated with CO_2; ii) diborane; or iii) with the borane adduct $BH_3{\cdot}THF$. Work reported in this thesis, however, uses the adduct $BH_3{\cdot}SMe_2$ rather than the THF adduct, due to its availability and low cost.

Reaction of one equivalent of $BH_3{\cdot}SMe_2$ with one equivalent of Me_3P gives the air stable colourless solid **36** in quantitative yield (Scheme 2.2).

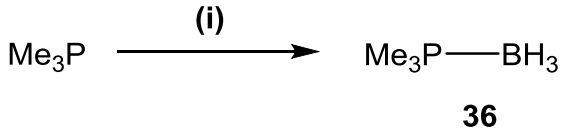

Scheme 2.2. Synthesis of **36**. Reagents and conditions: i) $BH_3{\cdot}SMe_2$, r.t., Et_2O, 1 h.

The preparation of **36** and its α-metalated species must be carried out in a grease-free Schlenk. If the metalation of **36** is carried out in normal silicone-greased Schlenks, an unexpected reaction of the simple phosphine-borane-stabilised carbanion occurs with the siloxanes present within the silicone grease to give an alkyl siloxide cluster (Scheme 2.3).[3] It is therefore imperative to exclude silicone grease during the synthesis of **36**.

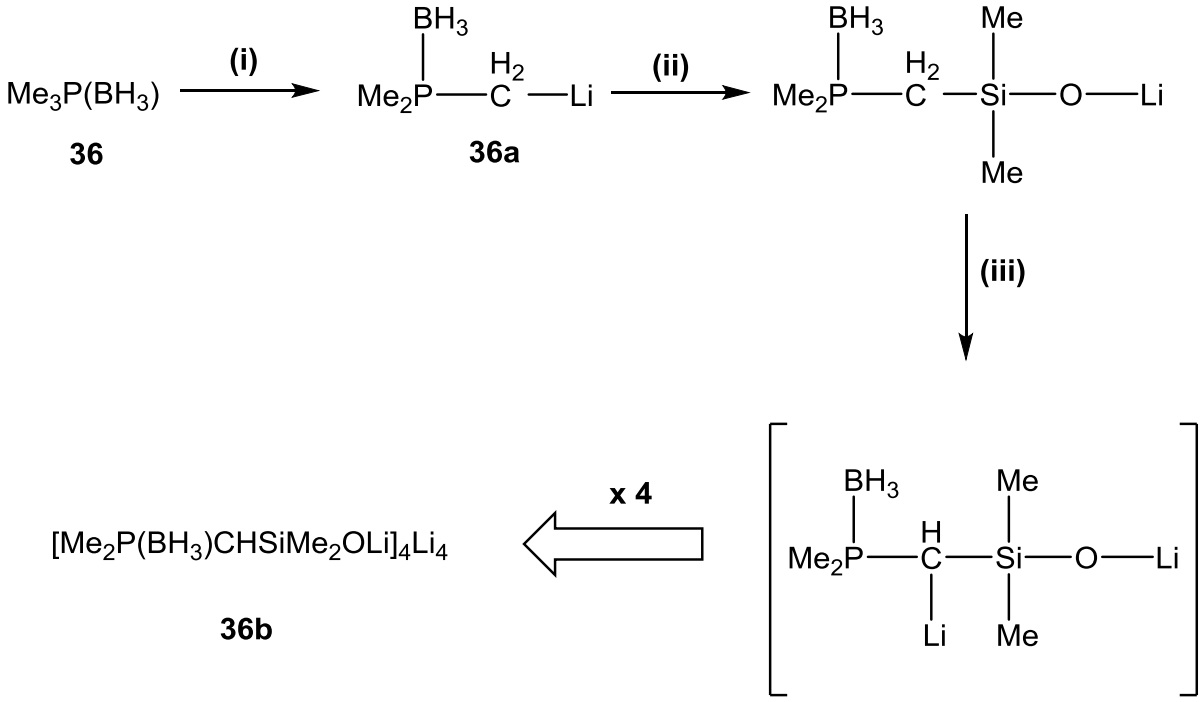

Scheme 2.3. Synthesis of an unusual complex containing $[Me_2P(BH_3)CHSiMe_2O]^{2-}$ siloxy-functionalised carbanions formed via the reaction between intermediate **36a** and silicone grease. Reagents and conditions: i) ^{n}BuLi, THF, r.t., 2 h. ii) Silicone grease, Et_2O, r.t., 2 h. iii) + **36a, - 36**.

The product **36b** crystallises as a cluster containing siloxy-functionalised carbanions (Figure 2.1). Izod and co-workers have suggested that the reaction with the silicon grease could be due to increased negative charge around the carbanion centre, due to a decrease in delocalisation around the molecule compared to Si-substituted analogues such as $[Me_3SiCHP(BH_3)Me_2]^{-}$. This therefore, increases the nucleophilicity of the carbanion centre and so it is more reactive towards silicone grease than its phenyl-substituted analogue **38**.

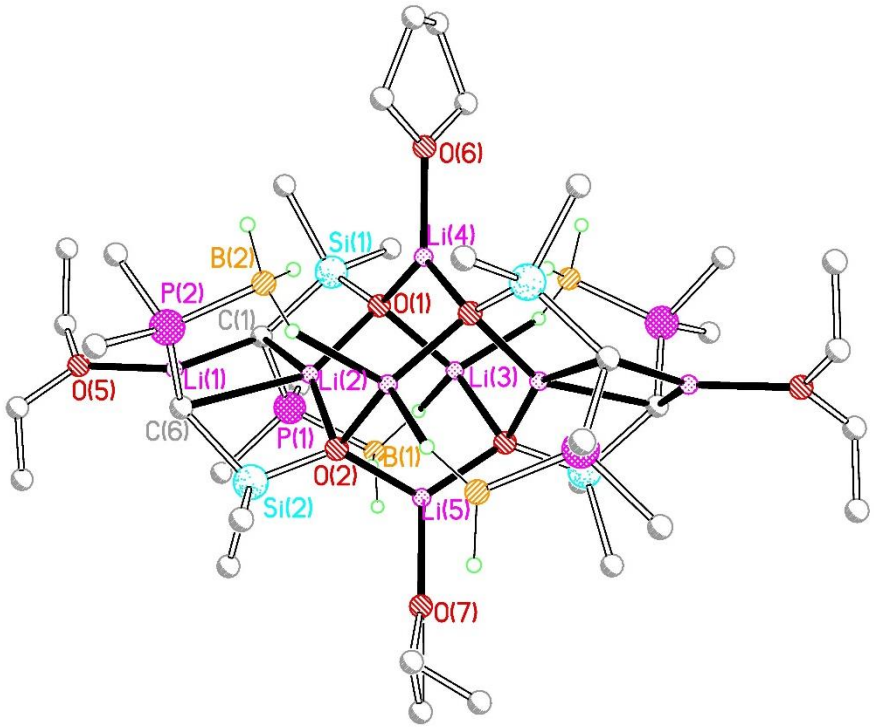

Figure 2.1. Molecular structure of one independent molecule of **36b** with all H atoms (except for those bound to boron) omitted for clarity.

2.2.2 $[Me_2P(BH_3)CH_2SiMe_2CH_2]_2$ (37)

One equivalent of ^{n}BuLi was added to **36** and the resulting mixture was added *in situ* to half an equivalent of 1,2-bis(chlorodimethylsilyl)ethane to give the linear bis(phosphine-borane) **37** in very good yield (Scheme 2.4).

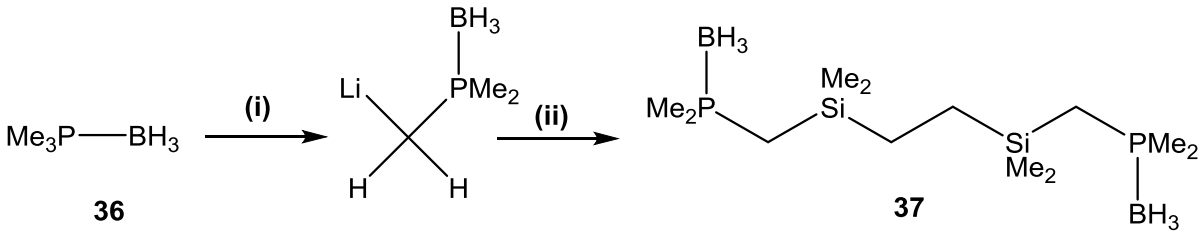

36 **37**

Scheme 2.4. Metalation of **36** and synthesis of **37**. Reagents and conditions: i) ^{n}BuLi, THF, r.t., 1 h. ii) $ClSiMe_2CH_2CH_2SiMe_2Cl$, THF, r.t., 1 h.

Compound **37** is isolated as an essentially pure compound but can be crystallised from hot methylcyclohexane to form colourless single crystals suitable for X-ray crystallography. The structure of **37** is of interest for comparison of its bond lengths and angles with α-

metalated phosphine-borane analogues (see Chapter 3.2 for further information). Below are selected bond lengths and angles for **37** (Table 2.1) along with its molecular structure (Figure 2.2).

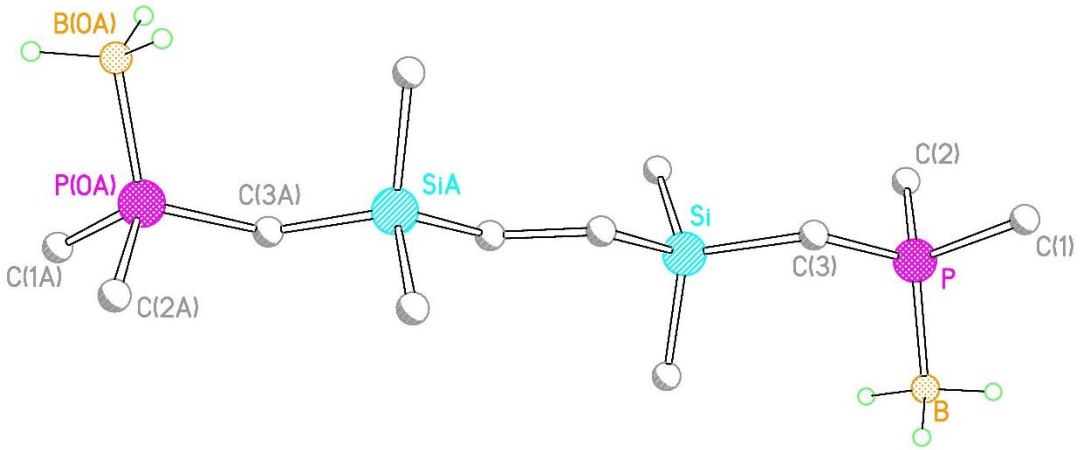

Figure 2.2. Molecular structure of **37** with H atoms (except for those bound to boron) omitted for clarity.

P-B	1.917(4)	B-P-C(3)	115.5(1)
P-C(3)	1.800(2)	B(0A)-P(0A)-C(3A)	115.5(1)
C(3)-Si	1.892(2)		
P-C	1.811(2)		
P-C(2)	1.807(2)		

Table 2.1. Selected bond lengths (Å) and angles (°) for **37**.

The $^{1}H\{^{11}B\}$, $^{11}B\{^{1}H\}$, $^{13}C\{^{1}H\}$ and $^{31}P\{^{1}H\}$ NMR spectra of compound **37** are as expected. In $CDCl_3$ the $^{1}H\{^{11}B\}$ NMR spectrum of **37** contains a multiplet at 0.5 ppm which corresponds to the two BH_3 moieties and the CH_2CH_2 backbone, and a broad singlet at 0.51 ppm due to the CH_2P protons. The $^{11}B\{^{1}H\}$ NMR spectrum contains a doublet at -37.5 ppm and the $^{31}P\{^{1}H\}$ NMR spectrum contains a quartet at 3.4 ppm (J_{PB} = 58.8 Hz).

The solid state structure of compound **37** is as expected. The C-Si and P-B distances [C(3)-Si 1.892(2) and B-P 1.917(4) Å] are typical of such compounds, [3-9] whereas the P-C

distance [P-C(3) 1.800(2) Å] is somewhat shorter than the corresponding P-C distance [P-C 1.826(2) Å] in the previously reported linear bis(phosphine-borane) $[Me_2P(BH_3)CH(SiMe_3)SiMe_2CH_2]_2$ (**38**) (Figure 2.3).

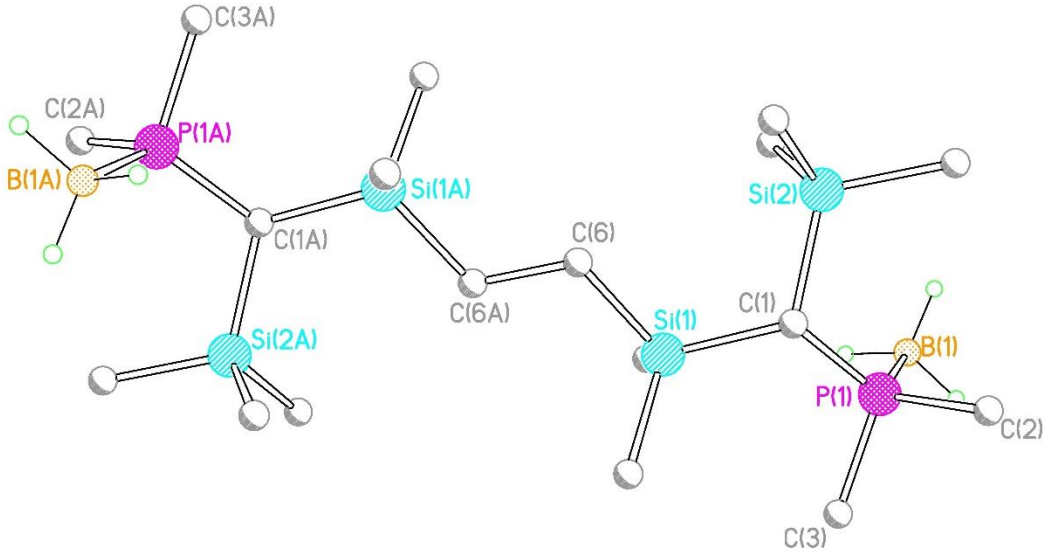

Figure 2.3. Molecular structure of **38** with H atoms (except for those bound to boron) omitted for clarity.[10]

2.2.3 $Ph_2(Me)P(BH_3)$ (39)

Compound **39** was prepared by a modified literature procedure where the phosphine-borane was made via the chlorodiphenylphosphine rather than diphenylmethylphosphine.[11] Chlorodiphenylphosphine was alkylated using methylmagnesium bromide and was then boronated using $BH_3{\cdot}SMe_2$ to give **39** as a viscous colourless liquid in excellent yield (Scheme 2.5).

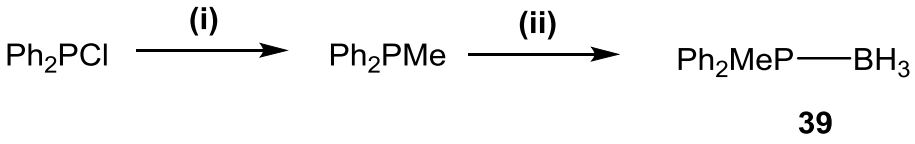

Scheme 2.5. Synthesis of **39**. Reagents and conditions: i) MeMgBr, THF, 0 °C, 1 h. ii) $BH_3{\cdot}SMe_2$, THF, r.t., 16 h.

The ^1H, $^{13}C\{^1H\}$, $^{11}B\{^1H\}$ and $^{31}P\{^1H\}$ NMR data for compound **39** correspond to the data reported previously.[11]

2.2.4 $[Ph_2P(BH_3)CH_2SiMe_2CH_2]_2$ (40)

One equivalent of ^{n}BuLi was added to **39**, resulting in a dark orange solution. This solution was added *in situ* to 0.5 equivalent of 1,2-bis(chlorodimethylsilyl)ethane. Recrystallisation from hot methylcyclohexane/THF gave **40** as a colourless crystalline solid in good yield (Scheme 2.6).

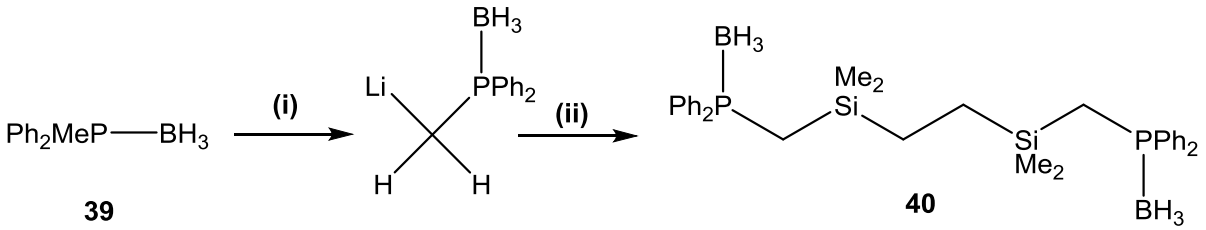

39 **40**

Scheme 2.6. Synthesis of **40**. Reagents and conditions: i) ^{n}BuLi, THF, r.t., 1 h. ii) $ClSiMe_2CH_2CH_2SiMe_2Cl$, THF, r.t., 1 h.

The $^{1}H\{^{11}B\}$, $^{11}B\{^{1}H\}$, $^{13}C\{^{1}H\}$ and $^{31}P\{^{1}H\}$ NMR spectra of compound **40** are as expected. In $CDCl_3$ the $^{1}H\{^{11}B\}$ NMR spectrum of **40** contains a doublet at 1.04 ppm which corresponds to the two BH_3 moieties, a doublet at 0.30 ppm (J_{PH} = 5.00 Hz) due to the CH_2P protons, and, a complex multiplet between 7.39 and 7.44 ppm due to the aromatic protons. The $^{11}B\{^{1}H\}$ NMR spectrum contains a broad peak at -38.9 ppm on which coupling to ^{31}P is not resolved and the $^{31}P\{^{1}H\}$ NMR spectrum contains a quartet at 13.5 ppm (J_{PB} = 69.5 Hz).

It is notable that throughout these investigations with phosphine-boranes, the $^{31}P\{^{1}H\}$ NMR spectra do not exhibit a typical quartet (Figure 2.4). The spin of ^{11}B is I = 3/2 and therefore, the ^{31}P NMR spectrum of a phosphine-borane obtained should exhibit a quartet with line ratios of 1:1:1:1.[12] However, the $^{31}P\{^{1}H\}$ NMR spectra recorded during these investigations show an increase in line height for the two middle peaks of the quartet. This increase in height is due to low abundant ^{10}B with a spin of I = 3. With ^{10}B, the septet produced by this nucleus lies underneath the original ^{11}B quartet, and so increases the two middle signals of the quartet to give the appearance of a Pascals quartet. There is also a significant amount of line broadening of the $^{31}P\{^{1}H\}$ NMR spectra of phosphine-borane compounds due to ^{11}B and ^{10}B possessing a relatively large quadrupole moment (4.059 and 8.459×10^{-30} Q m^2, respectively).[12]

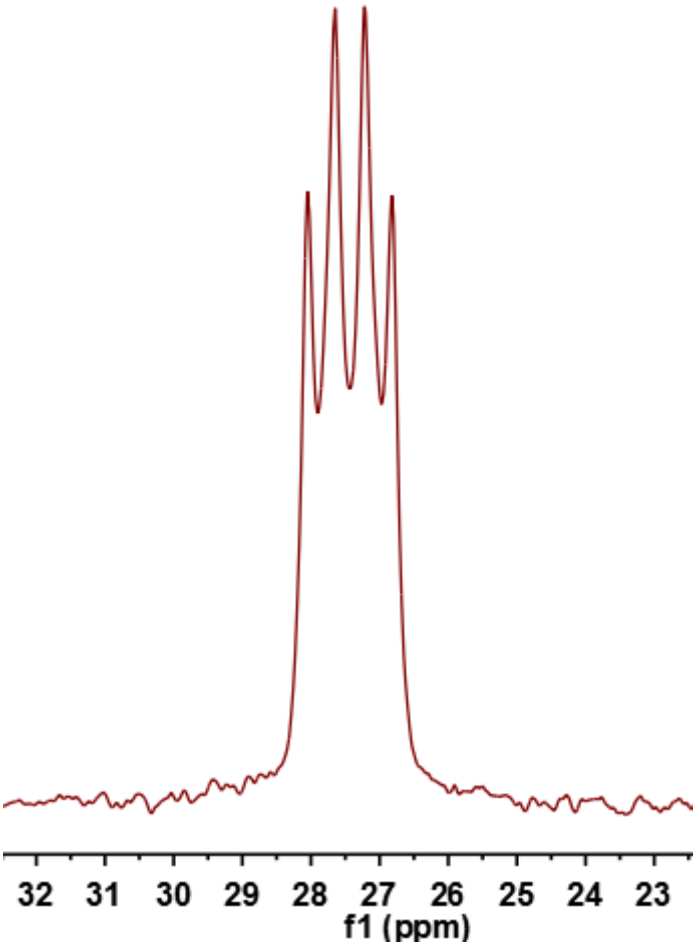

Figure 2.4. $^{31}P\{^{1}H\}$ NMR spectrum of a phosphine-borane without typical 1:1:1:1 line ratios.

2.3 Synthesis and characterisation of Group B precursors [*o*-phenylene-bridged bis(phosphine-boranes)]

2.3.1 $R_2PH(BH_3)$ [R = ^{i}Pr (41), Ph (42) or Cy (43)]

A solution of diisopropylchlorophosphine in THF was heated under reflux with one equivalent of $LiAlH_4$ and the resulting product was treated with the adduct $BH_3{\cdot}SMe_2$ to give a colourless oil in fairly good yield (Scheme 2.7). An acidic aqueous workup with dilute HCl was needed to dissolve any remaining salts that resulted from the use of $LiAlH_4$ in order to isolate **41**.

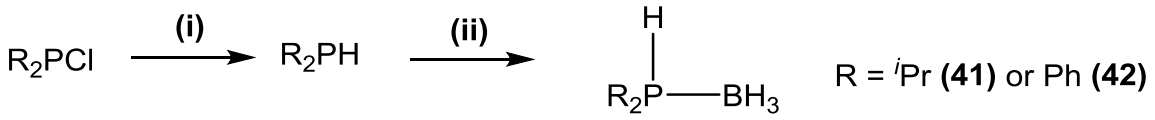

Scheme 2.7. Synthesis of **41** and **42**. Reagents and conditions: i) $LiAlH_4$, THF, ~80 °C, 1 h. ii) $BH_3{\cdot}SMe_2$, THF, r.t., 1 h.

When diphenylchlorophosphine was reacted with one equivalent of $LiAlH_4$ followed by an *in situ* boronation (Scheme 2.7) a mixture of $Ph_2PH(BH_3)$ (**42**) and other impurities was isolated. Distillation of this mixture gave a pure sample of **42** in an excellent yield. Both **42** and **43** [$Cy_2PH(BH_3)$] can be made via a straightforward boronation from the relevant phosphine. This, however, is a much more expensive way of making the corresponding phosphine-boranes; however, compound **43** [$Cy_2PH(BH_3)$] was always made via its phosphine to optimise yield.

2.3.2 1,2-$C_6H_4\{CH_2PR_2(BH_3)\}_2$ [R = ^{i}Pr (44), Ph (45) and Cy (46)]

Compounds **41**, **42** and **43** were metalated by treatment with ^{n}BuLi and these solutions were added to 0.5 equivalent of *α,α,*-dichloro-*o*-xylene to give **44**, **45** and **46**, respectively as colourless solids after an aqueous workup (Scheme 2.8).[13]

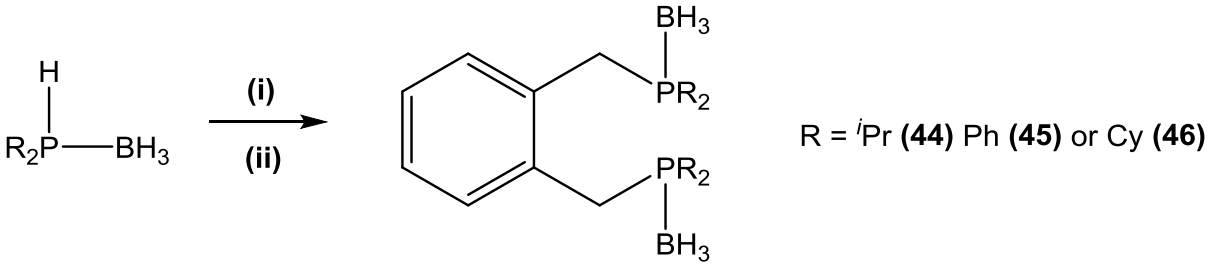

Scheme 2.8. Synthesis of **44**, **45** and **46**. Reagents and conditions: i) ^{n}BuLi, THF, r.t., 1 h. ii) 1,2-$C_6H_4(CH_2Cl)_2$, THF, r.t., 16 h.

It has been previously reported that similar reactions between 1,2-$C_6H_4(CH_2Br)_2$ and $R_2P(BH_3)Li$ gave a mixture of products.[13] This mixture of products was likely due to quaternisation of the resulting phosphine-borane (Scheme 2.9), due to favoured oxidative addition of the benzylic bromide to the phosphorus centre.[14]

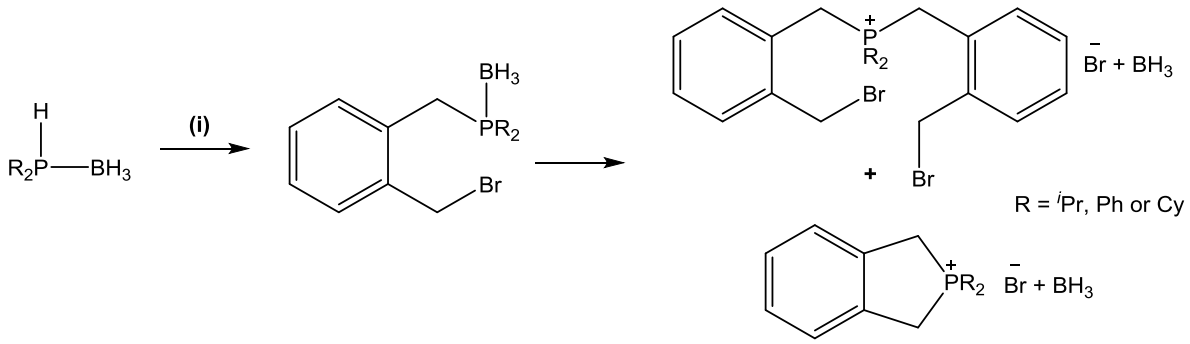

Scheme 2.9. Possible products formed via quaternisation of tertiary phosphine-boranes with 1,2-$C_6H_4(CH_2Br)_2$.

The $^{1}H\{^{11}B\}$, $^{11}B\{^{1}H\}$, $^{13}C\{^{1}H\}$ and $^{31}P\{^{1}H\}$ NMR spectra of compounds **44**-**46** are as expected. In $CDCl_3$ the $^{1}H\{^{11}B\}$ NMR spectrum of **44** contains a doublet at 0.33 ppm (J_{PH} = 14.5 Hz) which corresponds to the two BH_3 moieties, a pair of doublet of doublets at 1.13 ppm (J_{PH} = 13.8, J_{HH} = 7.1 Hz) and 1.20 ppm (J_{PH} = 14.1, J_{HH} = 7.3 Hz) which are due to the CH_3 groups on the $^{i}Pr_2$ substituents and a doublet at 3.32 ppm (J_{PH} = 11.6 Hz) which is due to the CH_2P protons. The $^{11}B\{^{1}H\}$ NMR spectrum contains a doublet at -44.3 ppm (J_{PB} = 49.0 Hz) and the $^{31}P\{^{1}H\}$ NMR spectrum contains a broad peak at 35.2 ppm in which coupling to ^{11}B is not resolved. In $CDCl_3$ the $^{1}H\{^{11}B\}$ NMR spectrum of **45** contains a doublet at 0.9 ppm (J_{PH} = 15.5 Hz) which corresponds to the two BH_3 moieties and a doublet at 3.53 ppm (J_{PH} = 11.7 Hz) due to the CH_2P protons. The $^{11}B\{^{1}H\}$ NMR spectrum contains a broad peak at -40.1 ppm and the $^{31}P\{^{1}H\}$ NMR spectrum contains a broad peak at 18.3 ppm. In $CDCl_3$ the $^{1}H\{^{11}B\}$ NMR spectrum of **46** contains a doublet at 0.29 ppm (J_{PH} = 15.1 Hz) which corresponds to the two BH_3 moieties and a doublet at 3.29 ppm (J_{PH} = 11.5 Hz) due to the CH_2P protons. The $^{11}B\{^{1}H\}$ NMR spectrum contains a broad peak at -43.6 ppm and the $^{31}P\{^{1}H\}$ NMR spectrum contains a broad peak at 27.8 ppm.

Compound **44** is isolated as an essentially pure compound but can be recrystallised to form single crystals suitable for X-ray crystallography from cold (-30 °C) toluene. Below are selected bond lengths and angles for **44** (Table 2.2) along with its molecular structure (Figure 2.5).

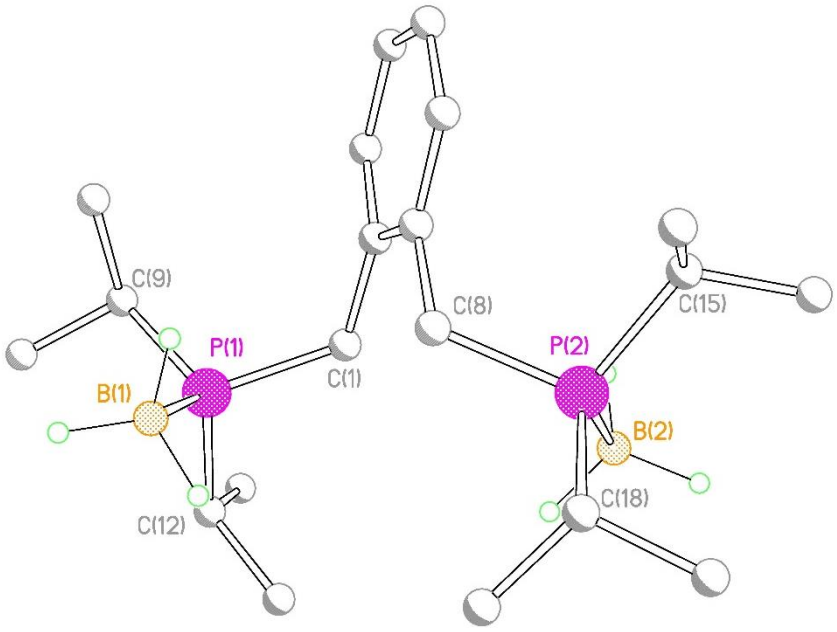

Figure 2.5. Molecular structure of **44** with H atoms (except for those bound to boron) omitted for clarity.

B(1)-P(1)	1.914(2)	P(2)-C(15)	1.8365(13)
P(1)-C(1)	1.8392(11)	P(2)-C(18)	1.8338(12)
P(1)-C(9)	1.8413(12)	B(2)-P(2)	1.923(2)
P(1)-C(12)	1.8375(11)	C(18)-P(2)-B(1)	113.29(6)
P(2)-C(8)	1.8372(11)	C(16)-P(1)-B(2)	115.34(6)

Table 2.2. Selected bond lengths (Å) and angles (°) for **44**.

Compound **44** crystallises as a discrete molecular species where the two $^{i}Pr_2P(BH_3)$ fragments lie on opposites sides of the phenylene linker. The B-P bond lengths [B(1)-P(2), 1.914(2); B(2)-P(1), 1.923(2) Å] for compound **44** are similar to the corresponding B-P distance in compound **37** [B-P, 1.917(4) Å], whereas the P(1)-C(benzyl) bond lengths in **44** [P(1)-C(1), 1.8392(11); P(2)-C(8), 1.8372(11) Å] are significantly longer than the corresponding distances in **37** [P(1)-C(3), 1.800(2) Å].

2.4 Synthesis and characterisation of Group C precursors (benzyl-substituted phosphine-boranes)

2.4.1 $C_6H_5CH_2PR_2(BH_3)$ [R = ^{i}Pr (47), Ph (48) and Cy (49)]

Benzylic-substituted phosphine-boranes $C_6H_5\{CH_2PR_2(BH_3)\}$ [R = ^{i}Pr (**47**), Ph (**48**) and Cy (**49**)] were made via the corresponding precursors **41**, **42** and **43** respectively. Compounds **41**, **42** and **43** were reacted with one equivalent of ^{n}BuLi followed by one equivalent of benzyl bromide to form a colourless oil (**47**), and colourless solids (**48** and **49**) in relatively good yields after an aqueous workup (Scheme 2.10). Compounds **48** and **49** were isolated as essentially pure solids but **48** can be recrystallised from hot toluene to give single crystals suitable for X-ray crystallography. Below are selected bond lengths and angles for **48** (Table 2.3) along with its molecular structure (Figure 2.6).

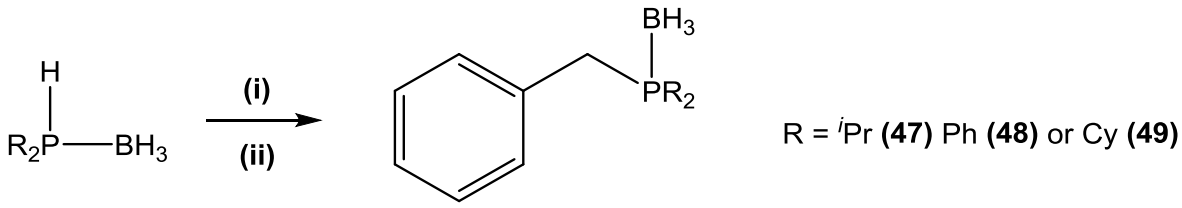

Scheme 2.10. Synthesis of **47**, **48** and **49**. Reagents and conditions: i) ^{n}BuLi, THF, r.t., 1 h. ii) Benzyl bromide, THF, r.t., 16 h.

Quantities of the benzyl bromide have to be 1 mol equivalent as this reaction will yield quaternisation products in the presence of an excess of benzyl bromide (Scheme 2.11).

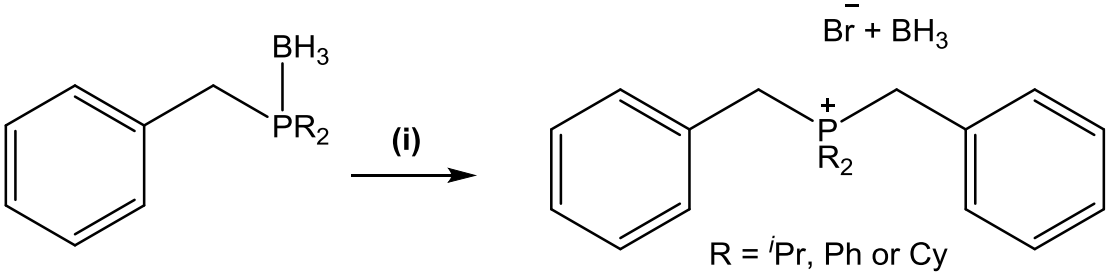

Scheme 2.11. Quaternisation of tertiary phosphine-boranes. Reagents and conditions: i) excess benzyl bromide.

The use of benzyl chloride could eliminate this issue, however as long as care is taken using benzyl bromide **47**, **48** and **49** may be isolated in excellent purity and yield.

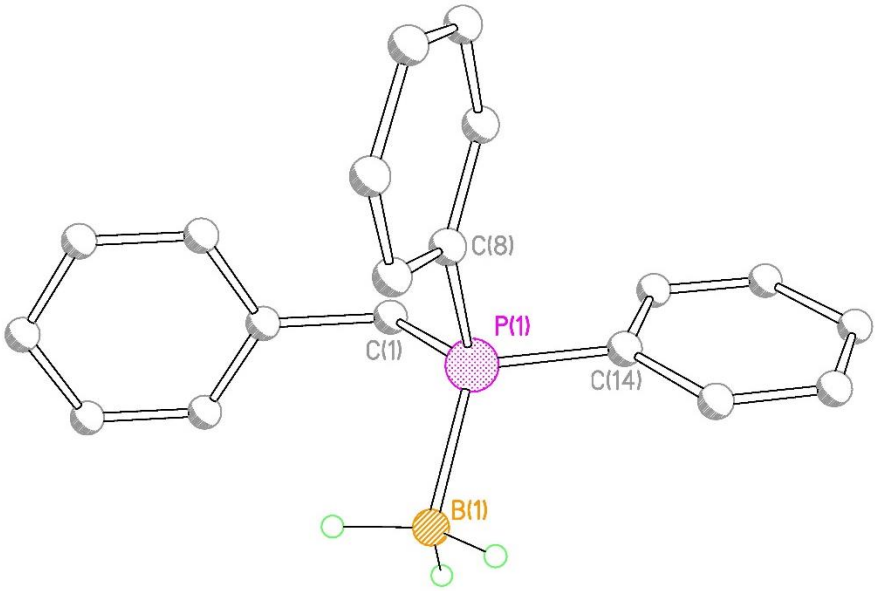

Figure 2.6. Molecular structure of **48** with H atoms (except for those bound to boron) omitted for clarity.

P(1)-B(1)	1.918(2)	B(1)-P(1)-C(1)	113.00(8)
P(1)-C(1)	1.825(2)		
B(1)-H(1C)	1.11(2)		
B(1)-H(1D)	1.12(2)		
B(1)-H(1E)	1.14(2)		

Table 2.3. Selected bond lengths (Å) and angles (°) for **48**.

The $^{1}H\{^{11}B\}$, $^{11}B\{^{1}H\}$, $^{13}C\{^{1}H\}$ and $^{31}P\{^{1}H\}$ NMR spectra of compounds **47**-**49** are as expected. In $CDCl_3$ the $^{1}H\{^{11}B\}$ NMR spectrum of **47** contains a doublet at 0.35 ppm (J_{PH} = 15.0 Hz), which corresponds to one BH_3 unit, and a pair of doublet of doublets

(Figure 2.7) at 1.07 ppm (J_{HH} = 3.00 Hz, J_{PH} = 9.00 Hz) due to the methyl protons, as well as a doublet at 2.98 ppm (J_{PH} = 11.5 Hz) corresponding to the CH_2P protons.

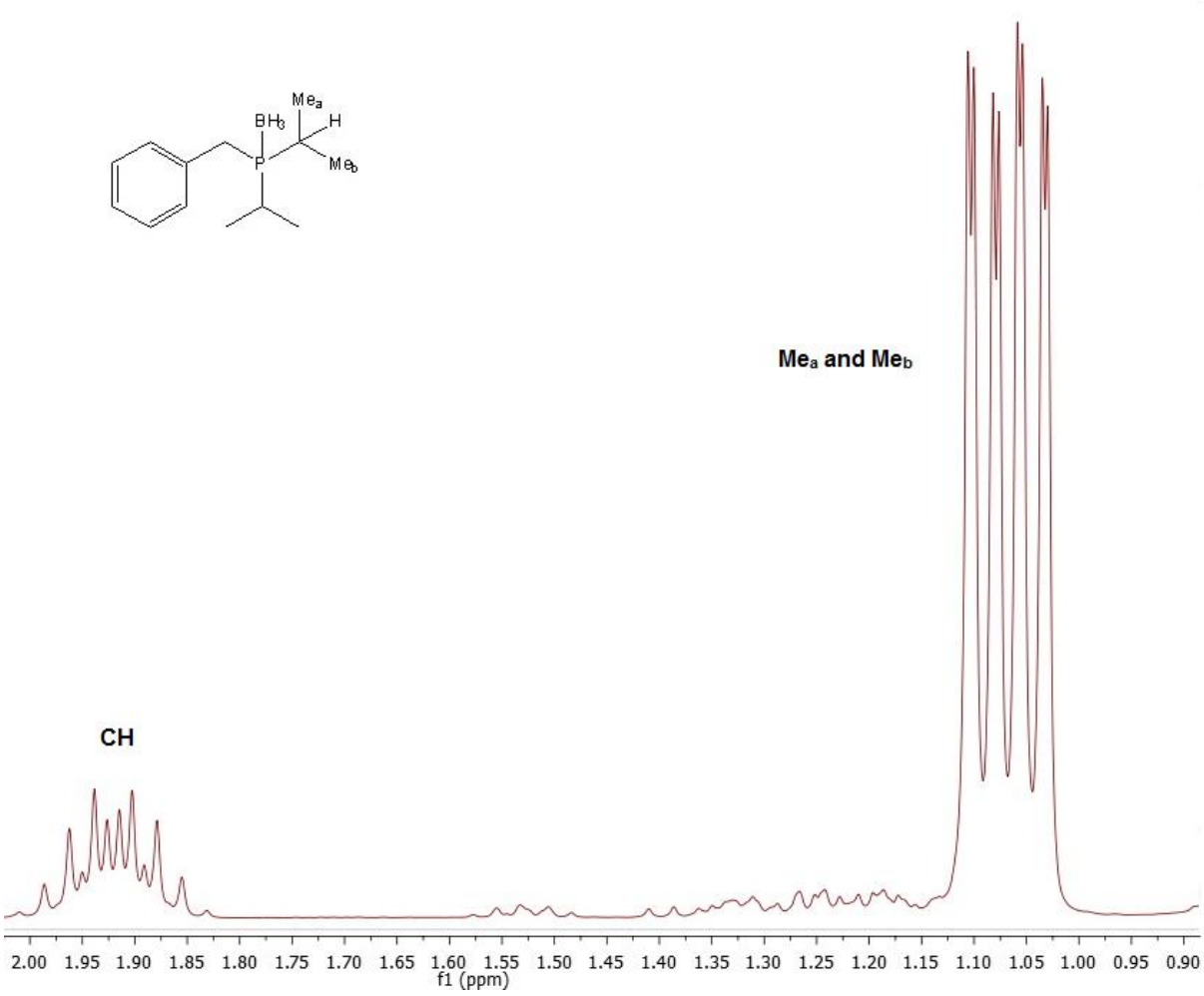

Figure 2.7. $^1H\{^{11}B\}$ NMR spectrum of **47** in $CDCl_3$ showing diastereotopic methyl groups and CH fragment of the isopropyl substituents.

This splitting pattern arises due to the fact that both methyl groups within the isopropyl substituents are diastereotopic so Me_a can never be in the same chemical environment as Me_b (Figure 2.8).

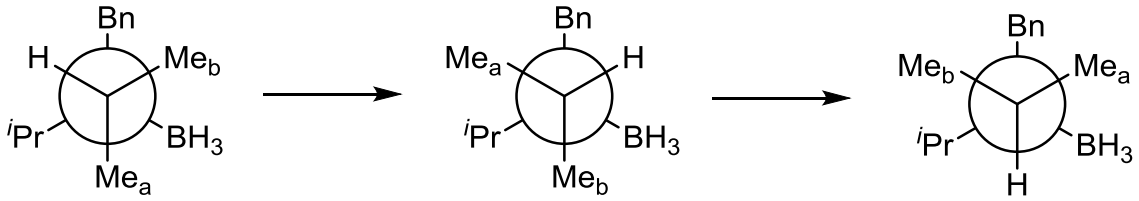

Figure 2.8. Newman projections along the C-P bond showing the diastereotopic nature of Me_a and Me_b in the isopropyl substituents of **47**.

The $^{11}B\{^1H\}$ NMR spectrum of **47** contains a doublet at -43.2 ppm (J_{PB} = 59.7 Hz) and the $^{31}P\{^1H\}$ NMR spectrum contains a quartet at 34.0 ppm (J_{PB} = 59.7 Hz). In $CDCl_3$ the $^1H\{^{11}B\}$ NMR spectrum of **48** contains a doublet at 0.9 ppm (J_{PH} = 15.9 Hz) which corresponds to the BH_3 unit, and a doublet at 3.15 ppm (J_{PH} = 11.8 Hz) due to the CH_2P protons. The $^{11}B\{^1H\}$ NMR spectrum contains a doublet at -39.1 ppm (J_{PB} = 49.3 Hz) and the $^{31}P\{^1H\}$ NMR spectrum contains a quartet at 18.0 ppm (J_{PB} = 49.3 Hz). In $CDCl_3$ the $^1H\{^{11}B\}$ NMR spectrum of **49** contains a doublet at 0.40 ppm (J_{PH} = 15.0 Hz) which corresponds to the BH_3 unit, and a doublet at 3.04 ppm (J_{PH} = 15.0 Hz) which corresponds to the CH_2P protons. The $^{11}B\{^1H\}$ NMR spectrum contains a doublet at -43.5 ppm (J_{PB} = 57.8 Hz) and the $^{31}P\{^1H\}$ NMR spectrum contains a quartet at 27.2 ppm (J_{PB} = 57.8 Hz).

Compound **48** crystallises as a discrete molecular species. The B-P bond length [B(1)-P(1), 1.918(2) Å] for compound **48** is similar to the corresponding B-P distances in compounds **37** [B-P, 1.917(4) Å] and **44** [P(1)-B(1), 1.914(2), P(2)-B(2), 1.923(2) Å], whereas the P(1)-C(benzyl) bond length in **48** [P(1)-C(1), 1.825(2) Å] is significantly shorter than the corresponding distances in compound **44** [P(1)-C(1), 1.8392(11); P(2)-C(8), 1.8372(11) Å] and significantly longer than the corresponding distance in **37** [P(1)-C(3), 1.800(2) Å].

2.5 Synthesis and characterisation of Group D precursors [$SiMe_3$-substituted and linear bis(phosphine-boranes)]

2.5.1 $C_6H_5\{CH(SiMe_3)PCy_2(BH_3)\}$ 50

Compound **49** undergoes an α-metalation by ^{n}BuLi followed by a silicon-carbon bond formation with chlorotrimethylsilane to form essentially pure **50** as a colourless solid in a relatively good yield (Scheme 2.12).

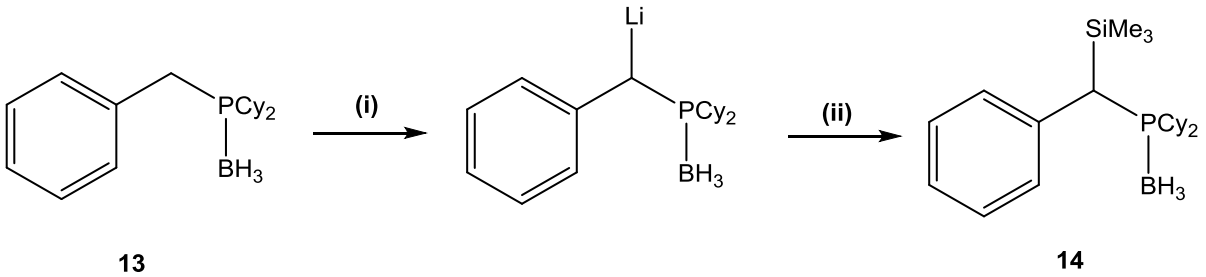

13 **14**

Scheme 2.12. Synthesis of **50**. Reagents and conditions: i) ^{n}BuLi, THF, r.t., 30 mins. ii) Me_3SiCl, THF, r.t., 30 mins.

The $^1H\{^{11}B\}$, $^{11}B\{^1H\}$, $^{13}C\{^1H\}$ and $^{31}P\{^1H\}$ NMR spectra of compound **50** are as expected. In $CDCl_3$ the $^1H\{^{11}B\}$ NMR spectrum of **50** contains a doublet at 0.65 ppm (J_{PH} = 14.2 Hz) which corresponds to the BH_3 unit, and a doublet at 2.72 ppm (J_{PH} = 20 Hz) which corresponds to the PCHSi proton. The $^{11}B\{^1H\}$ NMR spectrum contains a doublet at -40.3 ppm (J_{PB} = 64.2 Hz) and the $^{31}P\{^1H\}$ NMR spectrum contains a quartet at 29.2 ppm (J_{PB} = 64.2 Hz).

2.5.2 $\{CH_2CH_2PCy_2(BH_3)\}_2$ 51

Two equivalents of **43** underwent an α-metalation with ^{n}BuLi followed by addition to one equivalent of 1,4-dibromobutane to form an air stable colourless solid with good purity and yield (Scheme 2.13).

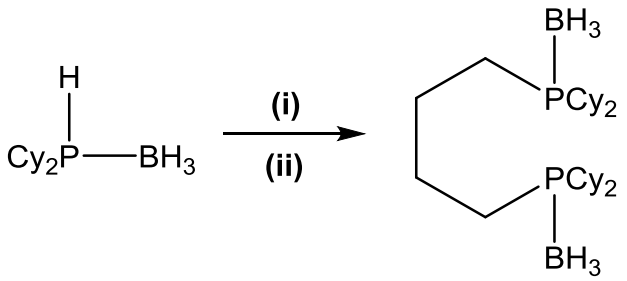

43 **51**

Scheme 2.13. Synthesis of **51**. Reagents and conditions: i) ^{n}BuLi, THF, r.t., 1 h. ii) 1,4-dibromobutane, THF, r.t., 16 h.

The $^{1}H\{^{11}B\}$, $^{11}B\{^{1}H\}$, $^{13}C\{^{1}H\}$ and $^{31}P\{^{1}H\}$ NMR spectra of compound **51** are as expected. In $CDCl_3$ the $^{1}H\{^{11}B\}$ NMR spectrum of **51** contains a doublet at 0.29 ppm (J_{PH} = 15.1 Hz) which corresponds to the two BH_3 moieties, the $^{11}B\{^{1}H\}$ NMR spectrum contains a doublet at -44.3 ppm and the $^{31}P\{^{1}H\}$ NMR spectrum contains a quartet at 25.2 ppm (J_{PB} = 49.0 Hz).

2.6 Conclusion

The phosphine-borane precursors **37**, **40**, **41-51** have been successfully synthesised and characterised by multi-element NMR spectroscopy. Crystals suitable for X-ray crystallography were isolated for compounds **37** and **48** and the molecular structures are typical for this type of compound. The $^{1}H\{^{11}B\}$, $^{11}B\{^{1}H\}$, $^{13}C\{^{1}H\}$ and $^{31}P\{^{1}H\}$ NMR spectra of compounds **37**, **40**, **41-51** are as expected. During the synthesis of compound **37** grease-free apparatus was essential in order to eliminate the competing reaction of $Me_2P(BH_3)CH_2Li$ with silicone grease. During the synthesis of compounds **44-46** 1,2-$C_6H_4(CH_2Cl)_2$ was used instead of 1,2-$C_6H_4(CH_2Br)_2$ in order to eliminate quaternisation as the competing reaction. Problems with low yield and purity of compounds **45** and **48** meant no further investigations into these compounds were carried out.

2.7 References

1. T. Imamoto, *Pure Appl. Chem.*, 1993, **65**, 655-660.
2. A. R. Muci, K. R. Campos and D. A. Evans, *J. Am. Chem. Soc.*, 1995, **117**, 9075-9076.
3. K. Izod, C. Wills, W. Clegg and R. W. Harrington, *Organometallics*, 2007, **26**, 2861-2866.
4. K. Izod, W. McFarlane, B. V. Tyson, I. Carr, W. Clegg and R. W. Harrington, *Organometallics*, 2006, **25**, 1135-1143.
5. K. Izod, C. Wills, W. Clegg and R. W. Harrington, *Organometallics*, 2006, **25**, 5326-5332.
6. K. Izod, C. Wills, W. Clegg and R. W. Harrington, *Organometallics*, 2006, **25**, 38-40.
7. K. Izod, C. Wills, W. Clegg and R. W. Harrington, *J. Organomet. Chem.*, 2007, **692**, 5060-5064.
8. K. Izod, C. Wills, W. Clegg and R. W. Harrington, *Dalton Trans.*, 2007, 3669-3675.
9. K. Izod, C. Wills, W. Clegg and R. W. Harrington, *Inorg. Chem.*, 2007, **46**, 4320-4325.
10. K. Izod, L. J. Bowman, C. Wills, W. Clegg and R. W. Harrington, *Dalton Trans.*, 2009, 3340-3347.
11. F. Dornhaus, M. Bolte, H. W. Lerner and M. Wagner, *Eur. J. Inorg. Chem.*, 2006, 1777-1785.
12. H. Friebolin, *Basic One- and Two-Dimensional NMR Spectroscopy*, Wiley-VCH, 2005, 3.
13. K. Izod, C. M. Dixon, E. McMeekin, L. Rodgers, R. W. Harrington and U. Baisch, *Organometallics*, 2014, **33**, 378-386.
14. J. Uziel, N. Riegel, B. Aka, P. Figuiere and S. Juge, *Tetrahedron Lett.*, 1997, **38**, 3405-3408.

Chapter 3. Synthesis and structural characterisation of α-metalated phosphine-borane precursors

3.1 Introduction

Phosphine-borane-stabilised carbanions have been used for many years for the synthesis of chiral diphosphines, such as DIPAMP (bis[(2-methoxyphenyl)phenylphosphine]ethane)[1, 2], which have many applications as supporting ligands in catalysis.[3-5] However, it is only recently that phosphine-borane-stabilised carbanions have been of interest in their own right as they are usually prepared and used *in situ* and so little is known about their structures; this is surprising given that $Me_2P(BH_3)$ is isoelectronic with $SiMe_3$. In order to investigate the extent of the stabilisation afforded by phosphine-borane substituents, Izod and co-workers synthesised the phosphine-borane-stabilised carbanion complex $Me_2P(BH_3)CH_2Li$, which undergoes an unusual reaction with silicone grease to yield a complex with a novel siloxy-functionalised alkyl ligand (discussed further in Chapter 1.4);[6] unfortunately, even with the absence of grease $\{Me_2P(BH_3)CH_2\}Li$ was not isolated cleanly. This greater reactivity towards silicone grease in comparison to $[(Me_3Si)_2C\{Me_2P(BH_3)\}]^-$ was attributed to the former exhibiting greater negative charge on the carbanion, due to a decrease in negative hyperconjugation (due to the lack of $SiMe_3$ groups) which leads to an increase in nucleophilic character on the carbanion.[6] From Izod and co-workers' ongoing investigations it is apparent that, even though $PMe_2(BH_3)$ and $SiMe_3$ groups are isoelectronic, silicon-stabilised carbanions and phosphine-borane-stabilised carbanions show different characteristics in their metal complexes (discussed further in Chapter 1.4).

This chapter discusses the synthesis and characterisation of an array of structurally different phosphine-borane-stabilised carbanions. Group A (compounds **44**-**46**) are linear and group B (compounds **47**-**49**) are phosphine-boranes that contain a phenylene linker in order to incorporate a rigid backbone (see Chapter 2.2 and 2.3 for a more detailed discussion). The ultimate aim was to synthesise the stannylenes of group A and B ligands and to compare the structures of group B with A in order to determine if the introduction of a rigid linker affects the overall structure; the main point of interest is the B-H···Sn interactions. Group C (compounds **50** and **51**) are analogues of the silicon-substituted ligands used in the previously published stannylenes $\{(Me_3Si)_2CH\}_2Sn$[7] and $[(Me_3Si)\{Me_2(BH_3)P\}CH]_2Sn$[8] from Lappert

and Izod, respectively, where $SiMe_3$ groups are absent in group C. The removal of the sterically demanding trimethylsilyl group and how that affects the structures of the corresponding stannylenes will be discussed further in Chapter 6.2. In order to progress towards the stannylenes of these phosphine-borane-stabilised carbanions, their alkali metal derivatives must first be investigated. This chapter discusses the synthesis of the phosphine-borane-stabilised carbanions of groups A, B and C along with characterisation; as well as the attempted synthesis of group D complexes and the reasons why investigations into group D were not carried any further.

3.2 Synthesis and characterisation of Group A phosphine-borane-stabilised carbanions

Treatment of the linear bis(phosphine-boranes) **37** and **40** with two equivalents of ^{n}BuLi and tmeda in THF yields the corresponding doubly-deprotonated complexes $[Li(tmeda)]_2[Me_2P(BH_3)CHSi(Me_2)CH_2]_2$ (**37a**) and $[Li(THF)_2]_2[Ph_2P(BH_3)CHSi(Me_2)CH_2]_2$ (**40a**), respectively, as yellow crystalline solids. Similarly, the reaction between **40** and two equivalents of $PhCH_2K$ in the presence of the tertiary amine pmdeta, yields the potassium complex $[K(pmdeta)]_2[CH_2SiMe_2CHP(BH_3)Ph_2]_2$ (**40b**) as yellow blocks after recrystallisation from hot toluene (Scheme 3.1).

The $^{1}H\{^{11}B\}$, $^{11}B\{^{1}H\}$, $^{13}C\{^{1}H\}$ and $^{31}P\{^{1}H\}$ NMR spectra of compounds **37a**, **40a** and **40b** are as expected. In deuterated benzene the $^{1}H\{^{11}B\}$ NMR spectrum of **37a** contains a doublet at -1.05 ppm (J_{PH} = 6.4 Hz) corresponding to the two protons bonded to the carbanion centres and a doublet at 1.05 ppm (J_{PH} = 11.5 Hz) which corresponds to the two BH_3 units. The $^{11}B\{^{1}H\}$ NMR spectrum contains a doublet at -33.0 ppm (J_{PB} = 88.3 Hz) and the $^{31}P\{^{1}H\}$ NMR spectrum contains a quartet at -4.8 ppm (J_{PB} = 88.3 Hz) whilst the ^{7}Li NMR spectrum contains a singlet at 1.0 ppm. In deuterated benzene the $^{1}H\{^{11}B\}$ NMR spectrum of **40a** contains a doublet at -0.10 ppm (J_{PH} = 25.0 Hz) corresponding to the two protons bonded to the two carbanion centres. The $^{11}B\{^{1}H\}$ NMR spectrum contains a doublet at -35.7 ppm and the $^{31}P\{^{1}H\}$ NMR spectrum contains a quartet at 12.5 ppm (J_{PB} = 88.2 Hz), whilst the ^{7}Li NMR spectrum contains a singlet at 1.2 ppm. Once isolated, compound **40b** has limited solubility in aromatic solvents, such as toluene, but has good solubility in ethereal solvents, such as THF. In deuterated THF the $^{1}H\{^{11}B\}$ NMR spectrum of **40b** contains a doublet at -0.53 ppm (J_{PH} = 25.0 Hz) corresponding to the two protons which are bonded to the two carbanion centres and a doublet at 0.95 ppm (J_{PH} = 15.0 Hz) which corresponds to the two

BH_3 units. The $^{11}B\{^1H\}$ NMR spectrum contains a doublet at -34.7 ppm (J_{PB} = 113.8 Hz) and the $^{31}P\{^1H\}$ NMR spectrum contains a quartet at 11.7 ppm (J_{PB} = 113.8 Hz).

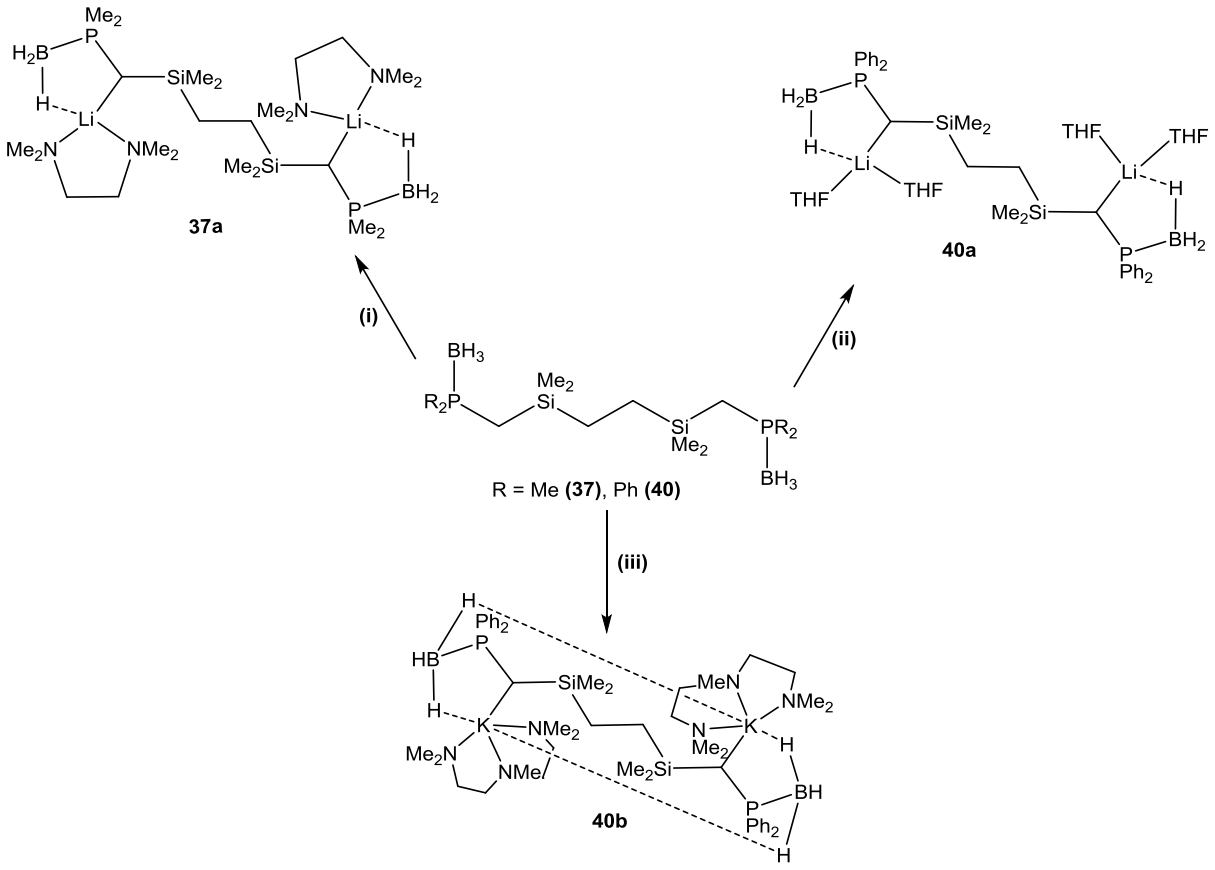

Scheme 3.1: Synthesis of **37a**, **40a** and **40b**. Reagents and conditions: i) 2 equivalents of ^{n}BuLi, THF, r.t., 1 hr. ii) 2 equivalents of ^{n}BuLi, tmeda, THF, r.t., 1hr. iii) 2 equivalents of BnK, pmdeta, THF, r.t., 16 hr.

Metalation of **37** and **40** with ^{n}BuLi results in a small downfield shift of the $^{11}B\{^1H\}$ NMR signal (**37**, -37.5 ppm; **37a**, -33.0 ppm; **40**, -38.9 ppm; **40a**, -35.7 ppm) and a small upfield shift in the $^{31}P\{^1H\}$ NMR signal (**37**, 3.4 ppm; **37a**, -4.8 ppm; **40**, 13.5 ppm; **40a**, 12.5 ppm). Metalation also leads to a large increase in the ^{31}P-^{11}B coupling constant (**37**, 58.8 Hz; **37a**, 88.3 Hz; **40**, 69.5 Hz; **40a**, 107.9 Hz).

With decreasing electronegativity of the metal centre there is also a slight upfield shift in the $^{31}P\{^1H\}$ NMR signal (**40a**, 12.5 ppm; **40b**, 11.7 ppm), while the $^{11}B\{^1H\}$ NMR signal moves very slightly to lower field (**40a**, -35.7 ppm; **40b**, -34.7 ppm). The ^{31}P-^{11}B coupling constant also shows a slight increase with decreasing electronegativity of the metal centre (**40a**, 107.9 Hz; **40b**, 113.8 Hz).

There is a noticeable difference between the ^{31}P-^{11}B coupling constants of compounds **37** and **40**, where a 10 Hz increase is observed going from a methyl (sp^3) to a phenyl (sp^2) substituent, respectively. This change in coupling can be explained using Bent's rule (Figures 3.1 and 3.2).[9]

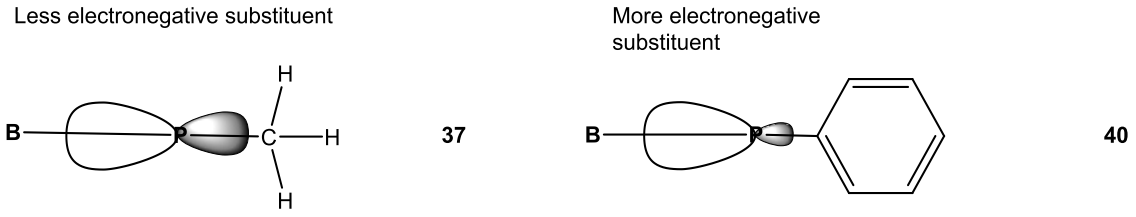

Figure 3.1: Atomic orbitals on P of compounds **37** and **40** indicating the change in s-character along the P-B bond when going from a sp^3 to an sp^2 carbon atom, respectively.

The s/p contribution of bonding in orbitals can be explained with the use of Bent's rule which proposes that the more electronegative a substituent is, the more s-character that substituent will possess. Therefore, the more electronegative sp^2 carbon centre in compound **40** compared to compound **37** has greater carbon s-character which results in greater phosphorus p-character which will then lead to the P-B bond having less phosphorus p- but greater s-character than the sp^3 carbon atom in **37**. Greater s-character leads to an increase in the ^{31}P-^{11}B coupling constant, which can also be seen in the phosphine-borane-stabilised carbanion complexes **37a** and **40a** (J_{PB} = **37**, 58.8 Hz; **40**, 69.5 Hz; **37a**, 88.3 Hz; **40a**, 107.9 Hz).[10]

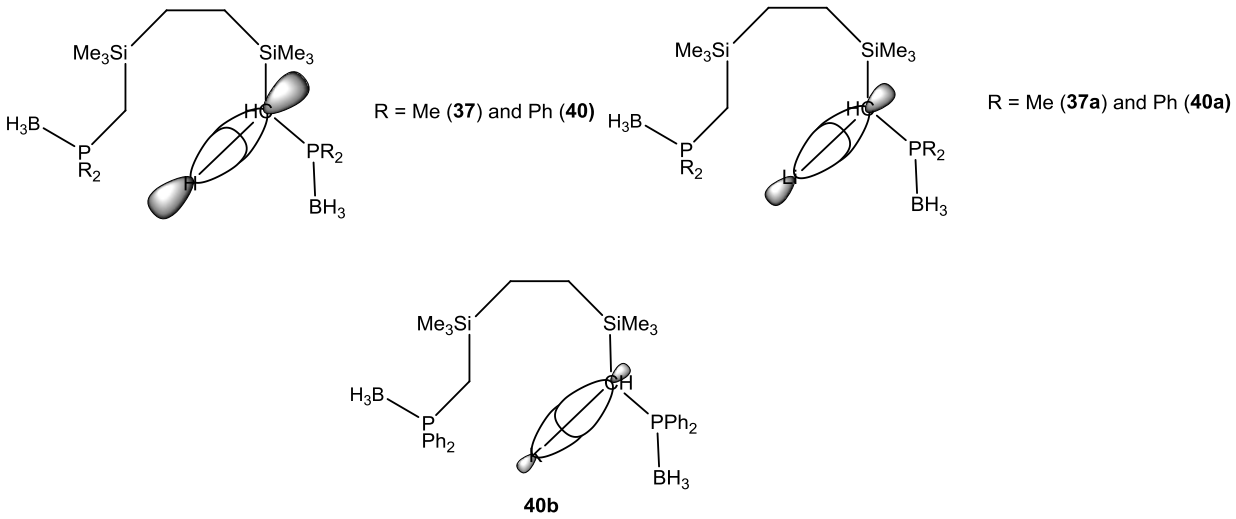

Figure 3.2: Atomic orbitals of compounds **37**, **37a** and **40**-**40b** showing the increase in s-character with increase in electropositivity on the carbanion.

With increase in electropositivity on the carbanion centre [C-H (**37** and **40**), to C-Li (**37a** and **40a**) and then to C-K (**40b**)] the C-M (M = H, Li and K) bond has more carbon s-character in **37a** and **40b** compared to **37** and **40**. If the C-M bond has more s-character, then this will affect the C-P bond resulting in more carbon p-character; overall leading to greater phosphorus s-character in the P-B bond. This increase in phosphorus s-character across the P-B bond results in an increase in the J_{PB} coupling constants in **37**, **37a** (**37**, J_{PB} = 58.8 Hz; **37a**, 88.3 Hz) and **40**, **40a** and **40b** (**40**, J_{PB} = 69.5 Hz; **40a**, 88.3 Hz; **40b**, 113.8 Hz). This trend is consistent with other examples where an increase of 20-50 Hz in J_{PB} is observed upon α-metalation of phosphine-borane compounds.[6, 11-22]

Crystals suitable for X-ray crystallography of **37a** have so far not been isolated; however, compounds **40a** and **40b** have been isolated as colourless crystals and yellow blocks, respectively, and so their solid-state structures have been obtained. Both **40a** and **40b** crystallise as monomeric units but adopt very different structures; the molecular structures of **40a** and **40b** are shown in Figures 3.3 and 3.4, respectively, along with selected bond lengths and angles (Tables 3.1 and 3.2).

The Li-C distance in **40a** [2.194(6) Å] is similar to that in previously reported examples, such as $[CH_2SiMe_2C(SiMe_3)_2LiC(SiMe_3)_2SiMe_2CH_2][Li(TMEDA)_2]$ (**52**) which has a Li-C distance of 2.156(4) Å.[23] Compound **52** is bulkier than compound **40a**, however, in **52**, one $SiMe_3$ unit is isoelectronic with the Me_2P-BH_3 groups in **40a**. Although the Li-C bond lengths are similar to each other in **40a** and **52**, the resulting structures are noticeably

different. Compound **40a** crystallises as a linear dicarbanion with an inversion centre midway along the C(2)-C(2′) bond; the C(2) atoms and their symmetry equivalents are disordered over two positions with equal occupancy. In contrast, **52** crystallises as a separated ion pair containing a chelating lithate anion and [Li(TMEDA)$_2$] cation resulting in a bent linear C-Li-C core (C-Li-C = 171.4(7) °)[23] and showing clearly two Li environments in the ^{7}Li NMR spectrum. Compound **40a** adopts a distorted tetrahedral structure at the lithium centres [O(1)-Li-C(1) = 113.7(3) °, O(2)-Li-C(1) = 137.6(3) °] due to interactions with the carbanion centres, an η^1-BH_3 group and the oxygen atoms of two THF molecules. A potential reason why these dicarbanions are structurally different could be due to the presence of the phosphine-borane unit in **40a**, where the η^1 interaction with the BH_3 moieties hinders chelation of the lithium ion by the two carbanion centres.

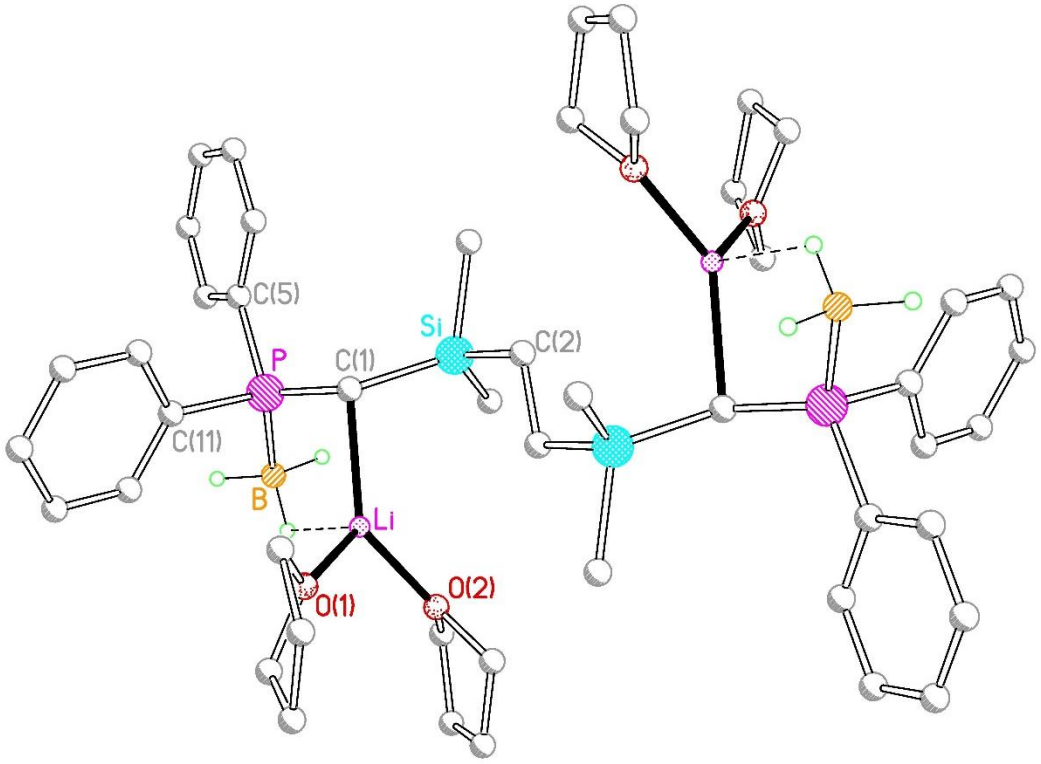

Figure 3.3: Molecular structure of **40a** with H atoms (except for those bound to boron) omitted for clarity.

P(1)-C(1)	1.729(2)	Li-O(1)	1.903(6)
P(1)-B(1)	1.924(3)	Li-O(2)	1.928(6)
B(1)-H(B)	1.07(3)	B-H(A)	1.06(4)
Li(1)-H(B)	2.22(3)	B-H(C)	1.07(3)
C(1)-Si	1.829(3)		
Li(1)-C(1)	2.194(6)	C(1)-P(1)-B(1)	114.14(14)

Table 3.1: Selected bond lengths (Å) and angles (°) for **40a**.

Compound **40b** crystallises as discrete molecules with an unusual cyclic structure with a C_2 axis perpendicular to the C(2)-C(2A) bond (Figure 3.4). Each potassium cation has contacts with a carbanion centre, one η^1-BH_3 group at one end of the phosphine-borane-stabilised carbanion, three nitrogen atoms of a molecule of pmdeta and an η^1-BH_3 group of the second half of the molecule. This results in each BH_3 group bridging the two potassium ions in a μ-η^1:η^1 fashion to generate a $(K\text{-}H\text{-}B\text{-}H)_2$ cycle to each K. The K-C bond length of 3.173(4) Å is significantly longer than the K-C distance in the silicon-substituted examples $(C_6H_6)_2KC(SiMe_3)_2SiMe_2CH_2CH_2Me_2Si(Me_3Si)_2CK(C_6H_6)_2$ and $(THF)_2KC(SiMe_3)_2SiMe_2CH_2CH_2Me_2Si(Me_3Si)_2CK(THF)_2$ [2.953(4) Å and 2.937(3) Å, respectively]. This longer bond length could be due to either the increase in the number of metal-ligand contacts in **40b** or the two pseudo-four-membered rings being strained enough to lengthen the K-C bond.

Comparison of the structures of **40a** and **40b** with that of the closely related precursor **37** shows a significant shortening of the C-P bond upon metalation (**37**, 1.8000(19) Å; **40a**, 1.729(3) Å; **40b**, 1.716(5) Å], which is consistent with extensive delocalisation of charge from the carbanion centre into the P-C σ^* orbital;[24] this is also true for the C-Si distances [**37**, 1.892(2) Å; **40a**, 1.829(3) Å; **40b**, 1.804(4) Å]. This shortening may also be attributed to the increased electron donation in the agostic-type H-B···M interactions. The P-B distances in compounds **40a** and **40b** are similar to that in **37** [**37**, 1.917(3) Å; **40a**, 1.924(3) Å; **40b**, 1.921(5) Å). The K···H distances in **40b** are significantly longer than the Li···H distances in **40a** [**40a**, 2.22(3) Å; **40b**, 2.78(6) and 2.82(6) Å], which may be attributed to the increased ionic radius of a potassium cation compared to lithium.

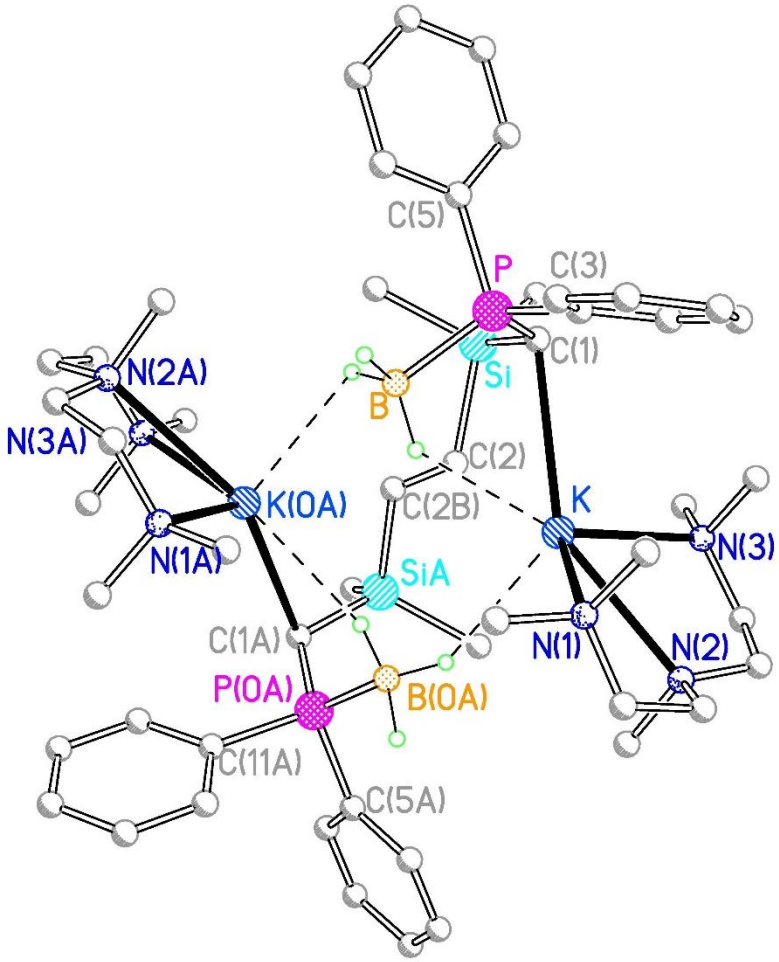

Figure 3.4: Molecular structure of **40b** with H atoms (except for those bound to boron) omitted for clarity.

P(1)-C(1)	1.716(5)	C(1)-Si	1.804(4)
P(1)-B(1)	1.921(5)		
B(1)-H(A)	1.14(7)	B(1)-H(B)	1.07(3)
B(1)-H(C)	1.17(4)	K-N(1)	2.833(4)
K(1)-H(B)	2.78(6)	K-N(2)	2.966(4)
K(1)-H(A)	2.82(6)	K-N(3)	2.906(4)
K(1)-C(1)	3.173(4)	C(1)-P(1)-B(1)	114.14(14)

Table 3.2: Selected bond lengths (Å) and angles (°) for **40b**.

3.3 Synthesis and characterisation of Group B phosphine-borane-stabilised carbanions

1,2-$C_6H_4\{CH_2P(BH_3)R_2\}_2$ [R = ^{i}Pr (**44**), Ph (**45**) or Cy (**46**)] undergo α-metalation with two equivalents of ^{n}BuLi and tmeda to yield the corresponding phosphine-borane-stabilised carbanions $[1,2\text{-}C_6H_4\{CHP(BH_3)R_2\}_2][Li(tmeda)]_2\cdot nL$ (R = ^{i}Pr, n = 0 (**44a**); R = Ph, nL = THF (**45a**); R = Cy, nL = 2PhCH$_3$ (**46a**)) (Scheme 3.2). Compound **45a** was made by a previous research student (Emma McMeekin) but data has been used in order to compare bond lengths and angles.

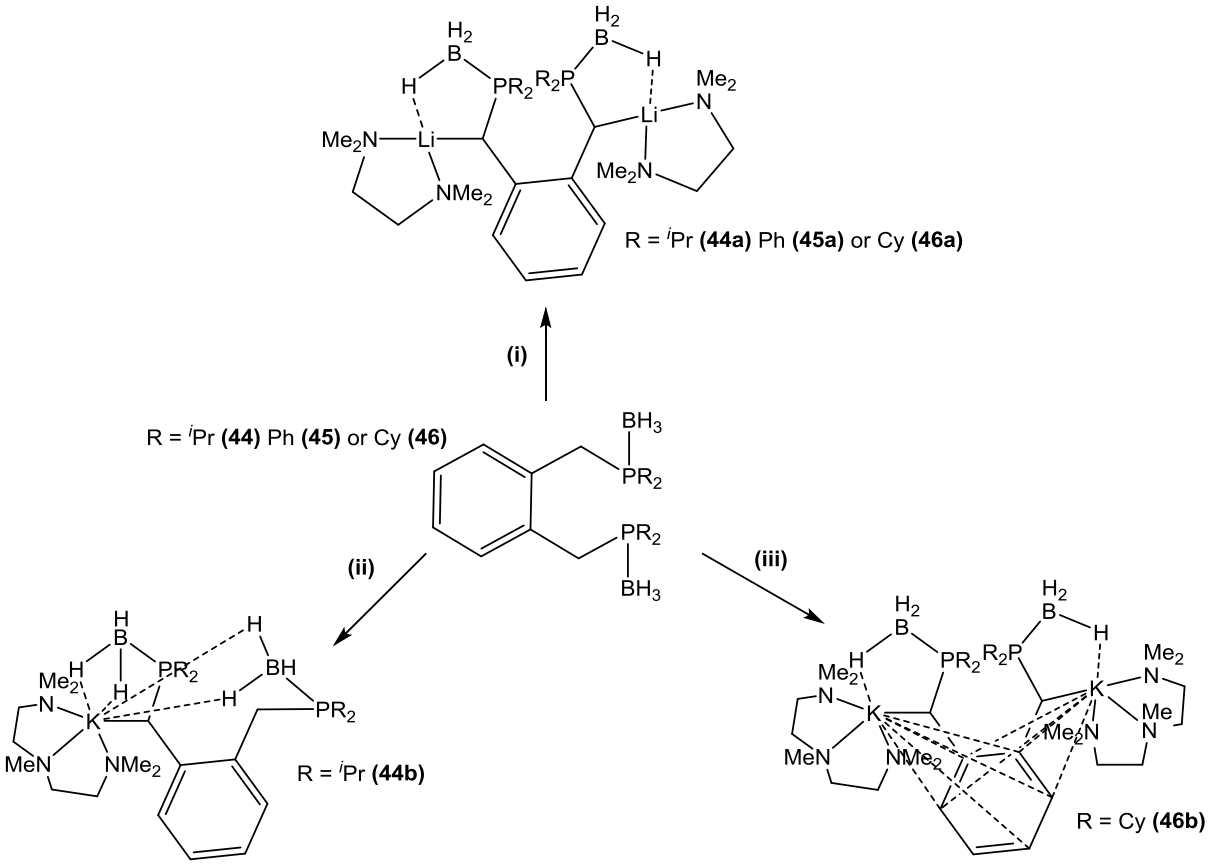

Scheme 3.2: Synthesis of **44a**-**46a**, **44b** and **46b**. Reagents and conditions: i) 2 equivalents of ^{n}BuLi, THF, tmeda, r.t., 1 hr. ii) 2 equivalents of MeK, pmdeta, Et_2O, r.t., 1hr. ii) 2 equivalents of BnK, pmdeta, THF, r.t., 16 hr.

The $^1H\{^{11}B\}$, $^{11}B\{^1H\}$, $^{13}C\{^1H\}$, ^7Li and $^{31}P\{^1H\}$ NMR spectra of compounds **44a**-**46a** are as expected. The $^1H\{^{11}B\}$ spectra of **44a**, **45a** and **46a** exhibit a doublet at 0.32 ppm (J_{PH} = 14.2 Hz), 0.99 ppm (J_{PH} = 14.6 Hz) and 0.33 ppm (J_{PH} = 15.0 Hz), respectively, which corresponds to the BH_3 protons. In the $^1H\{^{11}B\}$ NMR spectrum of compounds **44a** and **45a** the CHLi proton can be distinguished from the phosphorus substituents as doublets at 1.45 ppm (J_{PH} = 9.7 Hz) and 2.20 ppm (J_{PH} = 14.4 Hz), respectively; no coupling to Li^7 is

observed. In the $^{1}H\{^{11}B\}$ NMR spectrum of compound **46a** in d_8-THF it is not possible to identify the CHLi peak due to the many cyclohexyl protons which occur in the same region. The CHLi peak can, however, be observed in the $^{13}C\{^{1}H\}$ NMR spectrum as a doublet (J_{PC} = 61.3 Hz) at 23.3 ppm. The ^{7}Li NMR spectra of **44a**-**46a** exhibit singlets in the range -0.9 to -1.0 ppm whilst in the $^{11}B\{^{1}H\}$ NMR spectrum of **44a** shows a doublet at -39.3 ppm (J_{PB} = 78.4 Hz), whereas **45a** and **46a** show broad signals at -34.4 ppm and -39.8 ppm, respectively. In the $^{31}P\{^{1}H\}$ NMR spectra, **44a** and **46a** show quartets at 16.3 ppm (J_{PB} = 78.4 Hz) and 12.3 ppm (J_{PB} = 105.3 Hz), respectively, whilst **45a** shows a broad signal at 6.2 ppm. This large increase in the ^{31}P-^{11}B coupling constant (**44**, 49.0 Hz; **44a**, 78.4 Hz) is consistent with the formation of a phosphine-borane-stabilised carbanion (see above).

In order to compare structural characteristics between the Li and K complexes of compound **44**, an attempt to prepare the potassium salt **44b** was performed by treating **44** with two equivalents of MeK in cold (-10 °C) diethyl ether. This did not result in double deprotonation at the benzylic centres, but only resulted in monodeprotonation; this was clearly shown in the crude $^{31}P\{^{1}H\}$ NMR spectrum, where two quartets were found at 16.7 ppm (J_{PB} = 83.3 Hz) and 34.2 ppm (J_{PB} = 41.7 Hz), which are due to the monodeprotonated phosphine-borane-stabilised carbanion site and the phosphine-borane site in **44b**, respectively.[24] With the addition of pmdeta, the monodeprotonated product **44b** was recrystallised as pale yellow single crystals from *n*-hexane in good yield.

The reactivity of MeK is typically much greater than ^{n}BuLi and so it was surprising that double deprotonation did not occur. However, the monodeprotonation may be attributed to the competing reaction of MeK and diethyl ether which would leave only one equivalent of MeK available. Even though the initial deprotonation at one benzylic site is rapid, the second deprotonation is much slower and so the side reaction between MeK and diethyl ether dominates. Benzyl potassium is less basic than MeK and does not react with diethyl ether at room temperature, so an attempt was made to doubly deprotonate **44**-**46** with this reagent. Treatment of **44**-**46** with two equivalents of $PhCH_2K$ and pmdeta yielded the corresponding phosphine-borane-stabilised carbanions $[K(pmdeta)]_2[1,2\text{-}C_6H_4\{CHPR_2(BH_3)\}_2]$ [R = ^{i}Pr (**44b**), Ph (**45b**) and (**46b**)]. Despite repeated attempts, compounds **44b** and **45b** could not be isolated cleanly, however, crude $^{31}P\{^{1}H\}$ NMR spectra of the reaction mixtures show a typically large increase in the ^{31}P-^{11}B coupling constant upon formation of the dipotassium salts (J_{PB} = 85.8 and 89.6 Hz, for **44b** and **45b,** respectively). The $^{1}H\{^{11}B\}$, $^{11}B\{^{1}H\}$, $^{13}C\{^{1}H\}$ and $^{31}P\{^{1}H\}$ NMR spectra of compound **46b** are as expected. In the $^{1}H\{^{11}B\}$ NMR spectrum

of **46b** in d_8-toluene it is not possible to identify the CHK proton due to the many cyclohexyl and pmdeta protons, however, the corresponding carbon can be seen in the $^{13}C\{^1H\}$ NMR spectrum as a doublet (J_{PC} = 36.5 Hz) at 37.8 ppm; the $^{11}B\{^1H\}$ NMR and $^{31}P\{^1H\}$ spectra of **46b** contain broad peaks at -40.3 ppm and 12.7 ppm, respectively, on which ^{31}P-^{11}B coupling is not resolved.

Compounds **44a**-**46a** crystallise as discrete monomers which are similar in structure but which are not isostructural. Compound **44a** crystallises with no solvent associated with its asymmetric unit, whilst **45a** contains a molecule of THF and **46a** contains two molecules of toluene in their asymmetric units which are only weakly held in place and which are lost after about 15 minutes of the samples being under vacuum; the ^1H NMR spectrum of **46a** shows no solvent peaks. The molecular structures of **44a**, **45a** and **46a** are shown in Figures 3.5, 3.6 and 3.7, along with selected bond lengths and angles (Tables 3.3, 3.4 and 3.5).

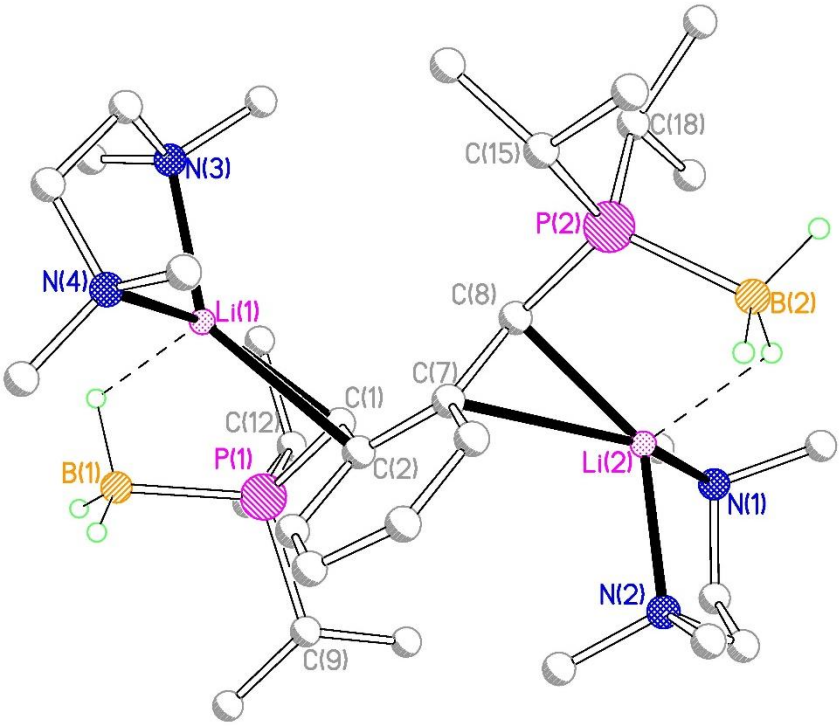

Figure 3.5: Molecular structure of **44a** with H atoms (except for those bound to boron) omitted for clarity.

P(2)-B(2)	1.929(3)	P(1)-B(1)	1.934(3)
B(2)-H(2C)	1.15(3)	B(1)-H(1C)	1.19(3)
Li(2)-C(8)	2.227(5)	Li(1)-C(1)	2.235(5)
Li(2)-C(7)	2.626(5)	Li(1)-C(2)	2.636(5)
P(2)-C(8)	1.755(3)	P(1)-C(1)	1.748(3)
Li(1)-H(1C)	2.08(3)	Li(2)-H(2C)	2.03(2)
Li(1)-N(3)	2.147(5)	Li(1)-N(4)	2.124(5)
Li(2)-N(1)	2.146(5)	Li(2)-N(2)	2.110(5)
P(1)-C(1)	1.748(3)	P(2)-C(8)	1.755(3)
C(8)-P(2)-B(2)	114.13(13)	C(1)-P(1)-B(1)	113.77(14)
Li(2)-C(8)-P(2)	92.23(16)	Li(1)-C(1)-P(1)	93.27(15)

Table 3.3: Selected bond lengths (Å) and angles (°) for **44a**.

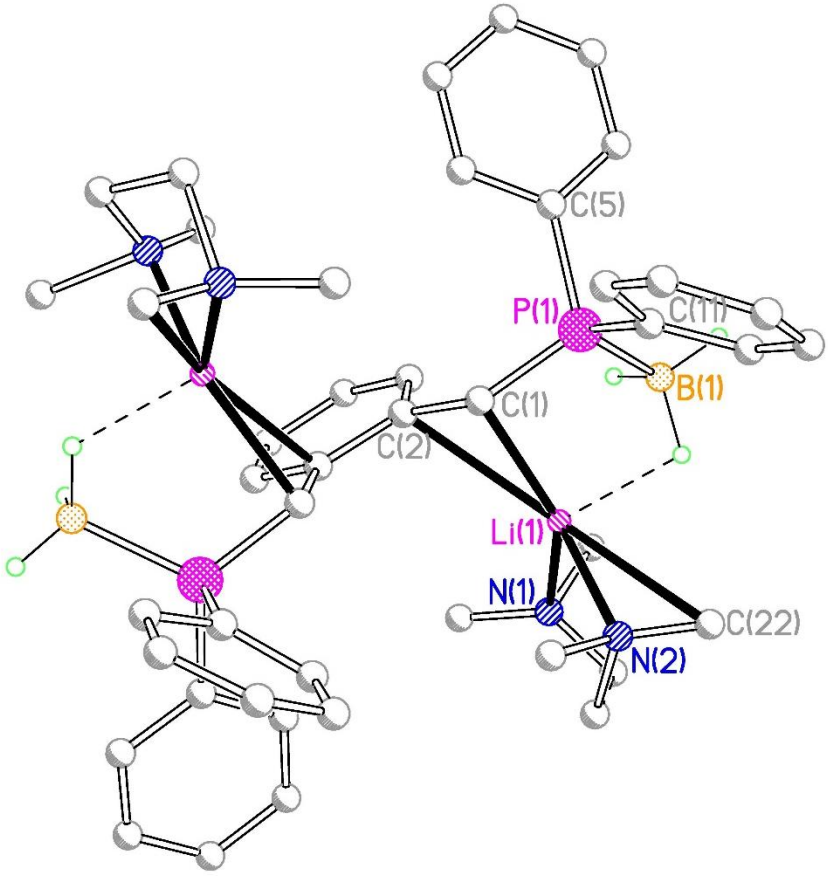

Figure 3.6: Molecular structure of **45a** with H atoms (except for those bound to boron) and solvent of crystallisation omitted for clarity.

P(1)-B(1)	1.925(2)	Li(1)-C(22)	2.760(8)
P(1)-C(1)	1.7412(17)	Li-N(1)	2.066(4)
B(1)-H(1A)	1.19(2)	Li-N(2)	2.100(4)
Li(1)-H(1A)	2.04(2)	C(1)-P(1)-B(1)	115.34(10)
Li(1)-C(2)	2.698(4)	Li(1)-C(1)-P(1)	87.77(11)
Li(1)-C(1)	2.241(4)		

Table 3.4: Selected bond lengths (Å) and angles (°) for **45a**.

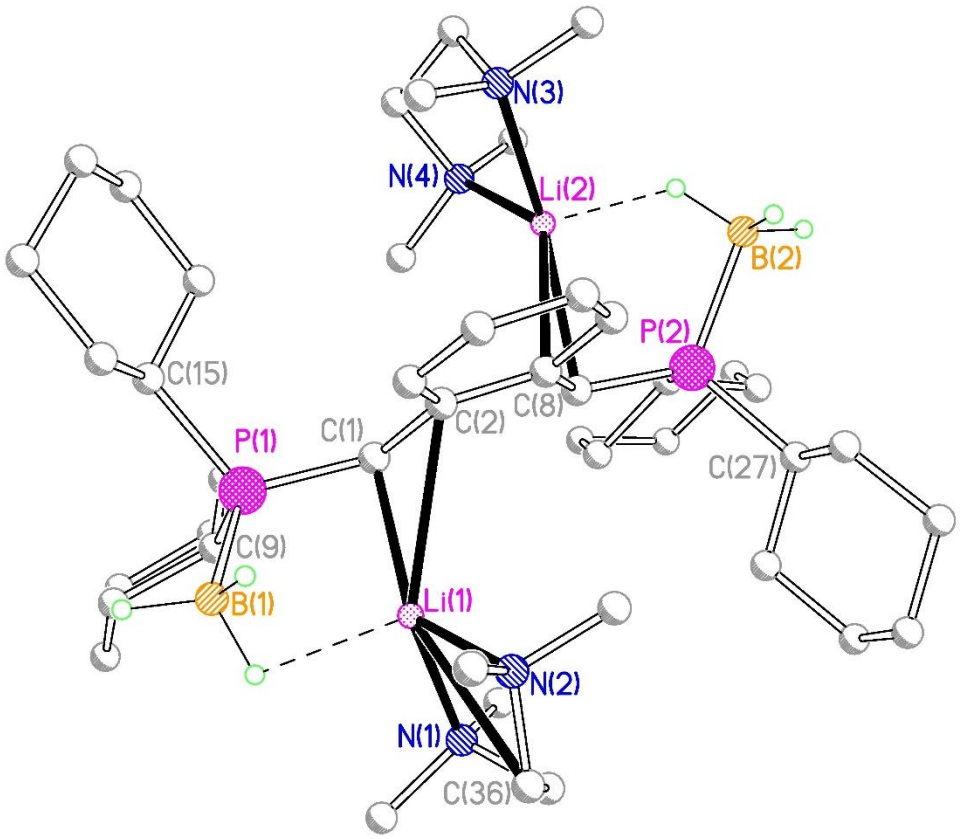

Figure 3.7: Molecular structure of **46a** with H atoms (except for those bound to boron) and solvent of crystallisation omitted for clarity.

P(2)-B(2)	1.951(3)	P(1)-B(1)	1.937(3)
B(2)-H(2A)	1.11(3)	B(1)-H(1B)	1.16(3)
Li(2)-C(8)	2.271(6)	Li(1)-C(1)	2.254(6)
Li(2)-C(7)	2.531(5)	Li(1)-C(2)	2.700(5)
P(2)-C(8)	1.739(3)	P(1)-C(1)	1.753(3)
Li(1)-N(1)	2.118(5)	Li(1)-N(2)	2.047(5)
Li(2)-N(3)	2.123(5)	Li(2)-N(4)	2.134(5)
C(8)-P(2)-B(2)	115.09(13)	C(1)-P(1)-B(1)	113.71(13)
Li(2)-C(8)-P(2)	88.36(16)	Li(1)-C(1)-P(1)	86.25(15)

Table 3.5: Selected bond lengths (Å) and angles (°) for **46a**.

In **44a** each lithium ion has a 5-coordinate geometry where each ion is bound to the carbanion centre, two nitrogen atoms of the tmeda co-ligand, the BH_3 unit in an η^1 fashion and an additional short contact with the *ipso* carbon atom within the *o*-phenylene linker adjacent to the carbanion centre; each Li ion is positioned on opposite sides of the essentially planar $C_6H_4(CP)_2$ fragment forming a distorted pentagonal ring. Compounds **45a** and **46a** adopt similar structures to **44a** but **45a** has an additional short contact between the Li cation and one of the methyl carbon atoms within the tmeda co-ligand whereas, **46a** has an additional short contact between the lithium ion and one of the methylene carbon atoms of the tmeda co-ligand. Compound **45a** also has a crystallographic C_2 axis which bisects the *o*-phenylene linker group.

The Li-C(carbanion) distances in compound **46a** (2.254(6) and 2.271(6) Å) are slightly longer than those in compounds **44a** and **45a** (2.235(5) and 2.227(5) Å, and 2.241(4) Å, respectively) which could be due to compound **46a** having the more sterically demanding cyclohexyl substituents compared to the ^{i}Pr and Ph groups in compounds **44a** and **45a**. The Li-C(carbanion) distances in compounds **44a**-**46a** are significantly longer than the corresponding distances in similar benzyl lithium compounds $[Li(Et_2O)(CH_2Ph)]_\infty$ [2.212(8) Å] and $Li(CH_2Ph)(tmeda)(THF)$ [2.210(5) Å], [25] but are similar to the Li-C distances in other phosphine-borane-stabilised carbanions (see above).[6, 11, 13, 14, 16-22]

The previously reported linear 1,4-dicarbanions $[[\{Ph_2P(BH_3)\}(Me_3Si)C(CH_2)]Li(THF)_3]_2\cdot 2THF$ (**53**) and $[(pmdeta)Li\{^{n}Pr_2P(BH_3)\}(Me_3Si)CCH_2]_2$ (**54**) adopt different structures to compounds **44a**-**46a** in the solid state (Scheme 3.3).[12, 18] Both **53** and **54** crystallise as discrete molecular species (the same as compounds **44a**-**46a**) and each lithium ion has contacts with the BH_3 hydrogens in an η^2-fashion at either end of the molecule. The lithium solvation sphere of **53** contains three molecules of THF whilst **54** has interactions to three nitrogen atoms in one molecule of pmdeta at each lithium ion and a crystallographic centre of inversion midway along the CH_2CH_2 bond; neither example has carbanion contacts with the lithium ion. The Li-H distances in compounds **44a** (2.08(3) and 2.03(2) Å), **45a** (2.04(2) Å) and **46a** (1.96(3) and 2.09(3) Å) are similar to those in **53** (2.13(3) and 1.97(3) Å) and **54** (1.94(3) and 2.05(3) Å).

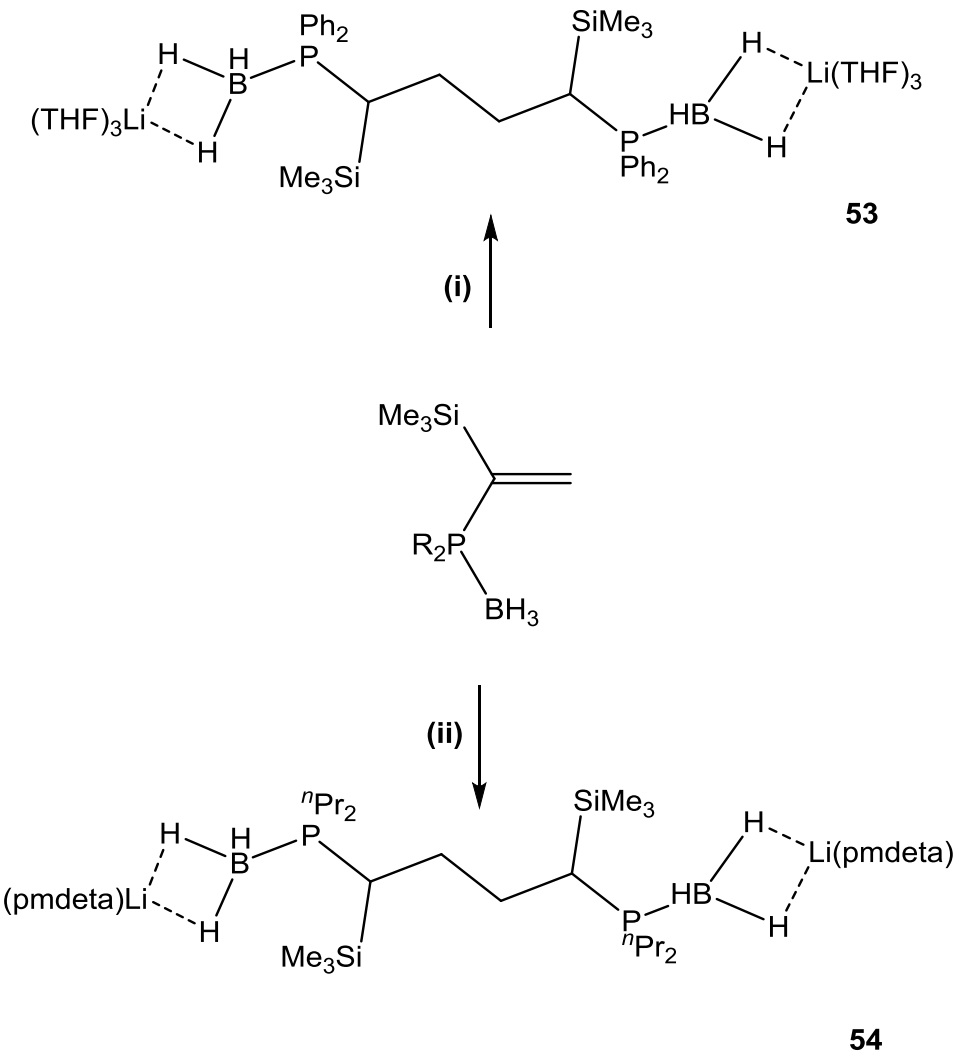

Scheme 3.3: Examples of Schlenk dimerisation to synthesise 1,4-dicarbanions. i) Li, THF. ii) Li, THF, pmdeta.

Compound **46b** also crystallises as a discrete monomer but adopts a different structure to compounds **44a**-**46a**. In compound **46b**, each potassium ion is bound to the carbanion centre, three nitrogen atoms and two carbon atoms of two methyl groups within the pmdeta co-ligand, in a η^1 fashion to the BH_3 unit and each potassium ion has additional short contacts with an *ipso* carbon atom in the *o*-phenylene linker adjacent to the carbanion centre C(5) and C(12); K(1) is also bound to the other carbanion centre and three carbon atoms of the aromatic ring whilst K(2) has short contacts to five carbon atoms within the phenylene ring and the benzylic carbon atom C(12). The molecular structure of **46b** is shown in Figure 3.8, along with selected bond lengths and angles (Table 3.6).

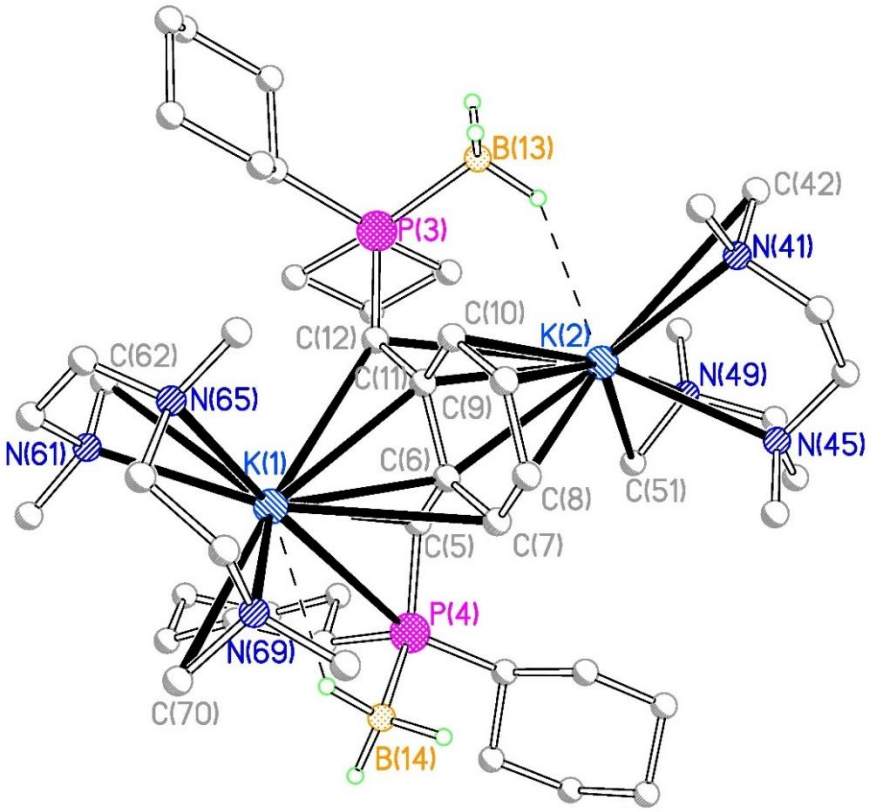

Figure 3.8: Molecular structure of **46b** with H atoms (except for those bound to boron) omitted for clarity.

K(1)-C(5)	3.1588(18)	K(2)-C(12)	3.446(2)
K(1)-C(12)	3.5133(19)	C(5)-P(4)	1.7277(17)
C(12)-P(3)	1.7252(18)	P(4)-B(14)	1.943(2)
P(3)-C(21)	1.8447(19)	P(3)-C(22)	1.8543(18)
P(4)-C(34)	1.8469(19)	P(4)-C(28)	1.8558(18)
K(1)-N(61)	2.8642(19)	K(2)-N(41)	2.8207(17)
K(1)-N(65)	2.926(5)	K(2)-N(45)	2.8914(17)
K(1)-N(69)	2.8167(18)	K(2)-N(49)	2.9092(16)
P(3)-B(13)	1.943(2)	P(4)-C(5)-C(6)	128.51(14)
		C(5)-K(1)-C(12)	50.68(4)

Table 3.6: Selected bond lengths (Å) and angles (°) for **46b**.

Compound **44b** crystallises as a discrete molecular species where the potassium ion is coordinated via the carbanion centre, by two BH_3 units in an η^2-fashion and by three nitrogen atoms of the pmdeta co-ligand. There are additional short contacts between the potassium ion and the *ipso* carbon atom of the aromatic ring adjacent to the pmdeta co-ligand.

The K(1)-C(5) bond length (3.1588(18) Å) in **46b** is similar to the K-C(carbanion) distance (3.211(8) Å) in the monosubstituted analogue [1,2-C_6H_4{$CHP(BH_3)^iPr_2$}{$CH_2P(BH_3)^iPr_2$}][K(pmdeta)] **44b**,[24] which are longer than K-C distances in previously reported carbanions which involve a benzylic centre; [25, 26] examples include $[(PhCH_2)K(pmdeta)]_\infty$[27] (K-C, 3.171(2) Å) and $[\{(Me_3Si)CH\}C_6H_4\text{-}2\text{-}NMe_2]K]_\infty$[28] (K-C, 2.966(4) Å).

3.4 Synthesis and characterisation of Group C phosphine-borane-stabilised carbanions

The benzyl-substituted phosphine-boranes $C_6H_5CH_2P(BH_3)R_2$ [R = ^{i}Pr (**47**) or Cy (**49**)] undergo α-metalation with one equivalent of ^{n}BuLi and tmeda to yield the corresponding phosphine-borane-stabilised carbanions $[C_6H_5CHP(BH_3)R_2][Li(tmeda)]$ [R = ^{i}Pr (**47a**), Cy (**49a**)] (Scheme 3.4) as judged by the $^{31}P\{^1H\}$ NMR spectra of the crude reaction solutions.

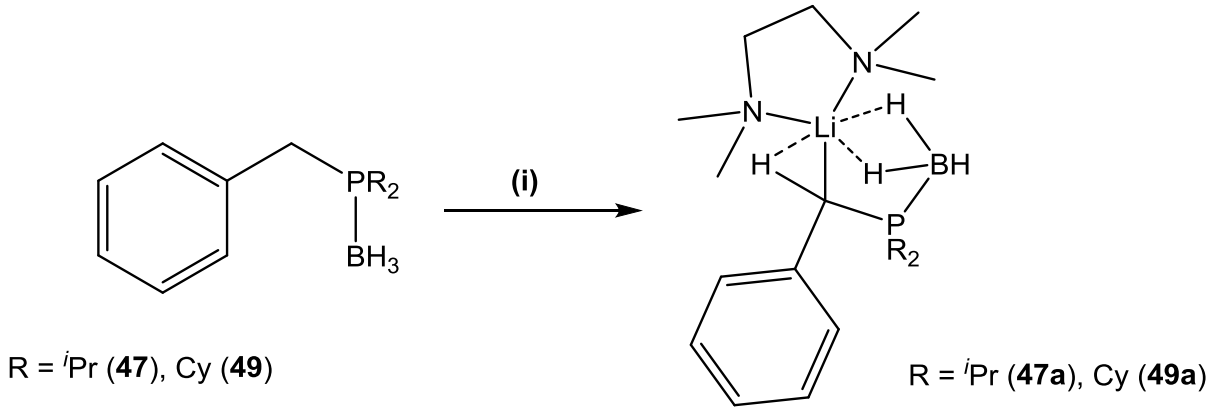

Scheme 3.4: Synthesis of **47a** and **49a**. Reagents and conditions: i) 1 eq. of ^{n}BuLi, THF, tmeda, r.t., 1 hr.

Compound **47a** has not been fully characterised due to difficulties with purification, however, the crude $^{31}P\{^1H\}$ NMR spectrum exhibits a quartet at 16.2 ppm (J_{PB} = 88.5 Hz) which is significantly different to the precursor **47** (quartet at 34.0 ppm, J_{PB} = 59.7 Hz) and

which shows a large increase in the ^{31}P-^{11}B coupling constant. Crystallisation was attempted with either tmeda or pmdeta as a co-ligand, with different solvents (Et_2O, toluene, light petroleum or methylcyclohexane) and solvent layering experiments; all of which have been attempted at different temperatures (r.t., 5 °C and -20 °C). However, unfortunately we were unable to isolate either clean samples or single crystals of **47a**. Compound **49a** was isolated as yellow single crystals suitable for X-ray crystallography from cold (5 °C) methylcyclohexane in good yield.

The $^{1}H\{^{11}B\}$, $^{11}B\{^{1}H\}$, $^{13}C\{^{1}H\}$, ^{7}Li and $^{31}P\{^{1}H\}$ NMR spectra of compound **49a** are as expected. The $^{1}H\{^{11}B\}$ NMR spectrum contains a doublet at 0.78 ppm (J_{PH} = 9.63 Hz) which is associated with the BH_3 unit; the CHLi proton is not observed in the $^{1}H\{^{11}B\}$ NMR spectrum due to the cyclohexyl substituents which give rise to a complex multiplet between 1.15 and 2.19 ppm which obscures the CHLi signal. The $^{13}C\{^{1}H\}$ NMR spectrum contains a doublet at 35.3 ppm (J_{PC} = 31.0 Hz) which corresponds to the CHLi carbon atom, the ^{7}Li NMR spectrum exhibits a singlet at 0.24 ppm and the $^{31}P\{^{1}H\}$ and $^{11}B\{^{1}H\}$ NMR spectra exhibit a quartet at 12.2 (J_{PB} = 81.5 Hz) and a doublet at -39.5 ppm (J_{PB} = 81.5 Hz), respectively. This large increase in the ^{31}P-^{11}B constant (**49**, 57.8 Hz; **49a**, 81.5 Hz) is consistent with the formation of a phosphine-borane-stabilised carbanion (see section 3.2 on Bent's rule).

In order to compare structural differences between complexes of Li and K ions the corresponding K compounds were prepared. Treatment of compounds **47** and **49** with an excess of BnK in THF results in the phosphine-borane-stabilised carbanion complexes $K[C_6H_5CHPR_2(BH_3)]$ [R = ^{i}Pr (**47b**), Cy (**49b**)]. Compounds **47b** and **49b** were isolated whilst trying to make the group 2 analogues using the method shown in Scheme 3.5; the synthesis of group 2 complexes of phosphine-borane-stabilised carbanions will be discussed in more detail in Chapter 4.

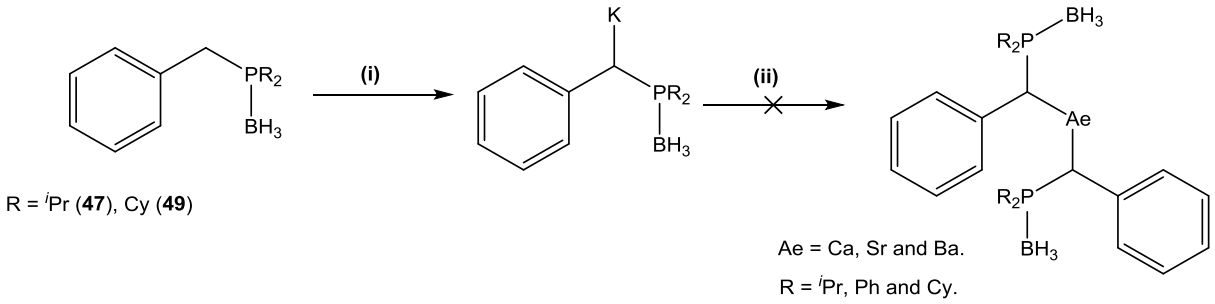

Scheme 3.5: Failed synthesis of group 2 complexes of a phosphine-borane-stabilised carbanion. Reagents and conditions: i) Excess BnK, THF, r.t., 1 hr. ii) AeI_2 (Ae = Ca, Sr and Ba), THF, r.t., 16 hr.

The $^{1}H\{^{11}B\}$, $^{11}B\{^{1}H\}$, $^{13}C\{^{1}H\}$ and $^{31}P\{^{1}H\}$ NMR spectra of compounds **47b** and **49b** are as expected. In the $^{1}H\{^{11}B\}$ NMR spectrum compound **47b** contains doublets at 0.34 ppm (J_{PH} = 13.1 Hz) and 1.83 ppm (J_{PH} = 4.8 Hz) which correspond to the BH_3 unit and the CHK fragment, respectively; the $^{11}B\{^{1}H\}$ NMR spectrum contains doublets at -41.0 ppm (J_{PB} = 81.3 Hz) and the $^{31}P\{^{1}H\}$ contains a quartet at 16.0 ppm (J_{PB} = 81.3 Hz).

In the $^{1}H\{^{11}B\}$ NMR spectrum compound **49b** contains doublets at 0.28 ppm (J_{PH} = 13.3 Hz) and 1.86 ppm (J_{PH} = 4.8 Hz) which correspond to the BH_3 unit and the CHK fragment, respectively; the $^{11}B\{^{1}H\}$ NMR spectrum contains a doublet at -40.2 ppm (J_{PB} = 79.2 Hz) and the $^{31}P\{^{1}H\}$ NMR spectrum contains a quartet at 8.80 ppm (J_{PB} = 79.2 Hz). This large increase in the ^{31}P-^{11}B coupling constant (**47**, 59.7 Hz; **47b**, 81.3 Hz; **49**, 57.8Hz; **49b**, 79.2 Hz) is consistent with the formation of a phosphine-borane-stabilised carbanion in each case.

Compounds **49a** and **49b** were isolated as single crystals suitable for X-ray crystallography. Compound **49a** crystallises as a discrete molecular species with coordination between the Li ion and the carbanion centre, BH_3 hydrogens in an η^2-fashion, the hydrogen atom associated with the carbanion centre and with the coordination sphere completed by two contacts to the two nitrogen atoms in one molecule of tmeda; the molecular structure of **49a** is shown in Figure 3.9, along with selected bond lengths (Table 3.7).

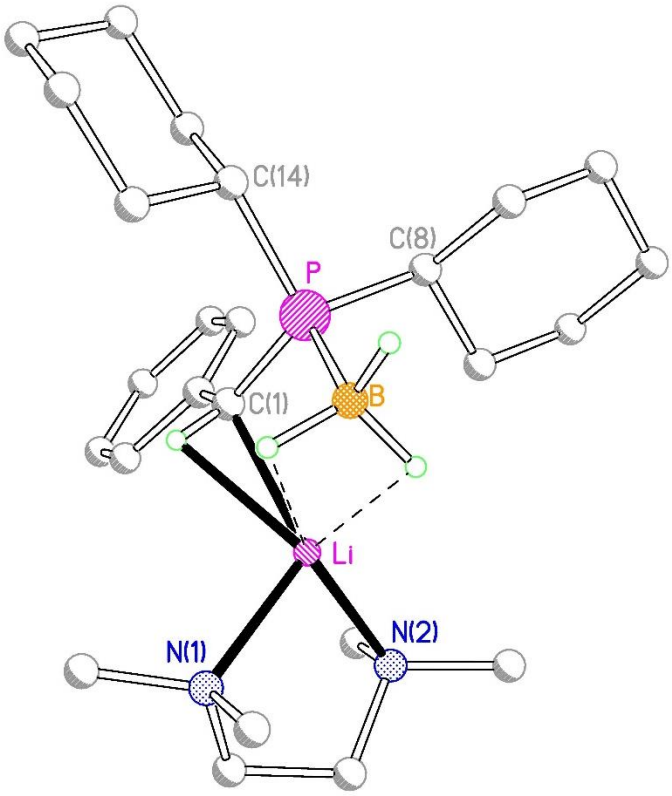

Figure 3.9: Molecular structure of **49a** with H atoms (except for those bound to boron) omitted for clarity.

Li-H(A)	2.328(16)	Li-N(1)	2.104(3)
Li-H(B)	2.035(16)	Li-N(2)	2.082(3)
Li-C(1)	2.267(3)	P-C(8)	1.8409(13)
Li-H(1)	2.130(16)	P-C(14)	1.8466(13)
P-C(1)	1.7403(14)	P-B	1.9349(16)

Table 3.7: Selected bond lengths (Å) and angles (°) for **49a**.

The Li-C(carbanion) bond length in compound **49a** (2.267(3) Å) is similar to the bond lengths in compound **46a** (2.254(6) and 2.271(6) Å); both compounds contain cyclohexyl substituents on the phosphorus atoms. Compound **49a** has longer Li-C(carbanion) contacts than compounds **40a**, **44a** and **45a** (all of which contain either phenyl or isopropyl

substituents on the phosphorus); this longer Li-C distance is consistent with the cyclohexyl groups being much larger and so elongating the Li-C(carbanion) contact.

The P-C and P-B distances in **49b** [1.7424(11) and 1.9365(13) Å, respectively] are similar to the corresponding P-C and P-B distances in **49a** [1.7403(14) and 1.9349(16) Å, respectively], however, the K-H distance in **49b** [2.82(2) Å] is significantly longer than the Li-H distances in **49a** [2.328(16) and 2.035(16) Å]; this may be attributed to the increased size of the potassium ion compared to the lithium ion.

Compound **49b** crystallises as a sheet polymer with disordered toluene molecules occupying spaces between the sheets. The packing shows bridging of the K cations by BH_3 in an η^2-fashion; along the *b*-axis, the potassium ions and phenyl rings alternate with each K ion coordinated by two η^6-coordinated rings. The asymmetric unit contains half a molecule of toluene disordered over an inversion centre; the molecular structure of **49b** is shown in Figures 3.10 and 3.11, along with selected bond lengths (Table 3.8).

Compound **49b** contains the more electropositive K ion which is also bigger in size than the Li ion in compound **49a**. It is common for K ions to complete their coordination sphere by having contacts with neighbouring sources of π-electrons due to its increased ionic radius as is seen in compound **49b**.[24]

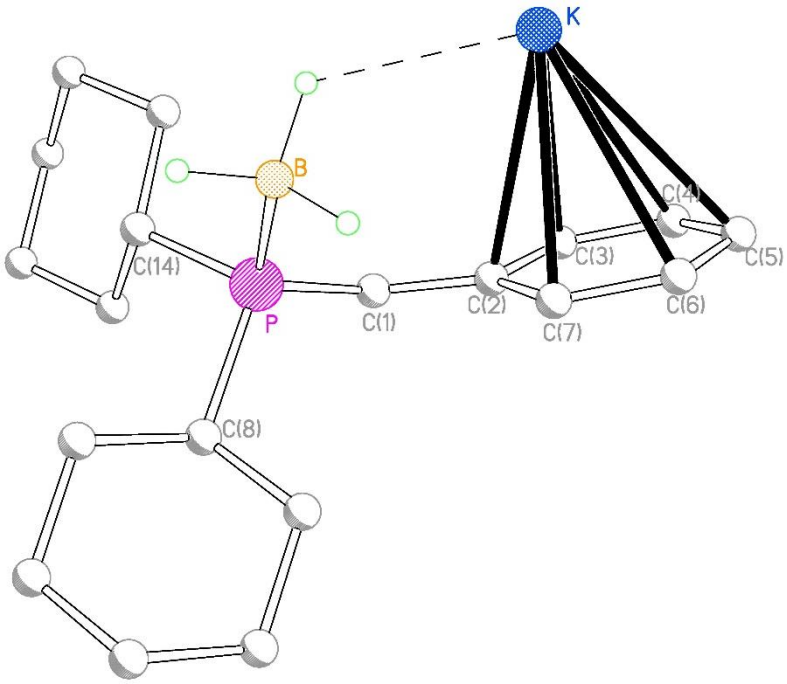

Figure 3.10: Asymmetric unit of **49b** with H atoms (except for those bound to boron) and solvent of crystallisation omitted for clarity.

K-H(OAa)	2.845(19)	P-B	1.9365(13)
K-H(OB)	2.82(2)	K-H(OCa)	2.68(2)
P-C(1)	1.7424(11)	K-C(2)	3.0205(11)
K-C(3)	3.1895(12)	K-C(4)	3.3269(12)
K-C(5)	3.3141(13)	K-C(6)	3.1574(13)
K-C(7)	3.0233(13)	K-C(2b)	3.2773(11)
K-C(3b)	3.1205(12)	K-C(4b)	3.0903(13)
K-C(5b)	3.1747(13)	K-C(6b)	3.2238(13)
K-C(7b)	3.2553(12)	K-B	3.6071(15)
K´-B	3.0152(12)		

Table 3.8: Selected bond lengths (Å) and angles (°) for **49b**.

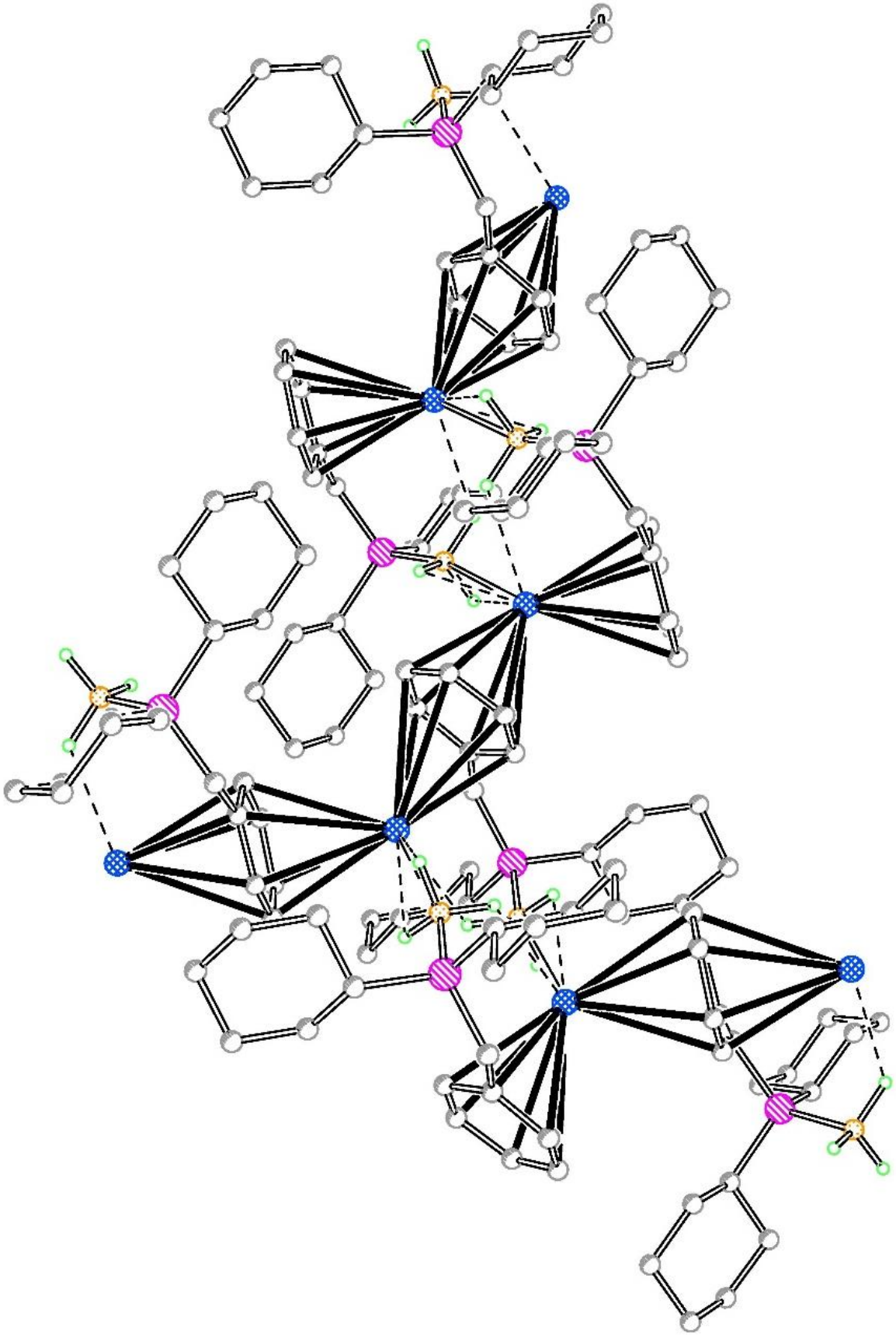

Figure 3.11: Sheet polymer structure of **49b** with H atoms (except for those bound to boron) and disordered toluene omitted for clarity.

3.5 Synthesis and characterisation of Group D phosphine-borane-stabilised carbanions

A number of different synthetic routes were attempted in order to achieve double deprotonation of the linear butylene-linked phosphine-borane $[CH_2CH_2PCy_2(BH_3)]_2$ (**51**); unfortunately, none of these were successful (Scheme 3.6).

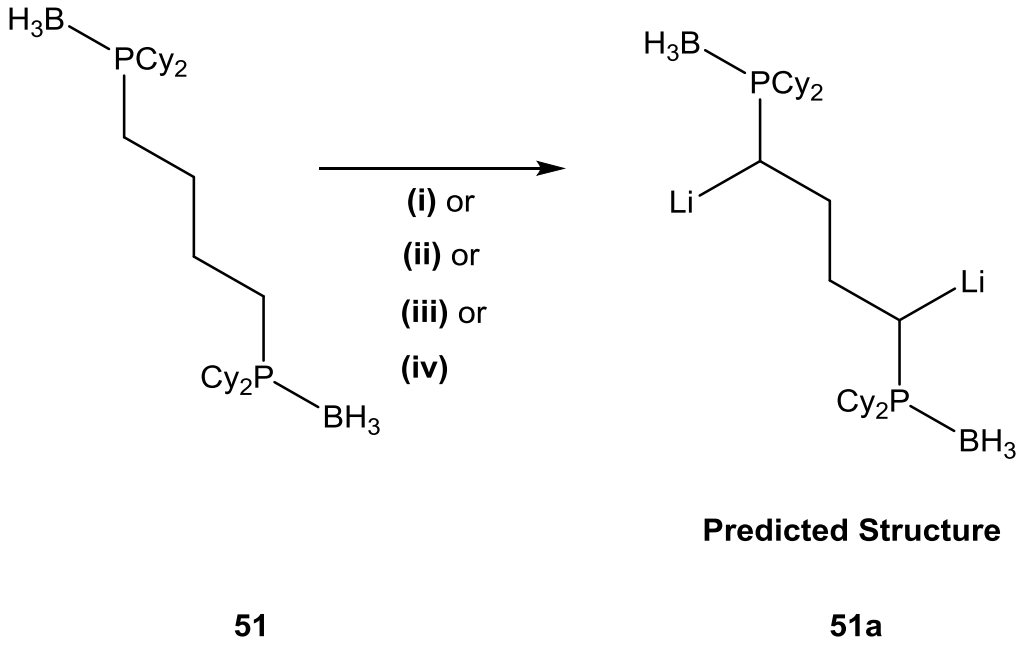

Scheme 3.6: Four different synthetic methods in the attempted deprotonation of compound **51**. Reagents and conditions: i) KO^{t}Bu, ^{n}BuLi, Et_2O. ii) ^{n}BuLi, THF, reflux 2 hrs. iii) ^{n}BuLi, tmeda, THF, reflux 2 hrs. iv) ^{t}BuLi, THF, -78 °C, 2 hrs.

The use of tmeda in a metalation reaction forms an interaction between the electropositive Li and the nitrogen atoms in the tmeda molecules (Figure 3.12); this interaction activates the ^{n}BuLi both kinetically and thermodynamically.

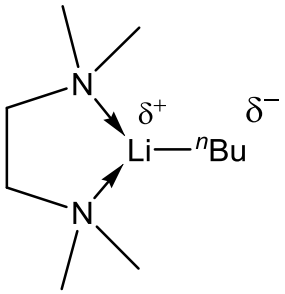

Figure 3.12: Thermodynamic and kinetic effects of tmeda with ^{n}BuLi.

The difference in reactions (i) and (ii) from Figure 3.13 is the use of tmeda in the latter method. At low temperatures or in THF an equilibrium of a mixture of dimers and tetramers of ^{n}BuLi will form whilst in hydrocarbon solvents ^{n}BuLi exists as a hexameric species.

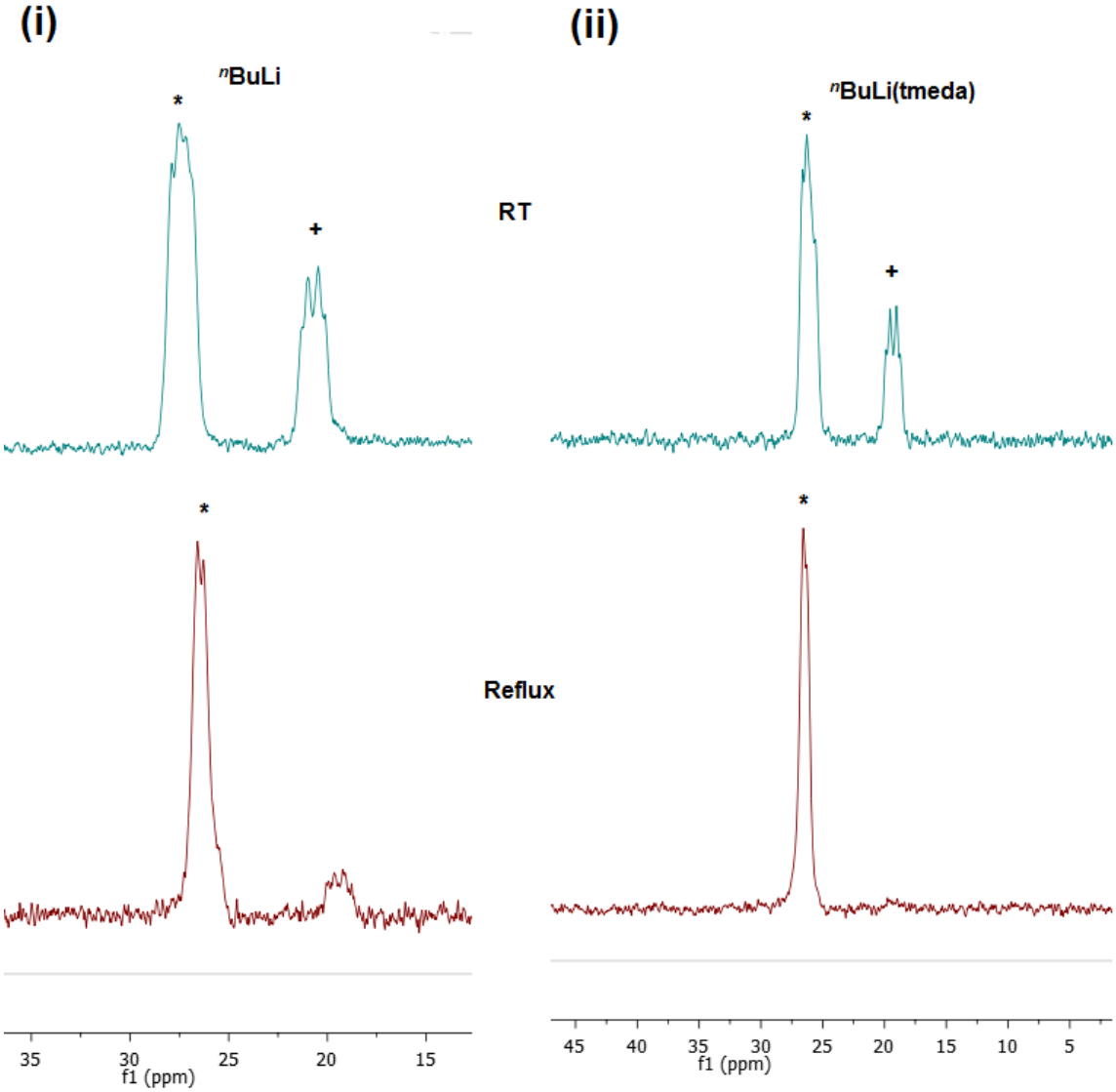

Figure 3.13: $^{31}P\{^{1}H\}$ NMR spectra of crude reaction solutions in THF. i) with ^{n}BuLi (Top) and under a 1 h reflux (Bottom). ii) with ^{n}BuLi, and tmeda (Top) and under reflux (Bottom). * Free phosphine-borane **51** and monodeprotonated phosphine-borane, + monodeprotonated phosphine-borane **51a**.

Kinetically, the organolithium is activated because the formation of these interactions between the Li ion and the nitrogen atom of the tmeda deoligormerises the oligomeric species

and so results in more reactive sites. Furthermore, the electron density located at the nitrogen atoms within the tmeda molecule is donated to the lithium centre. This leads to a greater amount of electron density at the alkyl substituent; this makes the alkyl group more electron rich and so a better nucleophile (Figure 3.12).

It can be seen from the $^{31}P\{^{1}H\}$ NMR spectra in Figure 3.13 that the metalation reactions do not go to completion and that after refluxing, any metalated compound is protonated back (usually from the solvent) to the free phosphine-borane precursor; this behaviour is the same when the reaction involving ^{t}BuLi warms up to room temperature. The instability of the phosphine-borane-stabilised carbanion may be attributed to the inductive effects of the CH_2CH_2 linker which increases the charge at the carbanion centre. Therefore, monodeprotonated **51** will exhibit an unstable carbanion with an increased charge, thus the monodeprotonated carbanion is subject to reacting with the protons from the THF solvent back to the free phosphine-borane; it is therefore, highly unlikely that compound **51** can undergo double deprotonation.

3.6 Conclusions

Compounds **40a** and **40b** both crystallise as monomeric units but adopt different structures where **40a** crystallises as a linear carbanion with an inversion centre midway along the C(2)-C(2′) bond and **40b** crystallises with a C_2 axis perpendicular to the C(2)-C(2A) bond; both **40a** and **40b** exhibit M-C(carbanion) contacts. Compounds **40a** and **52** crystallises differently, despite the isoelectronic nature of the $SiMe_3$ group with $R_2P(BH_3)$. Compound **40b** exhibits significantly longer K-C bond lengths compared to Si-substituted examples which may be attributed to either the increase in the number of contacts or the pseudo-four-membered being strained. Shortening of the C-P and C-Si bond lengths upon metalation in **40a** compared to **40b** is consistent with charge delocalisation from the carbanion centre into the C-P σ^*-orbital, or due to the increase in electron donation in the H-B···M agostic-type interactions. The lengthening of the K-H distances (2.78(6), 2.82(6) Å) compared to the Li-H distances (2.22(3) Å) in **40a** compared to **40b**, respectively, may be attributed to the increase in ionic radius of the potassium cation compared to the lithium cation.

Compounds **44a**-**46a** crystallise as discrete monomers, where **46a** and **45a** are similar to **44a** but have additional short contacts between the lithium cation and one methyl carbon atom within the tmeda co-ligand; all exhibit Li-C(carbanion) contacts.

Treatment of compound **44** with MeK yielded the monodeprotonated product **44b** due to competing reactions with MeK and the ethereal solvent; the double deprotonated product **46b** was obtained using BnK. Compounds **44b** and **46b** also crystallise as discrete monomers with K-C(carbanion) contacts but exhibit different structures to compounds **44a**-**46a** due to the increase cation size of K compared to Li, where K tends to coordinated to neighbouring sources of π-electrons.

Compounds **49a** and **49b** exhibit different solid state structures, where **49a** crystallises as a discrete monomer with Li-C(carbanion) contacts and **49b** crystallises as a sheet polymer with no K-C(carbanion) contacts. The may be attributed to the increase in cationic size in potassium compared to lithium and that potassium tends to complete its coordination sphere with neighbouring sources of π-electrons.

Compound **51** does not undergo double deprotonation due to the inductive nature of the CH_2CH_2 linker. In the crude $^{31}P\{^1H\}$ NMR for **51** the broad signals may exhibit a mixture of monodeprotonated and free phosphine-borane. When under reflux the unstable carbanion then deprotonates the THF solvent yielding free phosphine-borane, therefore, potentially unable to yield double deprotonation.

Overall, this chapter shows that phosphine-borane-stabilised carbanions adopt an array of differing crystal structures which depend on a number of different factors, such as, the phosphorus substituents, the size of the alkali metal, the presence of either a rigid or a flexible backbone linker and whether co-ligands (THF, tmeda or pmdeta) to the metal centre (Li or K) were used.

3.7 References

1. T. Imamoto, *Pure Appl. Chem.*, 1993, **65**, 655-660.
2. A. R. Muci, K. R. Campos and D. A. Evans, *J. Am. Chem. Soc.*, 1995, **117**, 9075-9076.
3. J. M. Brunel, B. Faure and M. Maffei, *Coord. Chem. Rev.*, 1998, **178**, 665-698.
4. M. Ohff, J. Holz, M. Quirmbach and A. Borner, *Synthesis-Stuttgart*, 1998, 1391-1415.
5. B. Carboni and L. Monnier, *Tetrahedron*, 1999, **55**, 1197-1248.
6. K. Izod, C. Wills, W. Clegg and R. W. Harrington, *Organometallics*, 2007, **26**, 2861-2866.
7. D. E. Goldberg, D. H. Harris, M. F. Lappert and K. M. Thomas, *J. Chem. Soc. Chem. Commun.*, 1976, 261-262.
8. K. Izod, C. Wills, W. Clegg and R. W. Harrington, *Organometallics*, 2009, **28**, 5661-5668.
9. J. E. Huheey, E. A. Keiter and R. L. Keither, *Inorganic Chemistry-Principles of Structure and Reactivity*, 4 edn., HarperCollins College Publishers, 1993, 225-229.
10. H. Friebolin, *Basic One- and Two-Dimensional NMR Spectroscopy*, Wiley-VCH, 2005, Chapter 3.2.
11. H. Schmidbaur and E. Weiss, *Angew. Chem. Int. Ed. Engl.*, 1979, **18**, 781-782.
12. K. Izod, W. McFarlane, B. V. Tyson, W. Clegg and R. W. Harrington, *Chem. Commun.*, 2004, 570-571.
13. X. M. Sun, K. Manabe, W. W. L. Lam, N. Shiraishi, J. Kobayashi, M. Shiro, H. Utsumi and S. Kobayashi, *Chem. Eur. J.*, 2005, **11**, 361-368.
14. K. Izod, C. Wills, W. Clegg and R. W. Harrington, *Organometallics*, 2006, **25**, 5326-5332.
15. K. Izod, C. Wills, W. Clegg and R. W. Harrington, *Inorg. Chem.*, 2007, **46**, 4320-4325.
16. K. Izod, C. Wills, W. Clegg and R. W. Harrington, *Dalton Trans.*, 2007, 3669-3675.
17. K. Izod, C. Wills, W. Clegg and R. W. Harrington, *J. Organomet. Chem.*, 2007, **692**, 5060-5064.
18. K. Izod, L. J. Bowman, C. Wills, W. Clegg and R. W. Harrington, *Dalton Trans.*, 2009, 3340-3347.
19. J. Langer, K. Wimmer, H. Goerls and M. Westerhausen, *Dalton Trans.*, 2009, 2951-2957.
20. L. Orzechowski, G. Jansen, M. Lutz and S. Harder, *Dalton Trans.*, 2009, 2958-2964.

21. K. Izod, C. Wills, W. Clegg and R. W. Harrington, *Organometallics*, 2010, **29**, 4774-4777.
22. J. Langer, V. K. Palfi, H. Gorls, M. Reiher and M. Westerhausen, *Chem. Commun.*, 2013, **49**, 1121-1123.
23. C. Eaborn, Z. R. Lu, P. B. Hitchcock and J. D. Smith, *Organometallics*, 1996, **15**, 1651-1655.
24. K. Izod, C. M. Dixon, E. McMeekin, L. Rodgers, R. W. Harrington and U. Baisch, *Organometallics*, 2014, **33**, 378-386.
25. A. Torvisco and K. Ruhlandt-Senge, *Inorg. Chem.*, 2011, **50**, 12223-12240.
26. J. D. Smith, *Adv. Organomet. Chem.*, 1999, **43**, 267-348.
27. B. C. Menon, H. F. Shurvell, J. P. Colpa and E. Buncel, *J. Mol. Struct.*, 1982, **78**, 29-41.
28. F. Feil and S. Harder, *Organometallics*, 2001, **20**, 4616-4622.

Chapter 4. Group 2 Phosphine-borane-stabilised carbanions

4.1 Introduction

Since analytical tools, such as NMR spectroscopy and X-ray crystallography, have improved greatly over the last 20 years, interest in heavier alkaline earth metal complexes has increased.[1-8] However, a common problem in group 2 complexes is their tendency to aggregate (due to their large ionic radii), resulting in insoluble products in organic solvents. To overcome this problem silicon-containing substituents are often used to disfavour aggregation and also to decrease the carbanion character of the ligand through negative hyperconjugation. The diorganophosphine-borane group $PR_2(BH_3)$ is isoelectronic and isosteric with the SiR_2Me substituent and so by substituting the silyl groups with phosphine-borane groups, the aggregation properties can be explored. It is surprising, however, that despite the isoelectronic and isosteric nature of these groups, little is known about heavier alkaline earth metal complexes of phosphine-borane-stabilised carbanions compared to their silyl-containing analogues.[9-13]

Izod and co-workers have previously carried out investigations in order to see the structural characteristics of the alkaline earth metal complexes of phosphine-borane-stabilised carbanions. Coordination of the metal by agostic-type interactions (B-H···Ae, Ae = Ca, Sr, Ba) dominates, however, complexes of silicon- and phosphine-borane-stabilised carbanions exhibit both agostic interactions and C-Ae contacts; the work carried out in this chapter is very much in its infancy but three different methods of synthesising group 2 complexes are reported herein.

4.2 Organolithium as a reagent

Treatment of one equivalent of *in situ* generated $Li_2[Me_2P(BH_3)CHSi(Me_2)CH_2]_2$ (**37a**) or two equivalents of $[(Me_3Si)CHP(BH_3)Me_2]Li$ with one equivalent of $MgCl_2$ in THF yields a colourless (***rac*-37c** and ***meso*-37c**) or a pale yellow (**55b**) solution, respectively. Both crude reaction mixtures of reactions 1 and 2 (Scheme 4.1) were extracted into diethyl ether, and $^{31}P\{^1H\}$ NMR spectra were recorded.

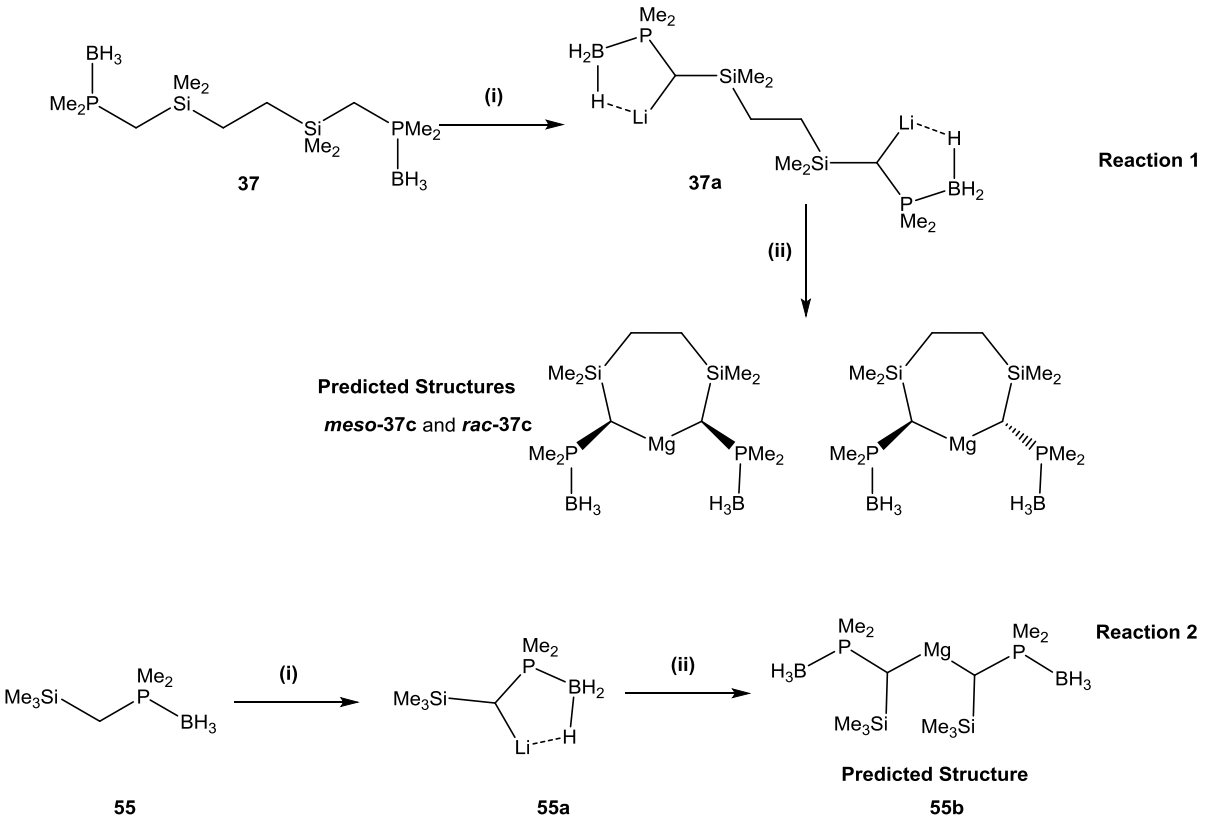

Scheme 4.1: Synthesis of alkaline earth metal complexes ***rac*-37c** and, ***meso*-37c** and **55b** (predicted structures). Reaction conditions. i) ^{n}BuLi, THF. ii) $MgCl_2$, THF.

The $^{31}P\{^{1}H\}$ NMR spectrum for unpurified ***rac*-37c** and ***meso*-37c** shows a broad multiplet at 4.6 ppm. Unfortunately, after repeated attempts at recrystallisations using diethyl ether and hot toluene, no solid was isolated.

The $^{31}P\{^{1}H\}$ NMR spectrum of unpurified **55b** (Figure 4.1) shows a broad quartet at 2.9 ppm. This broad quartet is due mainly to the free phosphine-borane precursor **55**, along with an unidentified product overlapping with the signal associated with **55**. Unfortunately, no solid was isolated after repeated attempts using diethyl ether and hot toluene and so it was not possible to fully investigate the unidentified product.

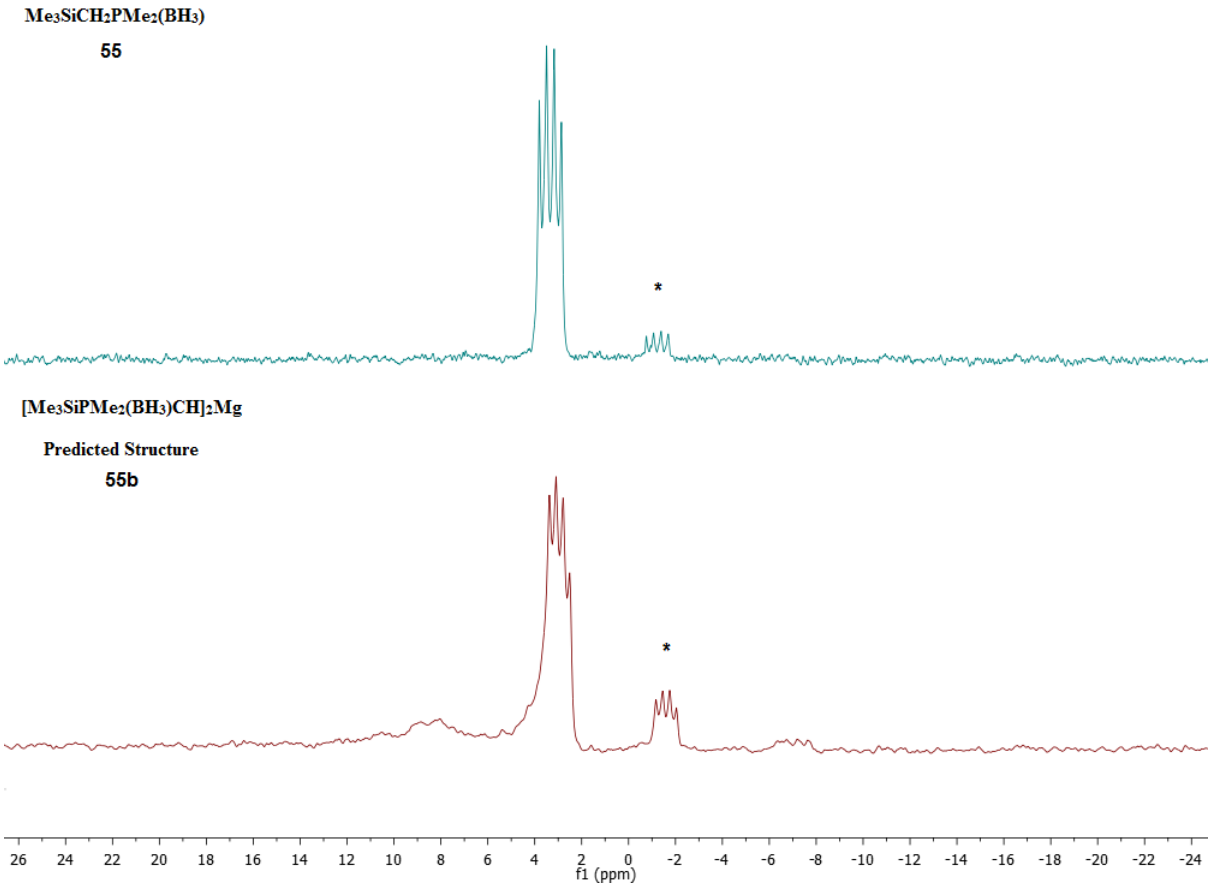

Figure 4.1: Crude $^{31}P\{^{1}H\}$ NMR spectra of **55** and **55b** in diethyl ether. *$PMe_3(BH_3)$

Treatment of two equivalents of *in situ* generated $Li[C_6H_5CHPCy_2(BH_3)]$ (**49a**) with one equivalent of AeI_2 (Ae = Ca, Sr) in THF yields yellow solutions of compounds **49c** and **49d** (Scheme 4.2).

The $^{31}P\{^{1}H\}$ NMR spectrum for unpurified **49c** and **49d** exhibit broad multiplets at 8.7 and 36.2 ppm, respectively. Unfortunately, after repeated attempts at recrystallisations using diethyl ether and hot toluene, no solid was isolated.

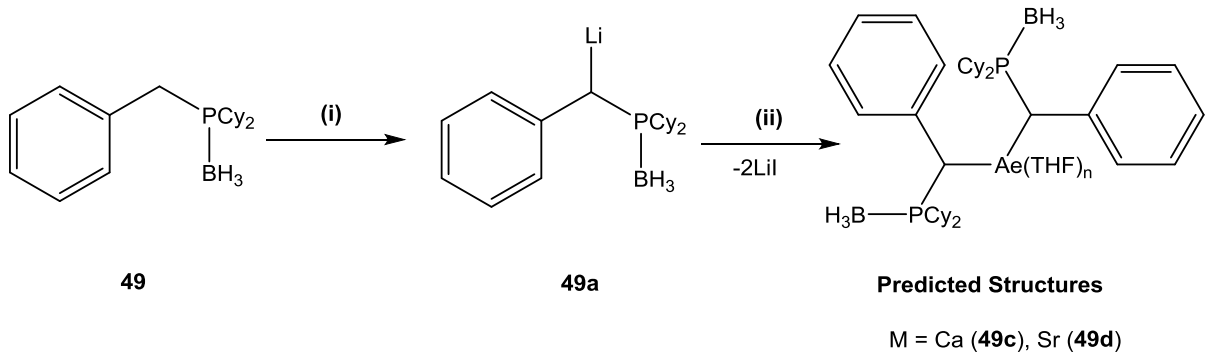

Scheme 4.2: Synthetic route for **49c** and **49d**. Reaction conditions. i) ^{n}BuLi, THF. ii) AeI_2, THF (Ae = Ca, Sr).

It is widely known that organolithiums have a tendency to form anionic 'ate' complexes when reacted with heavier group 2 halides.[14] In order to preclude this as a potential side reaction in the synthesis of group 2 phosphine-borane-stabilised carbanion compounds we set out to explore the use of organopotassium precursors, which do not normally yield ate complexes in their reactions with group 2 halides.

4.3 Benzylpotassium as a reagent

Treatment of two equivalents of *in situ* generated $K[C_6H_5CHPR_2(BH_3)]$ [R = ^{i}Pr (**47b**), Cy (**49b**)] with one equivalent of AeI_2 (Ae = Mg, Ca, Sr, Ba) in THF yields yellow solutions, presumably of compounds **47c**-**47f**, **49** (Scheme 4.3).

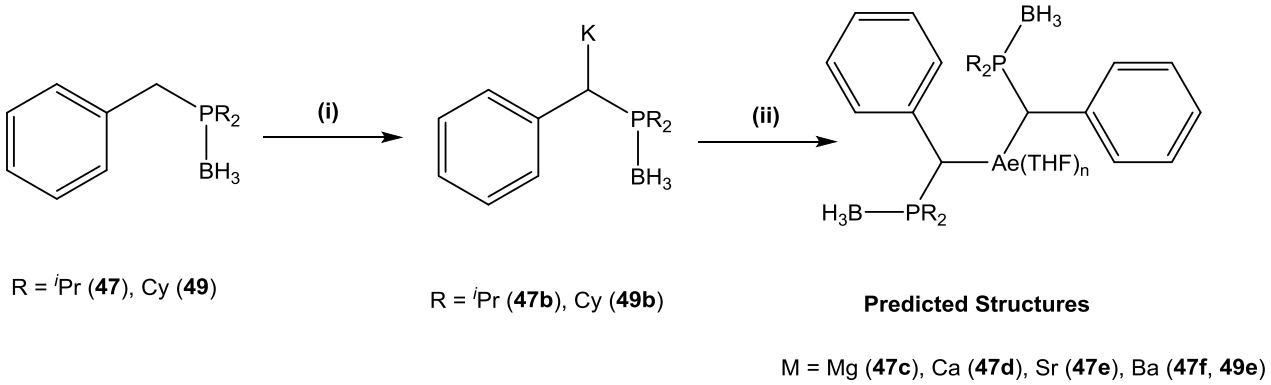

Scheme 4.3: Synthesis of **47c**, **47d**, **47e**, **47f** and **49e**. Reaction conditions. i) BnK, THF. ii) AeI_2, THF (Ae = Mg, Ca, Sr, Ba).

Recrystallisation of **47d-47f** using toluene yielded yellow crystalline solids which unfortunately, were not suitable for X-ray crystallography, however, did aid in gaining some NMR spectra. The $^{31}P\{^{1}H\}$ NMR spectra of compounds **47d-47f** exhibit quartets at 16.0 ppm (J_{PB} = 92.7 Hz) (Figure 4.2). The similarity in the $^{31}P\{^{1}H\}$ NMR spectra may be attributed to unreacted **47b** ($^{31}P\{^{1}H\}$ signal at 16.0 ppm, J_{PB} = 81.3 Hz), however, it is quite common for chemical shifts and coupling constants to not change significantly when converting from the potassium salt to the alkaline earth metal derivative.[15]

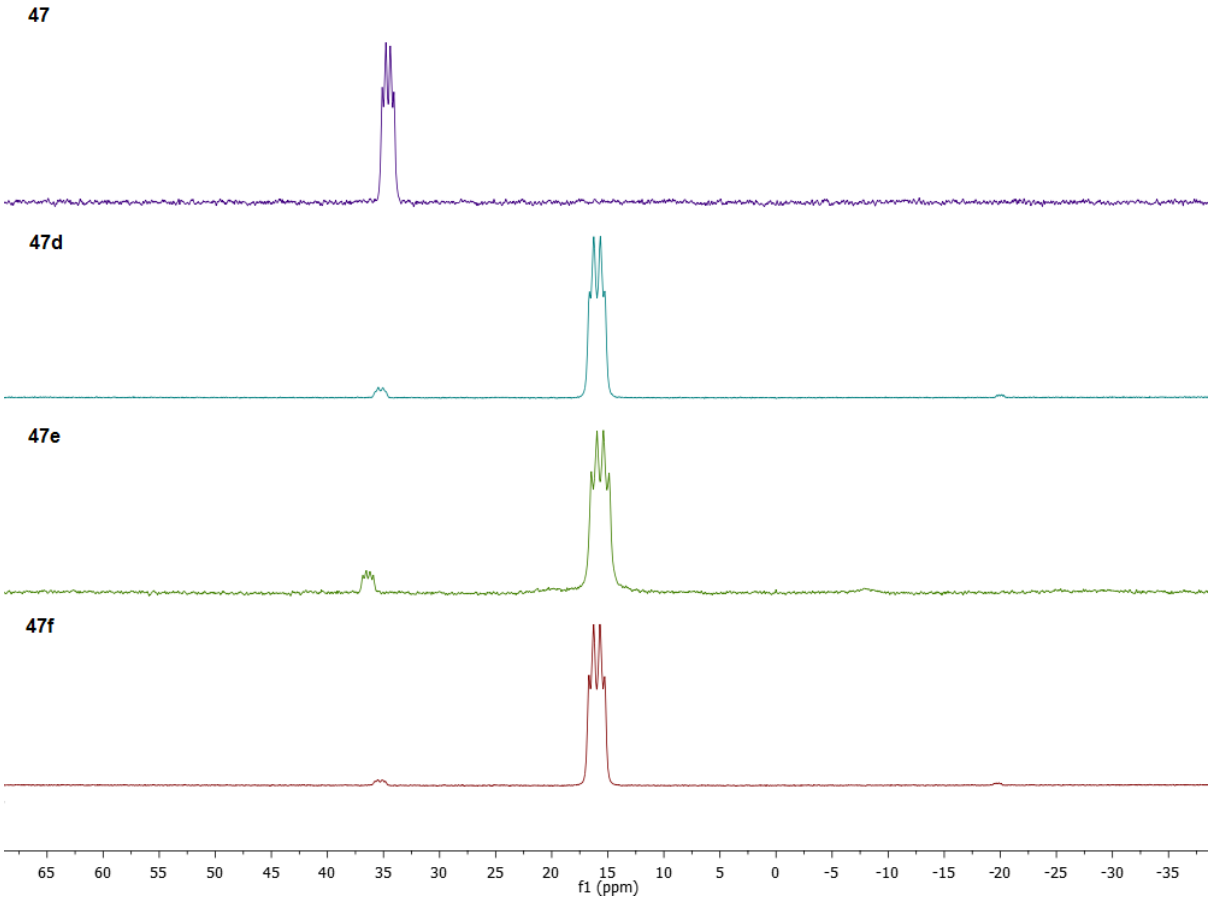

Figure 4.2: $^{31}P\{^{1}H\}$ NMR spectra for **47** and crude samples of **47d-47f** in THF.

The ^{1}H NMR spectra for **47d** (Figure 4.3) and **47f** show no THF signals which is unusual and not what would be expected for a group 2 complex due to the large ionic radii of the group 2 ions. Considering the similarity in the $^{31}P\{^{1}H\}$ NMR spectra of **47d**, **47e** and **47f** and that no THF remains coordinated to the metal centre suggests that in these reactions the predicted group 2 compounds are not formed and that the isolated solid is just the unreacted potassium compound **47b**.

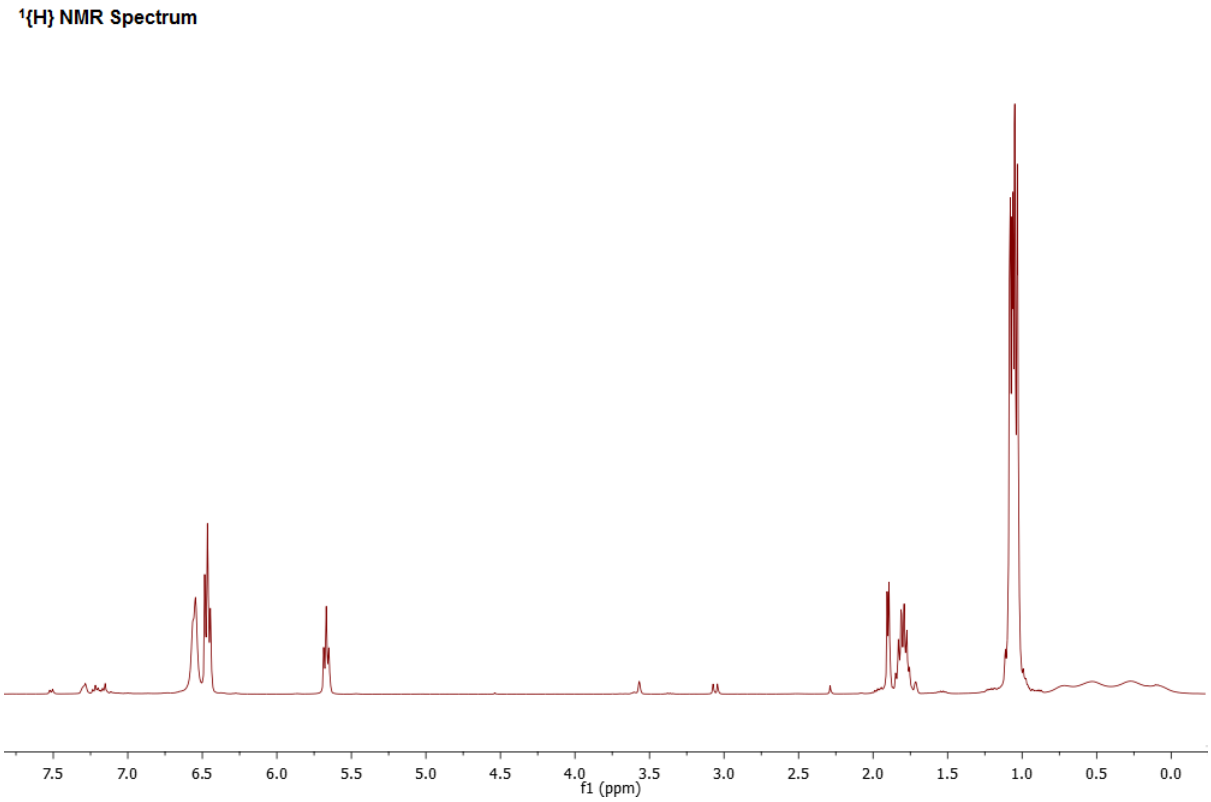

Figure 4.3: The ^{1}H NMR spectrum of crystalline **47d** in d_8-THF.

4.4 Dibenzylcalcium, -strontium and –barium as a reagent

Treatment of one equivalent of $(PhCH_2)_2Ae(THF)_n$, (Ae = Ca, n = 2; Sr, n = 1; Ba, n = 0.5) with two equivalents of **47** or **49** in THF yields yellow solutions, presumably of compounds **47g**-**47h** and **49f**-**49g** (Scheme 4.4).

The crude $^{31}P\{^1H\}$ NMR spectra for compounds **47g** and **47h** in THF show broad quartets at 17.3 ppm (J_{PB} = 98.7 Hz) and 15.9 ppm (J_{PB} = 102.0 Hz), respectively (Figure 4.4); the $^{31}P\{^1H\}$ NMR signals are shifted compared to **47b** (16.0ppm, J_{PB} = 93.9 Hz). In particular, the change in the ^{31}P-^{11}B coupling constants of **47b**, **47g** and **47h** may further verify **47g** and **47h** are the calcium and strontium complexes of the respective phosphine-borane-stabilised carbanions.

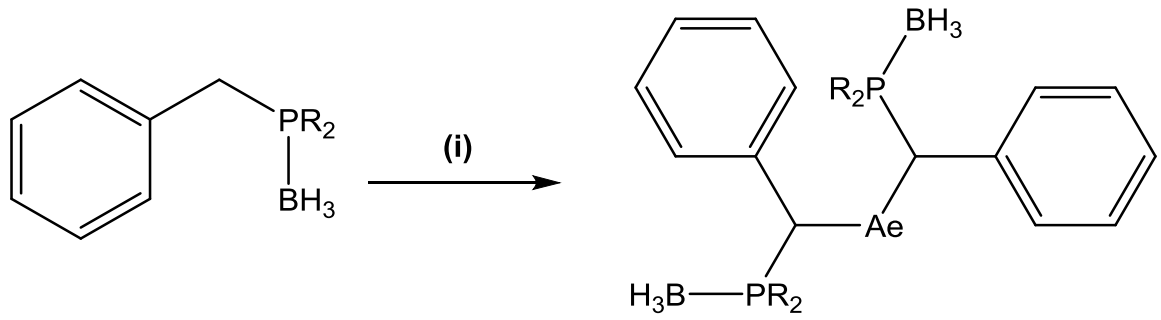

R = ^{i}Pr (**47**), Cy (**49**) Ae = Ca (**47g**, **49f**), Sr (**47h**, **49g**)

Scheme 4.4: Synthetic route for compounds **47g**-**47h** and **49f**-**49g**. Reaction conditions. i) $(PhCH_2)_2Ae(THF)_n$, (Ae = Ca, n = 2; Sr, n = 1; Ba, n = 0.5), THF.

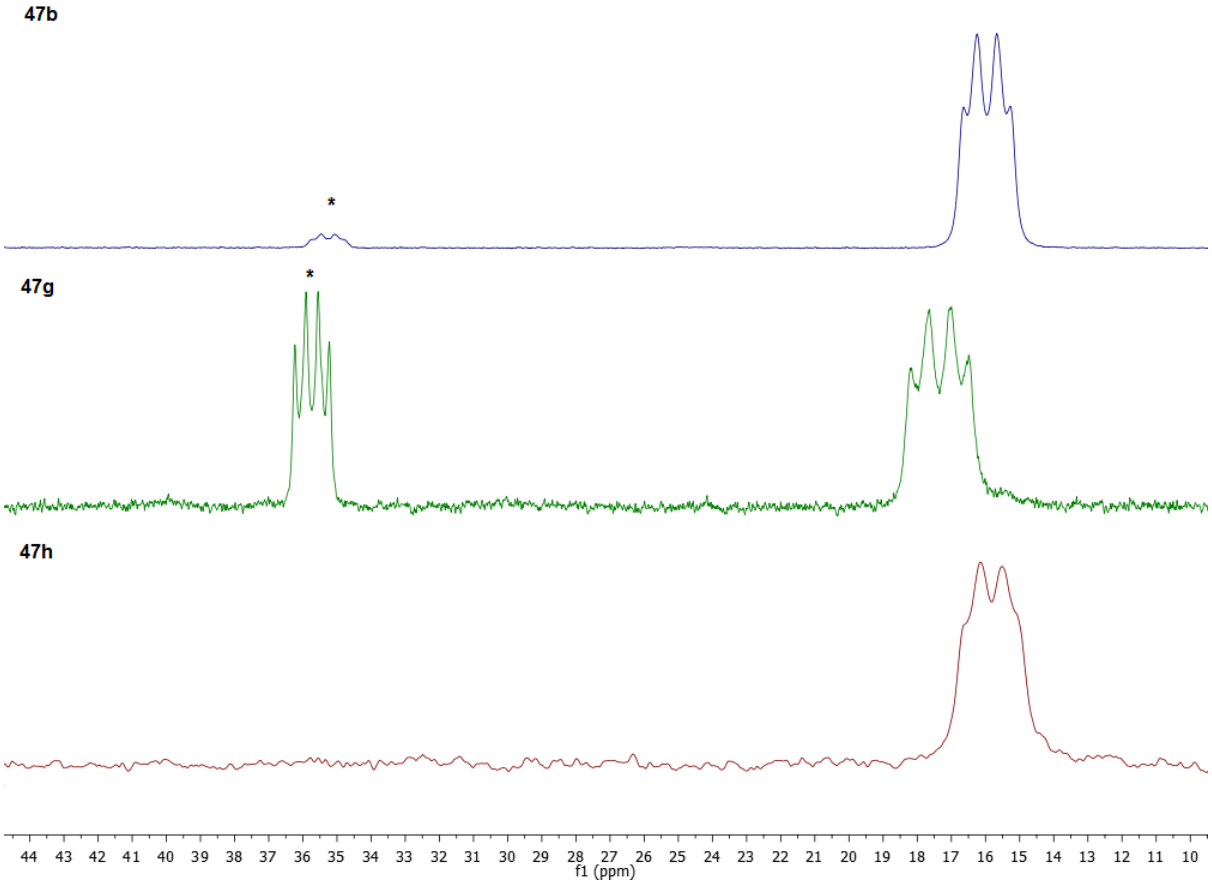

Figure 4.4: Crude $^{31}P\{^{1}H\}$ NMR spectra for compounds **47g** and **47h** in THF compared with the $^{31}P\{^{1}H\}$ NMR spectrum for compound **47b** THF. * Free phosphine-borane (**47**)

Unfortunately, after many attempts to isolate single crystals of **47g** and **47h** using many different solvents, no solid material was isolated and so a ^{1}H NMR was not recorded in order to see if THF was present; this could further indicate if **47g** and **47h** are alkaline earth metal complexes. However, previously reported compounds $[[PhP(BH_3)\{CH(SiMe_3)\}_2]Ca(OEt_2)]_2$ (**56**) and $[[PhP(BH_3)\{CH(SiMe_3)\}_2]Sr(THF)_{1.75}(OEt_2)_{0.25}]_2$ (**57**)[13] exhibit broad multiplets at 6.5 ppm (J_{PB} = 91.0 Hz) and 5.0 ppm (J_{PB} = 106.0 Hz) in their $^{31}P\{^{1}H\}$ NMR spectra where the ^{31}P-^{11}B coupling constants of **47g** and **47h** are remarkably similar to the coupling constants of both **56** and **57**. This huge rise in the ^{31}P-^{11}B coupling constant on metalation is also consistent with many examples of previously reported α-metalated phosphine-borane-stabilised carbanions.[9, 15-22]

The $^{31}P\{^{1}H\}$ NMR spectrum for compound **47g** (Figure 4.4) also exhibits a quartet at 35.7 ppm (J_{PB} = 98.7 Hz) which is associated with the free phosphine-borane **47**. The presence of **47** may be attributed to the decomposition of **47g** in THF at room temperature which is relatively common in alkaline earth metal complexes of phosphine-borane-stabilised carbanions.[13] It is not, however, clear what the decomposition pathway is but it may be due to the increased charge/size ratio of the calcium ion, which activates protons bound to the THF solvent which is coordinated to the metal centre.

The $^{31}P\{^{1}H\}$ NMR spectrum of **49g** (Figure 4.5) exhibits a broad quartet at 8.8 ppm (J_{PB} = 93.9 Hz) which is similar to that of the potassium complex **49b** (8.7 ppm, J_{PB} = 97.1 Hz). Compound **49** reacts with *in situ* generated $Bn_2Sr(THF)_2$; where $Bn_2Sr(THF)_2$ was synthesised using an excess of BnK. Single crystals suitable for X-ray crystallography from toluene were found to be the potassium complex **49b** which may be attributed to the *in situ* use of an excess of BnK. There are two pathways that could explain this:

1. Either $Bn_2Sr(THF)_2$ is decomposing in the THF solvent, and so, the excess BnK is reacting with the phosphine-borane precursor **49**.
2. Or that **49g** is being made, however, it deprotonates the solvent, resulting in the phosphine-borane precursor **49;** which then later reacts with the excess BnK to form **49b**.

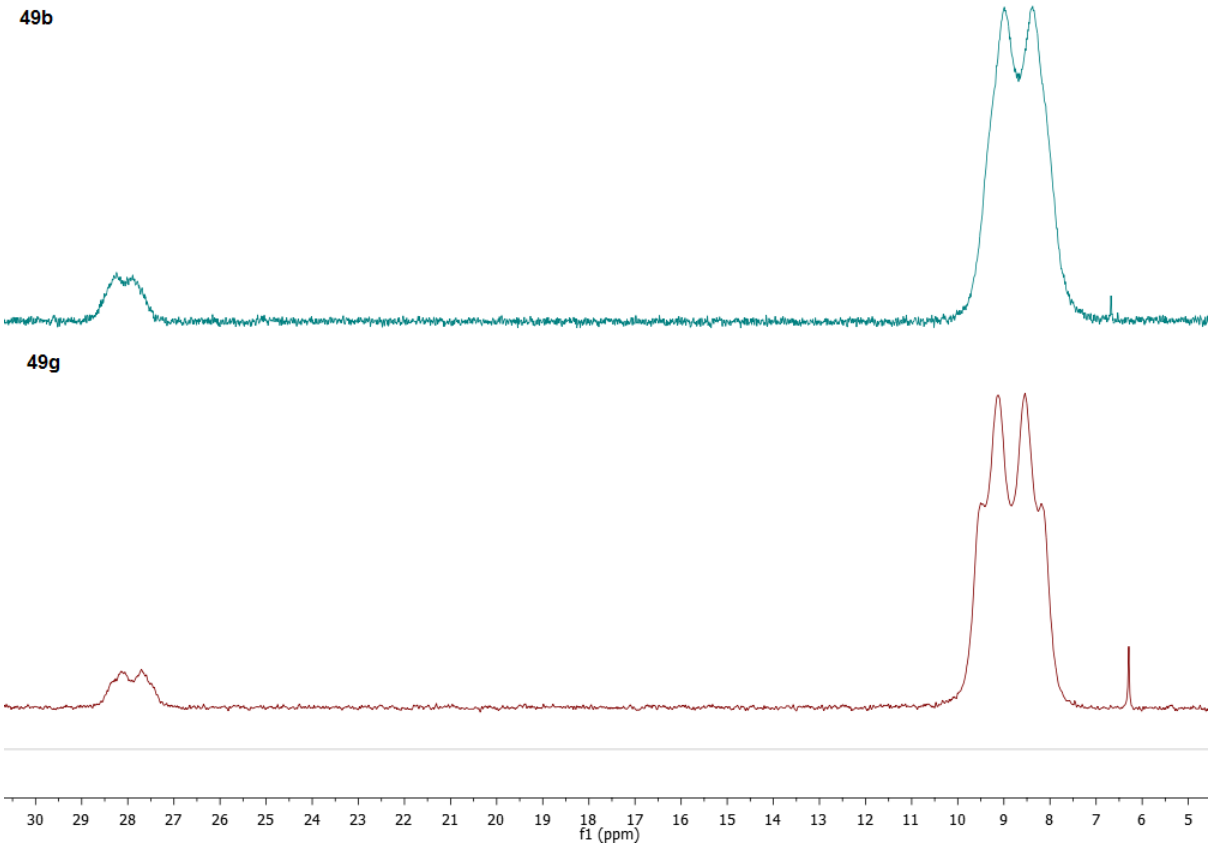

Figure 4.5: The $^{31}P\{^{1}H\}$ NMR spectrum of **49g** compared with **49b** in THF.

4.5 Conclusion

To summarise, this chapter provides an overview of three different synthetic routes to synthesise alkaline earth metal complexes of phosphine-borane-stabilised carbanions. The first method, using organolithiums is not commonly used in the synthesis of heavier group 2 complexes as this route has a tendency to form anionic 'ate' complexes. The second method, using benzylpotassium, is a fairly common synthetic approach, however, more investigations are needed in order to optimise the reactions conditions as unreacted **49b** is isolated. The third method, using dibenzylcalcium, -strontium and –barium is a relatively new approach to synthesising group 2 complexes and so is very much in its infancy, however, this synthetic approach seems to be the most promising method. There are still potential issues in terms of decomposition, especially with the calcium complex **47g** in THF solutions as there is the potential for deprotonation of the solvent molecules bound to the calcium metal centre, resulting in elimination of the phosphine-borane precursor **47**. It also seems vital that the dibenzylcalcium, -strontium and –barium complexes need to be isolated before reacting with phosphine-boranes as, if these are reacted *in situ*, any excess BnK that was used to synthesise

the group 2 complexes will compete and so react with the phosphine-borane precursors; hence resulting in the isolation of **49b**.

4.6 References

1. T. P. Hanusa, *Coord. Chem. Rev.*, 2000, **210**, 329-367.
2. J. S. Alexander and K. Ruhlandt-Senge, *Eur. J. Inorg. Chem.*, 2002, 2761-2774.
3. J. S. Alexander and K. Ruhlandt-Senge, *Chem. Eur. J.*, 2004, **10**, 1274-1280.
4. M. Westerhausen, *Dalton Trans.*, 2006, 4755-4768.
5. M. Westerhausen, M. Gaertner, R. Fischer and J. Langer, *Angew. Chem. Int. Ed.*, 2007, **46**, 1950-1956.
6. M. Westerhausen, M. Gartner, R. Fischer, J. Langer, L. Yu and M. Reiher, *Chem. Eur. J.*, 2007, **13**, 6292-6306.
7. M. Westerhausen, *Z. Anorg. Allg. Chem.*, 2009, **635**, 13-32.
8. C. Zeppek, J. Pichler, A. Torvisco, M. Flock and F. Uhlig, *J. Organomet. Chem.*, 2013, **740**, 41-49.
9. K. Izod, C. Wills, W. Clegg and R. W. Harrington, *Inorg. Chem.*, 2007, **46**, 4320-4325.
10. J. Langer, K. Wimmer, H. Goerls and M. Westerhausen, *Dalton Trans.*, 2009, 2951-2957.
11. L. Orzechowski, G. Jansen, M. Lutz and S. Harder, *Dalton Trans.*, 2009, 2958-2964.
12. J. Langer, V. K. Palfi, H. Gorls, M. Reiher and M. Westerhausen, *Chem. Commun.*, 2013, **49**, 1121-1123.
13. K. Izod, C. Wills, S. El-Hamruni, R. W. Harrington, P. G. Waddell and M. R. Probert, *Organometallics*, 2015, **34**, 2406-2414.
14. J. L. Wardell, *Comprehensive Organometallic Chemistry I*, Vol. 1, Eds: E. Abel, F. G. A. Stone, G. Wilkinson, Chapt. 2, Elsevier, 1982.
15. K. Izod, C. Wills, W. Clegg and R. W. Harrington, *Organometallics*, 2006, **25**, 38-40.
16. K. Izod, C. Wills, W. Clegg and R. W. Harrington, *Organometallics*, 2006, **25**, 5326-5332.
17. K. Izod, C. Wills, W. Clegg and R. W. Harrington, *Organometallics*, 2007, **26**, 2861-2866.
18. K. Izod, C. Wills, W. Clegg and R. W. Harrington, *Dalton Trans.*, 2007, 3669-3675.
19. K. Izod, C. Wills, W. Clegg and R. W. Harrington, *J. Organomet. Chem.*, 2007, **692**, 5060-5064.
20. K. Izod, L. J. Bowman, C. Wills, W. Clegg and R. W. Harrington, *Dalton Trans.*, 2009, 3340-3347.

21. K. Izod, C. Wills, W. Clegg and R. W. Harrington, *Organometallics*, 2010, **29**, 4774-4777.
22. H. Heuclin, M. Fustier-Boutignon, S. Y. F. Ho, X. F. Le Goff, S. Carenco, C. W. So and N. Mezailles, *Organometallics*, 2013, **32**, 498-508.

Chapter 5. Impact of a rigid backbone on the structure of an agostically-stabilised dialkylstannylene

5.1 Introduction

Recently, Izod and co-workers have investigated the extent to which agostic stabilisation of dialkylstannylenes inhibits their dimerisation. For example, $[(Me_3Si)\{Me_2P(BH_3)\}HC]_2Sn$ (**34**) (Figure 5.1), exhibits two stabilising B-H···Sn interactions and adopts a monomeric structure, whereas, $\{(Me_3Si)_2CH\}_2Sn$ (**28**),[1] which is isoelectronic and isosteric with compound **34** and in which such agostic-type interactions are absent, dimerises to the corresponding distannene in the solid state (Scheme 5.1).

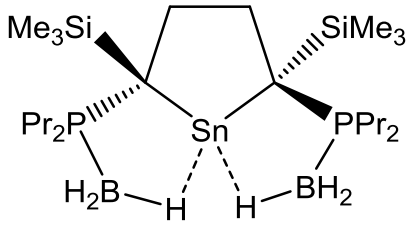

(**32**)

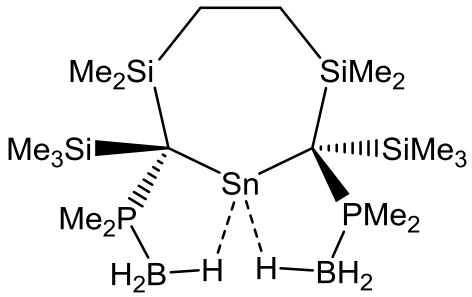

(**33**)

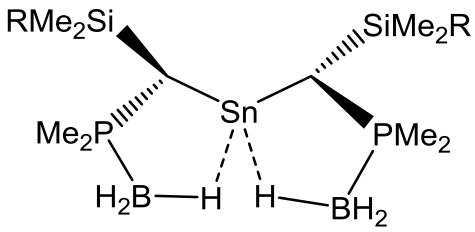

R = Me (**34**) and Ph (**35**)

Figure 5.1: Dialkylstannylenes exhibiting agostic-type stabilisation interactions.

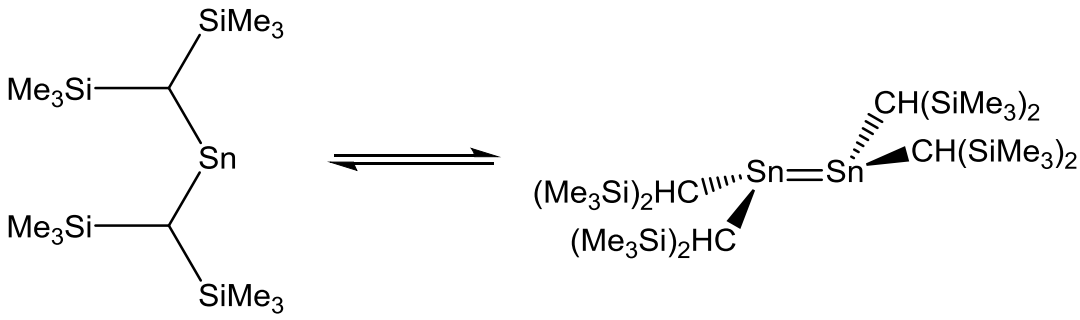

Scheme 5.1: Monomeric dialkylstannylene and the corresponding distannene.

In all of the dialkylstannylenes that Izod and co-workers have isolated (Figure 5.1), the supporting ligand is either monodentate (**34** and **35**), or has a flexible spacer group linking the two carbanion centres (**32** and **33**). This flexible spacer allows the phosphine-borane group to tilt towards the Sn centre, maximising the overlap between the B-H σ- orbital and the vacant p-orbital at Sn and so providing stabilisation at the electron deficient Sn(II) centre (Figure 5.2).

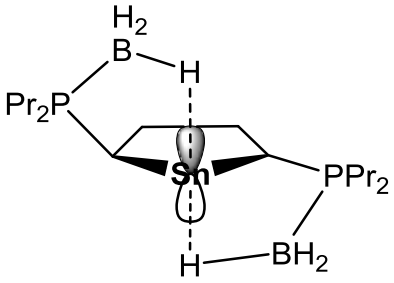

Figure 5.2: Compound **32** and orbital overlap between the B-H unit and the vacant p-orbital of Sn.

Previously reported work by Izod and co-workers and the work described in this chapter has begun to investigate the chemistry of phosphine-borane-stabilised dicarbanions in which the two carbanion centres are linked by an *ortho*-phenylene spacer.[2] The exploration of the impact of such a rigid ligand backbone on the strength of the B-H···Sn agostic-type interactions is of interest, since the rigidity of the ligand should limit the extent to which the BH_3 group can position itself near to the Sn centre and so affect the strength of the agostic-type stabilisation of the dialkylstannylene.

5.2 Synthesis of dialkylstannylenes

Treatment of *in situ*-generated [1,2-C_6H_4{$CHP(BH_3)Cy_2$}$_2$][$Li(THF)_n$]$_2$ with one equivalent of Cp_2Sn in toluene yields pale yellow crystals of [[1,2-C_6H_4{$CHP(BH_3)Cy_2$}$_2$]Sn]$_2$·3/2PhMe (**58**) (Scheme 5.2) suitable for X-ray crystallography. Once isolated, compound **58** has limited solubility in aromatic and ethereal solvents and this compound reacts rapidly with chlorinated solvents. Compound **58** also decomposes to the corresponding phosphine-borane and elemental tin with exposure to light or temperatures above 50 °C and, over a period of several hours, begins to decompose in THF solution at room temperature. Compound **58** is, however, sufficiently stable and soluble in THF for characterisation by NMR spectroscopy.

The reaction of Cp_2Sn with *in situ*-generated [1,2-C_6H_4{$CHP(BH_3)R_2$}$_2$][$Li(THF)_n$]$_2$ (R = ^{i}Pr, Ph and Cy) was expected to result in the agostically-stabilised dialkylstannylenes **59**-**61** shown in Scheme 5.2. However, the $^{31}P\{^1H\}$ NMR spectra of the crude reaction solutions exhibit several different phosphorus environments. A maximum of two phosphorus environments were predicted due to the *rac* and *meso* diastereomers of **58** and so the five broad peaks present in the crude reaction mixtures were initially attributed to impurities.

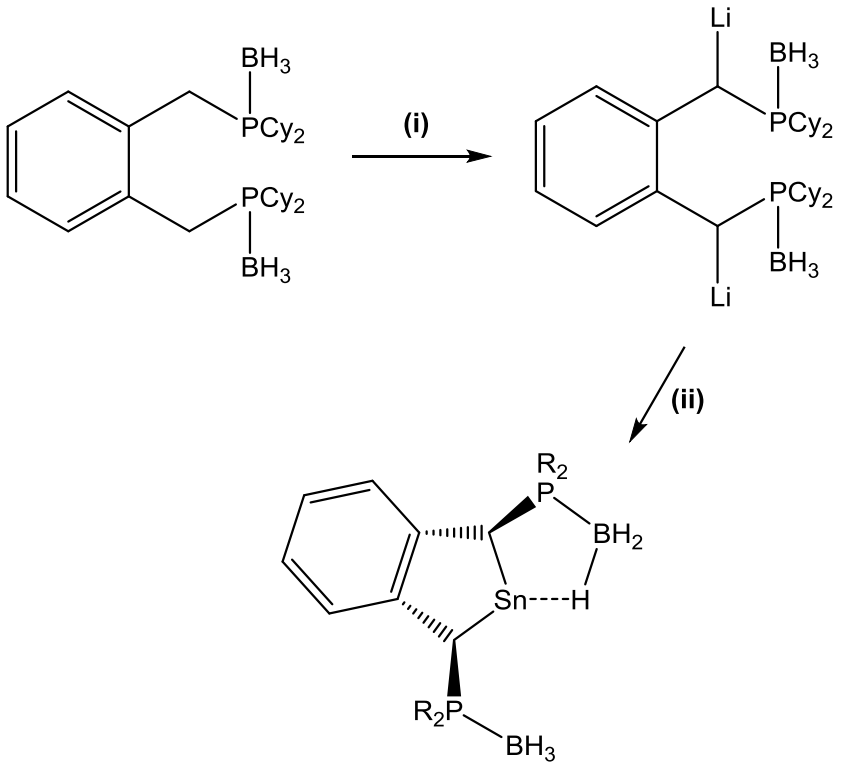

R = Cy (**59**), Ph (**60**), ^{i}Pr (**61**)

Scheme 5.2: Synthesis of Compound **58**. Reaction conditions. i) 2 equivalents of ^{n}BuLi, THF. ii) $SnCp_2$, toluene.

However, upon recrystallisation of compound **58** it was clear from the NMR data that the previously predicted structures given in Scheme 5.2 were incorrect. Instead of the usual dialkylstannylene structures, an unusual agostically-stabilised stannyl-stannylene with both chelating and bridging ligands was observed. The previously discounted $^{31}P\{^{1}H\}$ NMR spectra correlated with the solid state structure of compound **58** (Figure 5.3). The $^{31}P\{^{1}H\}$ NMR spectrum of crystalline compound **58** exhibits four broad signals at 27.2, 28.6, 30.0 and 35.4 ppm (Figure 5.4) while the $^{11}B\{^{1}H\}$ NMR spectrum exhibits two broad signals at -43.5 and -38.8 ppm (Figure 5.5) in an approximately 3:1 ratio. The unique high field signal (-38.8 ppm) in the latter spectrum may be attributed to the phosphine-borane which is associated with the short B-H···Sn interaction. These signals indicate that the dinuclear structure seen for compound **58** in the solid state (see below) persists in solution.

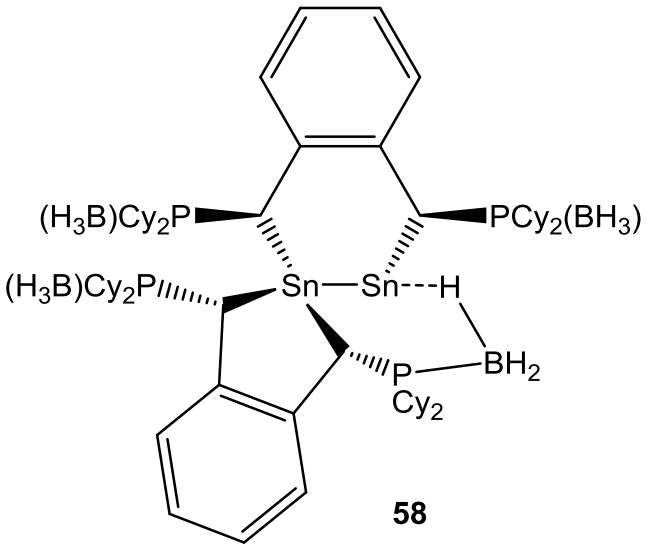

Figure 5.3: Schematic drawing of solid state structure of **58**.

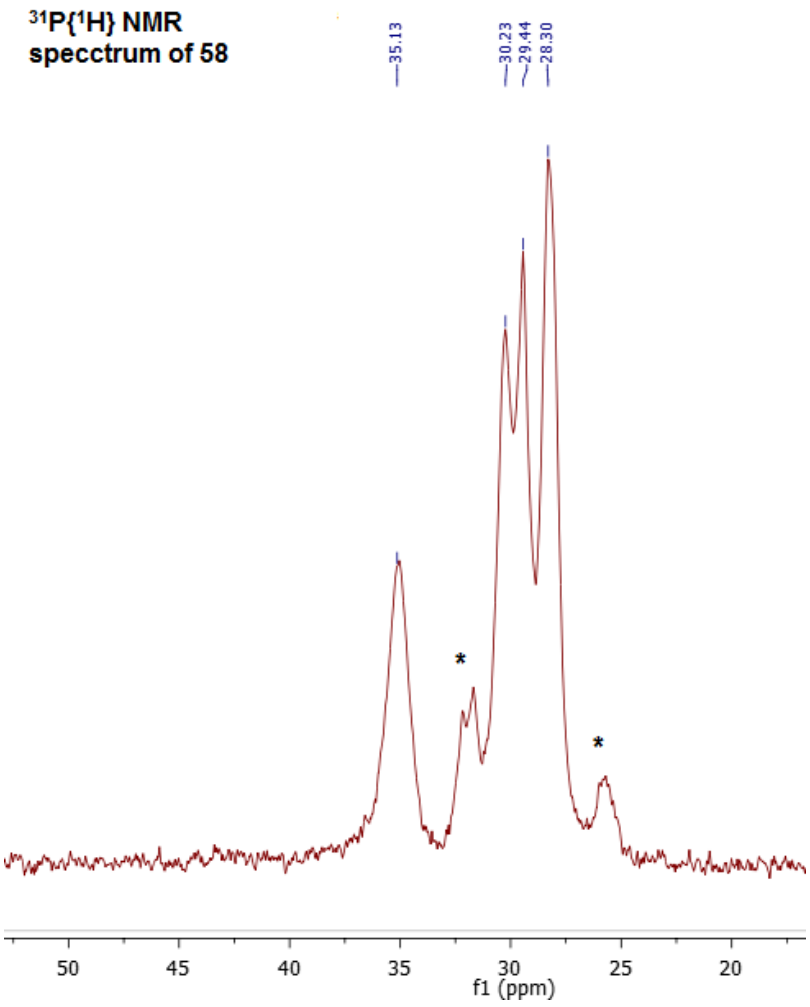

Figure 5.4: $^{31}P\{^{1}H\}$ NMR spectra of compounds **58**. * Unknown impurities

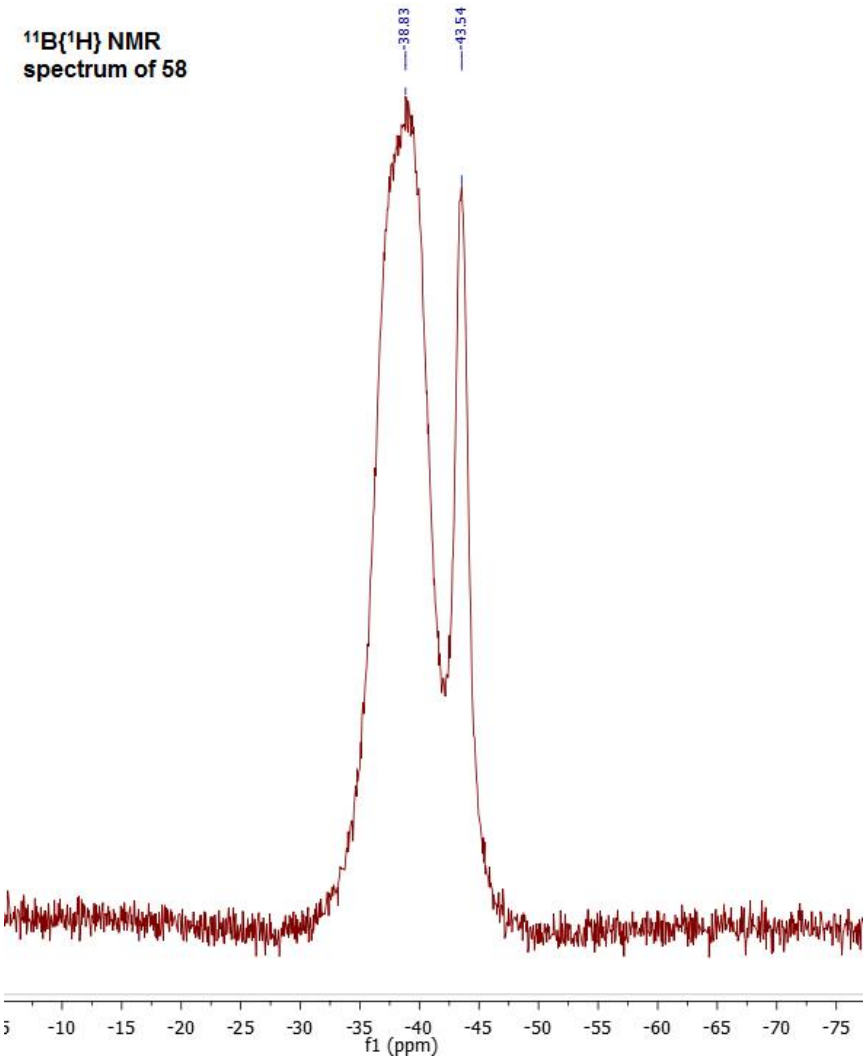

Figure 5.5: $^{11}B\{^{1}H\}$ NMR spectrum of compound **58** d_8-THF.

Furthermore, upon comparison of the crude $^{31}P\{^{1}H\}$ NMR spectra of compound **58** with those of **60** and **61** (Figure 5.6), it appears likely that these compounds also adopt a stannyl-stannylene structure.

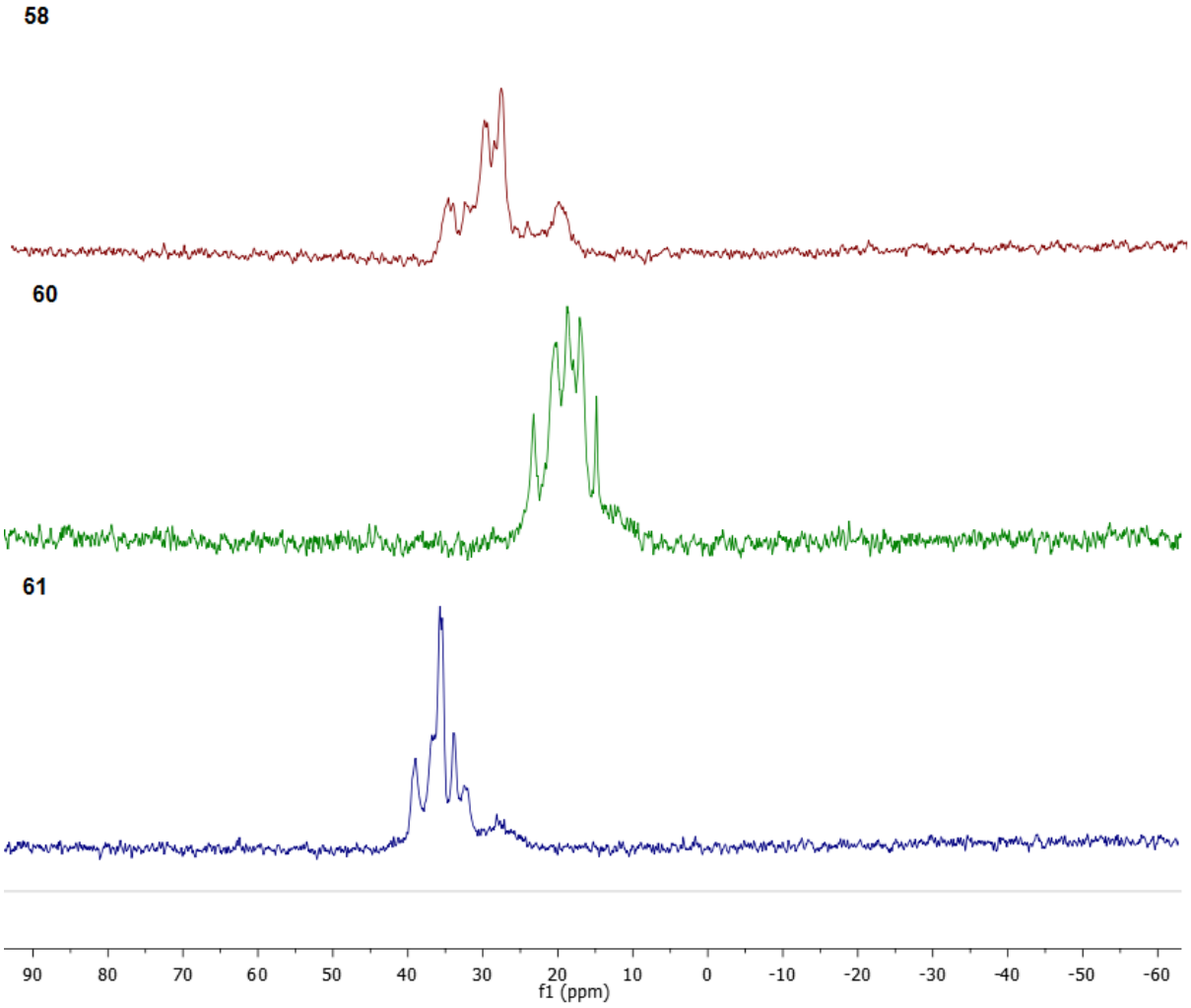

Figure 5.6: $^{31}P\{^{1}H\}$ NMR spectra of compounds **58**, **60** and **61** in the crude reaction mixture in THF.

The $^{31}P\{^{1}H\}$ NMR spectrum for the crude reaction mixture of compound **58** shows multiple broad and overlapping signals. This suggests that in addition to compound **58**, the solution contains the corresponding *rac* isomer, either as a monomeric or dimeric species; however, this species was not isolated. The presence of diastereomers will affect the potential yield that can be isolated; 50 % *rac* and 50 % *meso*. This explains why the overall yield of compound **58** initially seems relatively low. After considering the presence of diastereomers, it is unsurprising that the yield of **58** isolated is just 28%, which is in fact 56% of the potential *meso* diastereomer. It is also important to note that the less favourable *meso* conformation takes seven days to recrystallise. The ^{1}H NMR spectrum of compound **58** is complex and uninformative, due to the overlap of signals from the eight chemically inequivalent cyclohexyl groups (within which pairs of CH_2 groups are diastereotopic) and the signals from

four chemically inequivalent benzylic and BH_3 groups. The $^{119}Sn\{^1H\}$ NMR spectrum of compound **58** exhibits broad, featureless signals at -103 and 339 ppm (Figure 5.7), which may be attributed to the stannyl and stannylene centres, respectively; coupling between the two Sn centres is not resolved, due to the broad nature of these signals. The signal at -103 ppm is typical of tetravalent Sn centres,[3-5] while the signal at 330 ppm is similar to the chemical shifts in the previously reported agostically-stabilised dialkylstannylenes **32**-**35**, which fall in the range 320-787 ppm.[6-10]

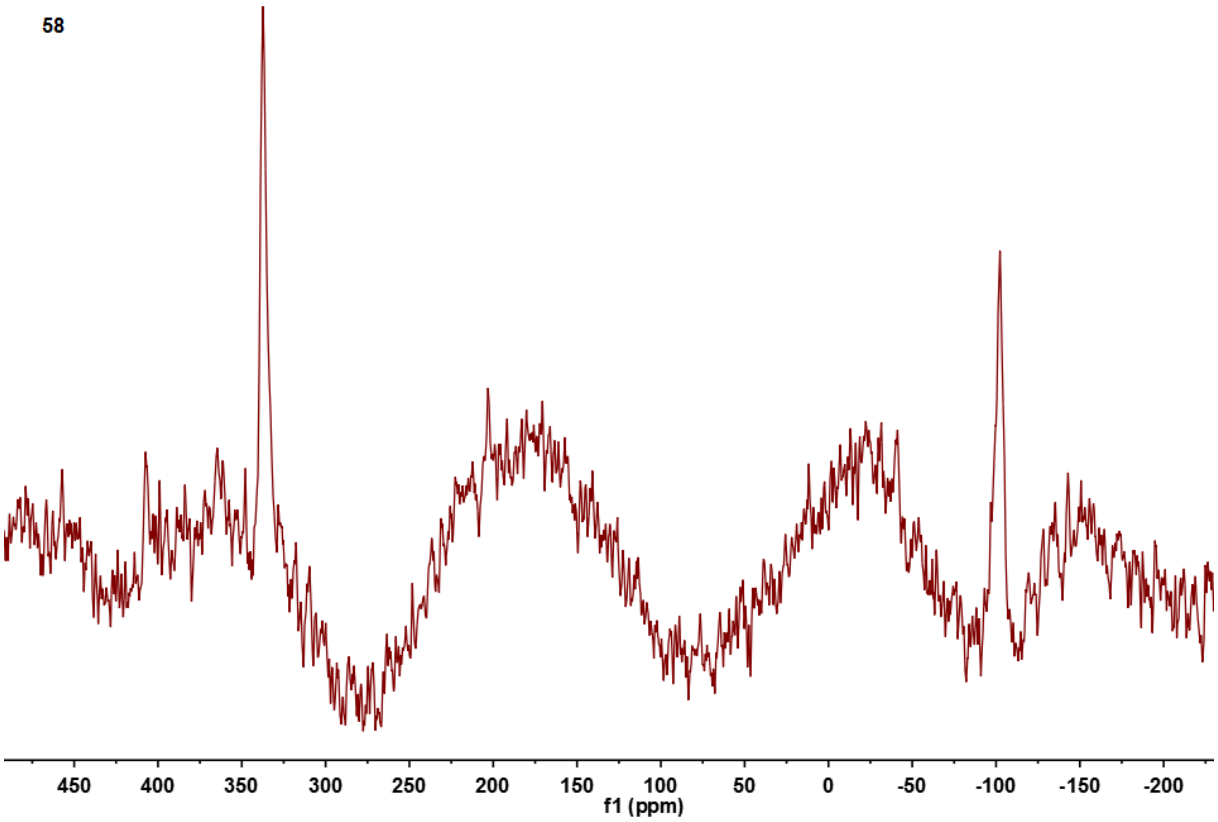

Figure 5.7: $^{119}Sn\{^1H\}$ NMR spectrum indicating two broad signals.

Compound **58** crystallises as a discrete molecular species containing two different Sn centres with formal oxidation states of I and III, joined by a formal Sn-Sn σ-bond and with 1½ molecules of toluene in the asymmetric unit; the solid state structure along with selected bond lengths can be seen in Figure 5.8 and Table 5.1, respectively.

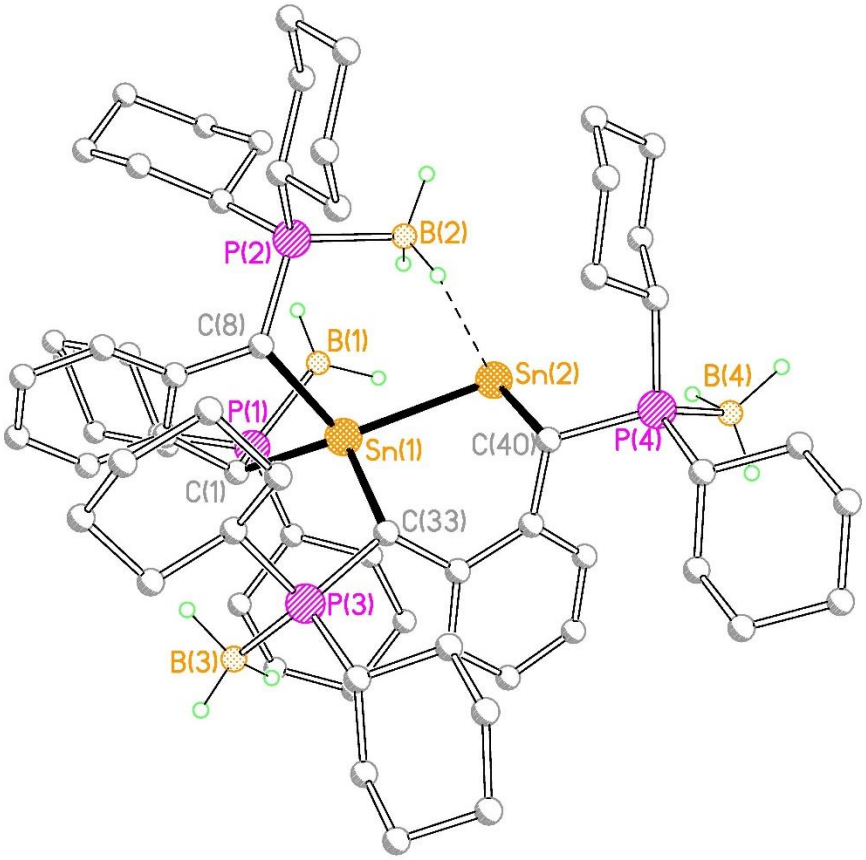

Figure 5.8: Molecular structure of compound **58** with solvent of crystallisation and H atoms (except those bound to boron) omitted for clarity.

Sn(1)-Sn(2)	2.81531(17)	Sn(1)-C(1)	2.1887(17)
Sn(1)-C(8)	2.2021(18)	Sn(1)-C(33)	2.2518(17)
Sn(2)-C(40)	2.3250(18)	Sn(2)-H(2B)	2.49(2)
P(1)-B(1)	1.931(2)	P(1)-C(1)	1.8373(18)
P(2)-B(2)	1.927(2)	P(2)-C(8)	1.8290(18)
P(3)-B(3)	1.939(2)	P(3)-C(33)	1.8218(17)
P(4)-B(4)	1.934(2)	P(4)-C(40)	1.8103(18)

Table 5.1: Selected bond lengths (Å) for compound **58**.

The formal Sn(III) centre is bonded to the two carbanion centres of a chelating dicarbanion ligand [Sn(1)-C(1) 2.1887(17) and Sn(1)-C(8) 2.2021(18) Å] and to a single

carbon atom of the second dicarbanion ligand [Sn(1)-C(33) 2.2518(17) Å], along with a short Sn-Sn contact. The Sn-C distances of the chelating dicarbanion ligand are similar to those in the tetravalent stannylene $C_6H_5CH_2SnR_3$ [R = $CH(SiMe_3)_2$] (**62**) published by Westerhausen [Sn-C 2.203(8), 2.193(8), 2.207(7), 2.201(8) Å],[11] however, the Sn-C distance of the second dicarbanion is significantly longer than the Sn-C distance in **62**; this may be attributed to compound **58** possessing a rigid linker which is bridging the two Sn centres, therefore, elongating the Sn-C distance in this case. The formal Sn(I) centre is bonded to the adjacent Sn atom and a carbon atom of the second dicarbanion ligand [Sn(2)-C(40) 2.3250(18) Å]; this distance is significantly longer than the Sn-C distance in the monomeric stannylene $Sn[CH(SiMe_3)_2]_2$ (**28**) [Sn-C 2.28 Å average from gas phase diffraction measurements].[1] The shorter Sn-C bond in **28** may be attributed to electron donation from the carbanion into the σ*-orbital on Si. The formal Sn(I) centre also has a short contact to a hydrogen atom of one of the BH_3 units of the ligand which chelates the formal Sn(III) centre [Sn(2)-H(2B) 2.49(2) Å]; this distance is similar to the H···Sn distances in compounds **32-35**, which are in the range of 2.03(5)-2.41(8) Å.[6-10] Although the location of H atoms by X-ray crystallography is not accurate, this distance is substantially shorter than the sum of the van der Waals radii of Sn and H (3.37 Å), which suggests that there is significant stabilisation via an agostic-type B-H···Sn interaction.

Formation of compound **58** results in one of the phosphine-borane-stabilised carbanion ligands chelating Sn(1), forming a five-membered C_4Sn heterocycle, whilst the second phosphine-borane-stabilised carbanion ligand bridges Sn(1) and Sn(2), generating a C_4Sn_2 six-membered heterocycle; each of these ligands adopts a *meso*-configuration. The Sn-Sn distance (2.81531(17) Å) is substantially shorter than the Sn-Sn distances in previously reported stannyl-stannylenes [formal oxidation states of Sn(I) and Sn(II)], which range from 2.865(6)-2.9688(5) Å[4, 12-26] and is similar to the Sn-Sn distance in grey tin (2.80 Å).[27] This short distance may be attributed to the incorporation of the Sn-Sn bond into a rigid six-membered ring.

5.3 DFT Calculations on a model stannyl-stannylene

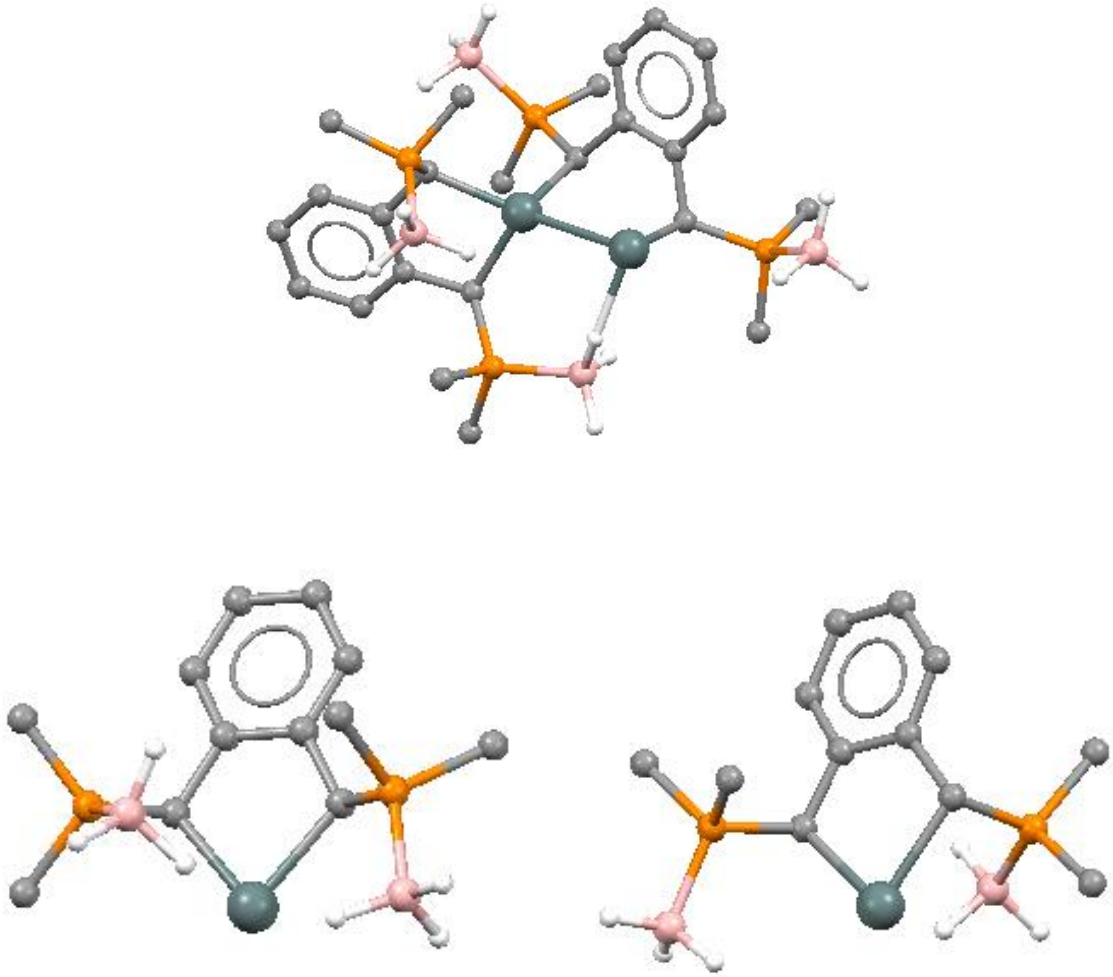

Figure 5.9: Optimised geometries of compound **63** (top), *meso*-**63** (bottom left) and *rac*-**63** (bottom right) with C-bound H atoms (except for those bound to boron) omitted for clarity.

DFT calculations on the complex [[1,2-C_6H_4{CHP(BH_3)Me_2}$_2$]Sn]$_2$ (**63**) (B3LYP/6-31G(2d, p)/Lanl2dz on Sn), in which the cyclohexyl groups have been replaced by smaller methyl substituents, reproduce the core structure of compound **58** observed in the solid state (Figure 5.9). In particular, one of the borane hydrogen atoms lies close to the divalent Sn centre (Sn···H, 2.13 Å), which is similar to the interaction observed in the solid-state structure of compound **58**. Natural Bond Orbital (NBO) analysis indicates that this interaction stabilises **63** by 28.8 kcal mol^{-1}, similar to the stabilisation energies calculated for **33**-**35** (even with the unusual bridging mode of the ligand in **63**).

In order to estimate the resulting stability of the stannyl-stannylene **63** in comparison to the monomer *meso*-[1,2-C_6H_4{CHP(BH_3)Me_2}$_2$]Sn (*meso*-**63**) the energies of both of these species have been calculated as well as that of the corresponding *rac* isomer (Figure 5.9). The optimised geometries for both *meso*- and *rac*-**63** have a single short B-H···Sn contact with Sn···H distances of 2.15 and 2.13 Å, respectively. This short interaction results in the C_4Sn five-membered ring being essentially planar for *meso*-**63**, however, for *rac*-**63** this interaction results in a twisting of both the five-membered ring and the aromatic ring. NBO analysis suggests that the B-H···Sn interactions stabilise *meso*- and *rac*-**63** by 41.4 and 33.1 kcal mol^{-1}, respectively. The calculations also suggest that *rac*-**63** is 1.8 kcal mol^{-1} more stable than *meso*-**63** and that *meso*-**63** is favoured by 1.1 kcal mol^{-1} compared to the stannyl-stannylene **63**. In previous examples, such as compounds **33**-**35**, the more energetically favourable conformation is the *rac* diastereomer as this allows both the BH_3 units to have Sn···H-B interactions whereas the less energetically favourable *meso* diastereomer just allows one BH_3 unit to have an Sn···H-B interaction. However, the lack of significant energetic preference calculated for *rac*-**63** and *meso*-**63** suggests that both will be in an approximately 1:1 mixture rather than the usual favoured *rac* diastereomer.

5.4 Conclusion

Multielement NMR spectroscopy indicated that the solid state structure of **58** persisted in solution; the $^{11}B\{^1H\}$ NMR spectrum of **58** exhibited a signal at -38.8 ppm which may be attributed to the phosphine-borane B-H···Sn interactions. The crude $^{31}P\{^1H\}$ NMR spectrum of **58** contains broad and overlapping peaks which may correspond to the *rac* isomer; this would explain why the isolation of **58** is in such poor yields. Furthermore, crude $^{31}P\{^1H\}$ NMR spectra for compounds **60** and **61** exhibited similar shaped signals to **58**, and so, similar structures may be predicted. The incorporation of the rigid linker may be the cause in the production of this type of unusual stannyl-stannylene rather than a usual dialkylstannylene. It is good to note that an agostic-type interaction still remains at the Sn(2) centre in compound **58**.

Compound **58** crystallises as a discrete molecular species containing two different Sn centres with formal oxidation states of I and III, including a formal Sn-Sn σ-bond. DFT calculations on **63** reproduce the core structure of compound **58** where NBO analysis exhibits a borane proton lying close to the divalent centre (similar to compound **58**) and stabilises compound **63** by 28.8 kcal mol^{-1}; similar to those calculated for **32**-**35**. The lack of energetic

preference calculated for *rac*-**63** and *meso*-**63** suggests that both will be in an approximately 1:1 mixture rather than the usual favoured *rac* diastereomer.

5.5 References

1. D. E. Goldberg, D. H. Harris, M. F. Lappert and K. M. Thomas, *J. Chem. Soc. Chem. Commun.*, 1976, 261-262.
2. K. Izod, C. M. Dixon, E. McMeekin, L. Rodgers, R. W. Harrington and U. Baisch, *Organometallics*, 2014, **33**, 378-386.
3. J. D. Cotton, P. J. Davidson and M. F. Lappert, *J. Chem. Soc. Dalton Trans.*, 1976, 2275-2286.
4. C. Eaborn, M. S. Hill, P. B. Hitchcock, D. Patel, J. D. Smith and S. B. Zhang, *Organometallics*, 2000, **19**, 49-53.
5. C. Wills, K. Izod, W. Clegg and R. W. Harrington, *Dalton Trans.*, 2010, **39**, 2379-2384.
6. K. Izod, W. McFarlane, B. V. Tyson, I. Carr, W. Clegg and R. W. Harrington, *Organometallics*, 2006, **25**, 1135-1143.
7. K. Izod, W. McFarlane, C. Wills, W. Clegg and R. W. Harrington, *Organometallics*, 2008, **27**, 4386-4394.
8. K. Izod, C. Wills, W. Clegg and R. W. Harrington, *Organometallics*, 2009, **28**, 2211-2217.
9. K. Izod, C. Wills, W. Clegg and R. W. Harrington, *Organometallics*, 2009, **28**, 5661-5668.
10. K. Izod, C. Wills, R. W. Harrington and W. Clegg, *J. Organomet. Chem.*, 2013, **725**, 11-14.
11. M. Westerhausen and T. Hildenbrand, *J. Organomet. Chem.*, 1991, **411**, 1-17.
12. H. Grutzmacher, H. Pritzkow and F. T. Edelmann, *Organometallics*, 1991, **10**, 23-25.
13. P. Jutzi, A. Becker, H. G. Stammler and B. Neumann, *Organometallics*, 1991, **10**, 1647-1648.
14. M. Kira, R. Yauchibara, R. Hirano, C. Kabuto and H. Sakurai, *J. Am. Chem. Soc.*, 1991, **113**, 7785-7787.
15. C. Drost, P. B. Hitchcock, M. F. Lappert and L. J. M. Pierssens, *Chem. Commun.*, 1997, 1141-1142.
16. C. Eaborn, T. Ganicz, P. B. Hitchcock, J. D. Smith and S. E. Sozerli, *Organometallics*, 1997, **16**, 5621-5622.
17. C. J. Cardin, D. J. Cardin, S. P. Constantine, A. K. Todd, S. J. Teat and S. Coles, *Organometallics*, 1998, **17**, 2144-2146.

18. M. Kira, S. Ishida, T. Iwamoto, M. Ichinohe, C. Kabuto, L. Ignatovich and H. Sakurai, *Chem. Lett.*, 1999, 263-264.
19. M. Kira, S. Ishida, T. Iwamoto and C. Kabuto, *J. Am. Chem. Soc.*, 1999, **121**, 9722-9723.
20. B. E. Eichler, B. L. Phillips, P. P. Power and M. P. Augustine, *Inorg. Chem.*, 2000, **39**, 5450-5453.
21. S. Wingerter, H. Gornitzka, R. Bertermann, S. K. Pandey, J. Rocha and D. Stalke, *Organometallics*, 2000, **19**, 3890-3894.
22. W. Setaka, K. Sakamoto, M. Kira and P. P. Power, *Organometallics*, 2001, **20**, 4460-4462.
23. C. Drost, M. Hildebrand and P. Lonnecke, *Main Group Met. Chem.*, 2002, **25**, 93-98.
24. B. E. Eichler, A. D. Phillips and P. P. Power, *Organometallics*, 2003, **22**, 5423-5426.
25. A. D. Phillips, S. Hino and P. P. Power, *J. Am. Chem. Soc.*, 2003, **125**, 7520-7521.
26. L. H. Pu, A. D. Phillips, A. F. Richards, M. Stender, R. S. Simons, M. M. Olmstead and P. P. Power, *J. Am. Chem. Soc.*, 2003, **125**, 11626-11636.
27. N. N. Greenwood and A. Earnshaw, *Chemistry of the Elements*, 2nd edn., Butterworth-Heinemann, 1997, 372.

Chapter 6. Replacement of a trimethylsilyl group and its impact on stability of dialkylstannylenes

6.1 Introduction

As discussed in Chapter 1.5, Lappert and co-workers reported the first dialkylstannylene $\{(Me_3Si)_2CH\}_2Sn$ in the 1970s (Scheme 6.1).[1] Compound **28** exists as a monomeric structure in the gas phase, but dimerises to the corresponding distannene **28a** in the solid state; compounds **28** and **28a** are in a dynamic equilibrium in solution.[2]

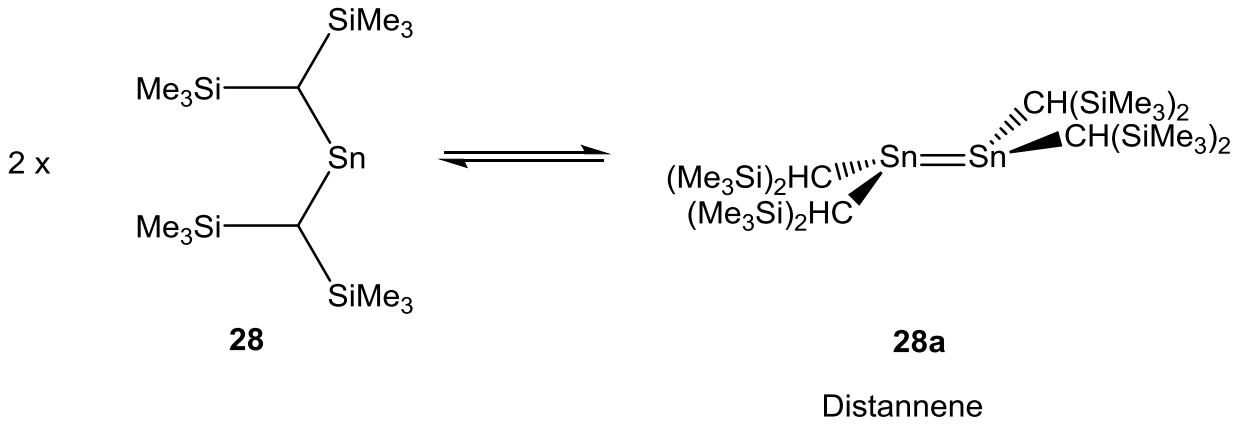

Scheme 6.1: Monomeric dialkylstannylene and the corresponding distannene.

Compounds **32** and **33** (discussed in chapter 1.5) (Scheme 6.2) are stabilised by a combination of steric bulk and agostic-type B-H···Sn interactions. Izod and co-workers reduced the steric bulk of the ligand in order to test the extent to which B-H···E interactions can stabilise dialkylstannylenes and therefore exhibit dimerisation to the corresponding $R_2Sn{=}SnR_2$. Compound **34** (Scheme 6.2), which contains the isoelectronic group Me_2PBH_3 instead of $SiMe_3$, was synthesised as an analogue of compound **28**. Izod and co-workers found that agostic-type interactions were stabilising enough to prevent dimerisation, and so compound **34** exists as a monomer in the solid state.[3]

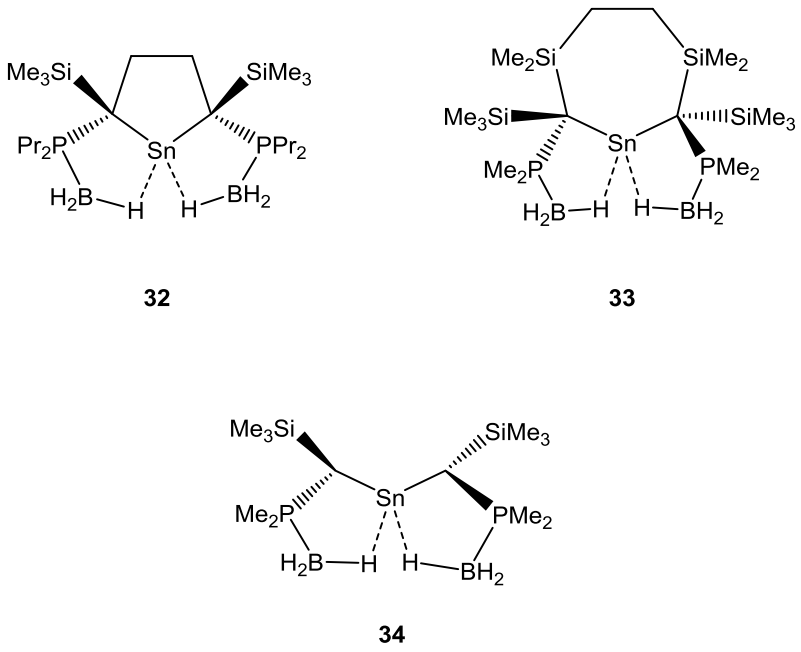

Scheme 6.2: Dialkylstannylenes exhibiting B-H···Sn agostic-type stabilisation interactions.

In the present work, the benzylic phosphine-borane precursors $C_6H_5CHPR_2(BH_3)$ [R = ^{i}Pr (**47**) and Cy (**49**)] were synthesised and used to develop new types of agostically-stabilised dialkylstannylenes. Compounds **47** and **49** are analogues of **34** in which the $SiMe_3$ has been removed and replaced with a phenyl ring; this change reduces steric bulk around the electron deficient Sn centre. Izod and co-workers investigated the structure of compound **34** and found that only the *rac* diastereomer is formed; no evidence of the *meso* diastereomer was found in the crude $^{31}P\{^1H\}$ NMR spectrum of the reaction mixture.[3] This structural preference was attributed to the electron deficient tin centre in **34** possessing two agostic-type B-H···Sn interactions compared to just one interaction, which is common in the *meso* diastereomer; overall, the *rac* diastereomer provides a larger stabilising effect compared to the *meso* diastereomer.[3] The development of the agostically-stabilised dialkylstannylenes using **47** and **49** is of interest to investigate whether the removal of the $SiMe_3$ group will affect the structures in each case.

6.2 Synthesis of dialkylstannylenes

6.2.1 Benzylic dialkylstannylenes

Treatment of one equivalent of $SnCl_2$ with two equivalents of *in situ*-generated [Li(tmeda)][$C_6H_5CHPR_2(BH_3)$] [R = ^{i}Pr (**47a**) and Cy (**49a**)] in diethyl ether yields the dialkylstannylenes Sn[$C_6H_5CHPR_2(BH_3)]_2$ [R = ^{i}Pr (**64**) and Cy (**65**)] (Scheme 6.3). Pale yellow crystals of **64** and **65** suitable for X-ray crystallography were isolated from cold (-20 °C) methylcyclohexane.

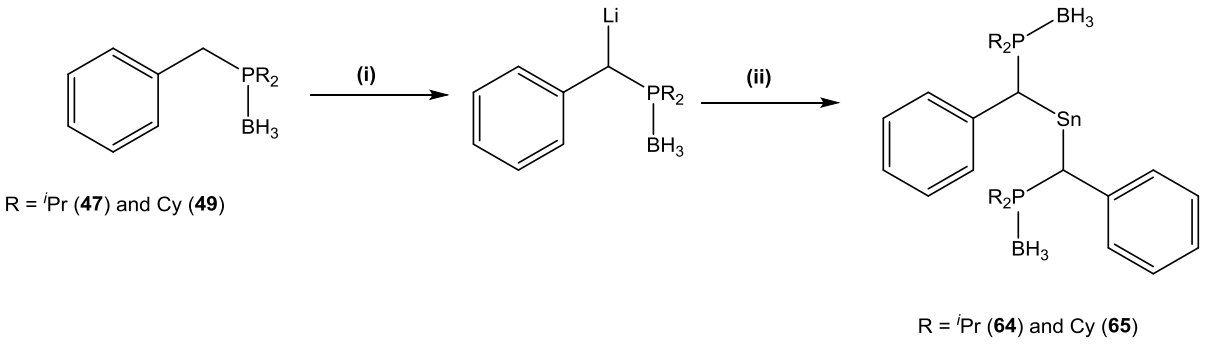

Scheme 6.3: Synthesis of Compounds **64** and **65**. Reaction conditions. i) ^{n}BuLi, THF. ii) 0.5$SnCl_2$, Et_2O.

Unfortunately, **65** could not be separated cleanly from side products (LiCl) and impurities (such as Sn[$C_6H_5CHPR_2(BH_3)$]Cl and $SnCl_2$) to obtain clean ^{1}H, ^{1}H{^{11}B}, ^{13}C{^{1}H} and ^{119}Sn{^{1}H} NMR spectra; therefore, compound **65** could not be fully characterised. Once isolated, both compounds **64** and **65** showed poor stability in many deuterated solvents ($CDCl_3$, d_8-THF and d_8-toluene) which resulted in decomposition to the free phosphine-boranes **47** and **49**.

It is worth noting here the differences in the experimental procedures between compounds **32**, **33**, **34** and that of **64** and **65** where **64** and **65** were made with the use of $SnCl_2$ and **32**, **33** and **34** were made with the use of $SnCp_2$. Compounds **32**, **33,** and **34** contain $SiMe_3$ groups and compounds **64** and **65** contain the more charge-delocalising phenyl group, which results in **64** and **65** being less nucleophilic and less reducing. The use of $SnCl_2$ with the more reducing compounds **32**, **33** and **34** results in deposition of elemental tin and formation of the corresponding phosphine-borane.[4]

6.2.2 Characterisation of compounds 64 and 65

Compounds **64** and **65** are chiral at both methine carbon atoms and so may form both *rac* and *meso* diastereomers (Figure 6.1). In an attempt to separate these diastereomers, diethyl ether was added to the solid crude reaction mixture of compound **65** resulting in a light yellow precipitate which was isolated and washed with cold diethyl ether. Both the precipitate and the filtrate were analysed using multinuclear NMR spectroscopy. In deuterated toluene the $^{1}H\{^{11}B\}$ NMR spectrum of the precipitate of **65** contains doublets at 0.62 ppm (J_{PH} = 8.5 Hz) and 0.91 ppm (J_{PH} = 10.0 Hz), which correspond to the two BH_3 units in the *rac* and *meso* diastereomers (Figure 6.2). The $^{1}H\{^{11}B\}$ NMR spectrum also exhibits a major doublet at 2.70 ppm (J_{PH} = 12.3 Hz) and a minor doublet (3:1 ratio) at 3.50 ppm (J_{PH} = 12.3 Hz) corresponding to the two hydrogens bonded to the two carbanion centres in each case (Figure 6.2). The $^{11}B\{^{1}H\}$ NMR spectrum contains a broad peak at -39.4 ppm. In deuterated toluene the $^{31}P\{^{1}H\}$ NMR spectrum of the precipitate contains a major peak at 26.7 ppm and a minor peak at 28.3 ppm whilst in diethyl ether the filtrate contains a major peak at 30.8 ppm and a minor peak at 29.0 ppm (Figure 6.3). The $^{119}Sn\{^{1}H\}$ NMR spectrum of the precipitate of **65** contains broad peaks at 359 and 370 ppm. This clearly suggests that while both diastereomers are formed, one has much reduced solubility in diethyl ether; however, it is unclear which chemical shifts correspond to which diastereomer in each case.

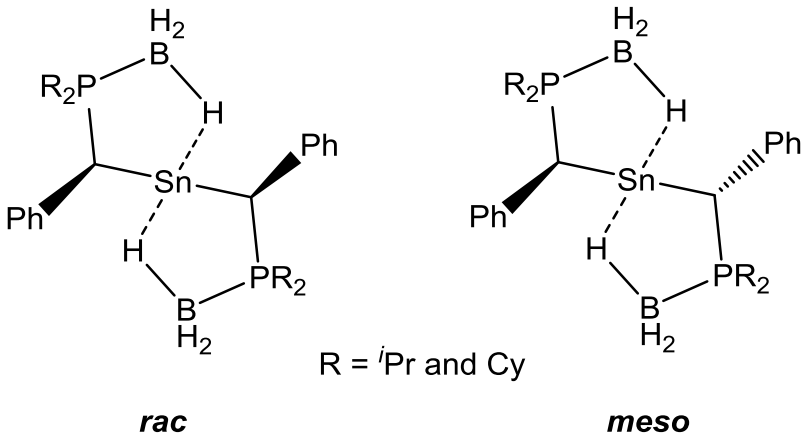

Figure 6.1: The proposed *rac* and *meso* diastereomers of compounds **64** and **65**.

The crude $^{11}B\{^{1}H\}$ NMR spectrum of compound **64** shows a broad doublet at -38.8 ppm (J_{PB} = 79.5 Hz) and the $^{31}P\{^{1}H\}$ NMR spectrum exhibits a broad peak at 34.6 ppm. Based on the NMR spectra of compound **65**, these broad peaks could also indicate the presence of *rac* and *meso* diastereomers (see discussion above).

The $^{119}Sn\{^{1}H\}$ NMR spectrum of **65** contains broad signals at 359 and 370 ppm which are similar to the $^{119}Sn\{^{1}H\}$ NMR signals of compounds *rac*-**32** (578 ppm)[4], *rac*-**33** (320 ppm)[5] and **34** (377 ppm)[3] but is significantly higher field than the isoelectronic compound **28** (2328 ppm).[1] These high field chemical shifts are consistent with the B-H···Sn contacts which are observed in the solid persisting in solution.[3]

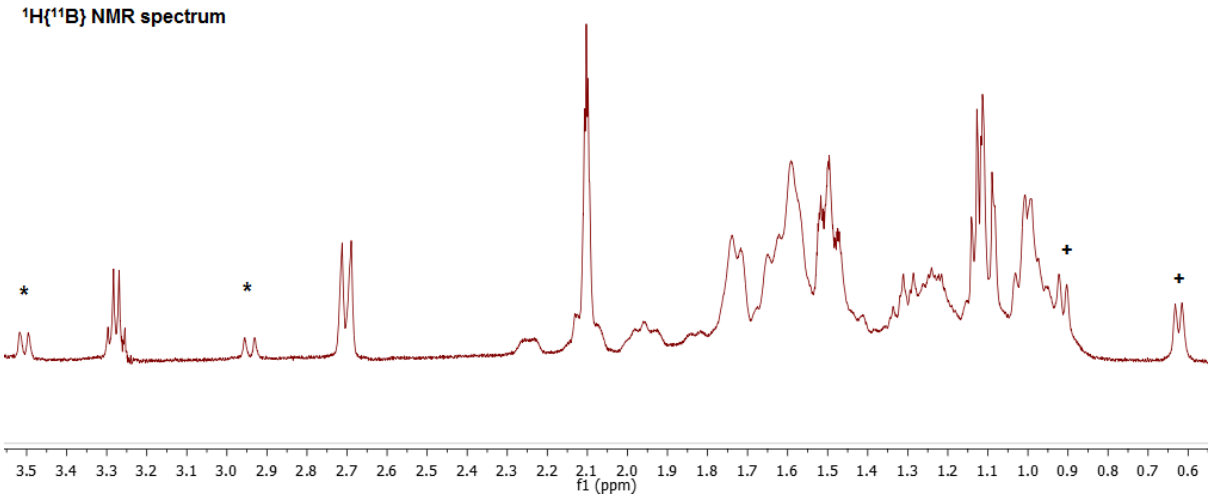

Figure 6.2: Evidence of *rac* and *meso* diastereomers in the $^{1}H\{^{11}B\}$ NMR spectrum of compound **65** d_8-toluene; CH protons (*) and BH_3 protons (+).

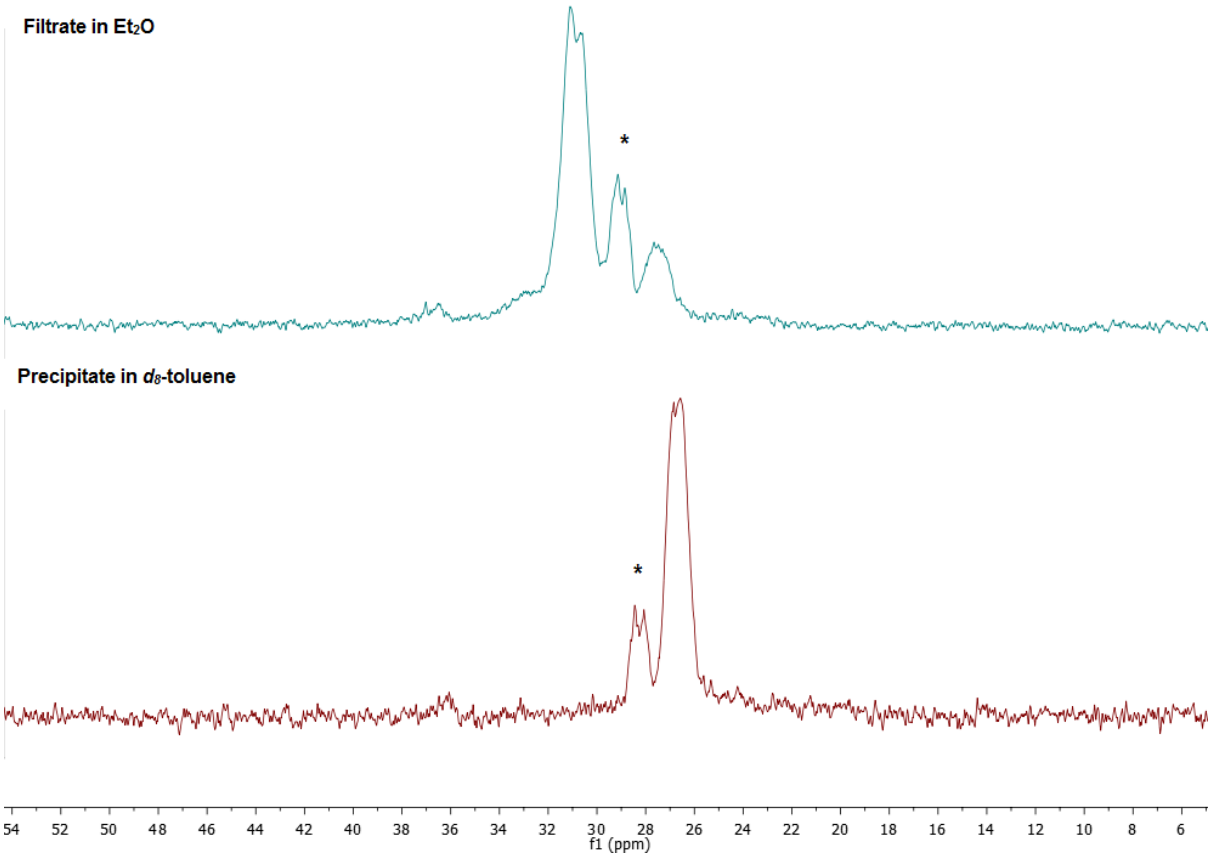

Figure 6.3: $^{31}P\{^{1}H\}$ NMR spectra of the precipitate and filtrate of compound **65**; * precursor **49** or *rac*-**65**.

Single crystals of ***rac*-64** and ***rac*-65** suitable for X-ray crystallography were obtained from cold methylcyclohexane or cold diethyl ether, respectively. Compounds ***rac*-64** and ***rac*-65** crystallise as discrete dialkyltetrylenes with effective disorder of the Sn atom and the methine CH groups over two sites with 60:40 occupancy. Both ***rac*-64** and ***rac*-65** have interactions between the Sn centre and one H atom from each of two separate BH_3 units in an η^1-fashion; ***rac*-64** and ***rac*-65** are isostructural but not isomorphous. The molecular structures of ***rac*-64** and ***rac*-65** are shown in Figures 6.4 and 6.5, respectively; selected bond lengths and angles are given in Tables 6.1 and 6.2 respectively.

The Sn-C distances of 2.282(10) and 2.314(10) Å in ***rac*-64** are similar to the corresponding distances in the previously reported compound **34** [2.3149(16) and 2.2864(16) Å]. The Sn-C distances of 2.176(5) and 2.275(4) Å in ***rac*-65** are shorter than those in compound **34**. The P-B distances [***rac*-64**, 1.925(14) and 1.919(14) Å; ***rac*-65**, 1.922(5) and 1.923(5) Å] and the C-P distances [***rac*-64**, 1.814(11) and 1.786(12) Å; ***rac*-65**, 1.798(4) and 1.806(5) Å] of both compounds are similar to the corresponding P-B [1.909(3)

and 1.918(2) Å] and C-P [1.7877(16) and 1.7919(18) Å] distances in compound **34**. The Sn···H distances of compounds ***rac*-64** (2.49(12) and 2.60(13) Å) and ***rac*-65** (2.38(4) and 2.35(4) Å) lie well within the sum of the van der Waals radii of H and Sn (3.37 Å) suggesting a significant H···Sn interaction. The H···Sn distances of compounds ***rac*-64** and ***rac*-65** are also similar to the corresponding distances in **34** (2.38(2) and 2.29(2) Å).[3]

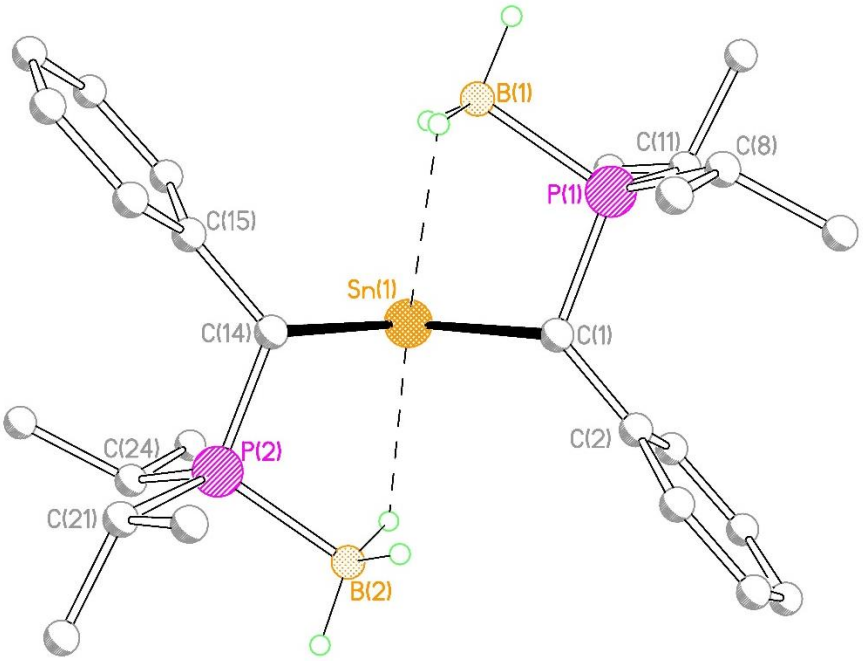

Figure 6.4: Molecular structure of ***rac*-64** H atoms (except those bound to boron) omitted for clarity.

Sn-C(1)	2.314(10)	Sn-C(14)	2.282(10)
C(1)-P(1)	1.814(11)	C(14)-P(2)	1.786(12)
P(1)-B(1)	1.925(14)	P(2)-B(2)	1.919(14)
Sn-H(1C)	2.60(13)	Sn-H(2A)	2.49(12)
		C(1)-Sn-C(14)	95.1(4)

Table 6.1: Selected bond lengths (Å) and angles (°) for ***rac*-64**.

The C-Sn-C angles of 95.1(4)° and 101.4(18)° in ***rac*-64** and ***rac*-65**, respectively are significantly different to the C-Sn-C angle observed for **6** [98.26(6)°]. Compound ***rac*-65** has

a C-Sn-C angle which is significantly greater than those of ***rac*-64** and **34** due to the larger cyclohexyl substituents on the phosphorus. The C-Sn-C angles for ***rac*-64** and ***rac*-65** are closer to 90° than to 120° which suggests unhybridised Sn orbitals (s and 3×p rather than sp^2 and p).

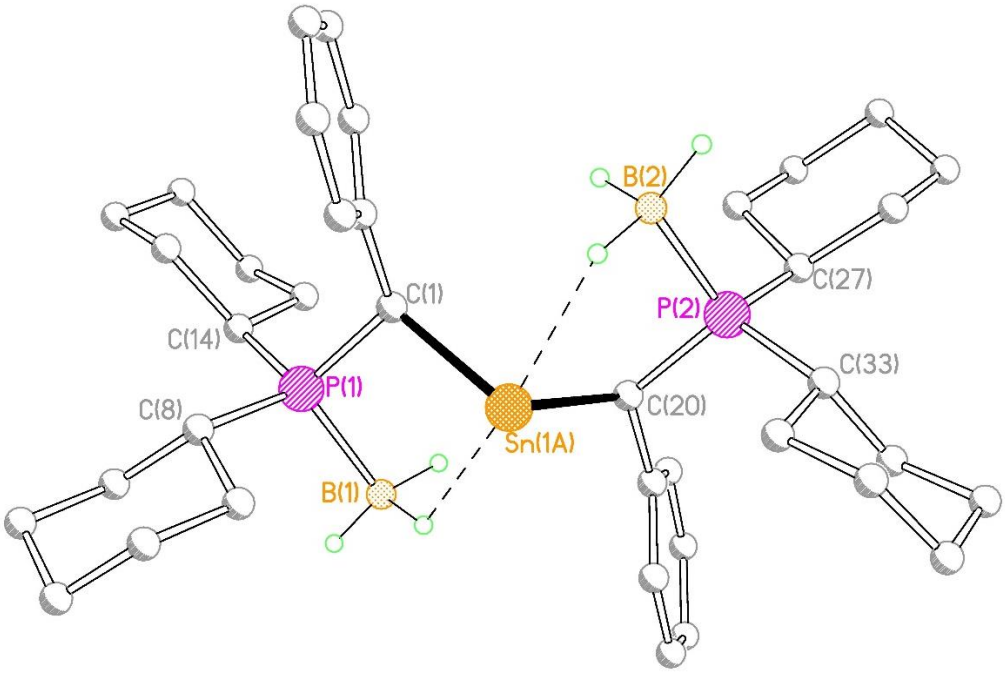

Figure 6.5: Molecular structure of compound ***rac*-65** with solvent of crystallisation and H atoms (except those bound to boron) omitted for clarity.

Sn-C(1)	2.176(5)	Sn-C(20)	2.275(4)
C(1)-P(1)	1.798(4)	C(20)-P(2)	1.806(5)
P(1)-B(1)	1.922(5)	P(2)-B(2)	1.923(5)
Sn-H(1A)	2.38(4)	Sn-H(2C)	2.35(4)
		C(1)-Sn-C(20)	101.4(18)

Table 6.2: Selected bond lengths (Å) and angles (°) for ***rac*-65**.

6.3 Conclusion

Overall, the removal of the trimethylsilyl group reduces the bulkiness within the agostically-stabilised dialkylstannylenes ***rac*-64** and ***rac*-65**. In compound **34** it was reported that there was no evidence to suggest that a mixture of *rac* and *meso* diastereomers had formed and so only ***rac*-34** was isolated and characterised.[3] This however, is not the case for compounds **64** and **65**; the NMR spectra of both compounds suggest the formation of a mixture of both *rac* and *meso* diastereomers. The $^{119}Sn\{^{1}H\}$ NMR spectrum of compound **65** exhibits two broad peaks of equal intensity, while the $^{1}H\{^{11}B\}$ and $^{31}P\{^{1}H\}$ NMR spectra of compound **65** show two separate chemical shifts for the mixture of diastereomers. This clear difference between compound **34** and **64**/**65** may be attributed to the removal of the $SiMe_3$ group in the latter compounds and the reduction in steric bulkiness. However, the increase in C-Sn-C angle in ***rac*-65** [101.4(18)°] compared to **34** [98.26(6)°] may indicate that ***rac*-65** contains more sterically hindered phosphorus substituents than **34** and yet still shows evidence for the formation of *rac* and *meso* diastereomers in **65**. However, the explanation as to why the removal of $SiMe_3$ may affect the structural outcome may also be attributed to the intermediates RSnCl [R = ($Me_3SiCHPMe_2(BH_3)$ (**66**), $C_6H_5CHP^iPr_2(BH_3)$ (**67**) or $C_6H_5CHPCy_2(BH_3)$ (**68**)] where intermediate **66** is more sterically hindered than **67** or **68**. The increase bulk in **66** will have a bigger influence in the addition of the second substituent than **67** or **68**, resulting in only the *rac* diastereomer seen for **34** and both *rac* and *meso* seen for **65**.

6.4 References

1. D. E. Goldberg, D. H. Harris, M. F. Lappert and K. M. Thomas, *J. Chem. Soc. Chem. Commun.*, 1976, 261-262.
2. K. W. Zilm, G. A. Lawless, R. M. Merrill, J. M. Millar and G. G. Webb, *J. Am. Chem. Soc.*, 1987, **109**, 7236-7238.
3. K. Izod, C. Wills, W. Clegg and R. W. Harrington, *Organometallics*, 2009, **28**, 5661-5668.
4. K. Izod, W. McFarlane, B. V. Tyson, I. Carr, W. Clegg and R. W. Harrington, *Organometallics*, 2006, **25**, 1135-1143.
5. K. Izod, C. Wills, W. Clegg and R. W. Harrington, *Organometallics*, 2009, **28**, 2211-2217.

Chapter 7. Heteroleptic dialkylstannylenes

7.1 Introduction

The synthesis of heteroleptic compounds via chlorostannylenes $SnCl[C_6H_5CHPR_2(BH_3)]$ [R = ^{i}Pr (**69**) and Cy (**70**)] is of interest in order to monitor agostic-interactions between the BH_3 unit and the electron-deficient tin centre; by changing the substituent X in the heteroleptic species RSnX, the stabilisation effects of the agostic interactions can be measured. Carbon based ligands may be the least π-donating whereas amines the most π-donating (Chart 7.1). This will lead to competition of the donation capabilities between the B-H σ-bonding electron density and the heteroatom lone pair into the empty p-orbital of the electron-deficient Sn centre. The Sn···H-B interactions should become weaker as the second ligand becomes more π-donating ligand, and so this may result in a reduction in agostic-interactions with the BH_3 unit and the electron deficient centre.

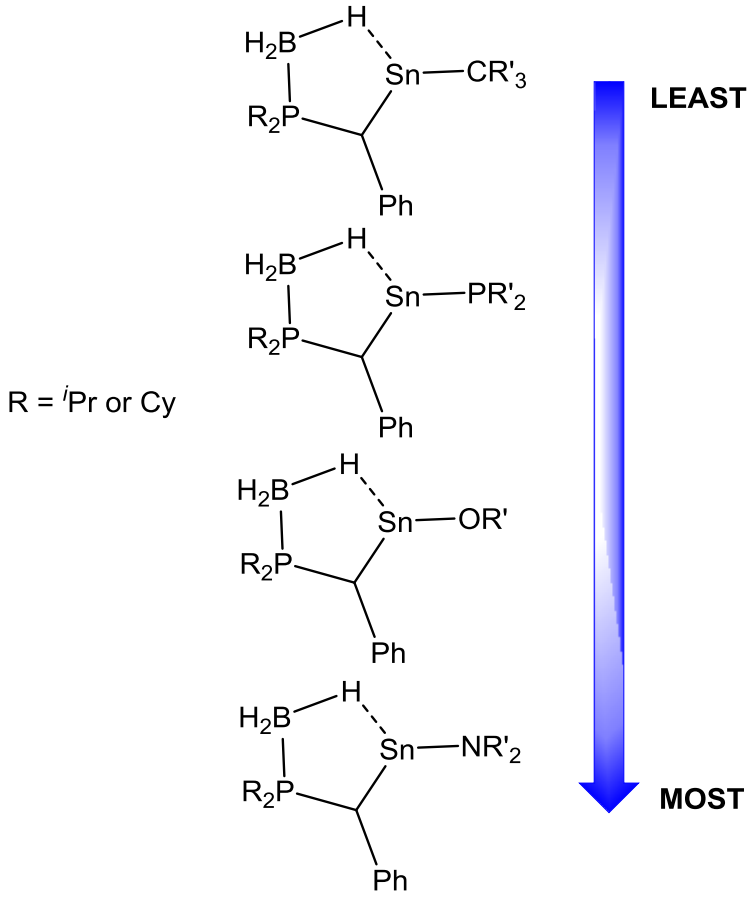

Chart 7.1: Heteroatoms from the least to the most π-donating.

In order to investigate this phenomenon, we sought to prepare a range of heteroleptic stannylenes [(PhCH$_2$)PR$_2$(BH$_3$)]SnX (X = -CH(SiMe$_3$)$_2$, -Dipp, -N(SiMe$_3$)$_2$, -O{2,6-^{t}Bu$_2$-4-MeC$_6$H$_2$}, -PTripp$_2$, -PDipp$_2$, -CH$_3$, -C$_6$H$_5$; R = ^{i}Pr and Cy) [Dipp = 2,6-^{i}Pr$_2$C$_6$H$_3$, Tripp = 2,4,6-^{i}Pr$_3$C$_6$H$_2$] and to probe the strength of the B-H···Sn interactions in each case.

7.2 Synthesis of heteroleptic dialkylstannylenes

Treatment of one equivalent of SnCl$_2$ with one equivalent of *in situ*-generated Li[C$_6$H$_5$CHPR$_2$(BH$_3$)] [R = ^{i}Pr (**47a**), Cy (**49a**)] in diethyl ether yields [C$_6$H$_5$CHPR$_2$(BH$_3$)]SnCl [R = ^{i}Pr (**69**), Cy (**70**)] (Scheme 7.1). A pale yellow solid precipitated with reduction of the ethereal solvent in each case.

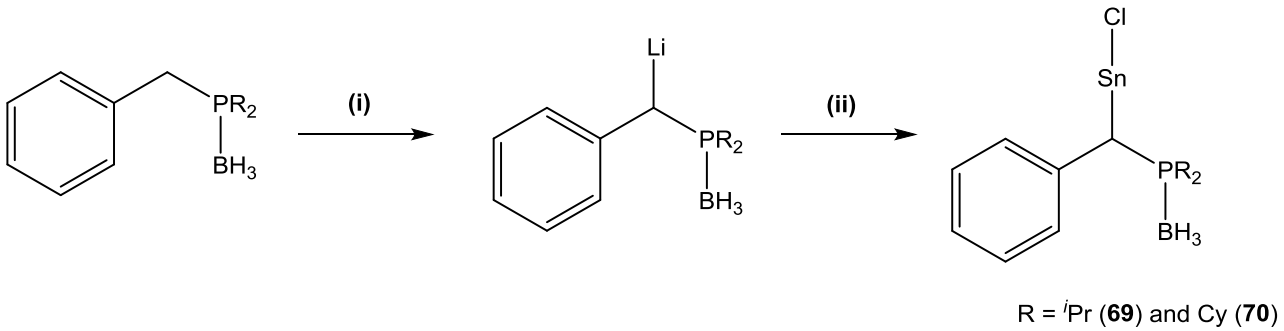

Scheme 7.1: Synthesis of compounds **69** and **70**. Reaction conditions. i) ^{n}BuLi, Et$_2$O. ii) SnCl$_2$, Et$_2$O.

Unfortunately, sufficiently clean solid was not obtained for compound **69** in order for full characterisation using NMR spectroscopy. The ^{1}H and ^{13}C{^{1}H} NMR spectra for compound **70** and the ^{11}B{^{1}H} and ^{31}P{^{1}H} NMR spectra for both compounds **69** and **70** are as expected. The ^{11}B{^{1}H} NMR spectrum of compound **69** contains a doublet at -39.2 ppm and the ^{31}P{^{1}H} NMR spectrum contains a quartet at 33.4 ppm (J_{PB} = 66.6 Hz). In deuterated THF the ^{1}H NMR spectrum of **70** contains a doublet at 3.05 ppm (J_{PH} = 11.7 Hz), corresponding to the methine proton bonded to the carbanion centre. The ^{11}B{^{1}H} NMR spectrum of **70** contains a broad peak at -39.8 ppm and the ^{31}P{^{1}H} NMR spectrum contains a broad peak at 27.7 ppm. The pale yellow solids isolated for compounds **69** and **70** were not suitable for X-ray crystallography.

7.3 Reactivity of heteroleptic alkylstannylenes with bulky reagents

7.3.1 Carbon-containing groups

Treatment of $[C_6H_5CHP^iPr_2(BH_3)]SnCl$ with one equivalent of either $LiCH(SiMe_3)_2$ or $Li\{2,6\text{-}^iPr_2\text{-}C_6H_3\}$ results in a colour change from a pale yellow to a dark red solution (Scheme 7.2).

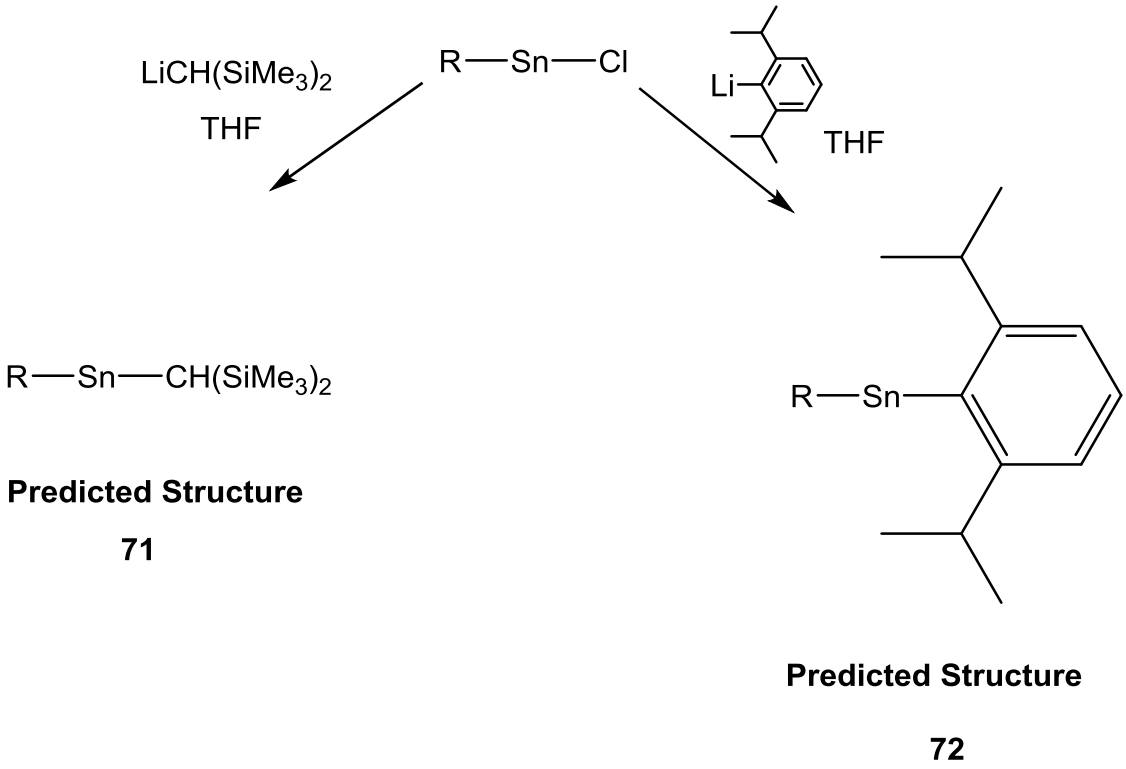

Scheme 7.2: Synthesis of compounds **71** and **72**.

Crude $^{31}P\{^1H\}$ NMR spectra of both reactions were recorded and both NMR spectra showed a change from the starting compound **69** (Figure7.1); unfortunately no other NMR data was obtained.

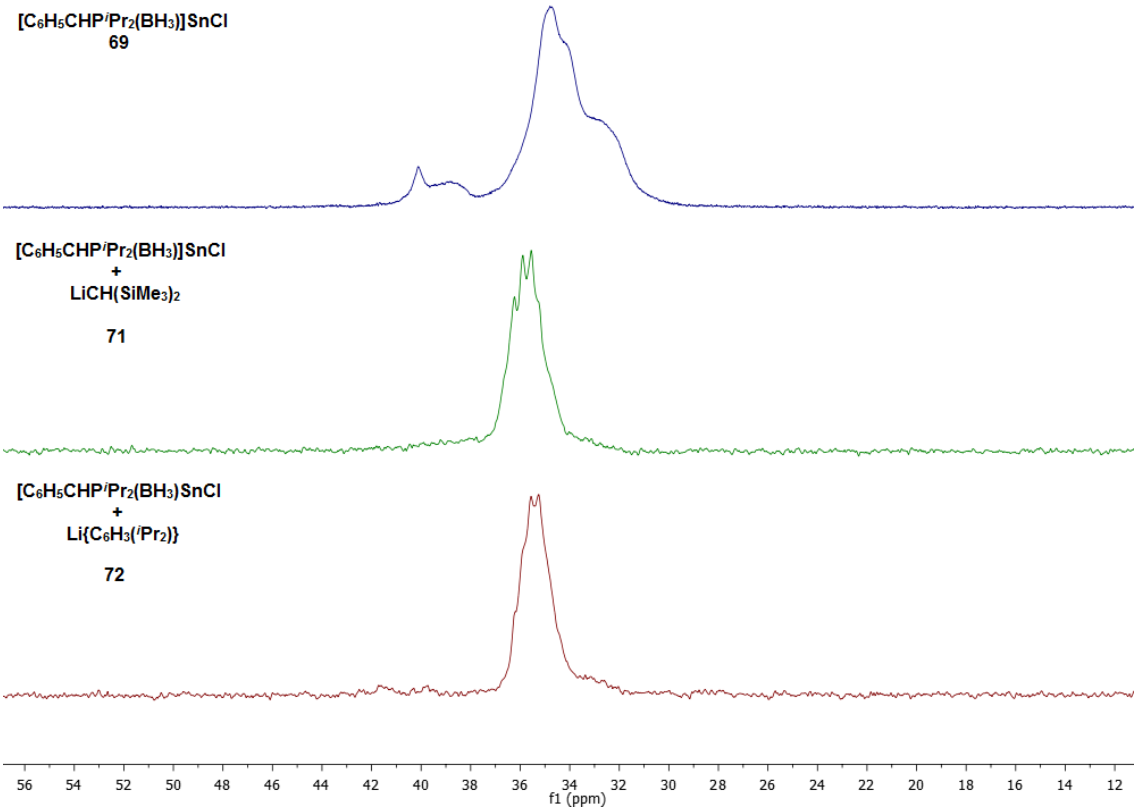

Figure 7.1: $^{31}P\{^{1}H\}$ NMR spectra of crude samples of **71** and **72** in diethyl ether compared to a crude $^{31}P\{^{1}H\}$ NMR spectrum of **69** diethyl ether.

Several solvents including diethyl ether, toluene, methylcyclohexane, *n*-hexane, ^{t}BuOMe and hexamethlydisiloxane (HMDSO) were used in order to isolate any form of solid to analyse via NMR spectroscopy or X-ray crystallography; unfortunately none of these solvents were successful.

7.3.2 Nitrogen- and oxygen-containing groups

Treatment of $[C_6H_5CHP^{i}Pr_2(BH_3)]SnCl$ with one equivalent of $LiN(SiMe_3)_2$ results in a colour change from pale yellow to a dark red solution (Scheme 7.3).

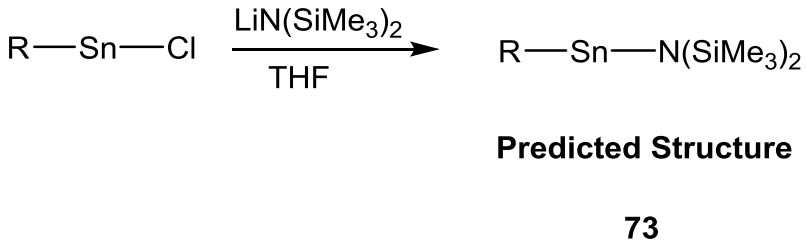

Scheme 7.3: Synthesis of compounds **73**.

A crude $^{31}P\{^{1}H\}$ NMR spectrum of the reaction with $LiN(SiMe_3)_2$ was taken and the $^{31}P\{^{1}H\}$ NMR spectra showed a change from the starting compound **69** (Figure 7.2).

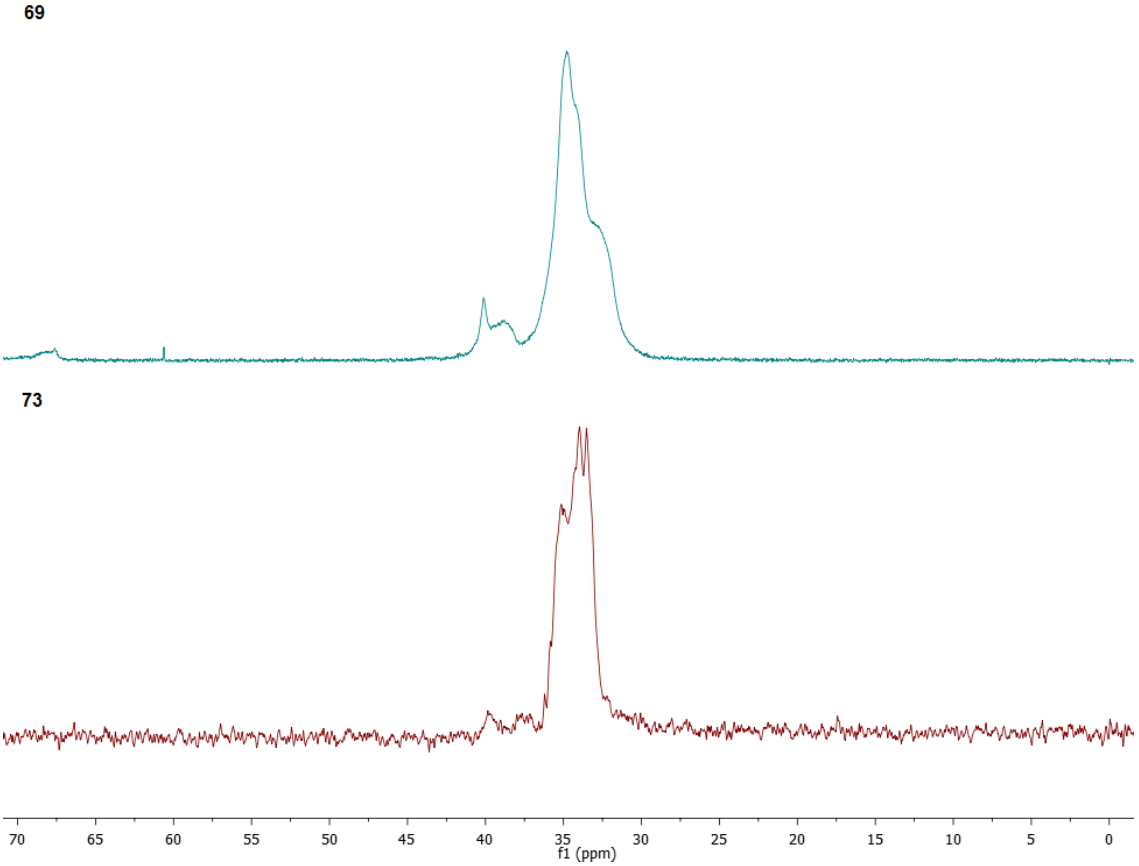

Figure 7.2: $^{31}P\{^{1}H\}$ NMR spectra of compound **73** in diethyl ether compared to **69** in diethyl ether.

Several solvents including diethyl ether, toluene, methylcyclohexane, *n*-hexane, ^{t}BuOMe and HMDSO were used in order to isolate any form of solid to analyse via NMR spectroscopy or X-ray crystallography; unfortunately none of these solvents were successful.

7.3.3 Phosphorus-containing groups

Treatment of $[C_6H_5CHP^iPr_2(BH_3)]SnCl$ with one equivalent of either $LiP(Dipp)_2$ or $LiP(Tripp)_2$ results in a colour change from pale yellow to a dark red solution (Scheme 7.4).

Work in the Izod group shows homoleptic diphosphatetrylenes $[Sn(PR_2)_2$ R = Tripp or Dipp] where the addition of tripp substituents are usually problematic due to decomposition to a diphosphine and the corresponding phosphine. The proposed route by which this decompositions occurs is via a triplet excited state which could be due to a small energy gap between the π and π^* orbitals (Figure 7.3).

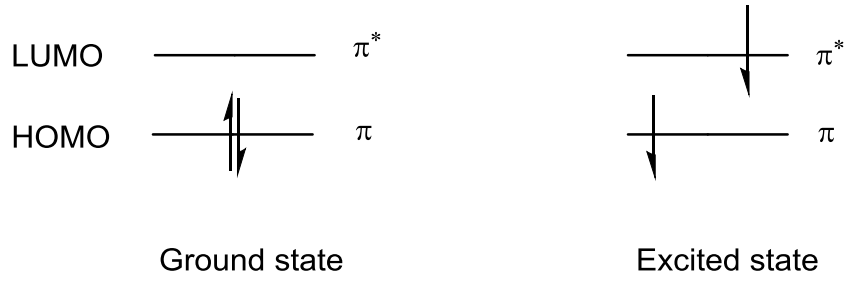

Figure 7.3: Molecular orbital diagrams of the ground and excited state of homoleptic diphosphatetrylenes $[Sn(PR_2)_2$ R = Tripp or Dipp].

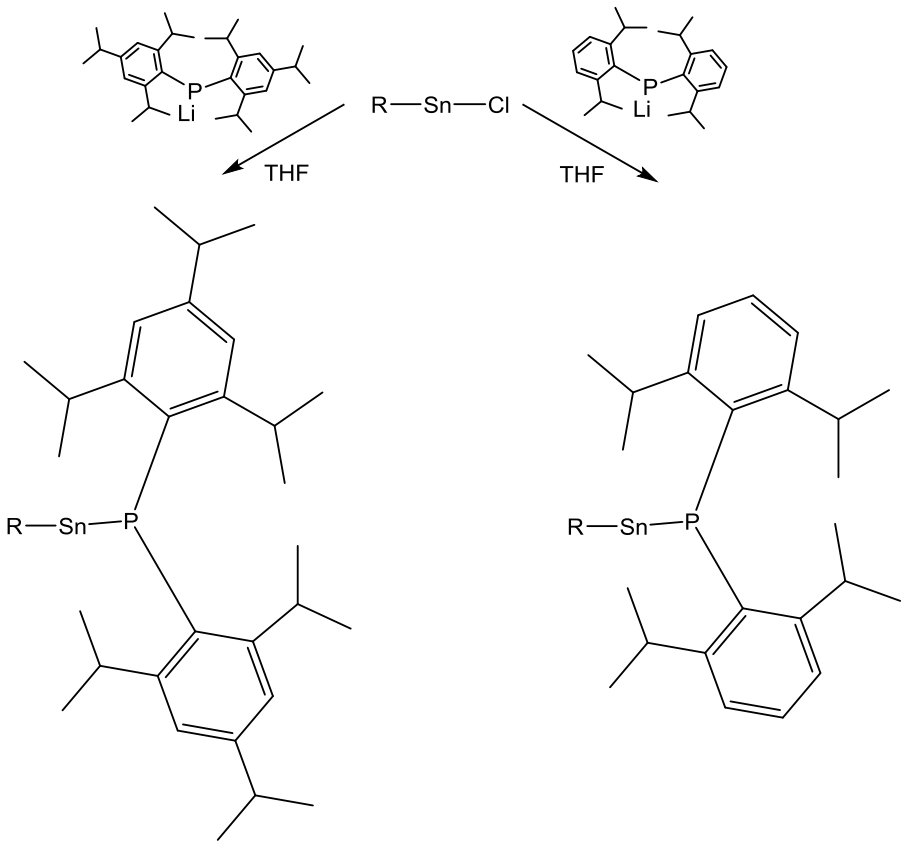

Scheme 7.4: Synthesis of compounds **74** and **75**.

This type of excited state may be attributed to the lone pair on the phosphorus atom donating to the empty p-orbital on the Sn centre (Figure 7.4).

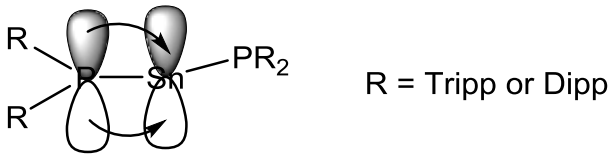

Figure 7.4: Orbital diagram showing the donation of the lone pair from the phosphorus into the empty p-orbital of the teteral centre.

The energy gap between the π and π^* orbitals for Dipp-substituted phosphines may be greater than those in Tripp-substituted phosphines, and so a triplet excited state is less likely; this prevents the decomposition to diphosphine and the corresponding phosphine.

The decomposition pathway seen in this type of phosphatetrylenes can also be seen in the reactions for compounds **74** and **75**, where the resulting heteroleptic phosphine-borane-substituted tetrylene now exhibits competing donation into the empty p-orbital from the diorganophosphine; this donation may supersede the usual agostic-type interactions (Figure 7.5).

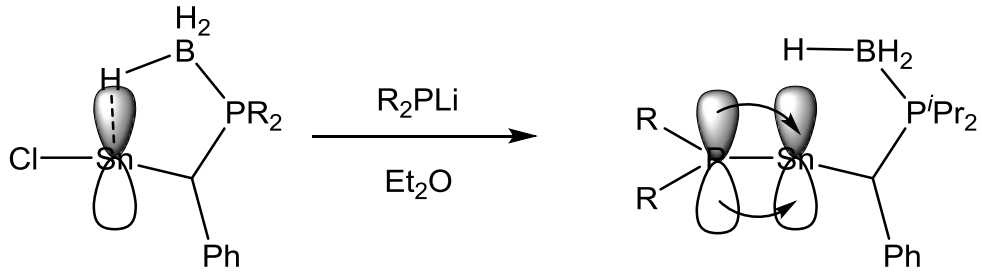

Figure 7.5: Orbital diagrams indicating the loss of agostic-type interactions.

Unpublished results in the Izod group regarding the reactions of Tripp and Dipp substituents with heavier group 14 metals show the formation of diphosphine and R_2PH (R = Dipp or Tripp). The production of the diphosphine and R_2PH may be attributed to the P-M bond being susceptible to reduction. This can also be seen in the crude reaction mixtures of compounds **74** and **75** (Figure 7.6) where the $^{31}P\{^{1}H\}$ NMR spectrum of **75** exhibits the least amount of decompostition products, along with a new signal at -25.3 ppm; indicating that Dipp is a more stable substituent than Tripp.

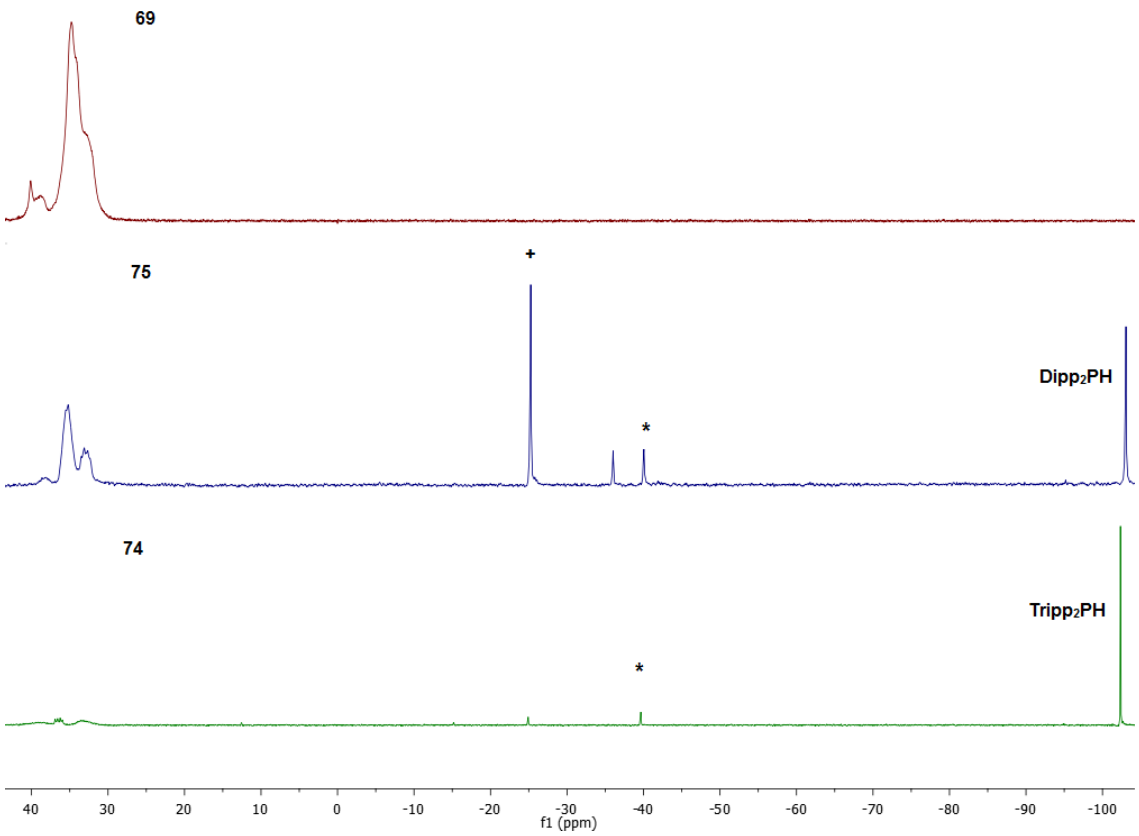

Figure 7.6: $^{31}P\{^{1}H\}$ NMR spectra of crude samples of **74** and **75** (+) compared to **69**; * R_2P-PR_2 [R = Dipp (middle), Tripp (bottom)].

Several solvents including diethyl ether, toluene, methylcyclohexane, *n*-hexane, ^{t}BuOMe and HMDSO were used in order to isolate any form of solid to analyse via NMR spectroscopy or X-ray crystallography; unfortunately none of these solvents were successful.

Furthermore, these bulky reagents make the products far too soluble to isolate any crystalline material in order to characterise via NMR spectroscopy or X-ray crystallography. In order to alter the highly soluble nature of these compounds, we decided to use much less sterically hindered reagents.

7.4 Reactivity of heteroleptic alkylstannylenes with less sterically hindered groups

Treatment of $[C_6H_5CHP^{i}Pr_2(BH_3)]SnCl$ with one equivalent of either MeMgBr or PhMgCl results in a colour change from pale yellow to a red solution (Scheme 7.5).

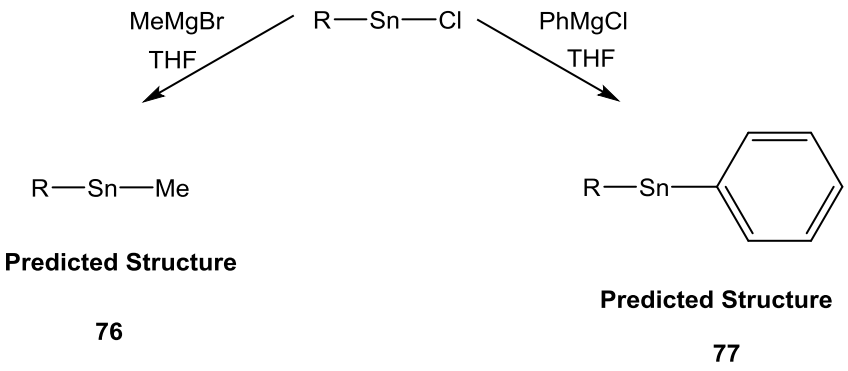

Scheme 7.5: Synthesis of compounds **76** and **77**.

Crude $^{31}P\{^{1}H\}$ NMR spectra were taken which show a change in the phosphine-borane species for both reactions (Figure 7.7).

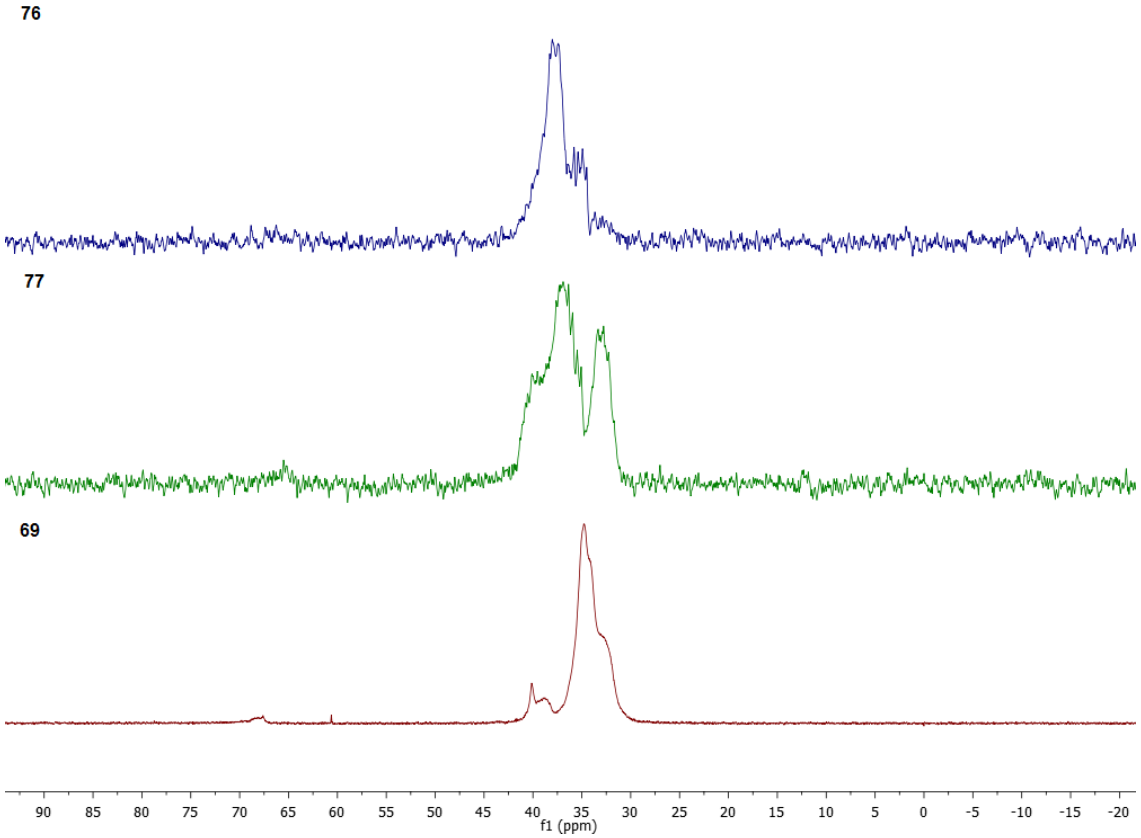

Figure 7.7: $^{31}P\{^{1}H\}$ NMR spectra of crude samples of **76** and **77** in diethyl ether compared to **69** in diethyl ether.

Both product mixtures were extracted into diethyl ether, the solvent was reduced and the solutions were cooled to 5 °C; crystalline **77** was obtained in this way, but unfortunately this was not suitable for X-ray crystallography.

7.5 Conclusions

Overall, sterically bulky ligands result in extremely soluble heteroleptic alkylstannylenes which could not be isolated. Compounds **71**-**75** exhibited a change in their crude $^{31}P\{^{1}H\}$ NMR spectra compared to the starting material **69**, however, even after using the very poor solvent HMDSO, no crystalline solid was isolated. This solubility issue led to the use of much less sterically demanding groups such as phenyl and methyl. Compounds **76** and **77** show a change in the $^{31}P\{^{1}H\}$ NMR spectra (Figure 7.7) and crystalline material was isolated for **77**. Unfortunately, this crystalline material was not suitable for X-ray crystallography and sufficiently clean NMR spectra were not obtained. However, the data obtained suggest that the use of small ligands should enable the isolation of heteroleptic alkylstannylenes, if suitable substituents are selected.

Chapter 8. Oxidation reactions of a phosphine-borane-stabilised dialkylstannylene

8.1 Introduction

The first example of the oxidative addition of an organohalide to a Sn(II) compound to give a tetravalent organotin compound, [Sn(Me)(Et)(Pr)I], was reported by Pope and Peachy in 1900.[1] To this date, there are a vast number of tetravalent organotin compounds, however, this investigation reported in this thesis will only consider the oxidative addition products containing $SiMe_3$ substituents, due to their isoelectronic relationship with $PMe_2(BH_3)$.

Treatment of acyclic SnR_2 (R = bis(trimethylsilyl)methyl) with MeI, HCl, RCl or RBr results in the products SnR_2MeI (**78**), SnR_2HCl (**79**), SnR_3Cl (**80**) and SnR_3Br (**81**), respectively as reported by Lappert and co-workers in 1976.[2] Investigations into compound **79** (via multielement NMR spectroscopy) indicated that the $SiMe_3$ groups were diastereotopic due to the tin centre exhibiting prochirality which can be seen in a simple Newmann projection diagram (Figure 8.1).[2]

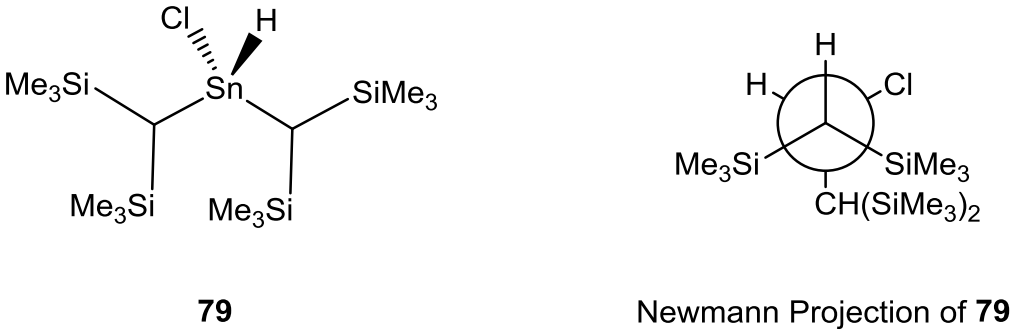

79 Newmann Projection of **79**

Figure 8.1: Newmann projection along the C-Sn bond indicating diastereotopic $SiMe_3$ groups in compound **79**.

It is of interest that a similar reaction between PbR_2 and HCl did not yield the oxidative addition product. Lappert thought the cause of this may be attributed to the increased reactivity and the weakness of the Pb-C bond, compared to Sn-C, therefore resulting in a decomposition product. Lappert and co-workers also referred to the reluctance of lead

compounds being able to achieve higher oxidation states needed for a four-coordinate oxidative addition product.[2]

Treatment of cyclic $Sn[C(SiMe_3)_2SiMe_2CH_2]_2$ (**30**) with MeI resulted in the oxidative addition product $Sn[C(SiMe_3)_2SiMe_2CH_2]_2(Me)I$ (**82**) published by Eaborn and co-workers in 2000; unfortunately, no investigations into the structure of compound **82** were undertaken.[3]

To date, there are very few examples of phosphine-borane-substituted Sn(IV) compounds and so this area of research is very much in its infancy, compared to the $SiMe_3$-substituted derivatives; compounds $[(Me_3Si)\{Me_2P(BH_3)CH]_2Sn(R)(X)$ [R = Me, X = I (**83**); R = CH_2CMe_3, X = I (**84**); R = CH_2Ph, X = Br (**85**)] were isolated and characterised by Izod and co-workers.[4] This chapter describes the synthesis of a new phosphine-borane-substituted Sn(IV) compound, along with its structural characterisation and a detailed investigation into its solution state structure using multielement NMR spectroscopy.

8.2 Synthesis of an oxidative addition product using MeI or BnBr

Treatment of a diethyl ether solution of $[C_6H_5CHP^iPr_2(BH_3)]_2Sn$ (**64**) with one equivalent of methyl iodide or benzyl bromide yields the corresponding oxidative addition products $[C_6H_5CHP^iPr_2(BH_3)]_2Sn(Me)I$ (**86**) and $[C_6H_5CHP^iPr_2(BH_3)]_2Sn(Bn)Br$ (**87**), respectively, as white powders over the course of 1-16 hrs (Scheme 8.1). Colourless crystals suitable for X-ray crystallography were grown by dissolving compound **86** in hot toluene and layering with diethyl ether. Compound **87** was crystallised via the same method but the crystalline material isolated was only suitable for elemental analysis and multielement NMR spectroscopy.

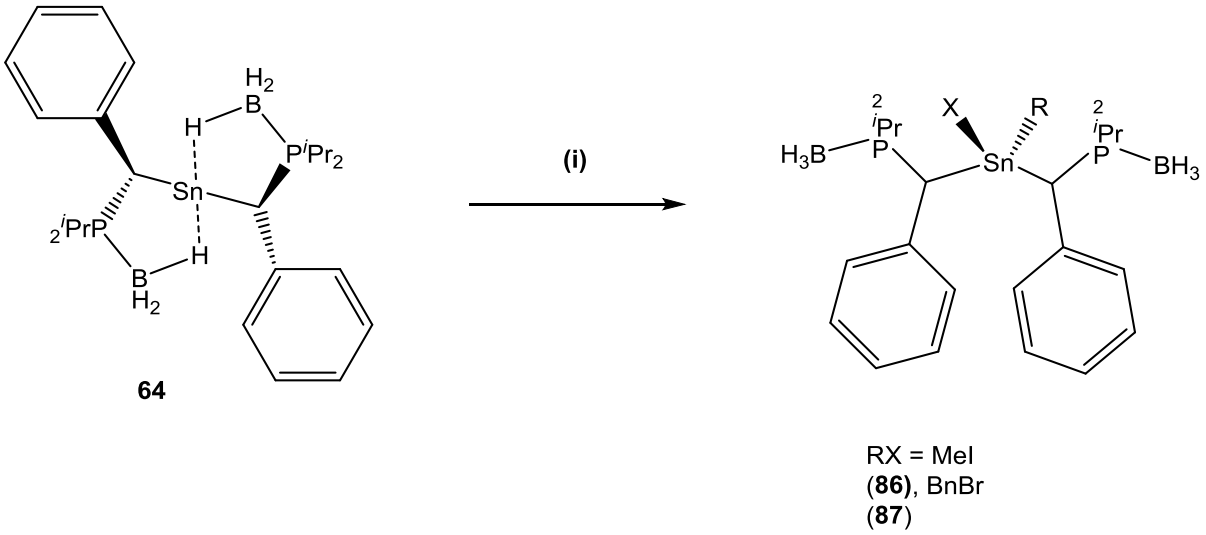

Scheme 8.1: Oxidation of compound **64**. Reagents and conditions: i) RX, diethyl ether, r.t., 16 hrs.

The solid state structure of compound **86** was determined by X-ray crystallography; the molecular structure is shown in Figure 8.2 and selected bond lengths and angles are given in Table 8.1. Compound **86** crystallises as a discrete monomer where the tin centre has contacts with two phosphine-borane fragments via the carbanion centres, a bond to the methyl carbon atom and a contact with an iodide in a distorted tetrahedral geometry; this compound has no agostic-type interactions between the borane hydrogens and the tin centre. Compound **86** lies on a *pseuo*-C_2 axis, with the methyl group and the iodine atom disordered over two sites each with equal occupancy, similar to the previously reported complex $[(Me_3Si)\{Me_2P(BH_3)\}CH]_2Sn(Me)(I)$ (**83**).[4]

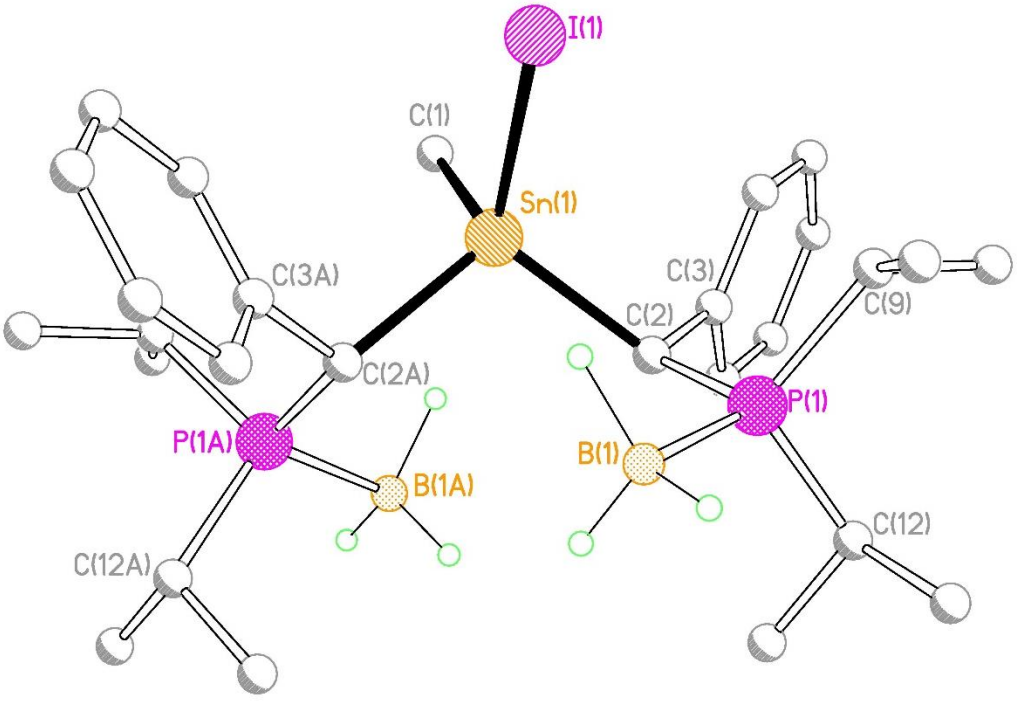

Figure 8.2: Molecular structure of **86** with H atoms (except for those bound to boron) and disorder component omitted for clarity.

Sn(1)-I	2.5611(15)	Sn-C(1)	2.25(3)
P(1)-B(1)	1.928(10)	Sn-C(2)	2.161(7)
P(1)-C(2)	1.842(8)	P(1)-C(9)	1.850(8)
P(1)-C(12)	1.843(9)	B(1)-H(1A)	1.09(10)
B(1)-H(1B)	1.23(11)	B(1)-H(1C)	1.08(10)
I-Sn-C(1)	103.7(6)	C2-Sn-C2(2A)	107.4(4)

Table 8.1: Selected bond lengths (Å) and angles (°) for **86**.

The Sn-I distance in compound **86** (2.5611(15) Å) is shorter than the Sn-I distances in other examples of tetravalent organotin(IV) iodides (typically 2.67-2.79 Å);[5-10] but it is of similar length to the corresponding distance in **83** (2.5626(7) Å). The Sn-I distance in compound **86** is also much shorter than that in the phosphine-borane-substituted organotin(IV) halide, $[(Me_3Si)\{Me_2P(BH_3)\}CH]_2Sn(CH_2CMe_3)(I)$ (**84**) (average of 2.7353 Å over three molecules in the asymmetric unit) which may be attributed to the greater steric

crowding at the tin centre in the latter example due to the larger neopentyl group compared to the methyl group in compound **86**.[4]

The Sn-C(carbanion) distance in compound **86** (2.253(3) Å) is within the typical range for tetrahedrally-coordinated organotin(IV) halides (Sn-C 2.04-2.33 Å) as well as other examples of phosphine-borane-substituted organotin(IV) halides (2.17-2.23 Å).[4-14] The Sn-C(carbanion) distance in compound **86** is between 0.03-0.06 Å shorter than the corresponding distances in the dialkylstannylene **64**, as expected, due to the increased formal charge at the tin centre in the oxidation product. The C(carbanion)-Sn-C(carbanion) bond angle increases significantly upon oxidation to form the tin(IV) centre; in the dialkylstannylene the C(carbanion)-Sn-C(carbanion) angle is 95.1(4) °, whereas the corresponding angle in compound **84** is 107.4(4) °.

In compound **86** the $^{119}Sn\{^{1}H\}$ NMR spectrum exhibits a doublet of doublets at -14.8 ppm (J_{SnP} = 20.5 Hz, $J_{SnP'}$ = 106.3 Hz). The rotational symmetry present in the dialkylstannylene is lost upon oxidative addition and formation of the Sn(IV) centre. This results in two distinct phosphorus centres, one in each phosphine-borane-stabilised carbanion ligand, along with the previously noted diastereotopic nature of the ^{i}Pr substituents; all of which can be seen in the NMR spectra of **86**. The $^{11}B\{^{1}H\}$ NMR spectrum of **86** exhibits a broad peak at 40.2 ppm which resolves into two distinct peaks (-40.1 ppm and -40.8 ppm) after carrying out broadband decoupling of ^{31}P (Figure 8.3). After selective ^{31}P decoupling the $^{11}B\{^{1}H, ^{31}P\}$ NMR spectra shows which boron is associated with which phosphorus.

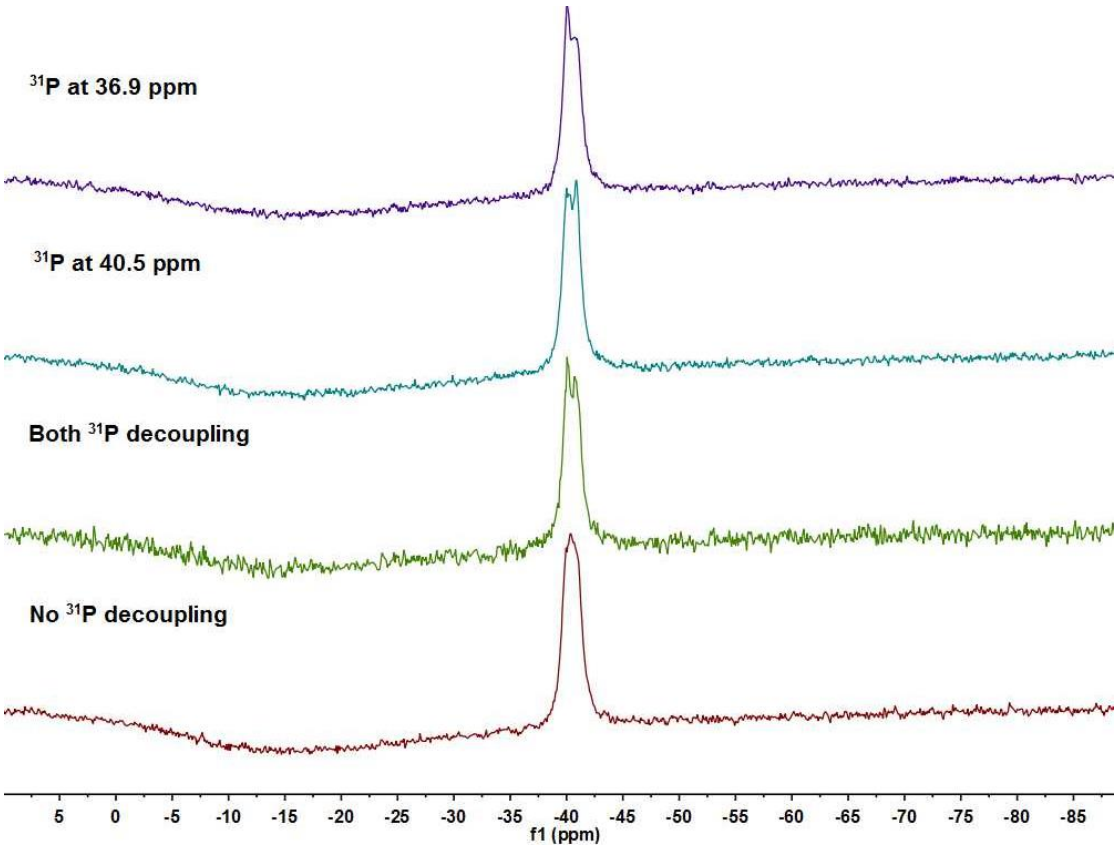

Figure 8.3: $^{11}B\{^{1}H, ^{31}P\}$ NMR spectra of compound **86** in $CDCl_3$ with selective ^{31}P decoupling.

The $^{31}P\{^{1}H\}$ NMR spectrum of **86** exhibits two broad peaks at 36.9 ppm and 40.5 ppm which are attributed to the two distinct phosphorus environments. Selective ^{11}B decoupling confirms that the phosphorus centre resonating at 36.9 ppm is associated with the boron at -40.1 ppm and the phosphorus at 40.5 ppm is associated with the boron at -40.8 ppm (Figure 8.4).

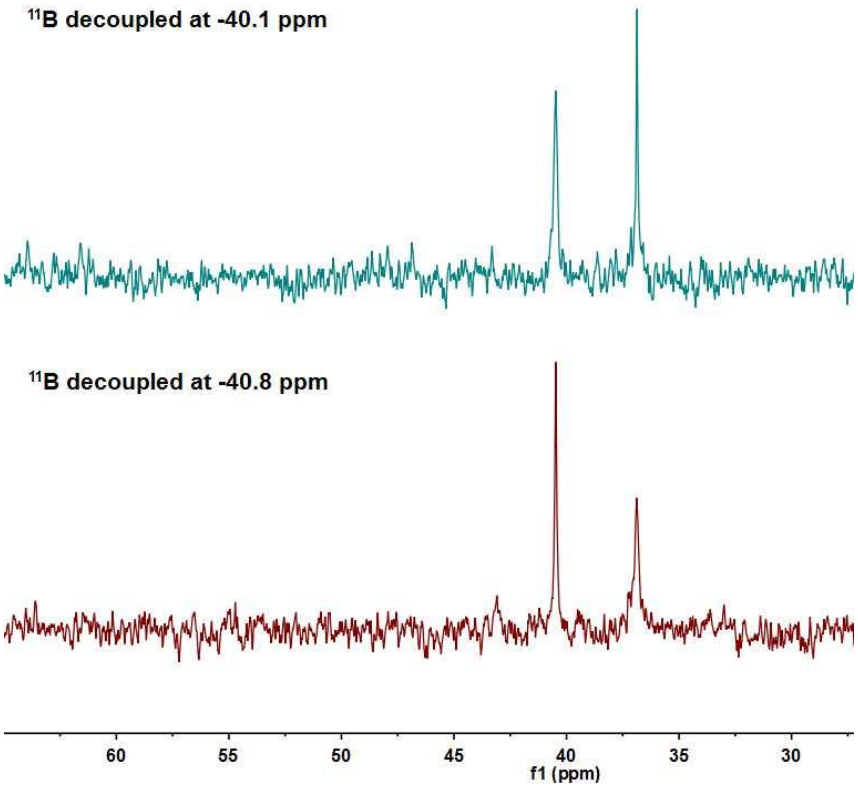

Figure 8.4: $^{31}P\{^{1}H\}$ NMR spectra of compound **86** in $CDCl_3$ with selective ^{11}B and ^{1}H decoupling.

It is much more complicated to assign the proton NMR spectrum of **86** (Figure 8.5) due to the chiral carbon centres which result in both the methine protons within the isopropyl substituents being diastereotopic; this means we expect four different methine proton environments and eight different isopropyl methyl environments along with other proton environments within compound **86**.

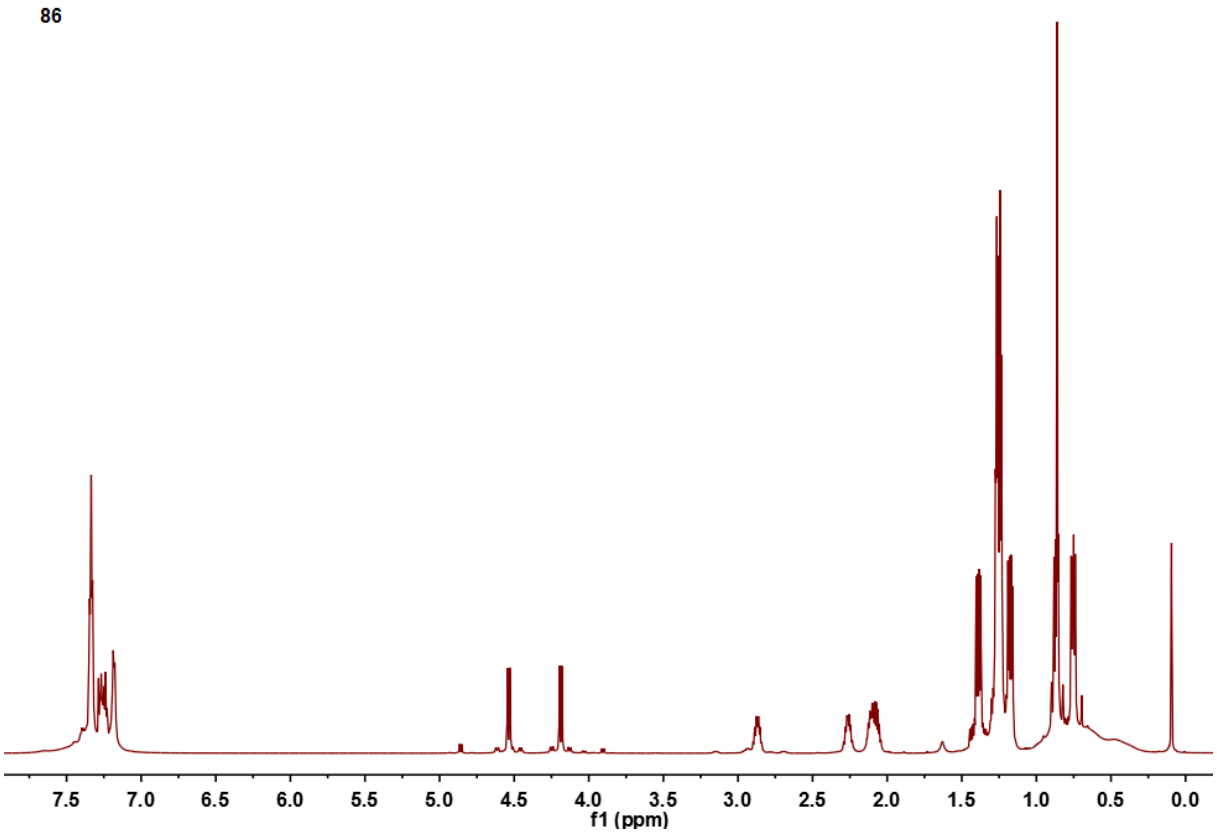

Figure 8.5: ^{1}H NMR spectrum of compound **86**.

To assign the ^{1}H NMR spectrum the following steps were carried out:

1. Firstly, the two doublets at 4.19 (J_{PH} = 15.0 Hz) and 4.54 ppm (J_{PH} = 15.0 Hz) are attributed to the protons at positions H^{1} and $H^{1'}$ (Figure 8.6) as these will be the most deshielded due to the tin centre and the phenyl rings. Selective ^{31}P decoupling at 36.9 and 40.5 ppm (Figure 8.7) allows assignment of H^{1} and $H^{1'}$ as the peak changes from a doublet to a singlet on decoupling. Therefore, H^{1} is assigned to the phosphorus centre labelled P^{2} and $H^{1'}$ to $P^{2'}$.

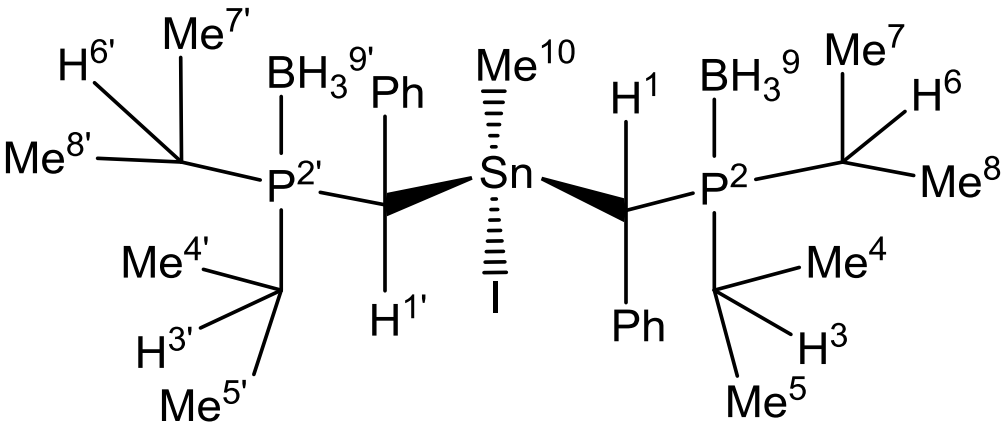

Figure 8.6: Compound **86** with atom labels

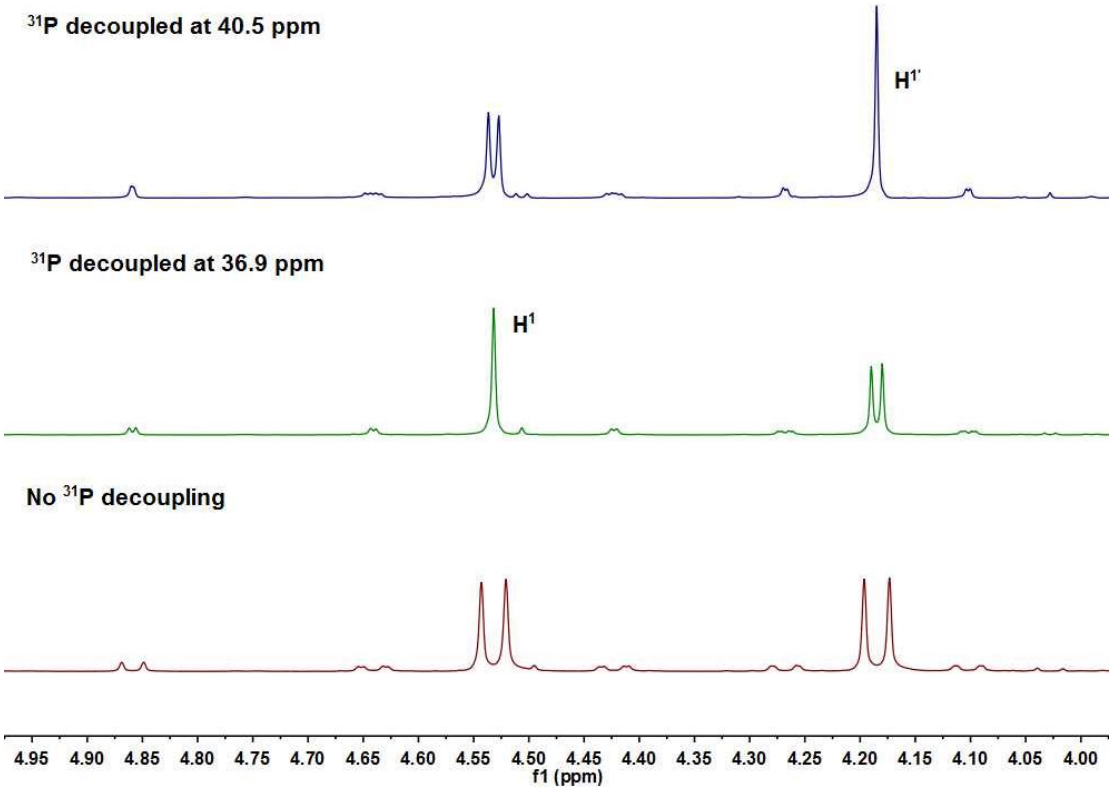

Figure 8.7: ^{1}H NMR spectra of compound **86** (benzylic region) with selective ^{31}P decoupling.

2. Moving upfield in the ^{1}H NMR spectrum, the two doublets of septets and the multiplet at 2.10 ppm are attributed to the four methine protons within the isopropyl substituents, the multiplet containing two protons. Again, by selectively decoupling at phosphorus, the isopropyl protons can be assigned to an individual phosphorus centre (Figure 8.8). By selectively decoupling at 36.9 ppm the doublet of septets at 2.26 ppm

and the left hand side of the multiplet resolves into a septet and therefore, the protons at positions H^3 and H^6 are associated with the phosphorus resonating at 36.9 ppm (P^2). By selectively decoupling at 40.5 ppm the doublet of septets at 2.87 ppm and the right hand side of the multiplet resolves into a septet and therefore the protons at positions $H^{3'}$ and $H^{6'}$ are associated with the phosphorus resonance at 40.5 ppm ($P^{2'}$).

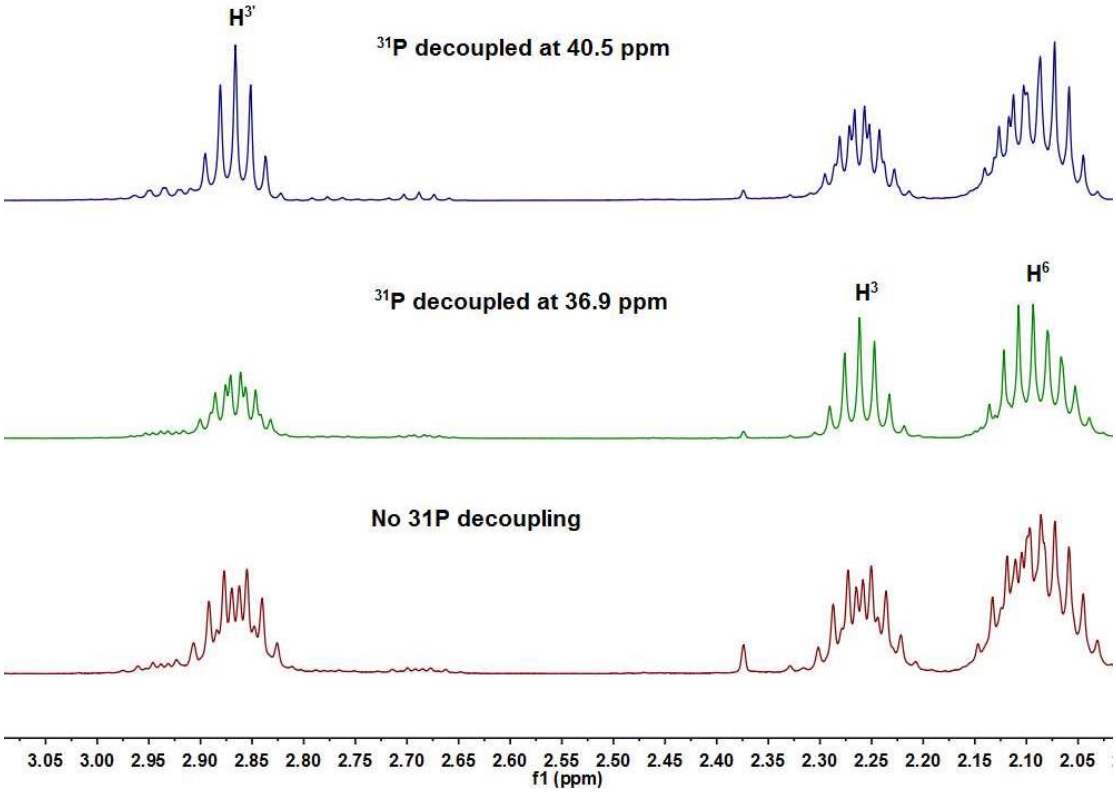

Figure 8.8: ^{1}H NMR spectra of compound **86** (C*H*^{i}Pr$_2$ region) in $CDCl_3$ with selective ^{31}P decoupling.

3. Moving further upfield in the ^{1}H NMR spectrum the four doublets of doublets (0.76, 0.87, 1.18 and 1.39 ppm) and the multiplet (1.25 ppm) are attributed to the eight different methyl groups within the isopropyl substituents; the ^{1}H NMR spectra with selective ^{31}P decoupling can be seen in Figure 8.9. With selective ^{31}P decoupling at 40.5 ppm the methyl groups at positions $Me^{4'}$, $Me^{5'}$, $Me^{7'}$ and $Me^{8'}$ resolve into single doublets and therefore, are associated with the phosphorus resonating at 40.5 ppm ($P^{2'}$) whilst the methyl groups at positions Me^4, Me^5, Me^7 and Me^8 are associated with the phosphorus at 36.9 ppm (P^2). The peak at 0.86 ppm is attributed to the methyl group directly bonded to the Sn centre (position Me^{10}).

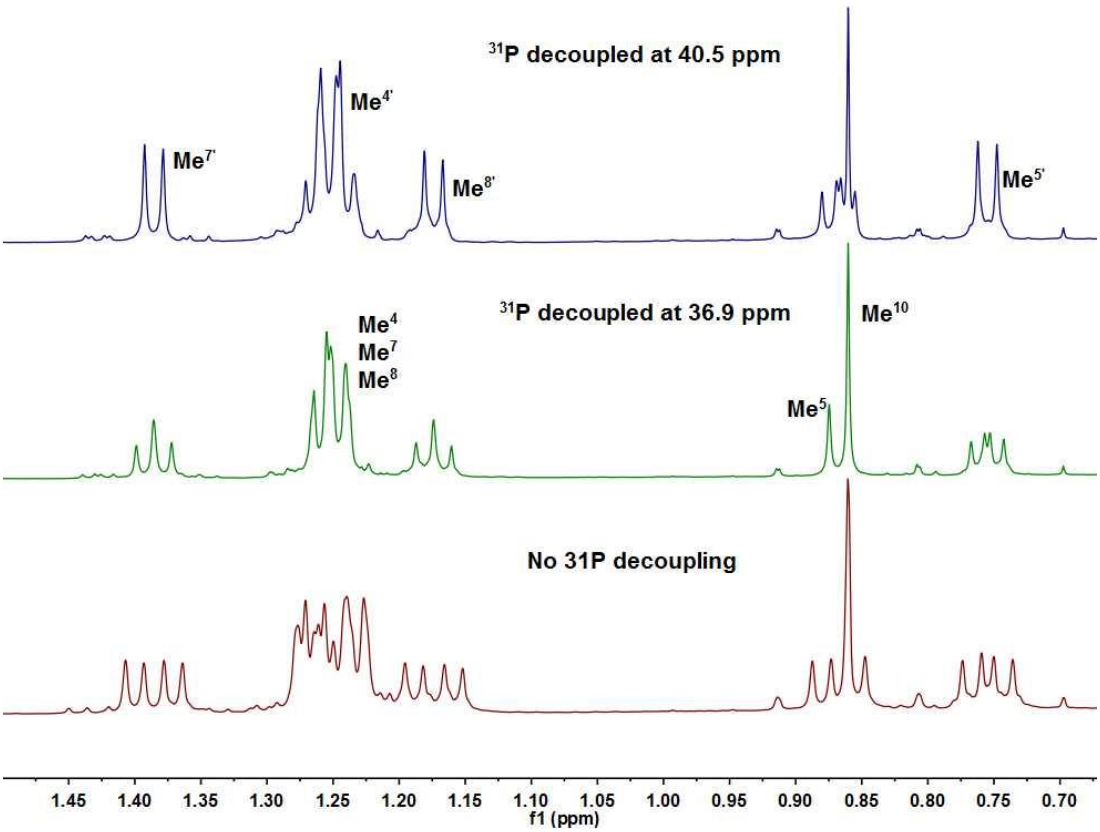

Figure 8.9: ^{1}H NMR spectra of compound **86** (methyl region) in $CDCl_3$ with selective ^{31}P decoupling.

4. Finally, a $^{1}H\{^{31}P\}$ COSY NMR spectrum was used to confirm the assignment of the protons and methyl groups within the isopropyl substituents.

To assign the ^{13}C peaks, the following steps were carried out:

1. An HSQC (Heteronuclear Single-Quantum Correlation) experiment was carried out in order to identify which protons were associated with which carbon atoms, as well as selective ^{31}P decoupling to identify which carbon atoms are associated with which phosphorus centre. The correlation between the protons and carbon atoms aided in the labelling of the overall structure seen in Figure 8.6 and a summary of $^{13}C\{^{1}H\}$ NMR signals can be seen in Table 8.2 below.
2. At room temperature, the $^{13}C\{^{1}H\}$ NMR spectrum showed very broad peaks in the aromatic region, therefore, VT (variable temperature) NMR spectroscopy (Figure 8.10) was needed, along with more NMR experiments (explained below) to assign the carbon atoms within the phenyl rings.

Atom Label	$^{1}H\{^{11}B\}$ NMR/ppm	$^{13}C\{^{1}H\}$ NMR/ppm/298 K
1	4.54 (J_{PH} = 15.0 Hz, J_{SnH} = 55.0 Hz)	34.79 (J_{PC} = 13.8 Hz)
2	-	-
3	2.26	21.46 (J_{PC} = 33.96 Hz)
4	1.25	19.51 (J_{PC} = 2.52 Hz)
5	0.87 (J_{HH} = 10.0 Hz, J_{PH} = 15.0 Hz)	17.19 (J_{PC} = 3.77 Hz)
6	2.10	22.00 (J_{PC} = 31.45 Hz)
7	1.25	
8	1.25	
9	0.56 (J_{PH} = 15.0 Hz)	-
10	0.86	5.56 (J_{P2C} = 1.80 Hz, $J_{P2'C}$ = 2.38 Hz)
1'	4.19 (J_{PH} = 15.0 Hz, J_{SnH} = 130.0 Hz)	35.68 (J_{PC} = 17.6 Hz)
2'	-	-
3'	2.87	21.24 (J_{PC} = 2.52 Hz)
4'	1.25	
5'	0.76 (J_{HH} = 10.0 Hz, J_{PH} = 15.0 Hz)	17.14 (J_{PC} = 5.03 Hz)
6'	2.10	21.00
7'	1.39 (J_{HH} = 10.0 Hz, J_{PH} = 15.0 Hz)	17.53
8'	1.18 (J_{HH} = 10.0 Hz, J_{PH} = 15.0 Hz)	18.24 (J_{PC} = 2.52 Hz)
9'	0.75 (J_{PH} = 10.0 Hz)	-

Table 8.2: Summary of ^{1}H and $^{13}C\{^{1}H\}$ signals of compound **86**.

3. The $^{13}C\{^{1}H\}$ NMR spectrum at 223 K shows two doublets at 135.90 (J_{PC} = 8.80 Hz) and 136.31 ppm (J_{PC} = 8.80 Hz) which are affiliated with the *ipso* carbons. The

carbons at the *para* position within the phenyl ring are associated with the signals at 126.75 (J_{PC} = 1.26 Hz) and 126.90 ppm (J_{PC} = 2.52 Hz) (Figure 8.10).

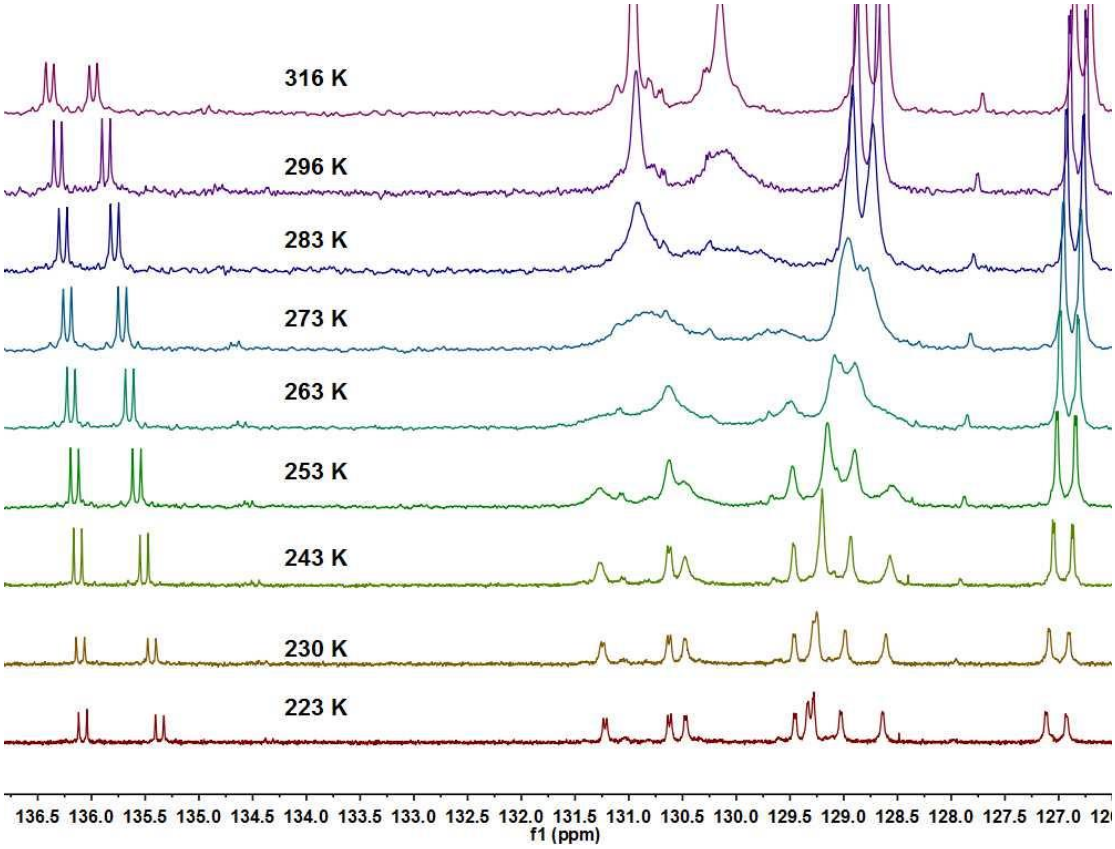

Figure 8.10: Variable temperature $^{13}C\{^{1}H\}$ NMR spectra of compound **86** in $CDCl_3$ showing the phenyl region.

4. To start assigning the phenyl region, a ^{13}C $\{^{1}H\}$ EXSY (Exchange Spectroscopy) NMR experiment was used to indicate which carbon atoms are exchanging within the same aromatic ring (Figure 8.11). The four peaks labelled (*) at 129.5, 130.5, 130.6 and 131.23 ppm are due to the *meta* carbon atoms and the three peaks labelled (+) at 128.6, 129.0 and 129.3 ppm are due to the *ortho* carbon atoms.

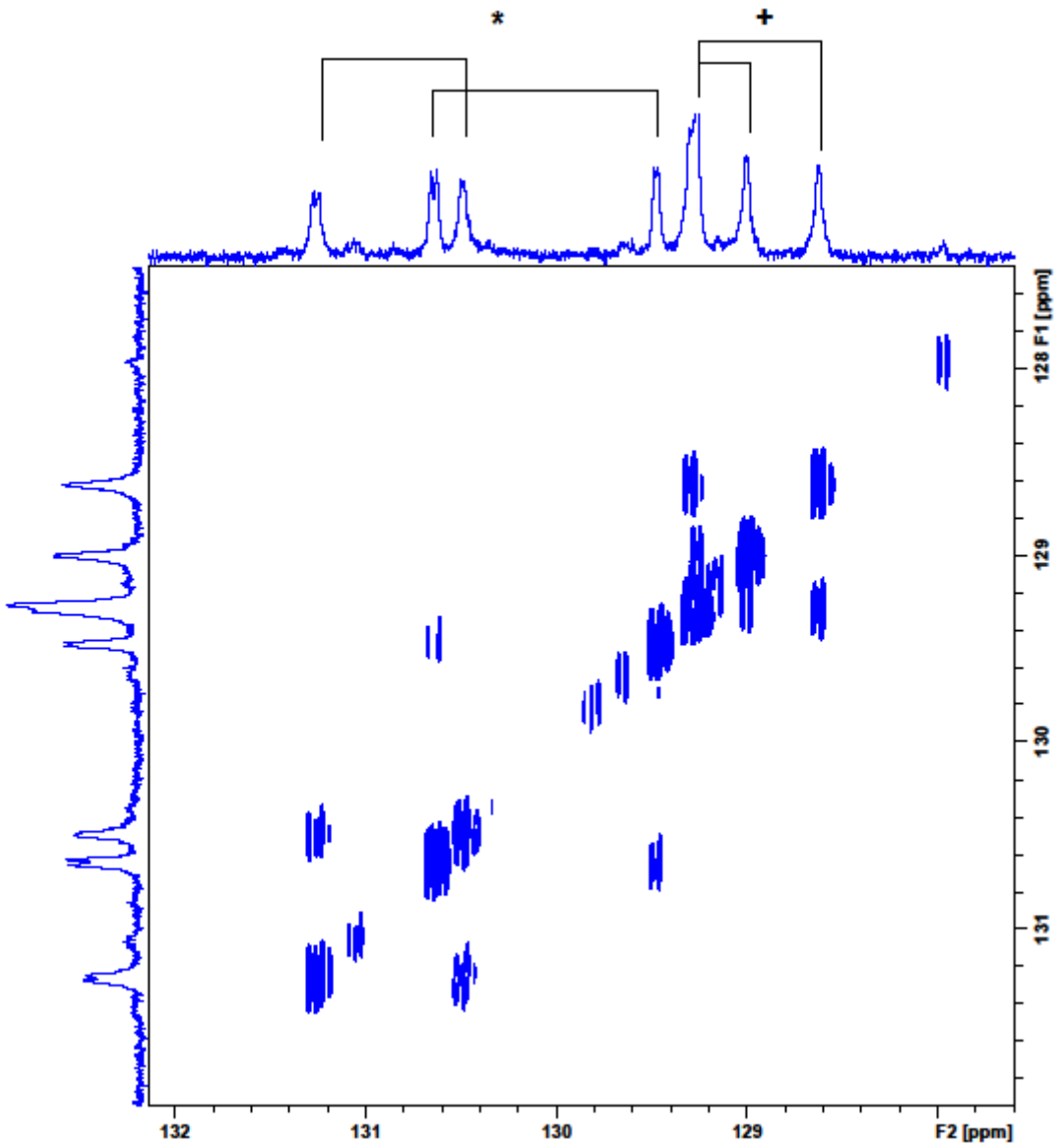

Figure 8.11: $^{13}C\{^{1}H\}$ EXSY NMR spectrum of **86** in $CDCl_3$ at 223 K indicating the *ortho* (*) and *meta* (+) protons in the phenyl region.

5. By looking at the HSQC spectrum the assignment of the *ortho* and *meta* carbon atoms can be used to assign the majority of the *ortho* and *meta* protons (Figure 8.12). The *meta* carbons at 130.5, 130.6 and 129.5 ppm correlate with the protons at 7.06 (J_{PH} = 10.00 Hz), 7.16 (J_{PH} = 5.00 Hz) and 7.51 ppm (J_{PH} = 5.00 Hz), respectively. Unfortunately, the multiplet at 7.31 ppm in the HSQC spectrum was unhelpful in determining the remainder of the *ortho* and *meta* protons. A summary of the ^{1}H and $^{13}C\{^{1}H\}$ NMR signals are presented in Table 8.2.

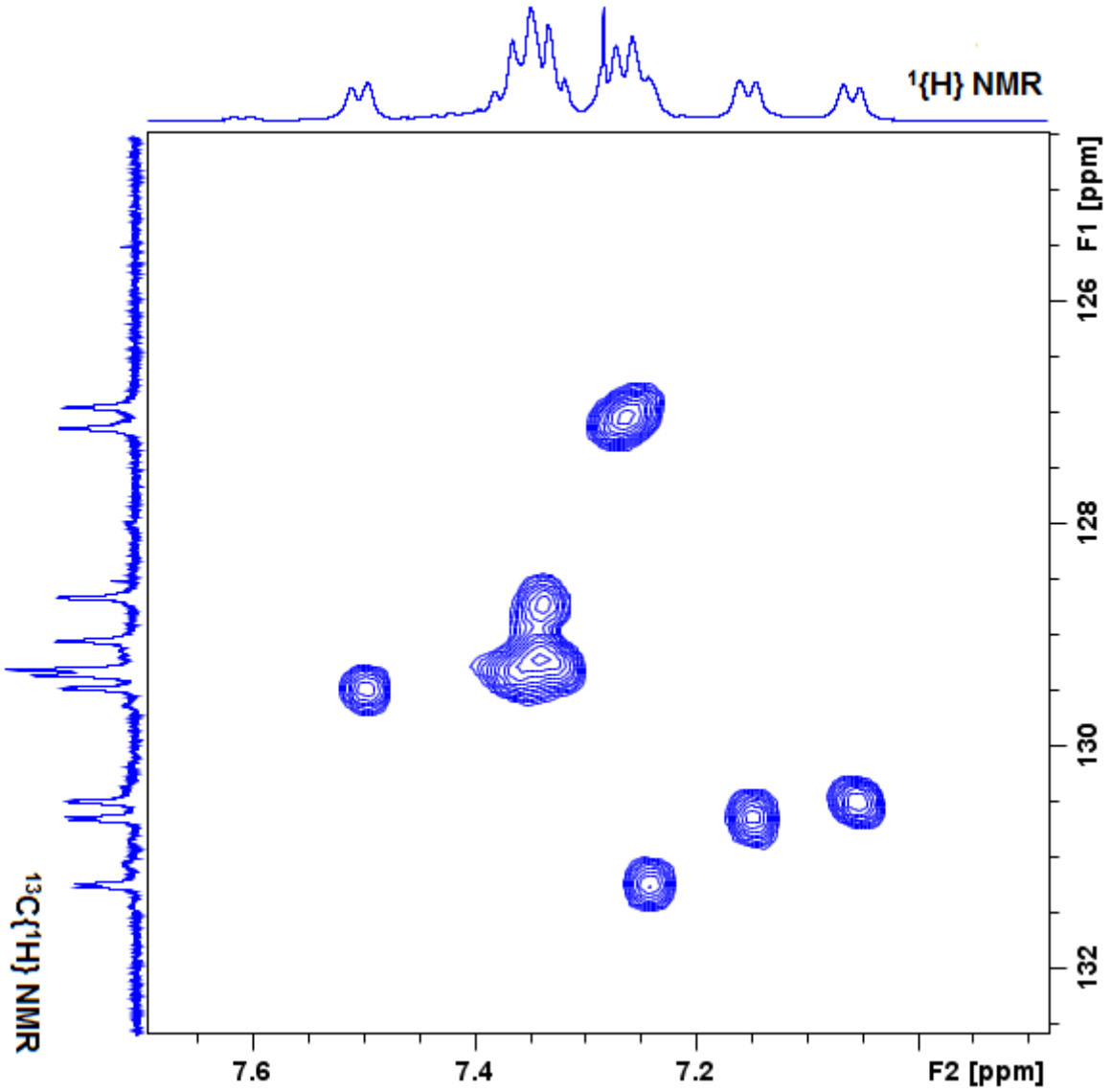

Figure 8.12: ^{1}H-^{13}C HSQC NMR spectrum of **86** in $CDCl_3$ indicating the correlation between *ortho* protons and carbons, and *meta* protons and carbons.

The ^{13}C{^{1}H} NMR spectrum at 296 K indicates dynamic behaviour in the *ortho* and *meta* carbon atoms which is identified by the broad nature of the signals between 128.5 and 131.5 ppm, and which may be attributed to restricted rotation of the phenyl rings about the P-C bond. It is of interest to investigate the *ortho* and *meta* carbon atoms in order to identify whether the rotation of the two aromatic rings exhibit different rotational energy barriers; this may be achieved by the use of the Eyring equation (Equation 8.1).

$$k = x\ \frac{k_B T}{h} e^{-\frac{\Delta G}{RT}}$$

k_B = Boltzmann constant (1.3805 x 10^{-23} JK^{-1})

x = transmission coefficient (assumed to be 1)

h = Planck's constant (6.6256 x 10^{-34} Js)

Equation 8.1: Eyring equation.

Equation 8.2 represents the correlation between the free enthalpy of activation ($\Delta G^{\ddagger}$), enthalpy of activation ($\Delta H^{\ddagger}$) and the entropy of activation ($\Delta S^{\ddagger}$).

$$\Delta G^{\ddagger} = \Delta H^{\ddagger} - T\Delta S^{\ddagger}$$

Equation 8.2: Correlation between $\Delta G^{\ddagger}$, $\Delta H^{\ddagger}$ and $\Delta S^{\ddagger}$.

Substituting equation 8.2 into equation 8.1 and rearrangement results in equation 8.3, with (lnk/T) as the subject.

$$ln\frac{k}{T} = ln\frac{k_B}{h} - \frac{\Delta H^{\ddagger}}{RT} + \frac{\Delta S^{\ddagger}}{R}$$

Equation 8.3: Result of substituting equation 2 into equation 3.

The experimental $^{13}C\{^{1}H\}$ NMR data at 223, 243, 253, 316 and 330 K (Figure 8.13) were used to help simulate the $^{13}C\{^{1}H\}$ NMR spectra (Figure 8.14) at these temperatures, in order to gain the rate constants associated with the exchange of the *ortho* carbon atoms in each aromatic ring. Using Figure 8.14 and the corresponding experimental $^{13}C\{^{1}H\}$ NMR spectra (Figure 8.13), both the simulated and experimental $^{13}C\{^{1}H\}$ NMR spectra are similar and therefore, the rate constants extracted from the simulated $^{13}C\{^{1}H\}$ NMR spectra can be used to carry out an Eyring plot that gives a straight line in each case (Figure 8.15). The gradient and the intercept of the graphs in Figure 8.15 can be calculated to produce the rotational energy barriers (Ring 1, $\Delta H^{\ddagger}$ = 53.2 kJ mol^{-1}; Ring 2, $\Delta H^{\ddagger}$ = 48.7 kJ mol^{-1}) and the entropy (Ring 1, $\Delta S^{\ddagger}$ = -9.50 J mol^{-1} K^{-1}; Ring 2, $\Delta S^{\ddagger}$ = -19.0 J mol^{-1} K^{-1}), respectively (Table

of T vs k can be seen in Appendix 2). This clearly shows that the barrier to rotation is different for the two phenyl rings in **86**, in spite of their rather similar chemical environments.

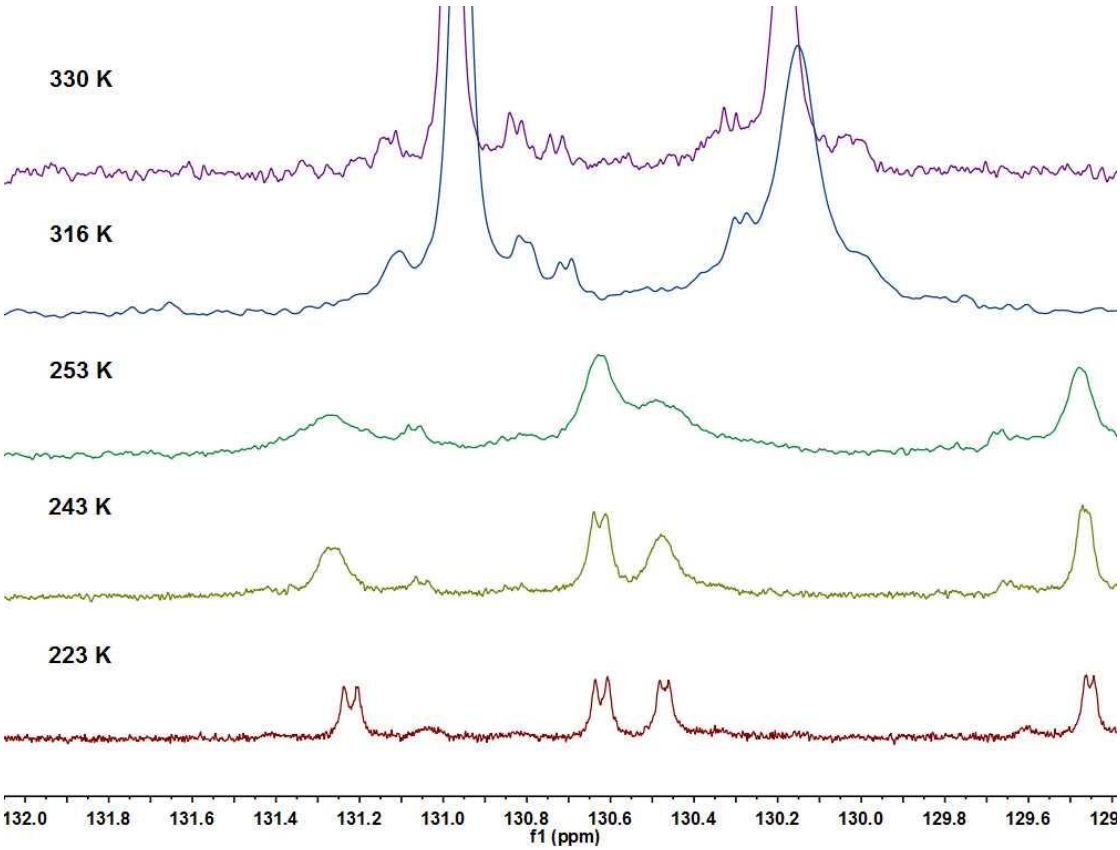

Figure 8.13: Experimental $^{13}C\{^{1}H\}$ NMR spectra of **86** in $CDCl_3$.

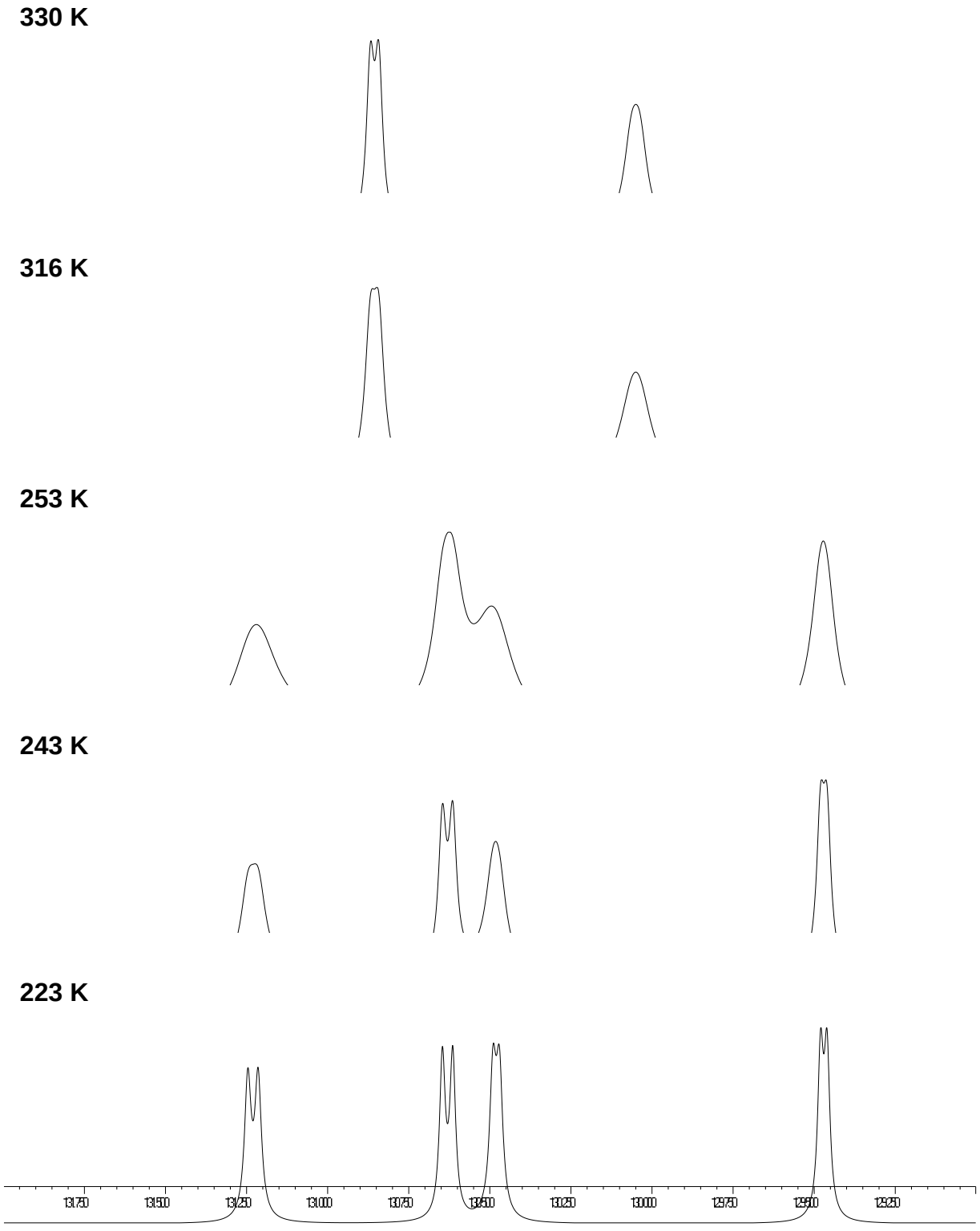

Figure 8.14: Simulated $^{13}C\{^{1}H\}$ NMR spectra of **86** using gNMR.

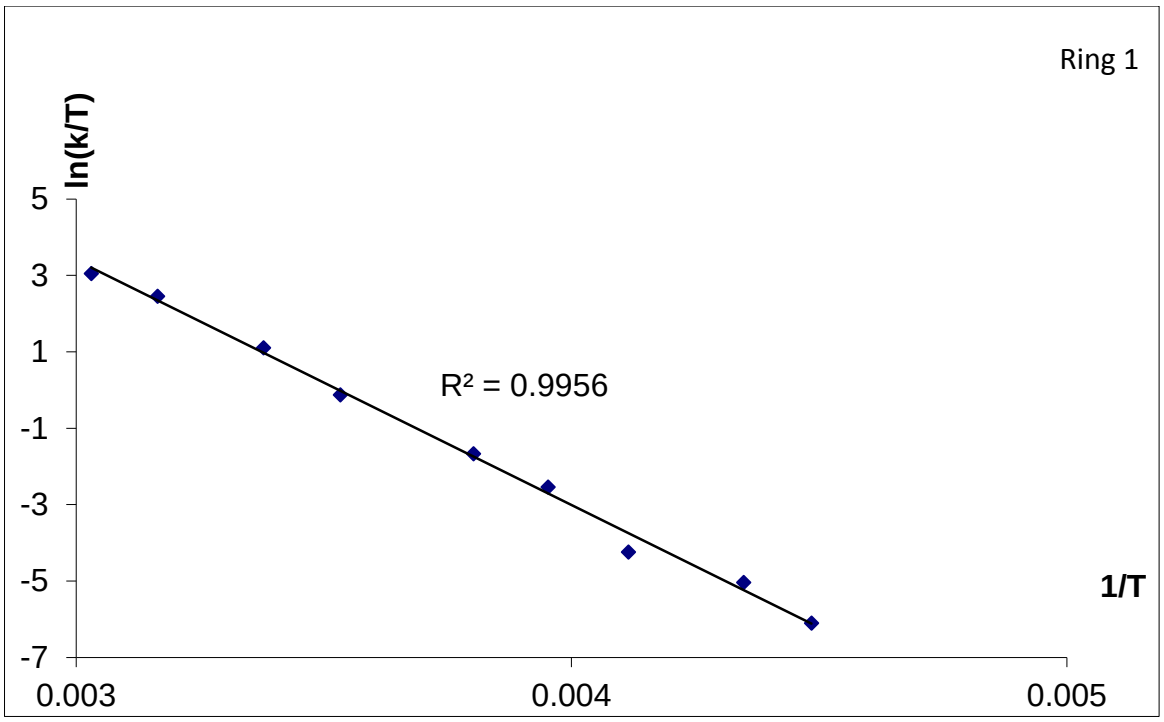

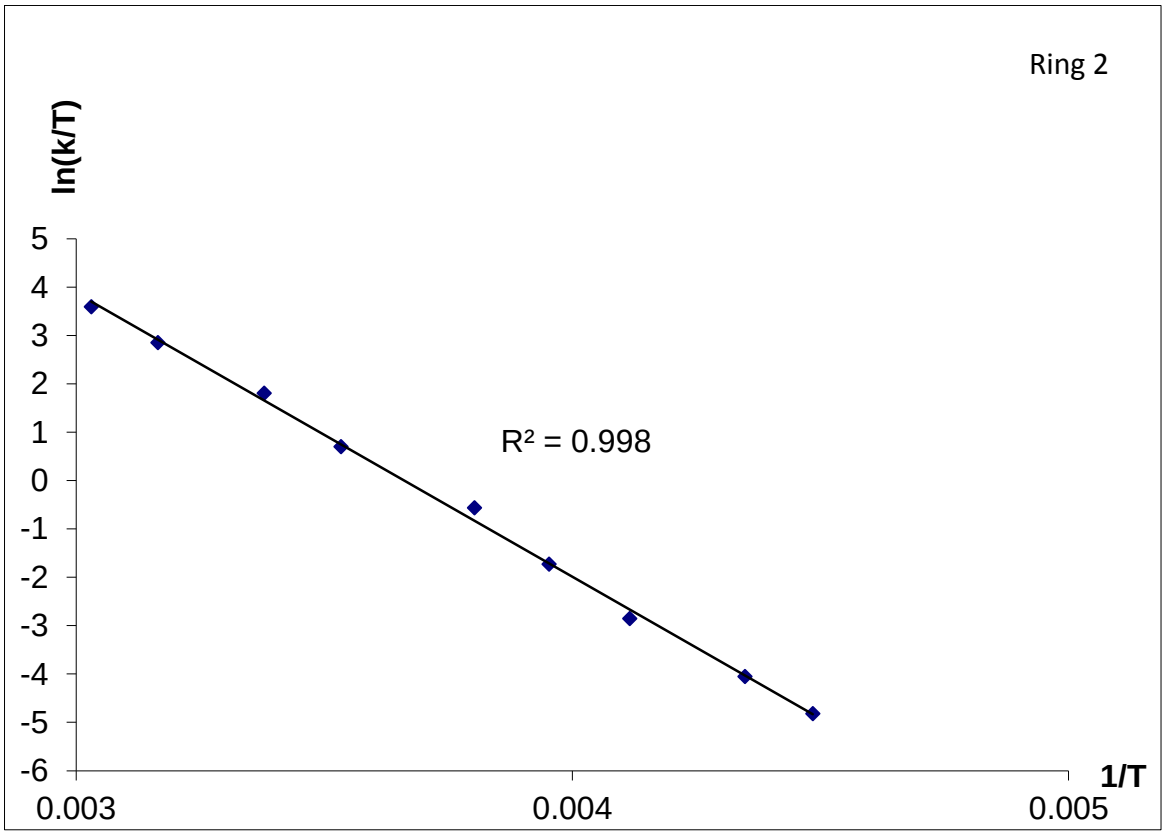

Figure 8.15: Eyring plots of ring 1 (top) and 2 (bottom) in compound **86**.

The $^{119}Sn\{^{1}H\}$ NMR spectrum of compound **87** exhibits three triplets at -22.8 (J_{SnP} = 28.0 Hz), -5.6 (J_{SnP} = 86.7 Hz) and -4.3 ppm (J_{SnP} = 85.8 Hz) where the triplet at -4.3 ppm is the major peak with similar structure to compound **86**, along with a low intensity doublet of doublets at 1.18 ppm (J_{SnP} = 126.8 Hz, $J_{SnP'}$ = 13.1 Hz) which is due to an impurity. The *meso* component of the starting material **64** may form two stereoisomers when reacted with benzyl bromide (Figure 8.16); these stereoisomers are assigned to the two minor triplet peaks (-22.8 and -5.6 ppm) in the $^{119}Sn\{^{1}H\}$ NMR spectrum of **87**.

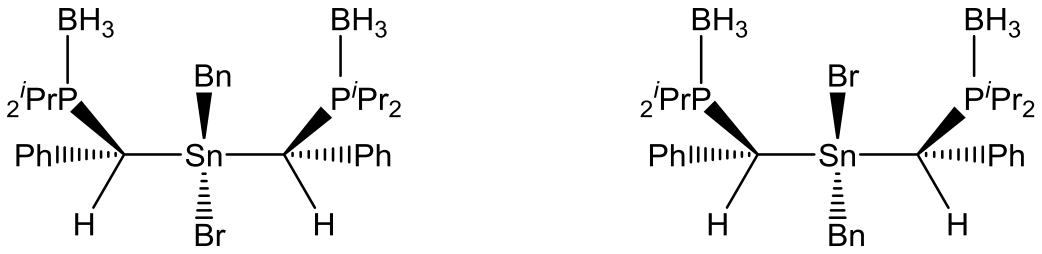

meso-**87**

Figure 8.16: Stereoisomers of *meso* **87**.

To summarise, due to the disorder (along the Me-Sn-I bonds) within the X-ray crystal structure, the solid state analysis shows that compound **86** possess rotational symmetry and therefore, ring 1 and 2 would be identical. However, it is clear in the extensive NMR investigation carried out within this chapter that compound **86** is not symmetrical and so results in two distinct phenyl rings, along with two different phosphorus centres, one on each of the phosphine-borane-stabilised carbanion ligand. This prevents absolute assignment of the NMR data; however, it is clear that the barrier to rotation of the two rings are different.

8.3 Oxidation addition reactions using compound 64

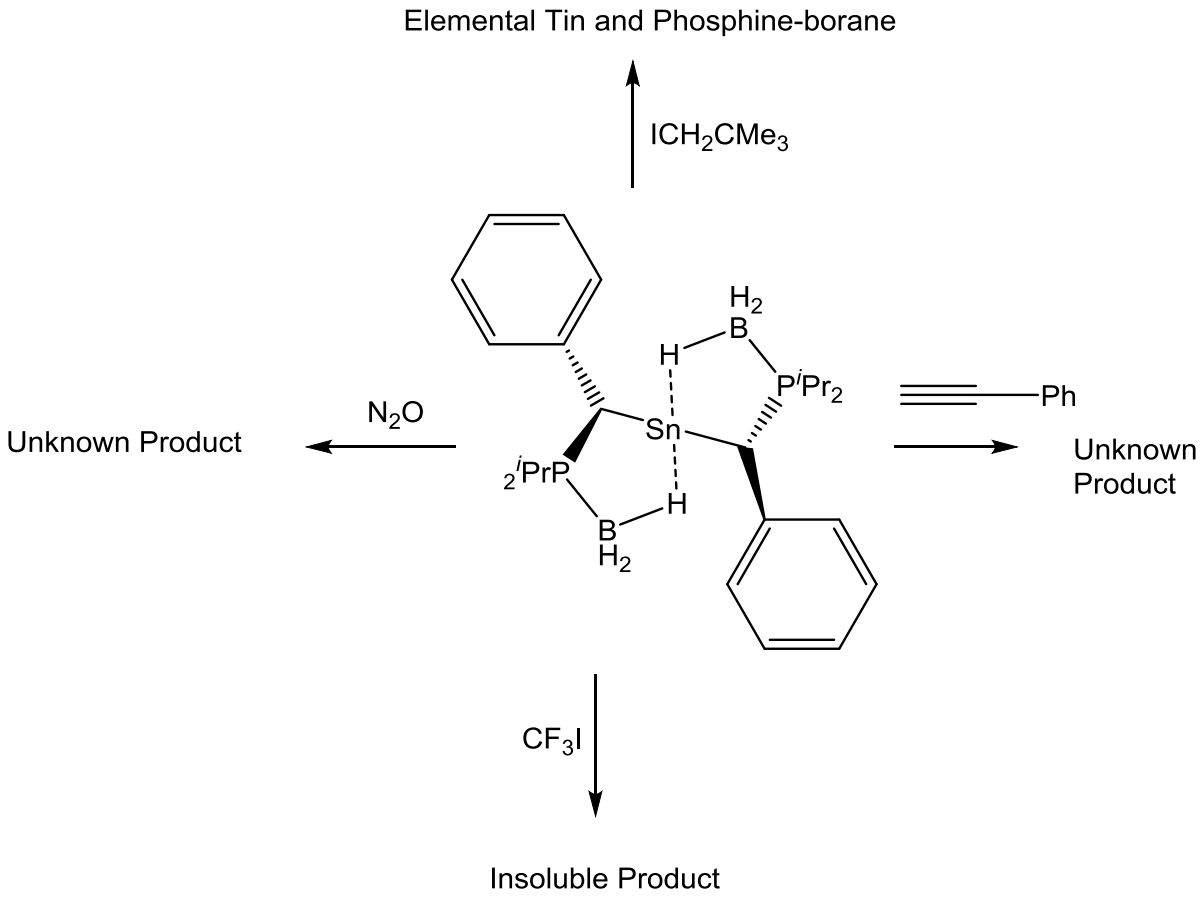

Scheme 8.2: Reactions of compound **64** with neopentyl iodide, nitrous oxide, trifluoroiodomethane and phenylacetylene.

Treatment of a solution of compound **64** in toluene with one equivalent of phenylacetylene yielded free phosphine-borane after stirring for 16 hrs (Scheme 8.2). The formation of free phosphine-borane may be attributed to the slightly acidic proton on the phenylacetylene protonating the dialkylstannylene; the progression of protonolysis can be seen in the $^{31}P\{^{1}H\}$ NMR spectrum (Figure 8.17). Treatment of a solution of compound **64** in diethyl ether with one equivalent of CF_3I yielded an insoluble (in THF, diethyl ether, toluene and DCM) colourless solid and so no NMR data could be obtained.

Treatment of a solution of compound **64** in diethyl ether with an excess of neopentyl iodide yielded elemental tin and free phosphine-borane after stirring for 16 hrs (Scheme 8.2). This may be attributed to compound **64** being too sterically bulky around the Sn centre and so the neopentyl iodide could not oxidise the dialkylstannylene. Over time the reaction mixture

was being exposed to more light and so compound **64** reduces down to elemental tin and free phosphine-borane; this is consistent with organotin complexes of this type being both light and thermally sensitive.

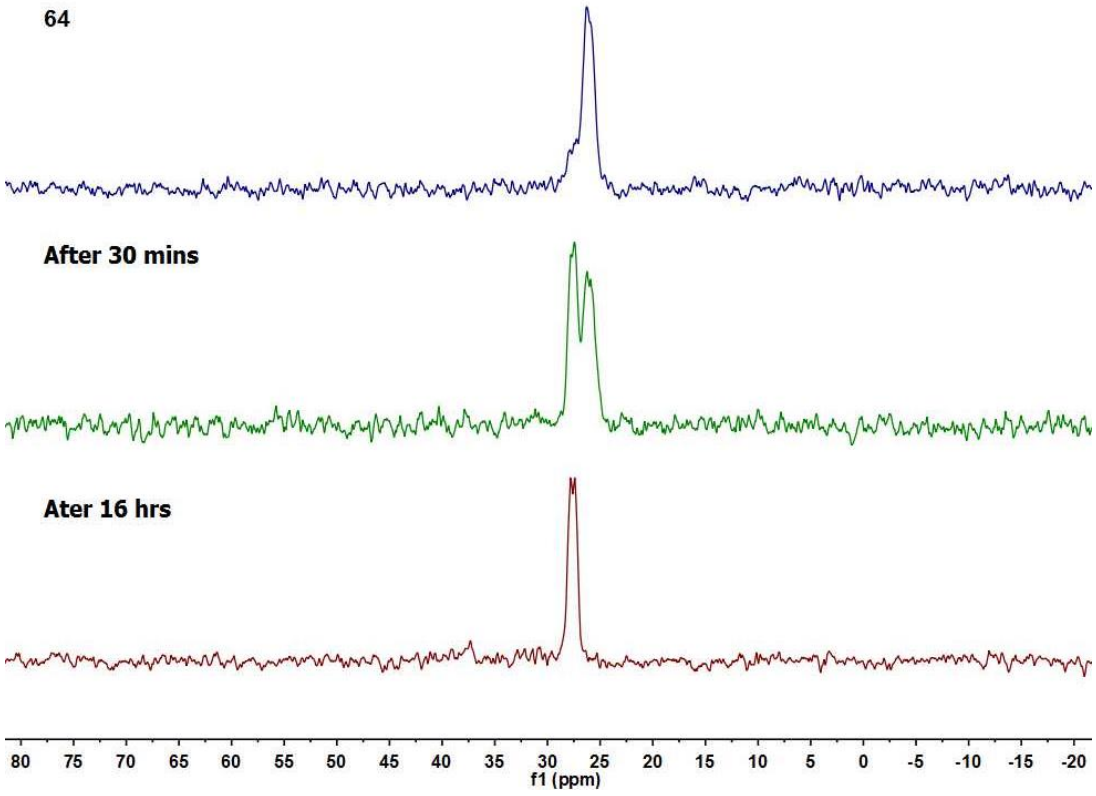

Figure 8.17: $^{31}P\{^{1}H\}$ NMR spectra of compound **64** in Et_2O with one equivalent of phenylacetylene. Compound **64** before addition of phenylacetylene (Top), after 30 mins (Middle) and after 16 hrs (Bottom).

Treatment of a solution of compound **64** in Et_2O with an excess of nitrous oxide yielded two phosphorus-containing species as seen in the $^{31}P\{^{1}H\}$ NMR spectrum of the crude reaction mixture (27.5 and 31.1 ppm) (Figure 8.18). It is possible that the peak at 27.5 ppm is due to **64** and so the peak at 31.1 ppm may be attributed to the oxidative addition of compound **64**. This reaction was left for 16 hrs and still showed two species in the $^{31}P\{^{1}H\}$ NMR spectrum with different intensities which indicates that the reaction had not gone to completion.

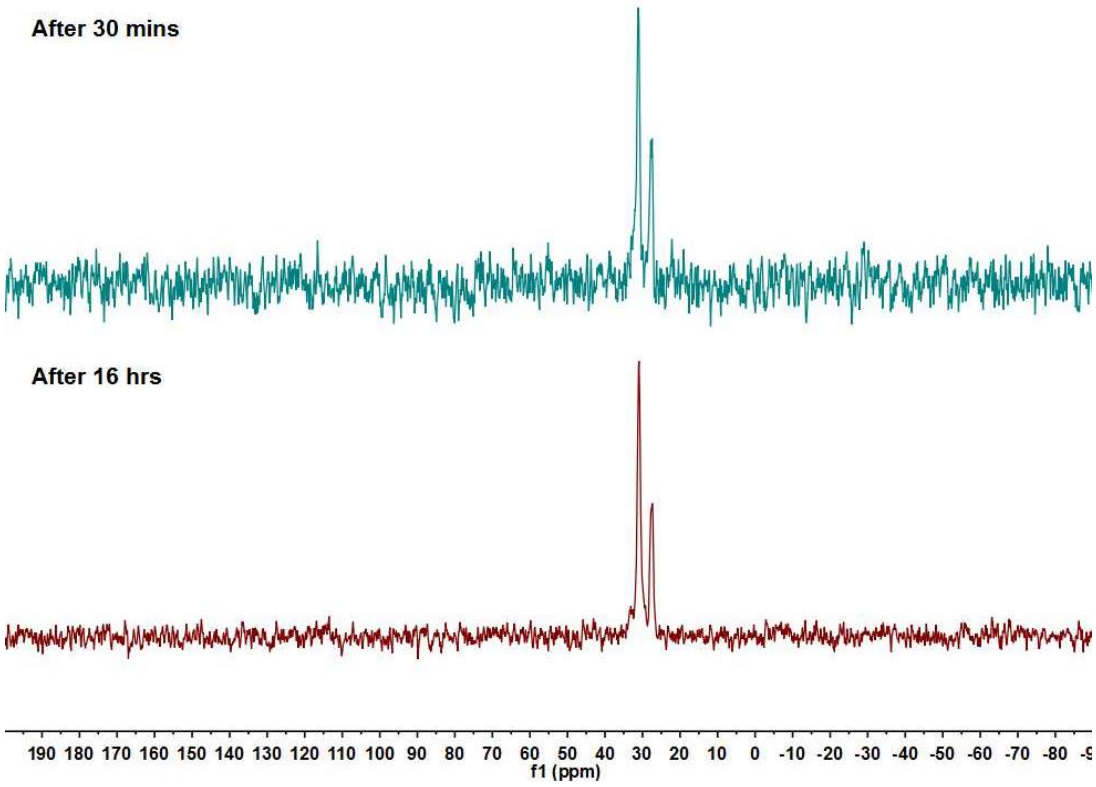

Figure 8.18: $^{31}P\{^{1}H\}$ NMR spectra of: i) Compound **64** with excess N_2O after 30 minutes. ii) Compound **64** with excess N_2O after 16 hrs.

If the relative intensities of the peaks in the $^{31}P\{^{1}H\}$ NMR were equal, then a 'puckered' species could have been postulated (Figure 8.19).

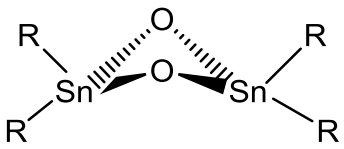

R = $Cy_2P(BH_3)CHPh$

Figure 8.19: 'Puckered' structure of a potential product between compound **64** and nitrous oxide.

8.4 Conclusion

Compound **86** was isolated as single colourless crystals and consists of a discrete monomer where the Sn centre has two contacts with two phosphine-borane fragments via a carbanion centre, a contact between the Sn centre and a methyl group, and a contact between the Sn centre and iodine. This distorted tetrahedral geometry loses rotational symmetry as well as agostic-type interactions upon oxidative addition; this loss of rotational symmetry can be seen in a detailed multi-element NMR spectroscopy investigation. As well as BnBr and MeI, other organic reagents were investigated, however, crude $^{31}P\{^{1}H\}$ NMR spectra suggest that these reactions give either free phosphine-borane or other unidentified species. Variable temperature $^{13}C\{^{1}H\}$ NMR spectra indicated dynamic behaviour of the aromatic rings in compound **86**. The experimental $^{13}C\{^{1}H\}$ NMR spectra were simulated using gNMR in order to calculate the rate constant, k, for the phenyl exchange process from line-shape analysis at various temperatures. Eyring plots were used to calculate the enthalpy of activation of the phenyl rings (Ring 1, 53.2 kJ mol^{-1}; Ring 2, 48.7 kJ mol^{-1}) which revealed that ring 2 is rotating at a faster rate than ring 1, despite their chemical equivalency.

8.5 References

1. W. J. Pope and S. J. Peachy, *Proc. Chem. Soc.*, 1900, **42**.
2. J. D. Cotton, P. J. Davidson and M. F. Lappert, *J. Chem. Soc. Dalton Trans.*, 1976, 2275-2286.
3. C. Eaborn, M. S. Hill, P. B. Hitchcock, D. Patel, J. D. Smith and S. B. Zhang, *Organometallics*, 2000, **19**, 49-53.
4. C. Wills, K. Izod, W. Clegg and R. W. Harrington, *Dalton Trans.*, 2010, **39**, 2379-2384.
5. N. W. Alcock and J. F. Sawyer, *J. Chem. Soc. Dalton Trans.*, 1977, 1090-1095.
6. J. S. Tse, M. J. Collins, F. L. Lee and E. J. Gabe, *J. Organomet. Chem.*, 1986, **310**, 169-178.
7. R. A. Howie, J. N. Ross, J. L. Wardell and J. N. Low, *Acta Crystallogr. Sect.*, 1994, **50**, 229-231.
8. S. Schwarz, F. Lissner and J. Weidlein, *Z. Anorg. Allg. Chem.*, 1999, **625**, 1807-1812.
9. B. Kasna, R. Jambor, L. Dostal, A. Ruzicka, I. Cisarova and J. Holecek, *Organometallics*, 2004, **23**, 5300-5307.
10. W. T. Mao, L. J. Tian, K. Q. Gu and Y. X. Sun, *Acta Crystallogr. Sect. E*, 2006, **62**, M3054-M3055.
11. C. R. A. Muchmore and M. J. Heeg, *Acta Crystallogr. Sect. C*, 1990, **46**, 1743-1745.
12. D. Zhang, S. Q. Dou and A. Weiss, *Z. Naturforsch. Sect. A*, 1991, **46**, 337-343.
13. D. Dakternieks, K. Dunn, D. J. Henry, C. H. Schiesser and E. R. T. Tiekink, *Organometallics*, 1999, **18**, 3342-3347.
14. G. Yamamoto, S. Ohta, M. Kaneko, K. Mouri, M. Ohkuma, R. Mikami, Y. Uchiyama and M. Minoura, *Bull. Chem. Soc. Jpn.*, 2005, **78**, 487-497.

Chapter 9. Conclusions

The work presented in this thesis has looked into an array of structurally different phosphine-boranes and their effect on the stabilities and structures of their main group derivatives. The specific ligand modifications considered include:

- the use of a rigid aromatic ring or a flexible backbone; with particular focus on the B-H···M agostic-type interactions;
- replacing a $SiMe_3$ group with a phenyl ring and the effect this has on the structure and reactivity.

9.1 Effects on the structures and stabilities on group 1 and 14 phosphine-borane-stabilised carbanions with either a rigid aromatic or flexible backbone.

Solid state characterisation of the linear bis(phosphine-boranes) $[Li(THF)_2]_2[Ph_2P(BH_3)CHSi(Me_2)CH_2]_2$ (**40a**), $[K(pmdeta)]_2[CH_2SiMe_2CHP(BH_3)Ph_2]_2$ (**40b**) shows key differences compared to the rigid *o*-phenylene-bridged systems $[1,2\text{-}C_6H_4\{CHP(BH_3)R_2\}_2][Li(tmeda)]_2\cdot n$L (R = ^{i}Pr, n = 0 (**44a**); R = Ph, nL = THF (**45a**); R = Cy, nL = $2PhCH_3$ (**46a**)) and $[K(pmdeta)]_2[1,2\text{-}C_6H_4\{CHPCy_2(BH_3)\}_2]$ (**46b**). Compounds **40a** and **40b** crystallise with pyramidal carbanions where **40b** exhibits an unusual cyclic structure with a $(K\text{-}H\text{-}B\text{-}H)_2$ cycle.[1] Compounds **44a**-**46a** and **46b** crystallise with planar carbanion centres due to delocalisation of charge into both the aromatic backbone and P-C σ^*-orbitals.[1] These overall differences between compounds **40a** and **40b**, and **44a**-**46a** and **46b** may be attributed to the difference in the backbone linkers. It is well known that potassium complexes favour coordination by π-electrons in order to complete their coordination sphere; this is seen for compound **46b** and other phosphine-borane-stabilised carbanions, such as **49a** and **49b (**Figure 9.1 and 9.2).[1]

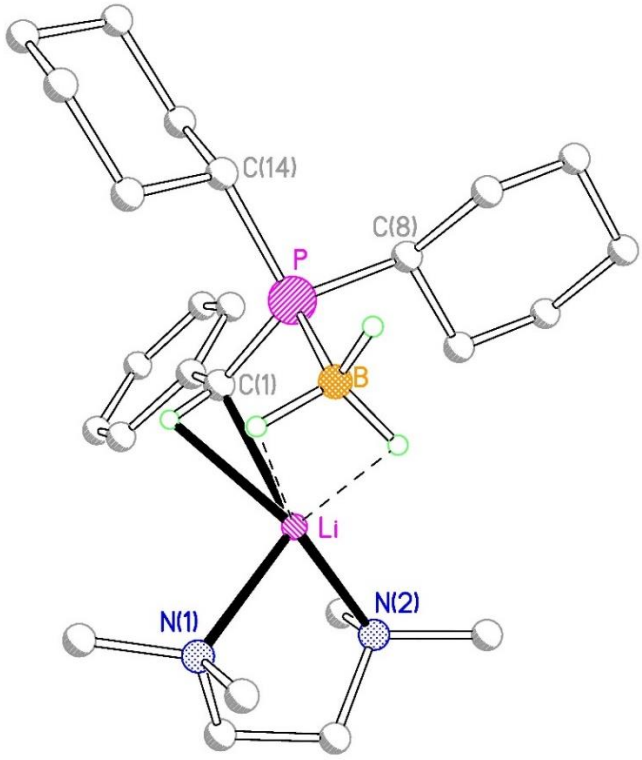

Figure 9.1: Molecular structure of **49a** with H atoms (except for those bound to boron) omitted for clarity.

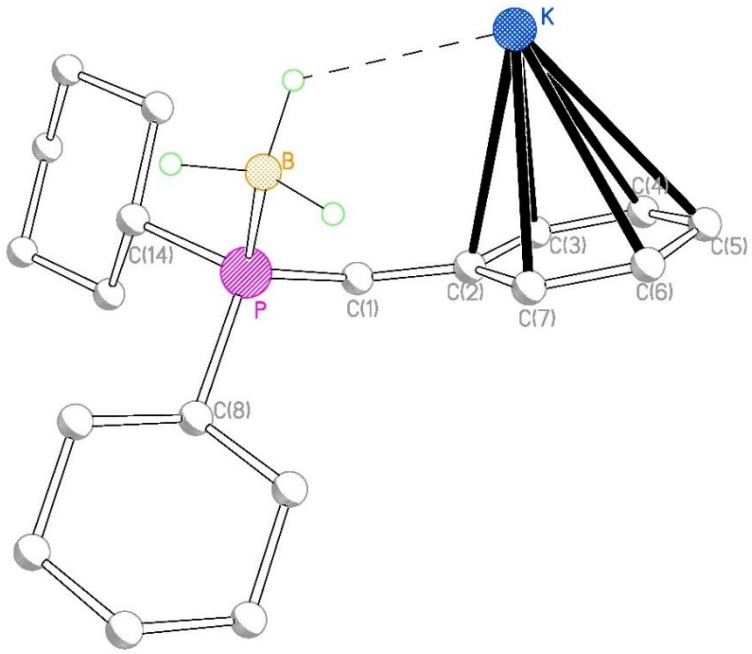

Figure 9.3: Asymmetric unit of **49b** with H atoms (except for those bound to boron) omitted for clarity.

However, compound **40b** does not exhibit interactions between the potassium cation and any aromatic groups, instead, compound **40b** adopts an unusual bent cyclic structure with two agostic-type interactions with one BH_3 unit at each end of the ligand, a feature that may not have been possible without a flexible linker (Figure 9.4).

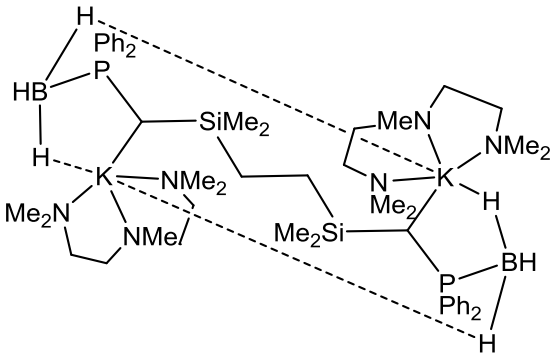

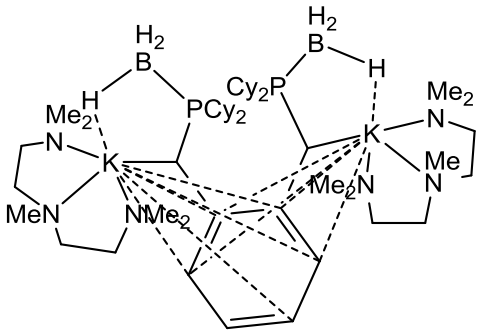

40b **46b**

Figure 9.4: Structures on compounds **40b** and **46b**.

Until recently, all phosphine-borane-substituted dialkylstannylenes contained a supporting ligand which is either monodentate or has a flexible spacer linking the two carbanion centres (Scheme 9.1).[2-5] The flexible spacer allows the supporting ligand to tilt towards the electron deficient Sn centre, which maximises the overlap between the B-H σ-orbital and the vacant p-orbital on Sn (Figure 9.5); this provides sufficient stabilisation against oligomerisation of the phosphine-borane-stabilised carbanion.

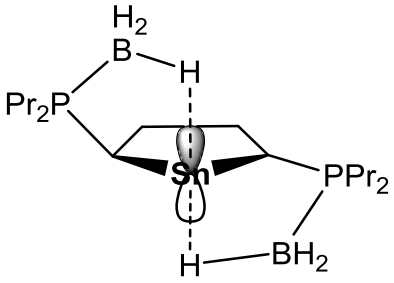

Figure 9.5: Compound **32** and orbital overlap between the B-H unit and the vacant p-orbital of Sn.

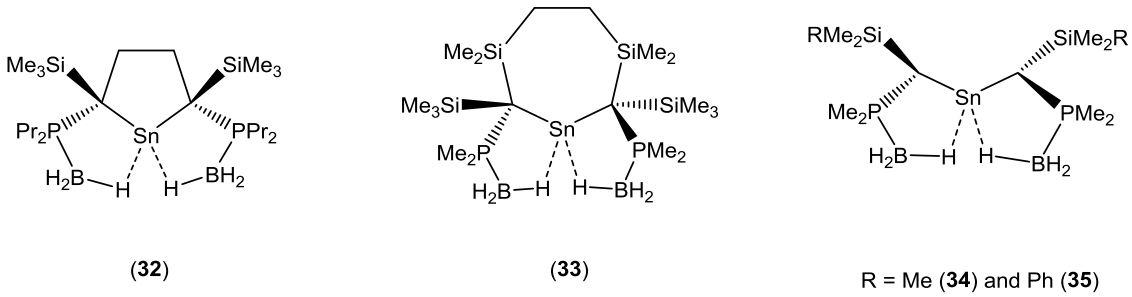

Scheme 9.1: Dialkylstannylenes with monodentate or flexible spacer supporting ligands.

Investigations into phosphine-boranes with a rigid linker show there is a limit to which the BH_3 group can position itself near the Sn centre and that this affects the overall structure of the dialkylstannylene **58** (Figure 9.6) yielding an unusual stannyl-stannylene $[[1,2\text{-}C_6H_4\{CHP(BH_3)Cy_2\}_2]Sn]_2 \cdot 3/2PhMe$.[6]

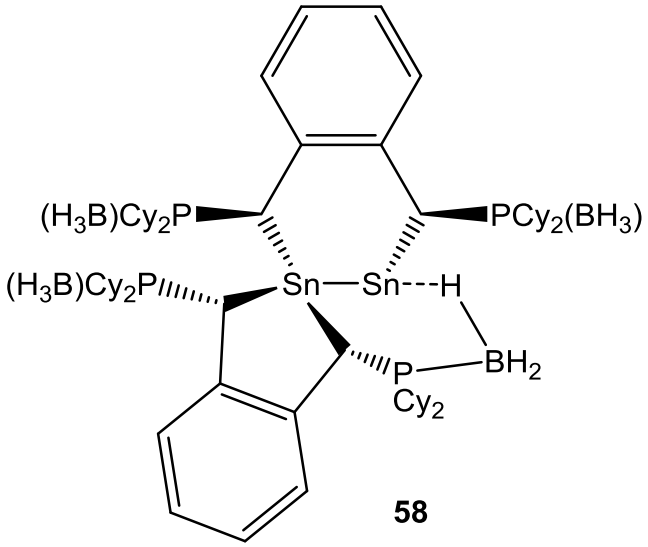

Figure 9.6: Schematic drawing of solid state structure of **58**.

Compound **58** still possesses a B-H···Sn agostic-type interaction, however due to the rigidity of the supporting ligands, compound **58** also exhibits a formal Sn-Sn bond with a chelating and bridging mode of two separate phosphine-borane fragments; a very different structure compared to compounds **32-35**.[6]

9.2 Replacement of a $SiMe_3$ group and its impact on the stability and structure of dialkylstannylenes.

Compounds **32-35**[2, 4] are stabilised by both steric bulk and agostic-type interactions. Izod and co-workers found that compound **35** is still monomeric in the solid state and that the agostic-type interactions were stabilising enough to prevent dimerisation. The dialkylstannylenes $Sn[C_6H_5CHPR_2(BH_3)]_2$ [R = ^{i}Pr (**64**) and Cy (**65**)] were synthesised in order to investigate whether agostic-type interactions alone were sufficiently stabilising against dimerisation. The $^{31}P\{^1H\}$ NMR spectra of compounds **64** and **65** indicate the presence of *rac* and *meso* diastereomers, however, only the *rac* diastereomer was isolated (Figure 9.7).

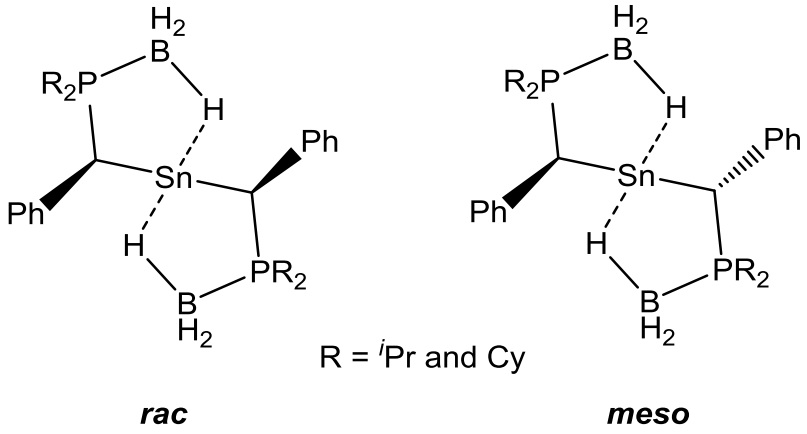

Figure 9.7: The proposed *rac* and *meso* diastereomers of compounds **64** and **65**.

Compounds **34** and **35** showed no evidence to suggest the formation of *rac* and *meso* diastereomers and so only the *rac* isomer was isolated and characterised.[4] This is not the case for compounds **64** and **65**, which may be attributed to the removal of the $SiMe_3$ group. This difference in structural preference may be attributed to the intermediates RSnCl [R = ($Me_3SiCHPMe_2(BH_3)$ (**66**), $C_6H_5CHP^iPr_2(BH_3)$ (**67**) or $C_6H_5CHPCy_2(BH_3)$ (**68**)] where **66** is the most sterically hindered. It is the bulkiness of the intermediate which has the biggest influence upon the addition of the second supporting ligand, resulting in only the *rac* diastereomer for **34**, but a mixture of *rac* and *meso* diastereomers for compound **64** and **65**. Furthermore, compounds **64** and **65** are monomeric in the solid state and so B-H agostic-type interactions sufficiently stabilise phosphine-borane-substituted dialkylstannylene of this type against dimerisation.

9.3 Difficulties in the isolation of heteroleptic alkylstannylenes

The synthesis of heteroleptic alkylstannylenes $[(PhCH_2)PR_2(BH_3)]SnX$ (X = -CH(SiMe$_3$)$_2$, -Dipp, -N(SiMe$_3$)$_2$, -O{2,6-^{t}Bu$_2$-4-MeC$_6$H$_2$}, -PTripp$_2$, -PDipp$_2$, -CH$_3$, -C$_6$H$_5$; R = ^{i}Pr and Cy) [Dipp = 2,6-^{i}Pr$_2$C$_6$H$_3$, Tripp = 2,4,6-^{i}Pr$_3$C$_6$H$_2$] via the chlorostannylenes $SnCl[C_6H_5CHPR_2(BH_3)]$ [R = ^{i}Pr (**69**) or Cy (**70**)] is of interest, in order to measure the extent at which the agostic-type interactions may be effected wither either carbon-, nitrogen-, oxygen- or phosphorus-containing ligands. It is predicted that the more π-donating ligand will weaken the B-H···Sn agostic-type interactions (Chart 9.1).

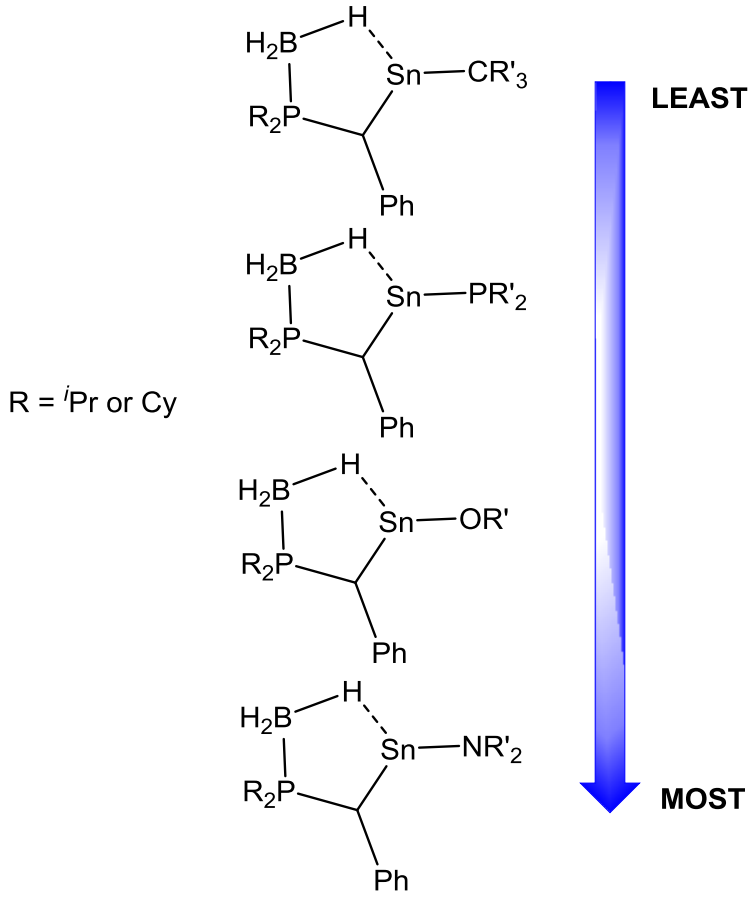

Chart 9.1: Heteroatoms from the least to the most π-donating.

However, the use of bulky ligands yielded extremely soluble products which could not be isolated but the data obtained suggest that the use of smaller ligands should enable the isolation of heteroleptic alkylstannylenes.

9.4 Dynamic behaviour of the oxidative addition product $[C_6H_5CHP^iPr_2(BH_3)]_2Sn(Me)I$ (86)

To date, very few examples of phosphine-borane-substituted Sn(IV) compounds have been isolated.[7] This thesis reports the two new oxidative addition products $[C_6H_5CHP^iPr_2(BH_3)]_2Sn(Me)I$ (**86**) and $[C_6H_5CHP^iPr_2(BH_3)]_2Sn(Bn)Br$ (**87**), where compound **86** yielded single crystals suitable for X-ray crystallography (Figure 9.8).

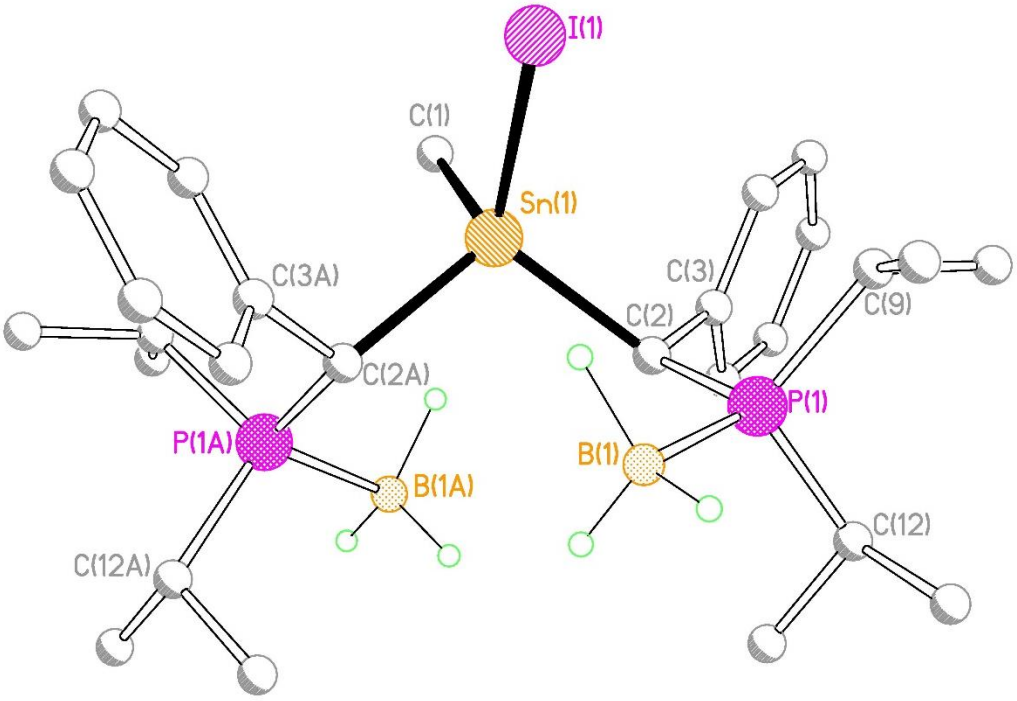

Figure 9.8: Molecular structure of **86** with H atoms (except for those bound to boron) omitted for clarity.

The $^{13}C\{^1H\}$ NMR spectrum of **86** at 296 K indicated dynamic behaviour in the phenyl region which was attributed to restricted rotation of the phenyl rings about the P-C bond. Eyring plots were used in order to measure the rotational energy barriers of both the phenyl rings in order to investigate whether they were rotating at different rates. The rotational energy barriers calculated (Ring 1, $\Delta H^{\ddagger}$ = 53.2 kJ mol^{-1}; Ring 2, $\Delta H^{\ddagger}$ = 48.7 kJ mol^{-1}) indicate that, despite their similar chemical environments, ring 1 and 2 show different barriers to rotation.

9.5 Possible future work

The work presented in this thesis has plenty of scope for future development. To date, there are only examples of acyclic phosphine-borane-substituted Sn(IV) compounds. It would be of great interest to develop the linear bis(phosphine-boranes) $[Me_2P(BH_3)CH_2SiMe_2CH_2]_2$ (**37**) and $[Ph_2P(BH_3)CH_2SiMe_2CH_2]_2$ (**40**) to synthesise and characterise the corresponding stannylenes followed by their oxidative addition products. The structures of compounds **37** and **40** would be compared to the more bulky stannylene $[CH_2SiMe_2C(SiMe_3)PMe_2(BH_3)]_2Sn$ (**33**) to determine any differences in their solid state structures and reactivity.

Little work has been carried out in the Izod group on phosphine-borane incorporated rhodium complexes and so far, none have been reported. Phosphine-borane-substituted dialkylstannylenes would be ideal ligands to investigate how *rac* and *meso* of these compounds changes the structure and reactivity of the corresponding rhodium complex.

Further investigations into small ligands for heteroleptic alkylstannylenes will be of interest in order to investigate how heteroatoms may affect the extent of agostic-type interactions.

The isolation of **58** is really the start of how rigid linkers may affect the structural outcome and so the agostic-type interactions of the corresponding stannylenes. Further work into this field would be beneficial and critical to gain a greater understanding into the effects of rigid versus flexible linkers. Chapter 5 discusses the reaction of Cp_2Sn with *in situ*-generated $[1,2\text{-}C_6H_4\{CHP(BH_3)R_2\}_2][Li(THF)_n]_2$ (R = ^{i}Pr, Ph or Cy) where compound **58** was isolated as an unusual stannyl-stannylene complex. In order to increase our understanding of how a rigid linker will affect the structural outcome and its reactivity of phosphine-borane-substituted dialkylstannylenes, the formation and the study of the ^{i}Pr and Ph analogues of **58** will be of significant interest.

9.6 References

1. K. Izod, C. M. Dixon, E. McMeekin, L. Rodgers, R. W. Harrington and U. Baisch, *Organometallics*, 2014, **33**, 378-386.
2. K. Izod, W. McFarlane, B. V. Tyson, I. Carr, W. Clegg and R. W. Harrington, *Organometallics*, 2006, **25**, 1135-1143.
3. K. Izod, L. J. Bowman, C. Wills, W. Clegg and R. W. Harrington, *Dalton Trans.*, 2009, 3340-3347.
4. K. Izod, C. Wills, W. Clegg and R. W. Harrington, *Organometallics*, 2009, **28**, 5661-5668.
5. K. Izod, C. Wills, W. Clegg and R. W. Harrington, *Organometallics*, 2009, **28**, 2211-2217.
6. K. Izod, C. M. Dixon, R. W. Harrington and M. R. Probert, *Chem. Commun.*, 2015, **51**, 679-681.
7. C. Wills, K. Izod, W. Clegg and R. W. Harrington, *Dalton Trans.*, 2010, **39**, 2379-2384.

Chapter 10. Experimental

10.1 General procedures

All manipulations were carried out using standard Schlenk techniques under an atmosphere of nitrogen/argon or in a nitrogen filled dry-box. Diethyl ether (Et_2O), THF, toluene, methylcyclohexane (MCH), benzene and petroleum ether (b.p. 40-60 °C) were pre-dried over sodium wire and distilled under nitrogen from sodium, potassium or sodium/potassium alloy. Dichloromethane (DCM) was distilled under nitrogen from CaH_2 (calcium hydride). THF and DCM were stored over activated 4Å molecular sieves; all other solvents were stored over a potassium mirror. Deuterated chloroform was distilled from CaH_2, and deuterated THF, toluene and benzene were distilled from potassium; all NMR solvents were deoxygenated by three freeze-pump-thaw cycles and were stored over activated 4Å molecular sieves.

Organolithiums were obtained from Aldrich and used as supplied; *n*-butyllithium was obtained as a 2.5 M solution in hexanes and *t*-butyllithium was obtained as a 1.6 M solution in pentane. The adduct $BH_3{\cdot}SMe_2$ was obtained as a 2.0 M solution in THF. Compounds PhMgCl, Me_3Al and $HNMe_2$ were obtained as 2.0 M solutions in THF, DiBAlH as a 1.0 M solution in THF and MeMgBr and MeMgCl as 3.0 M solutions in THF. KO^tBu (potassium *t*-butoxide), $NaBPh_4$ $PbCl_2$ and PbI_2 were heated under vacuum at 100 °C (0.01 mmHg) for 1 h prior to use. $SnCl_2$ and $ZnCl_2$ were dried using trimethylsilylchloride and then impurities removed under vacuum at room temperature (0.01 mmHg). All other compounds were used as supplied by the manufacturer with the exception of tmeda and pmdeta which were freshly distilled from CaH_2, and 12-crown-4 which was dried over activated 4 Å molecular sieves.

The compounds $Me_3P{\cdot}BH_3$,[1] 1,2-$C_6H_4\{CH_2PPh_2(BH_3)\}$,[2] 1,2-$C_6H_4\{CH_2P^iPr_2(BH_3)\}$,[2] [1,2-$C_6H_4\{CHP^iPr_2(BH_3)\}_2$][Li(tmeda)]$_2$,[2] [1,2-$C_6H_4\{CHPPh_2(BH_3)\}_2$][Li(tmeda)]$_2{\cdot}$THF,[2] BnK,[3, 4] MeK,[5-7] $SnCp_2$,[8] $PbCp_2$,[9] $^iPr_2PH(BH_3)$,[10] $Ph_2PH(BH_3)$,[11] $Cy_2PH(BH_3)$,[12] $Ph_2MeP(BH_3)$[11] and Bn_2M (M = Ca, Sr, Ba)[13] were prepared by previously published procedures.

10.2 NMR Spectroscopy and elemental analyses

^{1}H, $^{13}C\{^{1}H\}$, ^{7}Li, $^{11}B\{^{1}H\}$, $^{31}P\{^{1}H\}$ and $^{119}Sn\{^{1}H\}$ NMR spectra were recorded on a JEOL ECS 500 (operating at 500.16, 125.65, 194.25, 160.35, 202.35, and 186.51 MHz, respectively), JEOL ECS 400 (operating at 128.27, 161.83, 399.78 100.53, and 149.08 MHz), respectively or Bruker Avance I/III 300 NMR spectrometers (operating at 111.92, 300.13, 121.49, 96.29 and 75.48 MHz, respectively). ^{1}H and ^{13}C chemical shifts are quoted in ppm relative to tetramethylsilane; ^{7}Li, ^{11}B and ^{31}P chemical shifts are quoted in ppm relative to aqueous LiCl (1M), $BF_3(OEt)_2$ and 85% H_3PO_4, respectively; ^{119}Sn chemical shifts are quoted in ppm relative to tetramethyltin. Elemental analyses were obtained from the Elemental Analysis Service of London Metropolitan University.

10.3 Crystal structure determinations

Measurements for **37, 40a, 40b, 44, 44a, 45a, 46a, 46b, 48, 49a, 49b, 58, 64, 65** and **86** were made at 150K on an Oxford Diffraction Gemini A Ultra diffractometer. For all compounds cell parameters were refined from the observed positions of all strong reflections in each data set. Intensities were corrected semiemperically for absorption, based on a symmetry-equivalent and repeated reflections. The structures were solved by direct methods and were refined on F^2 values for all unique data. All non-H atoms were refined anisotropically, H atoms bonded to boron were freely refined isotropically, and the remaining H atoms were constrained with a riding model; U(H) was set at 1.2 (1.5 for methyl groups) times U_{eq} for the parent atom. Programs were AXS SMART and APEX2 (control) and SAINT (integration), Nonius COLLECT and associated programs, and SHELXTL for structure solution, refinement, and molecular graphics. Details of structure determination, atomic coordinates, and bond lengths and angles can be found in CIF format in the enclosed CD.

10.4 DFT calculations

Geometry optimisations on the gas-phase molecules were performed with the Gaussian09 suite of programs (revision D.01). Ground state optimisations were performed using the hybrid B3LYP functional,[14-16] the 6-31G(2d,p) all-electron basis set[17, 18] was used for all C, H, B and P atoms, while LanL2DZ effective core potential basis set was used for Sn

[default parameters were used throughout]. The identity of minima was confirmed by the absence of imaginary vibrational frequencies in each case. The stabilisation energy associated with the B-H···Sn interactions was calculated using the NBODel routine, in which the elements affording this interaction were selectively deleted.[19] Natural Bond Orbital analyses were performed using the NBO 3.1 module of Gaussian09.[20-25]

10.5 Preparative methods

$[Me_2P(BH_3)CH_2Si(Me_2)CH_2]_2$ (37): To a solution of Me_3P-BH_3 (6.31 g, 70.17 mmol) in THF (30 ml) was added ^{n}BuLi (28.07 ml of a 2.5 M solution in hexanes, 70.17 mmol) and the mixture was left to stir for 1 h at room temperature. This solution was added, dropwise, to a solution of 1,2–bis(chlorodimethylsilyl)ethane (7.55 g, 35.09 mmol) in THF (30 ml) and this solution was left to stir for 1 h at room temperature. To this mixture was added water (30 ml) and the organic phase was extracted into dichloromethane (3 x 30 ml). The combined organic extracts were dried over $MgSO_4$, filtered and the solvent was removed *in vacuo* from the filtrate to give a colourless solid. The crude product was crystallised from hot methylcyclohexane (15 ml) to give a colourless crystalline solid. Isolated yield: 6.97 g, 60%. $^1H\{^{11}B\}$ NMR (500.16 MHz, $CDCl_3$, 25 °C): δ 0.13 (s, 12H, $SiMe_2$), 0.50 (br.s, 6H, BH_3), 0.51 (br.s, 4H, PCH_2), 0.90 (d, J_{PH} = 15.1 Hz, 4H, CH_2CH_2), 1.29 (d, J_{PH} = 10.1 Hz, 12H, PMe_2). $^{13}C\{^1H\}$ NMR (125.77 MHz, $CDCl_3$, 25 °C): δ -1.54 ($SiMe_2$), 8.96 (CH_2CH_2), 13.45 (d, J_{PC} = 24.0 Hz, PCH_2), 15.55 (d, J_{PC} = 38.3 Hz, PMe_2). $^{11}B\{^1H\}$ NMR (160.47 MHz, $CDCl_3$, 25 °C): δ 37.5 (d, J_{PB} = 58.8 Hz). $^{31}P\{^1H\}$ NMR (202.47 MHz, $CDCl_3$, 25 °C): δ 3.4 (q, J_{PB} = 58.8 Hz).

$[Ph_2P(BH_3)CH_2Si(Me_2)CH_2]_2$ (40): To a cold (0 °C) solution of Ph_2PMe-BH_3 (4.76 g, 22.18 mmol) in THF (40 ml) was added ^{n}BuLi (8.89 ml of a 2.5 M solution in hexanes, 22.18 mmol) and this mixture was left to stir for 1 h at room temperature, resulting in a dark orange solution. This was added, dropwise, to a solution of 1,2-bis(chlorodimethylsilyl)ethane (2.39 g, 11.09 mmol) in THF (30 ml) and this mixture was left to stir for 1 h at room temperature resulting in a yellow mixture. To this mixture was added water (40 ml) and the organic phase was extracted into dichloromethane (3 x 30 ml). The combined organic extracts were dried over $MgSO_4$, filtered and the solvent was removed *in vacuo* from the filtrate to give a colourless solid. The crude product was crystallised from hot methylcyclohexane/THF

(15 ml/5 ml) to give a colourless crystalline solid. Isolated yield: 2.00 g, 32%. $^{1}H\{^{11}B\}$ NMR (500.16 MHz, $CDCl_3$, 25 °C): δ -0.11 (s, 12H, $SiMe_2$), 0.30 (d, J_{PH} = 5.00 Hz, 4H, PCH_2), 1.04 (d, J_{PB} = 20.0 Hz, 6H, BH_3), 1.52 (d, J_{PH} = 15.0 Hz, 4H, CH_2CH_2), 7.39-7.44 (m, 5H, PPh_2), 7.67-7.70 (m, 5H, PPh_2). $^{13}C\{^{1}H\}$ NMR (100.53 MHz, $CDCl_3$, 25 °C): δ -2.16 ($SiMe_2$), 8.48 (CH_2CH_2), 10.97 (d, J_{PC} = 25.1 Hz, PCH_2), 128.69 (d, J_{PC} = 10.1 Hz, Ar), 130.89 (d, J_{PC} = 2.01 Hz, Ar), 131.83 (d, J_{PC} = 9.1 Hz, Ar), 132.61 (d, J_{PC} = 54.3 Hz, Ar). $^{11}B\{^{1}H\}$ NMR (160.47 MHz, $CDCl_3$, 25 °C): δ -38.9 (br). $^{31}P\{^{1}H\}$ NMR (202.47 MHz, $CDCl_3$, 25 °C): δ 13.5 (q, J_{PB} = 69.5 Hz).

1,2-$C_6H_4\{CH_2P^iPr_2(BH_3)\}_2$ (44): To a solution of $^{i}Pr_2PH(BH_3)$ (1.61 g, 12.39 mmol) in THF (20 ml) was added ^{n}BuLi (4.96 ml of a 2.5M solution in hexanes, 12.39 mmol) and this mixture was left to stir for 1 h at room temperature. This solution was added, dropwise, to a solution of *α,α'*-dichloro-*o*-xylene (1.05 g, 6.19 mmol) in THF (20 ml) and this mixture was left to stir for 16 h at room temperature. To this mixture was added water (30 ml) and the organic phase was extracted into dichloromethane (3 x 20 ml). The combined organic extracts were dried over $MgSO_4$, filtered and the solvent was removed *in vacuo* from the filtrate to give a colourless solid. Single crystals suitable for X-ray crystallography were obtained from cold (-30 °C) toluene. Isolated yield: 1.45 g, 67%. $^{1}H\{^{11}B\}$ NMR (500.16 MHz, $CDCl_3$, 25 °C): δ 0.33 (d, J_{PH} = 14.5 Hz, 6H, BH_3), 1.13 (dd, $^{3}J_{PH}$ = 13.8, $^{3}J_{HH}$ = 7.1 Hz, 6H, CHMe*Me*), 1.20 (dd, $^{3}J_{PH}$ = 14.1, $^{3}J_{HH}$ = 7.3 Hz, 6H, CH*Me*Me), 2.00 (m, 4H, C*H*Me_2), 3.32 (d, $^{2}J_{PH}$ = 11.6 Hz, CH_2P), 7.15-7.24 (m, 4H, ArH). $^{13}C\{^{1}H\}$ NMR (125.77 MHz, $CDCl_3$, 25 °C): δ 17.2, 17.3 (CHMe_2), 22.0 (d, J_{PC} = 32.5 Hz, *C*HMe_2), 25.9 (d, J_{PC} = 26.3 Hz, *C*H_2P), 127.0, 131.5, 133.4 (Ar). $^{11}B\{^{1}H\}$ NMR (160.47 MHz, $CDCl_3$, 25 °C): δ -44.3 (d, J_{PB} = 49.0 Hz). $^{31}P\{^{1}H\}$ NMR (202.47 MHz, $CDCl_3$, 25 °C): δ 35.2 (m).

1,2-$C_6H_4\{CH_2PPh_2(BH_3)\}_2$ (45): To a solution of $Ph_2PH(BH_3)$ (1.64 g, 8.20 mmol) in THF (20 ml) was added ^{n}BuLi (3.28 ml of a 2.5M solution in hexanes, 8.20 mmol) and this mixture was left to stir for 1 h at room temperature. This solution was added, dropwise, to a solution of *α,α'*-dichloro-*o*-xylene (0.68 g, 4.10 mmol) in THF (20 ml) and this mixture was left to stir for 16 h at room temperature. To this mixture was added water (20 ml) and the organic phase was extracted into dichloromethane (3 x 20 ml). The combined organic extracts were dried over $MgSO_4$, filtered and the solvent was removed *in vacuo* from the filtrate to give a

colourless solid. Isolated yield: 1.61 g, 82%. $^{1}H\{^{11}B\}$ NMR (500.16 MHz, $CDCl_3$, 25 °C): δ 0.90 (d, J_{PH} = 15.5 Hz, 6H, BH_3), 3.54 (d, J_{PH} = 11.7 Hz, 4H, CH_2P), 6.51-7.62 (m, 24H, ArH). $^{13}C\{^{1}H\}$ NMR (125.77 MHz, $CDCl_3$, 25 °C): δ 30.9 (d, J_{PC} = 30.8 Hz, *C*H_2P), 126.7, 128.8, 128.9, 129.3, 131.4, 131.6 (Ar), 132.7 (d, J_{PC} = 8.6 Hz, Ar). $^{11}B\{^{1}H\}$ NMR (160.47 MHz, $CDCl_3$, 25 °C): δ -40.1 (br). $^{31}P\{^{1}H\}$ NMR (202.47 MHz, $CDCl_3$, 25 °C): δ 18.3 (br).

1,2-$C_6H_4\{CH_2PCy_2(BH_3)\}_2$ (46): To a solution of Cy_2PH (1.48 g, 7.45 mmol) in THF (20 ml) was added $BH_3{\cdot}SMe_2$ (3.73 ml of a 2.0 M solution in THF, 7.45 mmol) and this mixture was left to stir at room temperature for 30 mins. To a solution of $Cy_2PH(BH_3)$ (1.58 g, 7.45 mmol) in THF (20 ml) was added ^{n}BuLi (2.98 ml of a 2.5M solution in hexanes, 7.45 mmol) and this mixture was left to stir for 1 h at room temperature. This solution was added, dropwise, to a solution of *α,α'*-dichloro-*o*-xylene (0.61 g, 3.73 mmol) in THF (20 ml) and this mixture was left to stir for 16 h at room temperature. To this mixture was added water (30 ml) and the organic phase was extracted into dichloromethane (3 x 20 ml). The combined organic extracts were dried over $MgSO_4$, filtered and the solvent was removed *in vacuo* from the filtrate to give a colourless solid. Isolated yield: 1.42 g, 77%. $^{1}H\{^{11}B\}$ NMR (500.16 MHz, $CDCl_3$, 25 °C): δ 0.29 (d, J_{PH} = 15.1 Hz, 6H, BH_3), 1.16-1.93 (m, 44H, Cy) 3.29 (d, J_{PH} = 11.5 Hz, 4H, CH_2P), 7.09-7.35 (m, 4H, ArH). $^{13}C\{^{1}H\}$ NMR (125.77 MHz, $CDCl_3$, 25 °C): δ 25.8 (d, J_{PC} = 27.8 Hz, Cy), 26.1 (Cy) 27.0 (d, J_{PC} = 7.7 Hz, CH_2P), 27.1 (Cy), 32.0 (d, J_{PC} = 30.7 Hz, Cy), 126.8, 131.5, 133.7 (Ar). $^{11}B\{^{1}H\}$ NMR (160.47 MHz, $CDCl_3$, 25 °C): δ -43.6 (br). $^{31}P\{^{1}H\}$ NMR (202.47 MHz, $CDCl_3$, 25 °C): δ 27.8 (br).

$C_6H_5CH_2P^{i}Pr_2(BH_3)$ (47): To a solution of $^{i}Pr_2PH(BH_3)$ (2.66 g, 20.06 mmol) in THF (30 ml) was added ^{n}BuLi (8.54 ml of a 2.35M solution in hexanes, 20.06 mmol) and this mixture was left to stir for 1 h at room temperature. This solution was added, dropwise, to a solution of benzylbromide (2.39 ml, 20.06 mmol) in THF (30 ml) and the mixture was left to stir for 16 h at room temperature. To this mixture was added water (30 ml) and the organic phase was extracted into Et_2O (3 x 20 ml). The combined organic extracts were dried over $MgSO_4$, filtered and the solvent was removed *in vacuo* from the filtrate to give a colourless oil. Isolated yield: 3.26 g, 73%. $^{1}H\{^{11}B\}$ NMR (500.16 MHz, $CDCl_3$, 25 °C): δ 0.35 (d, J_{PH} = 15.0 Hz, 3H, BH_3), 1.04 (dd, $^{3}J_{PH}$ = 7.1, $^{3}J_{HH}$ = 1.5 Hz, 6H, CHMe*Me*), 1.09 (dd,

$^{3}J_{PH}$ = 7.1, $^{3}J_{HH}$ = 1.8 Hz, 6H, CH*Me*Me), 1.92 (m, 2H, C*H*Me$_2$), 2.98 (d, $^{2}J_{PH}$ = 11.5 Hz, 2H, CH$_2$P), 7.18-7.39 (m, 5H, ArH). $^{13}C\{^{1}H\}$ NMR (125.77 MHz, $CDCl_3$, 25 °C): δ 16.99, 17.08 (CH*Me*$_2$), 21.7 (d, J_{PC} = 30.4 Hz, *C*HMe$_2$), 28.26 (d, J_{PC} = 28.3 Hz, *C*H$_2$P), 126.87 (d, J_{PC} = 2.63 Hz, Ar), 128.49 (d, J_{PC} = 2.07 Hz, Ar), 129.92 (d, J_{PC} = 4.04 Hz, Ar), 133.50 (d, J_{PC} = 5.45 Hz, Ar) . $^{11}B\{^{1}H\}$ NMR (160.47 MHz, $CDCl_3$, 25 °C): δ -43.2 (d, J_{PB} = 59.7 Hz). $^{31}P\{^{1}H\}$ NMR (202.47 MHz, $CDCl_3$, 25 °C): δ 34.0 (q, J_{PB} = 59.7 Hz).

C$_6$H$_5${CH$_2$PPh$_2$(BH$_3$)} (48): To a solution of Ph$_2$PH (3.78 g, 20.30 mmol) in THF (30 ml) the adduct BH$_3$·SMe$_2$ was added (10.15 ml, 20.30 mmol) and this mixture was left to stir for 1 h at room temperature. To this mixture was added ^{n}BuLi (8.64 ml of a 2.35M solution in hexanes, 20.30 mmol) and the solution was left to stir for 1 h at room temperature. This solution was added, dropwise, to a solution of benzylbromide (2.41 ml, 20.30 mmol) in THF (30 ml) and this mixture was left to stir for 16 h at room temperature. To this mixture was added water (30 ml) and the organic phase was extracted into Et$_2$O (3 x 20 ml). The combined organic extracts were dried over MgSO$_4$, filtered and the solvent was removed *in vacuo* from the filtrate to give a colourless sticky solid. The product was extracted into hot toluene (20 ml), filtered and solvent removed *in vacuo* to yield a colourless solid. Single crystals suitable for X-ray crystallography were obtained from hot toluene. Isolated yield: 3.98 g, 68%. $^{1}H\{^{11}B\}$ NMR (500.16 MHz, $CDCl_3$, 25 °C): δ 0.87 (d, J_{PH} = 15.0 Hz, 3H, BH$_3$), 3.15 (d, J_{PH} = 11.8 Hz, CH$_2$P), 6.84-7.56 (m, 15H, ArH). $^{13}C\{^{1}H\}$ NMR (125.77 MHz, $CDCl_3$, 25 °C): δ 34.12 (d, J_{PC} = 32.66 Hz, *C*H$_2$P), 126.98 (d, J_{PC} = 3.47 Hz, Ar), 128.08 (d, J_{PC} = 1.90 Hz, Ar), 128.63, 128.76 (Ar), 130.29 (d, J_{PC} = 4.11 Hz, Ar), 131.87 (d, J_{PC} = 4.58 Hz, Ar), 133.22 (d, J_{PC} = 9.48 Hz, Ar), 141.79 (*ipso*-Ar) . $^{11}B\{^{1}H\}$ NMR (160.47 MHz, $CDCl_3$, 25 °C): δ -39.1 (d, J_{PB} = 49.3 Hz). $^{31}P\{^{1}H\}$ NMR (202.47 MHz, $CDCl_3$, 25 °C): δ 18.0 (q, J_{PB} = 49.3 Hz).

C$_6$H$_5${CH$_2$PCy$_2$(BH$_3$)} (49): To a solution of Cy$_2$PH (4.20 ml, 19.16 mmol) in THF (30 ml) the adduct BH$_3$·SMe$_2$ was added (9.58 ml, 19.16 mmol) and this mixture was left to stir for 1 h at room temperature. To this mixture was added ^{n}BuLi (7.67 ml of a 2.5M solution in hexanes, 19.16 mmol) and this solution was left to stir for 1 h at room temperature. This solution was added, dropwise, to a solution of benzylbromide (2.29 ml, 19.16 mmol) in THF (30 ml) and this mixture was left to stir for 16 h at room temperature. To this mixture was

added water (30 ml) and the organic phase was extracted into dichloromethane (3 x 20 ml). The combined organic extracts were dried over $MgSO_4$, filtered and the solvent was removed *in vacuo* from the filtrate to give a colourless solid. Single crystals suitable for X-ray crystallography were obtained from cold (0 °C) toluene. Isolated yield: 4.89 g, 84%. $^{1}H\{^{11}B\}$ NMR (500.16 MHz, $CDCl_3$, 25 °C): δ 0.40 (d, J_{PH} = 15.00 Hz, 3H, BH_3), 1.19-1.84 (m, 22H, PCy_2), 3.04 (d, J_{PH} = 15.0 Hz, 2H, CH_2P), 7.26-7.31 (m, 5H, ArH). $^{13}C\{^{1}H\}$ NMR (125.77 MHz, $CDCl_3$, 25 °C): δ 26.05, 26.84, 26.91, 26.99, 27.06 (Cy), 28.20 (d, J_{PC} = 28.9 Hz, Cy), 31.73 (d, J_{PC} = 31.4 Hz, CH_2P) , 126.90, 128.51, 130.01 (Ar), 133.81 (*ipso*-Ar). $^{11}B\{^{1}H\}$ NMR (160.47 MHz, $CDCl_3$, 25 °C): δ -43.5 (d, J_{PB} = 57.8 Hz). $^{31}P\{^{1}H\}$ NMR (202.47 MHz, $CDCl_3$, 25 °C): δ 27.2 (q, J_{PB} = 57.8 Hz).

$C_6H_5\{CH_2SiMe_3PCy_2(BH_3)\}$ (50): To a solution of $C_6H_5\{CH_2PCy_2(BH_3)\}$ (0.51 g, 1.66 mmol) in THF (20 ml) was added ^{n}BuLi (0.66 ml of a 2.5 M solution in hexanes, 1.66 mmol) and this solution was left to stir for 30 mins at room temperature. This solution was added, dropwise, to a solution of trimethylsilylchloride (0.21 ml, 1.66 mmol) in THF (20 ml) and this mixture was left to stir for another 30 mins at room temperature. To this mixture was added water (30 ml) and the organic phase was extracted into dichloromethane (3 x 20 ml). The combined organic extracts were dried over $MgSO_4$, filtered and the solvent was removed *in vacuo* from the filtrate to give a colourless solid. Isolated yield: 0.40 g, 65%. $^{1}H\{^{11}B\}$ NMR (500.16 MHz, $CDCl_3$, 25 °C): δ 0.12 ($SiMe_3$), 0.65 (d, J_{PH} = 14.2 Hz, 3H, BH_3), 1.00-2.18 (m, 22H, PCy_2), 2.72 (d, J_{PH} = 20.0 Hz, 1H, PCHSi), 7.14-7.25 (m, 5H, ArH). $^{13}C\{^{1}H\}$ NMR (125.77 MHz, $CDCl_3$, 25 °C): δ 0.39 (s, $SiMe_3$), 26.20 (d, J_{PC} = 1.26 Hz, Cy), 26.34 (d, J_{PC} = 1.26 Hz, Cy), 27.41 (br.d, Cy), 27.48 (br.d, Cy), 27.65 (d, J_{PC} = 3.77 Hz, Cy), 27.74 (d, J_{PC} = 3.77 Hz, Cy), 28.09 (d, J_{PC} = 5.03 Hz, Cy), 28.14 (br.d, Cy), 28.34 (d, J_{PC} = 3.77 Hz, Cy), 28.44 (s, SiCH), 28.50 (d, J_{PC} = 15.1 Hz, Cy), 34.40 (d, J_{PC} = 27.7 Hz, Cy), 35.53 (d, J_{PC} = 28.9 Hz, Cy), 125.87, 128.25, 130.75 (Ar), 136.92 (*ipso*-Ar). $^{11}B\{^{1}H\}$ NMR (160.47 MHz, $CDCl_3$, 25 °C): δ -40.3 (d, J_{PB} = 64.2 Hz). $^{31}P\{^{1}H\}$ NMR (202.47 MHz, $CDCl_3$, 25 °C): δ 29.2 (q, J_{PB} = 64.2 Hz).

$\{CH_2CH_2PCy_2(BH_3)\}_2$ (51): To a solution of Cy_2PH (4.20 ml, 19.16 mmol) in THF (30 ml) the adduct $BH_3{\cdot}SMe_2$ was added (9.58 ml of a 2.0M solution in THF, 19.16 mmol) and this mixture was left to stir for 1 h at room temperature. To this mixture was added ^{n}BuLi (8.33 ml of a 2.3M solution in hexanes, 19.16 mmol) and the solution was left to stir for 1 h at room temperature. This solution was added, dropwise, to a solution of 1,4-dibromobutane (2.07 g,

9.58 mmol) in THF (30 ml) and the solution was left to stir for 16 h at room temperature. To this mixture was added water (30 ml) and the organic phase was extracted into dichloromethane (3 x 20 ml). The combined organic extracts were dried over $MgSO_4$, filtered and the solvent was removed *in vacuo* from the filtrate to give a colourless solid. Isolated yield: 3.66 g, 80%. $^{1}H\{^{11}B\}$ NMR (500.16 MHz, $CDCl_3$, 25 °C): δ 0.29 (d, J_{PH} = 15.1 Hz 6H, BH_3), 1.22-1.82 (m, 48H, CyH + CH_2CH_2). $^{13}C\{^{1}H\}$ NMR (100.53 MHz, $CDCl_3$, 25 °C): δ 19.11 (d, J_{PC} = 31.2 Hz, Cy), 26.05 (Cy), 26.78 (d, J_{PC} = 2.01 Hz, Cy), 26.93 (d, J_{PC} = 1.01 Hz, Cy), 27.03 (br.d, Cy), 31.81 (d, J_{PC} = 33.2 Hz, PCH_2). $^{11}B\{^{1}H\}$ NMR (160.47 MHz, $CDCl_3$, 25 °C): δ -44.3 (d, J_{PB} = 49.0 Hz). $^{31}P\{^{1}H\}$ NMR (202.47 MHz, $CDCl_3$, 25 °C): δ 25.2 (q, J_{PB} = 49.0 Hz).

$[Li(tmeda)]_2[Me_2P(BH_3)CHSi(Me_2)CH_2]_2$ (37a): To a solution of $[Me_2P(BH_3)CH_2Si(Me_2)CH_2]_2$ (0.51 g, 1.55 mmol) in THF (30 ml) was added ^{n}BuLi (1.24 ml of a 2.5 M solution in hexanes, 3.10 mmol) and tmeda (0.46 ml, 3.10 mmol) and this mixture was left to stir for 1 h at room temperature. The solvent was removed from the mixture *in vacuo* to yield a colourless oil which was crystallised from cold (-20 °C) methylcyclohexane (10 ml) to yield colourless crystals. The solid was washed with cold (0 °C) petrol (3 x 5 ml) and isolated. Isolated yield: 0.39 g, 74%. Anal. Calcd for $C_{24}H_{68}B_2Li_2N_4P_2Si_2$ (566.50): C, 50.89; H, 12.10; N, 9.89. Found: C, 50.68; H, 12.15; N, 9.78. $^{1}H\{^{11}B\}$ NMR (500.16 MHz, d_6-benzene, 25 °C): δ -1.05 (d, J_{PH} = 6.4 Hz, 2H, LiCH), 0.30 (s, 12H, $SiMe_2$), 0.76 (s, 4H, CH_2CH_2), 1.43 (d, J_{PH} = 10.1 Hz, 12H, PMe_2), 1.78 (s, 8H, CH_2N), 2.05 (s, 24H, NMe_2). $^{13}C\{^{1}H\}$ NMR (125.77 MHz, d_6-benzene, 25 °C): δ 2.50 ($SiMe_2$), 3.20 (d, J_{PC} = 17.1 Hz, LiCH), 14.75 (CH_2CH_2), 19.66 (d, J_{PC} = 33.2 Hz, PMe_2), 45.8 (NMe_2), 56.3 (CH_2N). $^{7}Li\{^{1}H\}$ NMR (104.38 MHz, d_6-benzene, 25 °C): δ 1.0 (LiCH). $^{11}B\{^{1}H\}$ NMR (160.47 MHz, d_6-benzene, 25 °C): δ -33.0 (d, J_{PB} = 88.3 Hz). $^{31}P\{^{1}H\}$ NMR (202.47 MHz, d_6-benzene, 25 °C): δ -4.8 (q, J_{PB} = 88.3 Hz).

$[Li(THF)_2]_2[Ph_2P(BH_3)CHSi(Me_2)CH_2]_2$ (40a): To a solution of $[Ph_2P(BH_3)CH_2Si(Me_2)CH_2]_2$ (0.50 g, 0.88 mmol) in THF (40 ml) was added ^{n}BuLi (0.70 ml of a 2.5 M solution in hexanes, 1.75 mmol) and this mixture was left to stir for 1 h at room temperature. The solvent was removed *in vacuo* to yield a yellow oil which was crystallised from cold (-20 °C) Et_2O (10 ml) to yield yellow crystals. Isolated yield: 0.41 g, 80%. Anal.

calcd. for $C_{48}H_{26}B_2Li_2O_4P_2Si_2$ (870.74): C 66.21, H 8.80: Found: C, 66.11, H, 8.70%. $^1H\{^{11}B\}$ NMR (500.16 MHz, d_6-benzene, 25 °C): δ -0.10 (d, J_{PH} = 25.0 Hz, 2H, LiCH), 0.29 (s, 12H, $SiMe_2$), 0.86 (s, 4H, CH_2CH_2), 1.33 (m, 16H, THF), 3.52 (m, 16H, THF), 7.00-8.10 (m, 20H, PPh_2). $^{13}C\{^1H\}$ NMR (125.77 MHz, d_6-benzene, 25 °C): δ -1.24 (d, J_{PC} = 16.1 Hz, LiCH), 1.99 (d, J_{PC} = 6.0 Hz, $SiMe_2$), 15.24 (CH_2CH_2), 25.2 (THF), 68.0 (THF), 127.65, 128.4 (Ar), 131.4 (d, J_{PC} = 9.1 Hz, Ar), 141.9 (d, J_{PC} = 50.5 Hz, *ipso*-Ar). $^7Li\{^1H\}$ NMR (194.38 MHz, d_6-benzene, 25 °C): δ 1.2 (LiCH). $^{11}B\{^1H\}$ NMR (160.47 MHz, d_6-benzene, 25 °C): δ -35.7 (d, J_{PB} = 107.9 Hz). $^{31}P\{^1H\}$ NMR (202.47 MHz, d_6-benzene, 25 °C): δ 12.5 (q, J_{PB} = 107.9 Hz).

[1,2-C_6H_4{$CHPCy_2(BH_3)$}$_2$][Li(tmeda)]$_2$·2PhMe (46a): To a solution of 1,2-$C_6H_4[CH_2PCy_2(BH_3)]_2$ (1.00 g, 1.90 mmol) in THF (30 ml) was added ^{n}BuLi (1.52 ml of a 2.5M solution in hexanes, 3.79 mmol) and the solution was left to stir for 30 minutes at room temperature. The solvent was removed *in vacuo* to yield a dark orange oil. This oil was dissolved in toluene (30 ml) and tmeda (0.57 ml, 3.79 mmol) was added and the solution was left to stir for 5 minutes. The solvent was reduced to 20 ml and the solution was cooled (-20 °C) for 24 h, resulting in yellow crystals, which were washed with a small amount of cold (0 °C) petrol. Isolated yield: 1.04 g, 57%. Anal. calcd. for $C_{44}H_{88}B_2Li_2N_4P_2$ (770.65) [formula without toluene of crystallisation]: C, 68.57; H, 11.51; N, 7.27: Found: C, 68.53; H, 12.23; N, 7.04. $^1H\{^{11}B\}$ NMR (500.16 MHz, d_8-THF, 25 °C): δ 0.33 (d, J_{PH} = 15.0 Hz, 6H, BH_3), 1.12-2.02 (m, 46H, PCy_2 + CHLi), 2.16 (s, 24H, NMe_2), 2.31 (s, 8H, NCH_2) 5.86 (br, 2H, ArH), 6.59 (br, 2H, ArH). $^{13}C\{^1H\}$ NMR (125.77 MHz, d_8-THF, 25 °C): δ 23.30 (d, J_{PC} = 61.3 Hz, CHLi), 26.93, 27.65 (s, PCy_2), 27.83 (d, J_{PC} = 10.1 Hz, PCy_2), 28.08 (d, J_{PC} = 10.1 Hz, PCy_2), 28.54 (s, PCy_2), 34.84 (d, J_{PC} = 34.2 Hz, PCy_2), 45.36 (s, NMe_2), 57.90 (s, NCH_2CH_2N), 112.49 (Ar), 116.32 (d, J_{PC} = 6.0 Hz, Ar), 139.15 (d, J_{PC} = 15.1 Hz, *ipso*-Ar). $^7Li\{^1H\}$ NMR (194.38 MHz, d_8-THF, 25 °C): δ -1.0 (LiCH). $^{11}B\{^1H\}$ NMR (160.47 MHz, d_8-THF, 25 °C): δ -39.8 (br). $^{31}P\{^1H\}$ NMR (202.47 MHz, d_8-THF, 25 °C): δ 12.3 (q, J_{PB} = 105.3 Hz).

Li[$C_6H_5CHP^iPr_2(BH_3)$] (47a): To a solution of $C_6H_5\{CH_2P^iPr_2(BH_3)\}$ (1.00 g, 4.49 mmol) in Et_2O (30 ml) was added ^{n}BuLi (1.91 ml of a 2.4 M solution in hexanes, 4.49 mmol) and this mixture was left to stir for 1 h at room temperature. Crude $^{11}B\{^1H\}$ NMR (160.47 MHz,

25 °C): δ -39.8 (d, J_{PB} = 88.5 Hz). Crude $^{31}P\{^{1}H\}$ NMR (202.47 MHz, 25 °C): δ 16.2 (q, J_{PB} = 88.5 Hz).

[Li(tmeda)][$C_6H_5CHPCy_2(BH_3)$] (49a): To a solution of $C_6H_5\{CH_2PCy_2(BH_3)\}$ (1.00 g, 3.28 mmol) in THF (30 ml) was added ^{n}BuLi (1.43 ml of a 2.3 M solution in hexanes, 3.28 mmol) followed by tmeda (0.49 ml, 3.28 mmol) and this mixture was left to stir for 1 h at room temperature. The solvent was removed *in vacuo* and the resulting solid was crystallised from cold (-5 °C) methylcyclohexane to yield yellow crystals. Isolated yield: 1.07 g, 77%. Anal. calcd. for $C_{25}H_{47}BLiN_2P$ (424.38): C, 70.75; H, 11.16; N, 6.60. Found: C, 70.65; H, 10.88; N, 6.46. $^{1}H\{^{11}B\}$ NMR (500.16 MHz, d_8-toluene , 25 °C): 0.78 (d, J_{PH} = 9.63 Hz, 3H, BH_3), 1.15-2.19 (m, 39H, PCy_2 + CHLi + NMe_2 + NCH_2), 6.98-7.03 (m, 5H, ArH). $^{13}C\{^{1}H\}$ NMR (125.77 MHz, d_8-toluene, 25 °C): 26.64, 27.08 (PCy_2), 27.51 (d, J_{PC} = 4.36 Hz, PCy_2), 27.58 (PCy_2), 27.67 (d, J_{PC} = 4.46 Hz, PCy_2), 35.31 (d, J_{PC} = 30.99 Hz, CHLi), 45.26 (NMe_2), 56.20 (NCH_2CH_2N), 113.05 (Ar), 120.35 (d, J_{PC} = 9.6 Hz, Ar), 137.14 (Ar), 152.15 (*ipso*-Ar). $^{7}Li\{^{1}H\}$ NMR (194.38 MHz, d_8-toluene, 25 °C): δ 0.24 (LiCH). $^{11}B\{^{1}H\}$ NMR (160.47 MHz, d_8-toluene, 25 °C): δ -39.46 (d, J_{PB} = 81.5 Hz). $^{31}P\{^{1}H\}$ NMR (202.47 MHz, d_8-toluene, 25 °C): δ 12.24 (q, J_{PB} = 81.5 Hz).

[K_2{$Me_2P(BH_3)CHSi(Me_2)CH_2$}$_2$] (37b): To a solution of $[Me_2P(BH_3)CH_2Si(Me_2)CH_2]_2$ (0.50 g, 1.55 mmol) in THF (30 ml) was added, dropwise, a solution of benzylpotassium (0.40 g, 3.10 mmol) in THF (30 ml) and this solution was left to stir for 1 h at room temperature. The solvent removed *in vacuo* and the resulting solution was crystallised from cold (-20 °C) toluene/THF (10 ml/2 ml) to yield a red crystalline material. Isolated yield: 0.27 g, 43.0%. $^{31}P\{^{1}H\}$ NMR (202.47 MHz, d_6-benzene, 25 °C): δ -6.8 (q, J_{PB} = 97.2 Hz), 3.4 (q, J_{PB} = 58.7 Hz).

[K(pmdeta)]$_2$[$Ph_2P(BH_3)CHSi(Me_2)CH_2$]$_2$ (40b): To a solution of $[Ph_2P(BH_3)CH_2Si(Me_2)CH_2]_2$ (0.50 g, 0.88 mmol) in THF (20 ml) was added, dropwise, a solution of benzylpotassium (0.26 g, 2.00 mmol) in THF (10 ml), followed by pmdeta (0.37 ml, 1.75 mmol) and this solution was left to stir for 16 h at room temperature. The solvent was removed *in vacuo* from the resulting orange solution to yield a sticky yellow

solid, which was crystallised from cold (-20 °C) toluene (20 ml) as yellow blocks. Isolated yield: 0.53 g, 61%. Anal. calcd. for $C_{50}H_{90}B_2K_2N_6P_2Si_2$ (993.22): C 60.46; H 9.13; N, 8.46. Found: C, 60.34; H, 9.06; N, 8.31. $^1H\{^{11}B\}$ NMR (500.16 MHz, d_8-THF, 25 °C): δ -0.53 (d, J_{PH} = 25.0 Hz, 2H, KCH), -0.15 (s, 12H, $SiMe_2$), 0.43 (s, 4H, CH_2CH_2), 0.95 (d, J_{PH} = 15.0 Hz, 6H, BH_3), 2.16 (s, 12H, NMe_2), 2.19 (s, 3H, NMe), 2.32 (m, 8H, CH_2N), 2.43 (m, 8H, CH_2N), 7.00-8.10 (m, 20H, PPh_2). $^{13}C\{^1H\}$ NMR (125.77 MHz, d_8-THF, 25 °C): δ -2.2 (d, J_{PC} = 38.2 Hz, KCH), -0.1 ($SiMe_2$), 12.1 (d, J_{PC} = 5.0 Hz, CH_2CH_2), 40.5 (NMe), 43.5 (NMe_2), 54.6 (NCH_2), 124.9 (d, J_{PC} = 9.1 Hz, Ph), 125.0 (Ph), 129.3 (d, J_{PC} = 9.1 Hz, Ph), 129.9 (d, J_{PC} = 9.1 Hz, Ph). $^{11}B\{^1H\}$ NMR (160.47 MHz, d_8-THF, 25 °C): δ -34.7 (d, J_{PB} = 113.8 Hz). $^{31}P\{^1H\}$ NMR (202.47 MHz, d_8-THF, 25 °C): δ 11.7 (q, J_{PB} = 113.8 Hz).

$[K(pmdeta)]_2[1,2\text{-}C_6H_4\{CHPCy_2(BH_3)\}_2]$ (46b): To a solution of $1,2\text{-}C_6H_4[CH_2PCy_2(BH_3)]_2$ (0.50 g, 0.95 mmol) in THF (30 ml) was added, dropwise, a solution of benzylpotassium (0.30 g, 2.30 mmol) in THF (30 ml) followed by pmdeta (0.39 ml, 1.90 mmol) and this solution was left to stir for 1 h at room temperature. The solvent was removed *in vacuo* to yield a sticky orange solid which was dissolved in Et_2O (10 ml), filtered and this mixture was left to stand at room temperature for 24 h to yield yellow crystals. Isolated yield: 0.37 g, 41%. Anal. calcd. for $C_{50}H_{102}B_2K_2N_6P_2$ (949.15): C 63.27; H 10.83; N, 8.85. Found: C, 63.11; H, 11.01; N, 8.76. $^1H\{^{11}B\}$ NMR (500.16 MHz, d_8-toluene, 25 °C): δ 0.98 (d, J_{PH} = 12.0 Hz, 6H, BH_3), 1.09-2.23 (m, 67H, PCy_2 + CH_2N + NMe + NMe_2), 6.18 (s, 2H, ArH), 9.96 (s, 2H, ArH). $^{13}C\{^1H\}$ NMR (125.77 MHz, d_8-toluene, 25 °C): δ 27.2 (PCy), 27.6 (PCy_2), 27.8 (d, J_{PC} = 10.1 Hz, PCy_2), 28.0 (d, J_{PC} = 10.1 Hz, PCy_2) 28.5, 33.3 (d, J_{PC} = 30.1 Hz, PCy_2), 37.8 (d, J_{PC} = 36.5 Hz, CHK), 41.8 (NMe), 45.0 (NMe_2), 55.1, 57.0 (NCH_2), 111.2, 113.7 (Ar), 141.9 (d, J_{PC} = 3.9 Hz, Ar). $^{11}B\{^1H\}$ NMR (160.47 MHz, d_8-toluene, 25 °C): δ -40.3 (br). $^{31}P\{^1H\}$ NMR (202.47 MHz, d_8-toluene, 25 °C): δ 12.7 (br).

$K[C_6H_5CHP^iPr_2(BH_3)]$ (47b): To a solution of $C_6H_5\{CH_2P^iPr_2(BH_3)\}$ (0.50 g, 2.24 mmol) in THF (20 ml) was added, dropwise, a solution of BnK (0.34 g, 2.61 mmol) in THF (20 ml) and this solution was left to stir for 45 mins at room temperature. The solvent was removed *in vacuo* and the resulting solution was crystallised from cold (-20 °C) toluene to yield orange crystals which were washed with cold (0 °C) petrol (3 x 5 ml). Isolated yield: 0.28 g, 48%. Anal. calcd. for $C_{13}H_{23}BKP$ (260.81): C, 60.01; H, 8.91. Found: C, 59.99; H, 8.96. $^1H\{^{11}B\}$

NMR (500.16 MHz, d_8-toluene, 25 °C): δ 0.34 (d, J_{PH} = 13.09 Hz, 3H, BH_3), 0.96 (br.d, J_{PH} = 7.12, 6H, CHMe*Me*), 1.01 (dd, J_{PH} = 6.94, J_{HH} = 2.5 Hz, 6H, CH*Me*Me), 1.73 (m, 2H, C*H*Me_2), 1.83 (d, J_{PH} = 4.76 Hz, CHK), 5.58 (m, 1H, ArH), 6.34-6.48 (m, 4H, ArH). $^{13}C\{^1H\}$ NMR (125.77 MHz, d_8-toluene, 25 °C): δ 16.64, 17.51 (CH*Me*$_2$), 25.74 (d, J_{PC} = 36.06 Hz, *C*HMe_2), 34.00 (d, J_{PC} = 75.32 Hz, *C*HK), 106.87, 117.12, 127.82 (Ar), 153.92 (d, J_{PC} = 9.45 Hz, Ar). $^{11}B\{^1H\}$ NMR (160.47 MHz, d_8-toluene, 25 °C): δ -41.0 (d, J_{PB} = 81.3 Hz). $^{31}P\{^1H\}$ NMR (202.47 MHz, d_8-toluene, 25 °C): δ 16.0 (q, J_{PB} = 81.3 Hz).

K[C_6H_5CHPCy_2(BH_3)] (49b): To a solution of $C_6H_5\{CH_2PCy_2(BH_3)\}$ (0.50 g, 1.65 mmol) in THF (20 ml) was added, dropwise, a solution of BnK (0.30 g, 2.30 mmol) in THF (20 ml) and this solution was left to stir for 45 mins at room temperature. The solvent was removed *in vacuo* and the resulting solution was crystallised from cold (-5 °C) toluene to yield orange crystals which were washed with cold (0 °C) petrol (3 x 5 ml). Isolated yield: 0.62 g, 91%. Anal. calcd. for $C_{19}H_{31}BKP\cdot PhCH_3$ (386.38): C, 73.63; H, 9.61. Found: C, 73.49; H, 9.51. $^1H\{^{11}B\}$ NMR (500.16 MHz, d_8-THF, 25 °C): δ 0.28 (d, J_{PH} = 13.33 Hz 3H, BH_3), 1.15-1.83 (m, 22H, PCy_2), 1.86 (d, J_{PH} = 4.77 Hz, 1H, CHK), 2.28 (s, 3H, Toluene), 5.56 (m, 1H, ArH), 6.43-6.52 (m, 4H, ArH), 7.10-7.16 (m, 5H, Toluene). $^{13}C\{^1H\}$ NMR (125.77 MHz, d_8-THF, 25 °C): δ 26.40 (d, J_{PC} = 2.26 Hz, PCy_2), 26.66 (PCy_2), 27.36 (d, J_{PC} = 3.02 Hz, PCy_2), 27.50 (d, J_{PC} = 1.51 Hz, PCy_2), 28.11 (PCy_2), 28.23 (d, J_{PC} = 3.77 Hz, PCy_2), 33.77 (d, J_{PC} = 12.39 Hz, CHK), 36.21 (d, J_{PC} = 37.03 Hz, C*H*PCy_2), 125.05, 127.92, 128.68 (Ar), 137.44 (*ipso*-Ar). $^{11}B\{^1H\}$ NMR (160.47 MHz, d_8-THF, 25 °C): δ -40.2 (d, J_{PB} = 79.2 Hz). $^{31}P\{^1H\}$ NMR (202.47 MHz, d_8-THF, 25 °C): δ 8.8 (q, J_{PB} = 79.2 Hz).

[[1,2-C_6H_4{CHPCy_2(BH_3)}$_2$]Sn]$_2$·1½PhMe (58): To a solution of 1,2-$C_6H_4[CH_2PCy_2(BH_3)]_2$ (0.50 g, 1.17 mmol) in THF (20 ml) was added ^{n}BuLi (0.94 ml of a 2.5M solution in hexanes, 2.34 mmol) and this mixture was left to stir for 30 minutes at room temperature, which resulted in an orange solution. The solvent was removed *in vacuo* to yield a dark orange oil. This oil was dissolved in toluene (20 ml) and was added, dropwise, to a solution of $SnCp_2$ (0.29 g, 1.17 mmol) in toluene and this mixture was left to stir for 45 minutes at room temperature, with the exclusion of light. The mixture was filtered, the filtrate was reduced to 10 ml and then cooled (-20 °C) to crystallise. After 7 days yellow crystals were isolated and washed with petrol (3 x 5 ml). Isolated Yield: 0.23 g. 28%. The solvent is

gradually lost when the sample was put under vacuum and so no solvent peaks were observed in the NMR spectra. Anal. Calcd for $C_{64}H_{112}B_4P_4Sn_2$ (1286.1): C, 59.77; H, 8.78. Found: C, 59.68; H, 8.88. $^1H\{^{11}B\}$ NMR (500.15 MHz, d_8-THF, 25 °C): δ 0.50-2.67 (m, 107H, Cy + BH_3 + CHSn + Ph*Me*), 6.58 (m, 1H, ArH), 6.79 (m, 1H, ArH), 7.00 (m, 2H, ArH), 7.07-7.19 (m, 5H, *Ph*Me), 7.28 (m, 2H, ArH), 7.96 (m, 1H, ArH), 8.03 (m, 1H, ArH). $^{11}B\{^1H\}$ NMR (160.47 MHz, d_8-THF, 25 °C): δ -43.5, -38.8 (br). $^{31}P\{^1H\}$ NMR (202.47 MHz, d_8-THF, 25 °C): δ 27.4, 28.6, 30.0, 35.4 (br). $^{119}Sn\{^1H\}$ NMR (186.51 MHz, d_8-THF, 25 °C): δ -103 (br, FWHM = 770 Hz), 339 (br, FWHM = 480 Hz).

Sn[1,2-C_6H_4{$CHPPh_2(BH_3)$}$_2$] (60): To a solution of 1,2-$C_6H_4[CH_2PPh_2(BH_3)]_2$ (0.50 g, 1.00 mmol) in THF (20 ml) was added ^{n}BuLi (0.80 ml of a 2.5M solution in hexanes, 1.99 mmol) and this mixture was left to stir for 30 minutes at room temperature. The solvent was removed *in vacuo* to yield a red oil. This oil was dissolved in toluene (20 ml) and was added, dropwise, to a solution of $SnCp_2$ (0.25 g, 0.996 mmol) in toluene and this mixture was left to stir for 45 minutes at room temperature, with the exclusion of light, to give an orange solution; which was unable to isolate any solid material for full characterisation. Crude $^{31}P\{^1H\}$ NMR (202.47 MHz, Toluene, 25 °C): δ 14.8 (br), 16.9 (br), 18.8 (br), 20.4 (br), 23.1 (br).

Sn[1,2-C_6H_4{$CHP^iPr_2(BH_3)$}$_2$] (61): To a solution of 1,2-$C_6H_4[CH_2P^iPr_2(BH_3)]_2$ (0.50 g, 1.37 mmol) in THF (20 ml) was added ^{n}BuLi (1.14 ml of a 2.5M solution in hexanes, 2.73 mmol) and this mixture was left to stir for 30 minutes at room temperature The solvent was removed *in vacuo* to yield a dark orange oil. This oil was dissolved in toluene (20 ml) and was added, dropwise, to a solution of $SnCp_2$ (0.34 g, 1.37 mmol) in toluene and this mixture was left to stir for 16 h at room temperature, with the exclusion of light. The mixture was then filtered to give an orange solution which was unable to isolate any solid material for full characterisation. Crude $^{31}P\{^1H\}$ NMR (202.47 MHz, Toluene, 25 °C): δ 32.07 (br), 33.40 (br), 35.20 (br), 36.26 (br), 38.70 (br).

Sn[$C_6H_5CHP^iPr_2(BH_3)$]$_2$ (64): To a solution of $C_6H_5CHP^iPr_2(BH_3)$ (1.00 g, 4.49 mmol), in Et_2O (30 ml) was added ^{n}BuLi (1.91 ml of a 2.35 M solution in hexanes, 4.49 mmol) and this

solution was left to stir for 1 h at room temperature. This solution was added, dropwise, to a cold (-78 °C) solution of $SnCl_2$ (0.43 g, 2.24 mmol) in Et_2O (20 ml) and this mixture was left to stir overnight and attain room temperature. This mixture was filtered, solvent was removed *in vacuo* from the filtrate and the resulting solid was crystallised from cold (-20 °C) methylcyclohexane. Isolated Yield: 2.12 g, 84%. $^{11}B\{^1H\}$ NMR (160.47 MHz, 25 °C): δ -38.76 (d, J_{PB} = 79.47 Hz). $^{31}P\{^1H\}$ NMR (202.47 MHz, 25 °C): δ 34.59 (br).

Sn[$C_6H_5CHPCy_2(BH_3)]_2$ (65): To a solution of $C_6H_5CHPCy_2(BH_3)$ (1.00 g, 3.31 mmol), in Et_2O (30 ml) was added ^{n}BuLi (1.44 ml of a 2.3 M solution in hexanes, 3.31 mmol) and this mixture was left to stir for 1 h at room temperature. This solution was added, dropwise, to a cold (-78 °C) solution of $SnCl_2$ (0.31 g, 1.65 mmol) in Et_2O (20 ml) and this mixture was left to stir overnight and attain room temperature. This mixture was filtered, solvent was removed *in vacuo* from the filtrate and the resulting solid was crystallised from cold (5 °C) diethylether. Isolated Yield: 0.21 g, 17.7%. Anal. Calcd for $C_{38}H_{62}B_2P_2Sn$ (721.25): C, 63.29; H, 8.67. Found: C, 58.49; H, 8.18. $^1H\{^{11}B\}$ NMR (500.16 MHz, d_8-toluene, 25 °C): δ 0.62 (d, J_{PH} = 8.50 Hz, 6H, BH_3), 1.07-1.79 (m, 44H, PCy_2), 3.50 (d, J_{PH} = 11.25 Hz, 2H, CHSn), 7.10-7.28 (m, 10H, ArH). $^{11}B\{^1H\}$ NMR (160.47 MHz, d_8-toluene, 25 °C): δ -39.4 (br). $^{31}P\{^1H\}$ NMR (202.47 MHz, d_8-toluene, 25 °C): 32.0 (br). $^{119}Sn\{^1H\}$ NMR (186.51 MHz, d_8-toluene, 25 °C): δ 359 (br), 370 (br).

[$C_6H_5CHP^iPr_2(BH_3)$]SnCl (69): To a solution of $C_6H_5CHP^iPr_2(BH_3)$ (1.00 g, 4.49 mmol), in Et_2O (30 ml) was added ^{n}BuLi (1.91 ml of a 2.35 M solution in hexanes, 4.49 mmol) and this mixture was left to stir for 1 h at room temperature. This solution was added, dropwise, to a cold (-78 °C) solution of $SnCl_2$ (0.43 g, 2.24 mmol) in Et_2O (20 ml) and this mixture was left to stir overnight and attain room temperature. This mixture was filtered and a fine yellow solid deposited from solution; this was isolated and was washed with Et_2O (3 x 5 ml). Isolated Yield: 1.43 g, 84.7%. $^{11}B\{^1H\}$ NMR (160.47 MHz, 25 °C): δ -39.2 (d, J_{PB} = 66.6 Hz). $^{31}P\{^1H\}$ NMR (202.47 MHz, 25 °C): 33.4 (q, J_{PB} = 66.6 Hz).

[$C_6H_5CHPCy_2(BH_3)$]SnCl (70): To a solution of $C_6H_5CHPCy_2(BH_3)$ (0.50 g, 1.65 mmol), in Et_2O (20 ml) was added ^{n}BuLi (0.70 ml of a 2.35 M solution in hexanes, 1.65 mmol) and this

solution was left to stir for 1 h at room temperature. This solution was added, dropwise, to a cold (-78 °C) solution of $SnCl_2$ (0.31 g, 1.65 mmol) in Et_2O (20 ml) and this mixture was left to stir overnight and attain room temperature. This mixture was filtered, the filtrate was reduced in volume (10 ml) and a fine yellow solid precipitated which was washed with Et_2O (3 x 5 ml). Isolated Yield: 0.63 g, 83.6%. Anal. Calcd for $C_{19}H_{31}BClPSn$ (455.42): C, 50.11; H, 6.86. Found: C, 50.24; H, 6.99. $^{1}H\{^{11}B\}$ NMR (500.16 MHz, *d*$_8$-THF, 25 °C): 1.07-1.79 (m, 22H, PCy_2), 3.05 (d, J_{PH} = 11.69 Hz, 1H, CHSn), 7.10-7.28 (m, 5H, Ph). $^{13}C\{^{1}H\}$ NMR (125.77 MHz, *d*$_8$-THF, 25 °C): δ 26.04-28.01 (m, PCy_2), 31.71 (d, J_{PC} = 28.89 Hz, SnCH), 127.62, 128.00, 129.96, 130.00 (Ph). $^{11}B\{^{1}H\}$ NMR (160.47 MHz, *d*$_8$-THF, 25 °C): δ -39.8 (br). $^{31}P\{^{1}H\}$ NMR (202.47 MHz, *d*$_8$-THF, 25 °C): 27.7 (br).

$[C_6H_5CHP^iPr_2(BH_3)]_2Sn(Me)I$ (86): To a solution of $Sn[C_6H_5CHP^iPr_2(BH_3)]_2$ (10 ml of a 0.101 M solution in Et_2O, 1.01 mmol) was added MeI (0.06 ml, 1.01 ml) and this solution was left to stir for 16 h at room temperature. A colourless precipitate had formed which was isolated by decanting the supernatant and removing residual solvent *in vacuo* to yield a colourless solid. Single crystals were obtained suitable for X-ray crystallography by dissolving the crude product in hot toluene (5 ml) and layering with Et_2O (20 ml). Isolated Yield: 0.32 g, 45%. Anal. Calcd for $C_{27}H_{49}B_2IP_2Sn$ (702.91): C, 45.20; H, 7.15. Found: C, 45.27; H, 7.26. $^{1}H\{^{11}B\}$ NMR (500.16 MHz, $CDCl_3$, 25 °C): 0.56 (d, J_{PH} = 15.0 Hz, BH_3^9) 0.75 (d, J_{PH} = 10.0 Hz, $BH_3^{9'}$), 0.76 (dd, J_{HH} = 10.0 Hz, J_{PH} = 15.0 Hz, $CH_3^{5'}$), 0.86 (s, 3H, $SnCH_3$), 0.87 (dd, J_{HH} = 10.0 Hz, J_{PH} = 15.0 Hz, CH_3^5), 1.18 (dd, J_{HH} = 10.0 Hz, J_{PH} = 15.0 Hz, $CH_3^{8'}$), 1.25 (m, CH_3^4, CH_3^7, CH_3^8 AND $CH_3^{4'}$), 1.39 (dd, J_{HH} = 10.0 Hz, J_{PH} = 15.0 Hz, $CH_3^{7'}$), 2.10 (s, PCH^6 + $PCH^{6'}$), 2.26 (s, PCH^3), 2.87 (s, $PCH^{3'}$), 4.19 (d, J_{PH} = 15.0 Hz, J_{SnH} = 130.0 Hz, $SnCH^{1'}$), 4.54 (d, J_{PH} = 15.0 Hz, J_{SnH} = 55.0 Hz, $SnCH^1$). $^{13}C\{^{1}H\}$ NMR (125.77 MHz, $CDCl_3$, 25 °C): δ 5.56 (dd, J_{P2C} = 1.80 Hz, $J_{P2'C}$ = 2.38 Hz, $SnCH_3$), 17.14 (d, J_{PC} = 5.03 Hz, $CMe^{5'}$), 17.19 (d, J_{PC} = 3.77 Hz, CMe^5), 17.49 (s, CMe), 17.53 (s, $CMe^{7'}$), 18.00 (s, CMe), 18.24 (d, J_{PC} = 2.52 Hz, $CMe^{8'}$), 19.51 (d, J_{PC} = 2.52 Hz, CMe^4), 20.21 (d, J_{PC} = 3.77 Hz, CMe), 21.00 (s, $CMe^{6'}$), 21.24 (d, J_{PC} = 2.52 Hz, $CMe^{3'}$), 21.46 (d, J_{PC} = 33.96 Hz, CMe^3), 22.00 (d, J_{PC} = 31.45 Hz, CMe^6), 34.79 (d, J_{PC} = 13.8 Hz, CMe^1), 35.68(d, J_{PC} = 17.6 Hz, $CMe^{1'}$), $^{11}B\{^{1}H\}$ NMR (160.47 MHz, $CDCl_3$, 25 °C): δ -40.1 (br, BH_3^9), -40.8 (br, $BH_3^{9'}$). $^{31}P\{^{1}H\}$ NMR (202.47 MHz, $CDCl_3$, 25 °C): δ 36.9 (br, P^2), 40.48 (br, $P^{2'}$). $^{119}Sn\{^{1}H\}$ NMR (186.51 MHz, $CDCl_3$, 25 °C): δ -14.8 ppm (dd, (J_{HH} = 20.5 Hz, J_{PH} = 106.3 Hz).

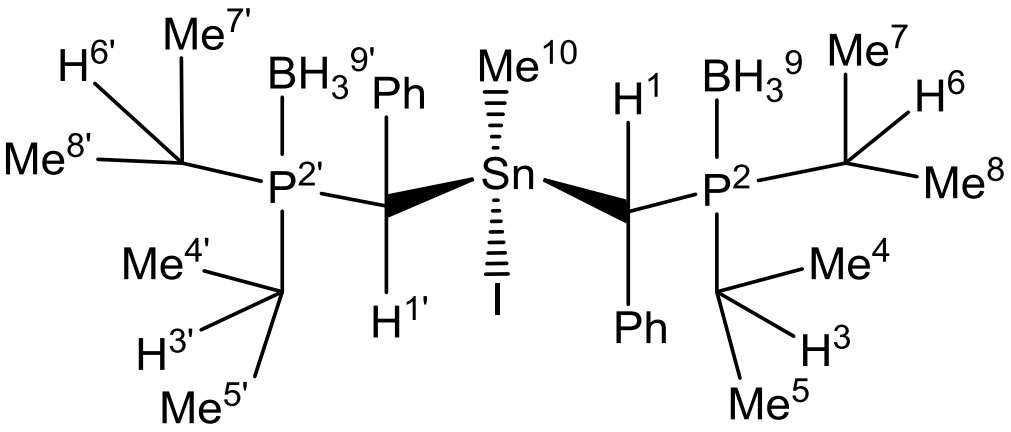

Compound **86** with atom labelling.

[$C_6H_5CHP^iPr_2(BH_3)]_2Sn(Bn)Br$ (87): To a solution of $Sn[C_6H_5CHP^iPr_2(BH_3)]_2$ (10 ml of a 0.101 M solution in Et_2O, 1.01 mmol) was added BnBr (0.12 ml, 1.01 ml) and this solution was left to stir for 16 h at room temperature. The resulting crude sample was reduced in volume (10 ml) and cooled (-5 °C) in order to precipitate compound **87** as a colourless solid. Single crystals were obtained suitable for X-ray by dissolving the crude product in hot toluene (5 ml) and layering with Et_2O (20 ml). Isolated Yield: 0.36 g, 49%. Anal. Calcd for $C_{33}H_{53}B_2BrP_2Sn$ (732.03): C, 54.15; H, 7.30. Found: C, 54.04; H, 7.20. ^{1}H NMR (500.16 MHz, $CDCl_3$, 25 °C): 0.39 (dd, J_{HH} = 5.00 Hz, J_{PH} = 10.0 Hz, 6H, CH_3), 0.94 (dd, J_{HH} = 10.0 Hz, J_{PH} = 15.0 Hz, 6H, CH_3), 1.08 (dd, J_{HH} = 10.0 Hz, J_{PH} = 15.0 Hz, 6H, CH_3), 1.23 (dd, J_{HH} = 5.00 Hz, J_{PH} = 15.0 Hz, 6H, CH_3), 2.70, 4.15 (d, J_{PH} = 15.0 Hz, 1H, SnC*H*), 7.79 (d, J_{PH} = 10.0 Hz, 1H, SnC*H*), 6.89-7.55 (m, 15H, Ar). ^{11}B{^{1}H} NMR (160.47 MHz, $CDCl_3$, 25 °C): δ -40.5 (br, BH_3). ^{31}P{^{1}H} NMR (202.47 MHz, $CDCl_3$, 25 °C): δ 36.2 (br), 38.3 (br), 40.74 (br). ^{119}Sn{^{1}H} NMR (186.51 MHz, $CDCl_3$, 25 °C): δ -22.8 (t, J_{SnP} = 28.0 Hz), -5.61 (t, J_{SnP} = 86.7 Hz). -4.31 ppm (t, J_{SnP} = 85.8 Hz), 1.17 ppm (dd, J_{SnP} = 126.8 Hz, $J_{SnP'}$ = 13.1 Hz).

10.6 References

1. H. Schmidbaur, E. Weiss and G. Muller, *Synth. React. Inorg. Met.-Org. Chem.*, 1985, **15**, 401-413.
2. K. Izod, C. M. Dixon, E. McMeekin, L. Rodgers, R. W. Harrington and U. Baisch, *Organometallics*, 2014, **33**, 378-386.
3. K. Izod, D. G. Rayner, S. M. El-Hamruni, R. W. Harrington and U. Baisch, *Angewandte Chemie-International Edition*, 2014, **53**, 3636-3640.
4. L. Lochmann and J. Trekoval, *J. Organomet. Chem.*, 1987, **326**, 1-7.
5. C. Eaborn, P. B. Hitchcock, K. Izod, A. J. Jaggar and J. D. Smith, *Organometallics*, 1994, **13**, 753-754.
6. E. Weiss and Sauerman.G, *Chemische Berichte-Recueil*, 1970, **103**, 265-&.
7. E. Weiss and Sauerman.G, *Angewandte Chemie (International ed. in English)*, 1968, **7**.
8. E. Fischer and H. Grubert, *Natureforsch*, 1956, **11b**.
9. K. Izod, W. McFarlane, C. Wills, W. Clegg and R. W. Harrington, *Organometallics*, 2008, **27**, 4386-4394.
10. A. Naghipour, S. J. Sabounchei, D. Morales-Morales, S. Hernandez-Ortega and C. M. Jensen, *J. Organomet. Chem.*, 2004, **689**, 2494-2502.
11. F. Dornhaus, M. Bolte, H. W. Lerner and M. Wagner, *Eur. J. Inorg. Chem.*, 2006, 1777-1785.
12. B. Mohr, D. M. Lynn and R. H. Grubbs, *Organometallics*, 1996, **15**, 4317-4325.
13. K. Izod and P. G. Waddell, *Organometallics*, 2015, **34**, 2726-2730.
14. A. D. Becke, *J. Chem. Phys.*, 1993, **98**, 5648-5652.
15. P. J. Stephens, F. J. Devlin, C. F. Chabalowski and M. J. Frisch, *J. Phys. Chem.*, 1994, **98**, 11623-11627.
16. R. H. Hertwig and W. Koch, *Chem. Phys. Lett.*, 1997, **268**, 345-351.
17. Harihara.Pc and J. A. Pople, *Theor. Chim. Acta*, 1973, **28**, 213-222.
18. M. M. Francl, W. J. Pietro, W. J. Hehre, J. S. Binkley, M. S. Gordon, D. J. Defrees and J. A. Pople, *J. Chem. Phys.*, 1982, **77**, 3654-3665.
19. M. W. Wong, *Chem. Phys. Lett.*, 1996, **256**, 391-399.
20. J. P. Foster and F. Weinhold, *J. Am. Chem. Soc.*, 1980, **102**, 7211-7218.
21. A. E. Reed and F. Weinhold, *J. Chem. Phys.*, 1983, **78**, 4066-4073.
22. A. E. Reed and F. Weinhold, *J. Chem. Phys.*, 1985, **83**, 1736-1740.
23. A. E. Reed, R. B. Weinstock and F. Weinhold, *J. Chem. Phys.*, 1985, **83**, 735-746.

24. J. E. Carpenter and F. Weinhold, *Journal of Molecular Structure-Theochem*, 1988, **46**, 41-62.
25. A. E. Reed, L. A. Curtiss and F. Weinhold, *Chem. Rev. (Washington, DC, U. S.)*, 1988, **88**, 899-926.

Appendix 1. X-ray crystallographic data

Compound No.	Formula	File No.
37	$[Me_2P(BH_3)CH_2Si(Me_2)CH_2]_2$	ki505
40a	$[Li(THF)_2]_2[Ph_2P(BH_3)CHSi(Me_2)CH_2]_2$	ki503
40b	$[K(pmdeta)]_2[Ph_2P(BH_3)CHSi(Me_2)CH_2]_2$	ki514
44	$1,2\text{-}C_6H_4\{CH_2P^iPr_2(BH_3)\}_2$	ki524
44a	$[1,2\text{-}C_6H_4\{CHP^iPr_2(BH_3)\}_2][Li(tmeda)]_2$	ki448
45a	$[1,2\text{-}C_6H_4\{CHPPh_2(BH_3)\}_2][Li(tmeda)]_2\cdot THF$	ki475
46a	$[1,2\text{-}C_6H_4\{CHPCy_2(BH_3)\}_2][Li(tmeda)]_2\cdot 2PhMe$	ki513
46b	$[K(pmdeta)]_2[1,2\text{-}C_6H_4\{CHPCy_2(BH_3)\}_2]$	ki523
48	$C_6H_5\{CH_2PPh_2(BH_3)\}$	ki533
49a	$[Li(tmeda)][C_6H_5CHPCy_2(BH_3)]$	ki516
49b	$K[C_6H_5CHPCy_2(BH_3)]$	ki532
58	$[[1,2\text{-}C_6H_4\{CHPCy_2(BH_3)\}_2]Sn]_2\cdot 1½PhMe$	ki506
64	$Sn[C_6H_5CHP^iPr_2(BH_3)]_2$	ki542
65	$Sn[C_6H_5CHPCy_2(BH_3)]_2$	ki519
86	$[C_6H_5CHP^iPr_2(BH_3)]_2Sn(Me)I$	ki549

Appendix 2. Eyring plot data

T (K)	k (s^{-1})	1/T	ln(k/T)
330	12000	0.0030303	3.593569
316	5500	0.0031646	2.856761
296	1800	0.0033784	1.805182
283	570	0.0035336	0.700189
263	150	0.0038023	-0.56152
253	45	0.0039526	-1.72673
243	14	0.0041152	-2.854
230	4	0.0043478	-4.05178
223	1.8	0.0044843	-4.81939

T (K)	k (s^{-1})	1/T	ln(k/T)
330	7000	0.0030303	3.054573
316	3700	0.0031646	2.460346
296	900	0.0033784	1.112035
283	250	0.0035336	-0.12399
263	50	0.0038023	-1.66013
253	20	0.0039526	-2.53766
243	3.5	0.0041152	-4.2403
230	1.5	0.0043478	-5.03261
223	0.5	0.0044843	-6.10032